UNIVERSITÀ POLITECNICA DELLE MARCHE

Department of Life and Environmental Sciences

XV PhD cycle in Life and Environmental Sciences

Curriculum Biomolecular Sciences (SB)

α-Hydrazido acids for the synthesis of bioactive amphiphilic compounds

PhD candidate:

Paolo Amabili

Supervisor:

Samuele Rinaldi, PhD

XXIX cycle PhD - 2013-2016

Abstract

Novel mimics of β-peptides based on the formal substitution Cβ→Nβ(acyl) were synthesized with the aim to obtain new *foldamers* (oligomers with a predictable folding). Thus, we modified pirrolidin-2-one tethered β-amino acids, previously used in our laboratory to prepare hexamers, devised a new imidazolidinone-tethered α-hydrazido acid (AOPIC) suitable to give oligomers that were analysed using spectroscopic (NMR and CD) and computational (MD) techniques. The computational analysis, besides furnishing the theoretical proof of the 8-helix as the only stable structure, strongly evidenced a "hydrazido-turn" sequence, where additional 5-membered H-bonded cycles were enclosed within the 8-membered ones.

In the search for simpler and cheaper analogues, we directed our attention towards analogues of the previously employed oligomers, where constrictions and chirality were missing, with the aim to obtain a secondary structure with minor synthetic effort and increased versatility in side chains substitution. In fact, an appropriate disposition of side chains could be a good starting point for the synthesis of amphiphilic foldamers to be tested as antibacterial agents.

Since many difficulties are connected with the use of peptide drugs, synthetic mimics of AMPs (SMAMPs) are receiving ever more interest and importance as new drug candidates, owing to the rapid and widespread development of antibiotic resistances. Thus, within this topic, we carried out the synthesis of amphiphilic α-hydrazido acid derivatives, which could be novel lead compounds for developing a new class of SMMAMPs.

The Minimum Inhibitory Concentration (MIC) was evaluated for a few properly derivatized α-hydrazido acid monomers, and the preliminary results showed a promising antimicrobial activity suitable for biological applications, eventually leading to a structure optimization for improvement of the pharmacological properties.

SUMMARY

CHAPTER 1:

Foldamers: an overview

1. FOLDAMERS: AN OVERVIEW

1.1 Introduction

In all the proteins, as well as in every peptidic structure, a correct *folding* is essential for the formation of the "active sites" where the functional groups, often separated along the amino-acidic chain, are rearranged in a predetermined three-dimensional structure, necessary for their activity. For understanding the close relationship between structure and activity and also the principles that are at the basis of a correct folding in an amino-acidic backbone, we could perform a *de novo* design of biomimetic polymers with unusual properties never seen in nature. Those syntheses could have important practical applications in pharmaceutical and material sciences. This represent the "Foldamers" field of study.[1]

"A foldamer is any oligomer that folds into a conformationally ordered state in solution, the structures of which are stabilized by a collection of non-covalent interactions between nonadjacent monomer units".[1] This definition has important implications:

- A foldamer is an *oligomer*, and this entail the presence of a regular repetitive structural motif (a *monomer*) in the backbone
- Foldamers are *oligomeric* and not *polymeric* structures
- The fact that the ordered conformation is "in solution", imply that the solvent covers an important role in the structure of these molecules and in the fluctuations of atomic coordinates in the preferred conformation
- The molecule has to organize with a dynamic process in (a) prevalent conformation(s): oligomers where there isn't such a possibility are not considered foldamers
- When the molecule is folded, it adopts a single set (or few of them) of superimposable conformations, that is to say a single secondary structure
- The secondary structure is stabilized by *non-covalent interaction between non-adjacent monomeric units*: if the potential energy surface of *intra*monomer covalent bonds and the steric effects between adjacent residues are the only reasons for the adopted secondary structure, an oligomer cannot be considered as a foldamer (e.g. polyproline, polyaldehydes, polymethacrylate, etc.). Furthermore, we cannot consider a foldamer the structure that present a secondary structure stabilized by hydrogen bonds between adjacent residues.

This last point is relevant, because it makes the definition of foldamer consistent with the "synthetic analogue of a natural secondary structure". In fact, every natural secondary structure

corresponds to this definition. Obviously, the torsional preferences for the dihedral angles and the steric effects between adjacent residues will contribute to determine the secondary structure, but they will not be sufficient in itself, exactly as in the natural α-peptides, where many other factors can influence the folding (e.g. H-bonding).

The pathway to create a new foldamer follows several steps:

i. Identification of new oligomeric backbones with a high tendency to fold into a well defined secondary structure. This imply the ability to predict the relationship between the conformational properties of the monomer and the corresponding oligomers.

ii. It's necessary to insert in the monomer suitable and well oriented chemical functionalities, in order to improve the folding propensities of oligomers (preorganization).

iii. The foldamers have to be obtained in a synthetically efficient way, through both a practical and stereoselective synthesis of enantiomerically pure monomers and a high-yielding oligomerization process.

In the last decades, several research groups have devoted their studies towards the development of new monomers to build novel foldamers.[1] According to the features of the monomeric units, all these oligomers could be grouped into two main principal classes (Figure 1): "aliphatic" and "aromatic" foldamers.

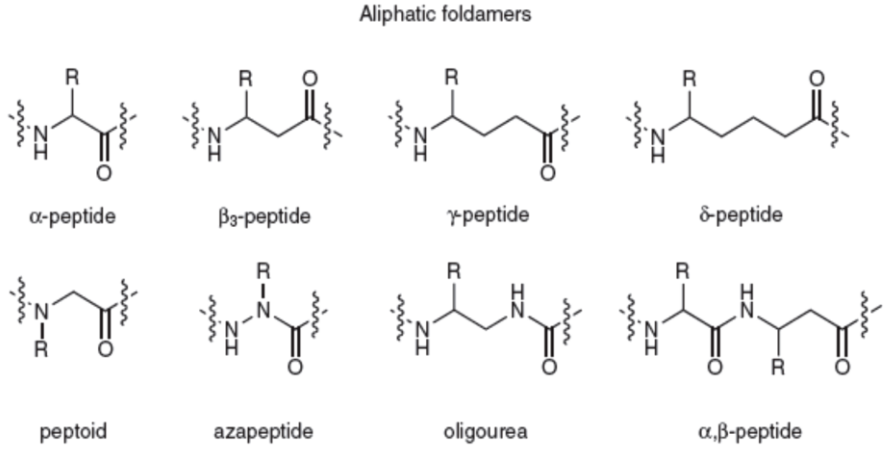

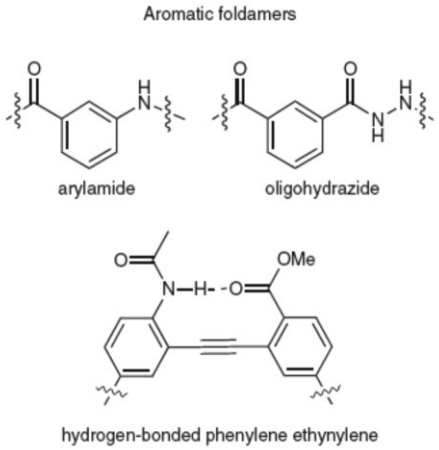

Figure 1. Examples of foldameric backbones.

The huge number of building monomers brought to a wide number of secondary and higher-order structures, some of which are reported in Figure 2.

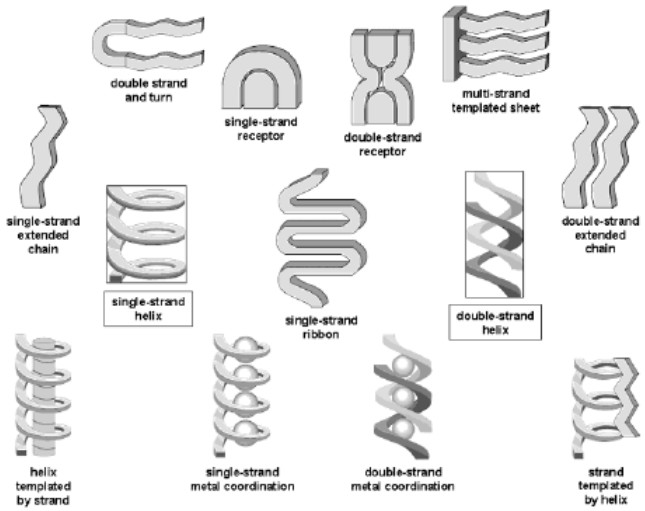

Figure 2. Some secondary and supersecondary structures adopted by foldamers.

1.2 β-Peptide Foldamers

Among aliphatic foldamers, the β-peptides family is the most interesting and the most studied for several reasons:

- They are the littlest structural variation with respect to the natural α-peptides.
- Generally, they are very stable towards proteases.
- Even though they have an extra C-C bond with free rotation, with the proper substitutions they can form secondary structures, especially helices, more stable than the ones of α-peptides.

- For both acyclic and cyclic monomers, there are many different techniques that allow the easy synthesis in enantiomerically pure form and with all the desired side chains/functionalities.
- With the β-amino acids it is possible to have much more substitution patterns in comparison to α-amino acids (Figure 3), thus offering an enhanced opportunity to control the conformation of the corresponding oligomers.

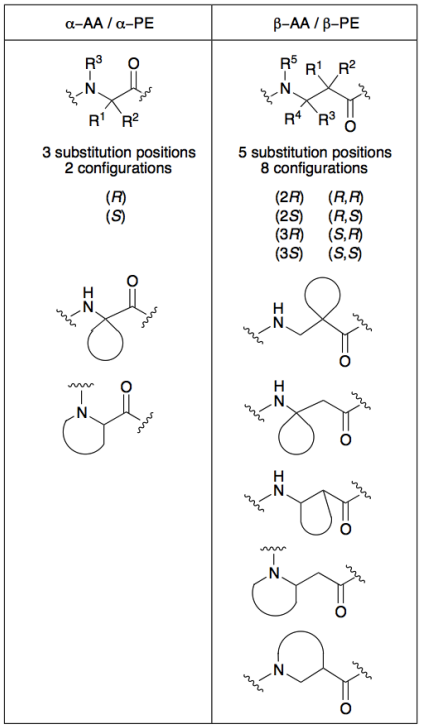

Figure 3. Substitution and cyclization scheme of α- and β-amino acids.

The conformations of β-peptides can be analysed in term of backbone torsional angles ω, φ, θ e ψ, as.[2] The effects of substituents on the conformation of β-peptides were investigated in a plethora of experimental studies,[1] and a generic example of how different substitution patterns in acyclic β-peptides can affect the observed folding is reported in Figure 4.[3]

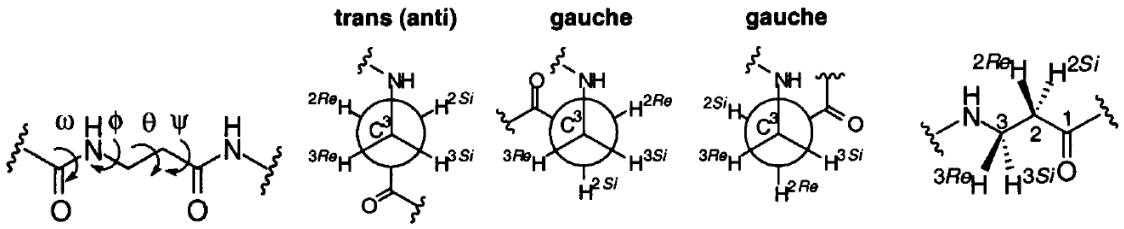

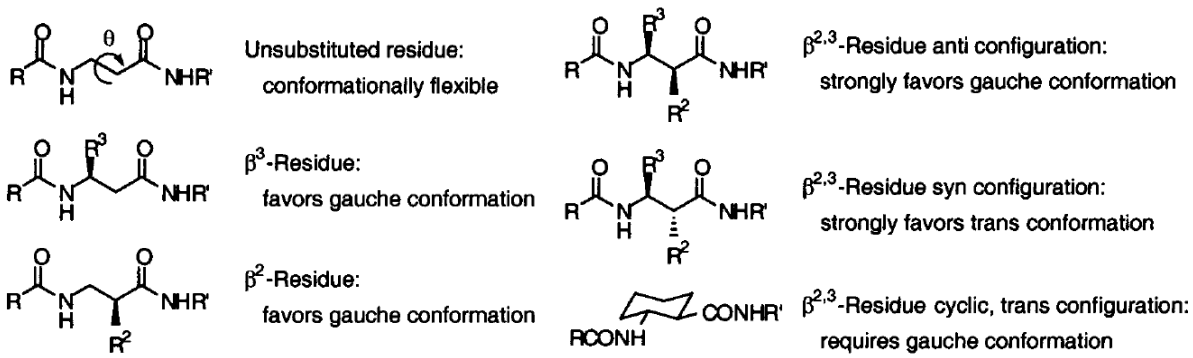

Figure 4. Effect of the substituents on the torsional dihedral angle θ.

Therefore, different substitution patterns influence the torsional angles, bringing to several stables conformations as helices, sheets or turns, even if the effect of all the noncovalent interactions must be accurately taken into account. For example, it was evidenced that *syn* and *anti*-$\beta^{2,3}$-peptides, obtained from β-lactams with *cis* and *trans* configuration, have the intrinsic conformational tendency to give different secondary structures due to steric hindrance between the substituents (Figure 5).[4]

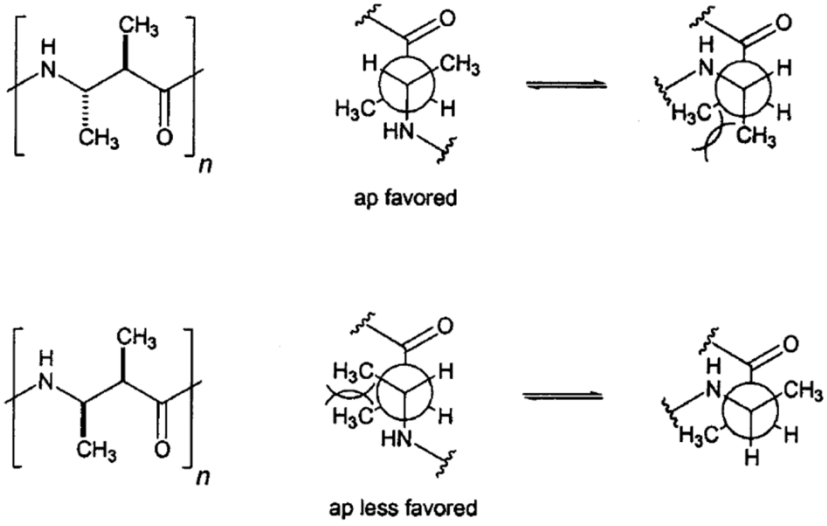

Figure 5. Intrinsic conformational preferences of *syn*- and *anti*-$\beta^{2,3}$-peptides.

In particular, an *anti* substitution leads to a preference for the β-strand (Figure 6), while a *syn* substitution facilitates the formation of helices.

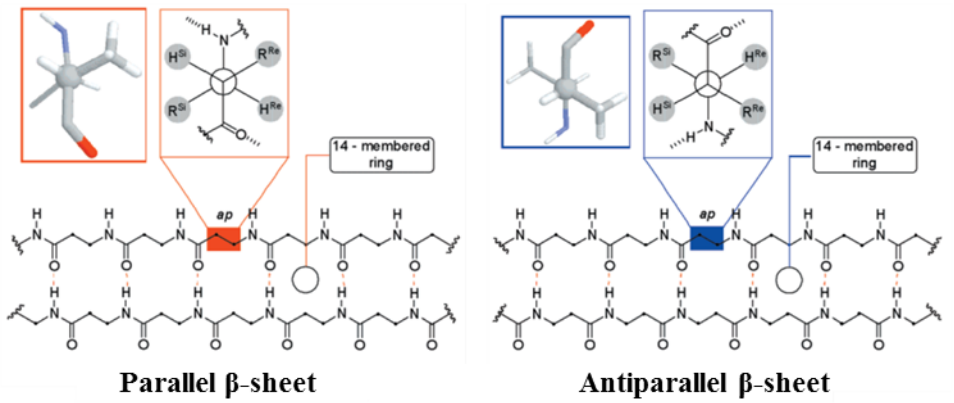

Figure 6. Preferential formation of β-sheets for *anti*-β^{2,3}-peptides.

The nomenclature of the helical conformations is very variable in literature.[3,5,6] The one reported in Figure 7, and used throughout the entire discussion, relies simply on the number of the atoms occurring between the C=O and N-H groups involved in the H-bond (Gellman's nomenclature).[3] Other nomenclatures will be used only when needed.

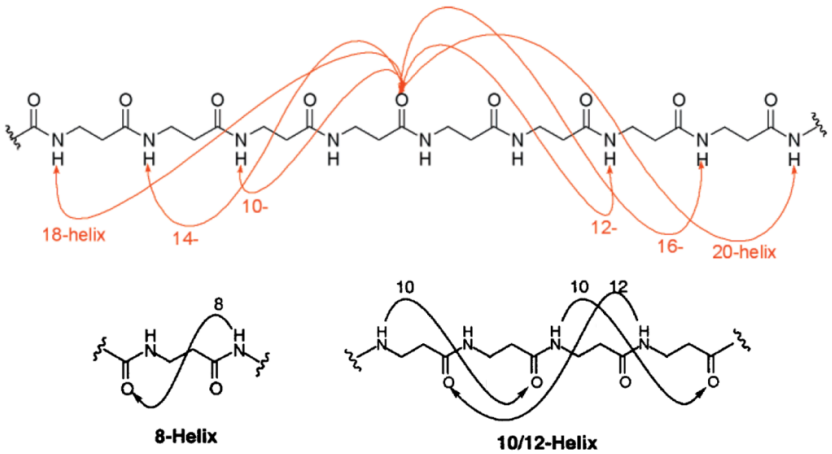

Figure 7. Different helix conformations for β-peptides.

The most common structure for various acyclic β^2-, β^3- and β^{2,3}-substituted amino acids is, by far, the 14-helix, where there is a C=O(*i*)•••H-N(*i*-*2*).[1] Anyway, exploiting a suitable substitution scheme in the monomers and a proper placement of differently substituted monomers in the peptidic sequence, other secondary structures such as 10/12-helices, 10-membered turns and β-sheets were obtained (Figure 8).[7]

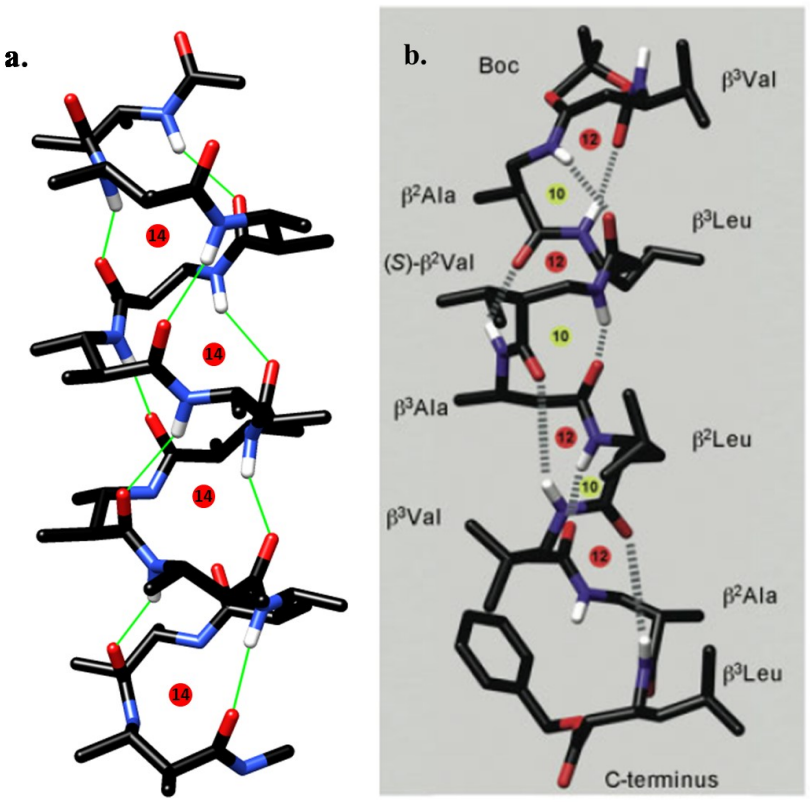

Figure 8. Examples of helices for substituted β-amino acids. (a) 14-helix of a dodecamer made of $\beta^{2,3}$-disobstituted-amino acids; (b) 10/12 helix of a peptide with an alternate placement of monosubstituted β^2- and β^3-amino acids. Only H-bonded hydrogens were displayed for clarity.

On the contrary, β-peptides containing the conformationally constrained cyclic amino acid *trans*-2-amino-cyclopentanecarboxylic acid (ACPC) adopt a 12-helix conformation, stabilized by H-bonding between amide carbonyl groups at position *i* and the amide proton at position *i+3*. On the other hand, when the monomer is the *trans*-2-aminocyclohexanecarboxylic acid (ACHC), the β-peptide folds in a 14-helix conformation, stabilized by H-bonding between the amide proton at position *i* and the carbonyl at position *i+2* (Figure 9).[8]

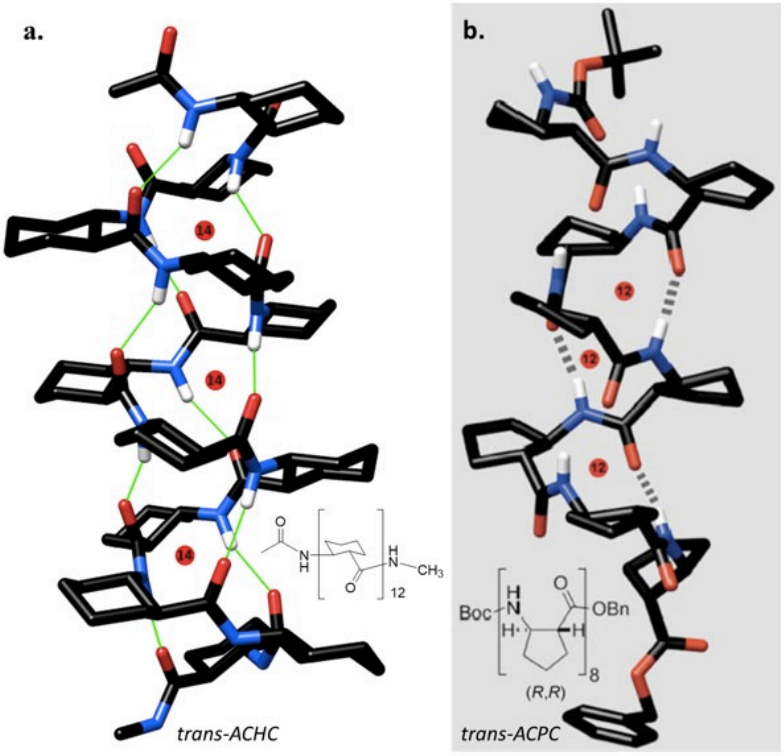

Figure 9. (a) 14-helix conformation for *trans*-ACHC; (b) 12-helix for an oligopeptide of *trans*-ACPC. Only H-bonded hydrogens were displayed for clarity.

1.3 Foldamers of β-Peptide Mimetics

The same reasons seen above, mainly related to the search for new secondary structures and an improved biological activity/stability, which had previously led to the expansion of β-peptides field, have subsequently also led to the expansion of the field of their mimetics.

In α-aminoxy acids, the β carbon is replaced with an oxygen atom, and the tendency to give 8-membered cycles by intramolecular hydrogen bonds (N-O turns) is already evident in suitably derivatized monomers (Figure 10).[9]

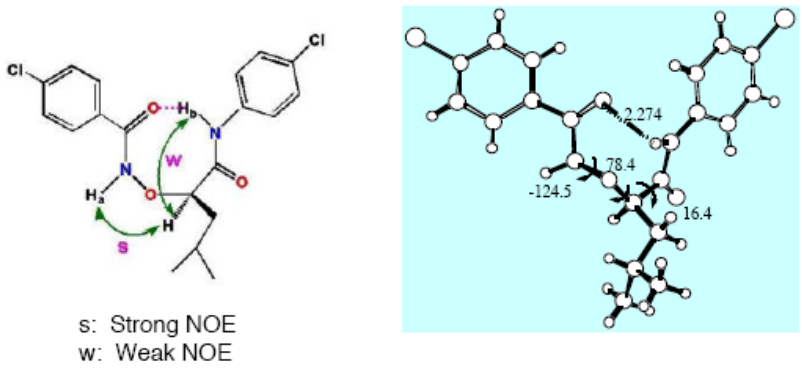

Figure 10. Structural determination of the N-O turns in α–aminoxy acid monomers (left: NOEs in solution; right: X-rays of the crystal structure).

The intramolecular hydrogen bonds formed by oligomers are very strong, as evidenced by the impressive chemical shift values of the protons involved, that is all the NHs except the one belonging to the first residue. Moreover, the striking overall stability of the resulting 8-helix structure is proven by the observations that all the intramolecularly H-bonded NHs are almost completely insensitive to unfolding processes caused by both intermolecular hydrogen bonding and competition of a strong H-bond-acceptor solvent, such as DMSO-d_6 (Figure 11).

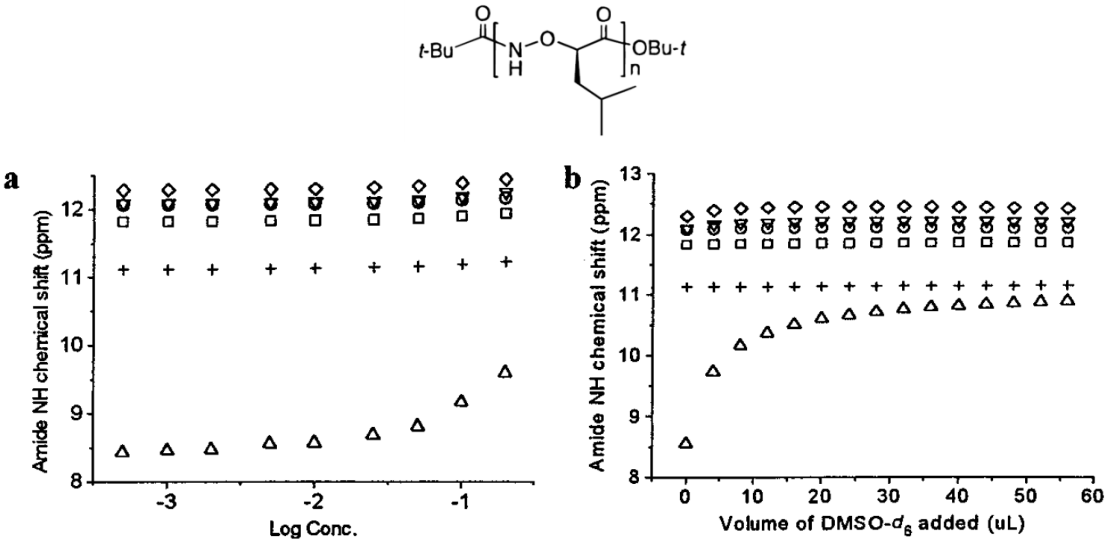

Figure 11. (a) δ of amide protons for the hexamer shown (n = 6) in $CDCl_3$ at 25 °C, as a function of logarithm of concentration. (b) δ of amide protons when increasing amounts of DMSO-d_6 were added to a 5 mM solution of the hexamer in 0.5 mL of $CDCl_3$ at 25 °C.

On the contrary, in the case of the 1st residue NH, which is the only one not involved in the formation of intramolecular hydrogen bonds, the expected substantial increase of δ due to either the H-bond-driven self-association or the formation of a strong hydrogen bond with DMSO-d_6 is readily evident. The most stable secondary structure deduced for those α-aminoxy-peptides, which was actually computed at the level HF/6-31G* on a simplified model tetramer (all the substituents are Me) with a C-terminal amide derivatization, is an 8-helix with a pitch very close to 2 residues, precisely a 1.8_8-helix, using the helix nomenclature.[6] In such a slightly twisted 2_8-helix, the sequence of N-O turns arranges the side chains alternate on opposite sides of the helix, in a β-strand-like fashion, with a pattern reminiscent of a twisted parallel β-sheet (Figure 12).

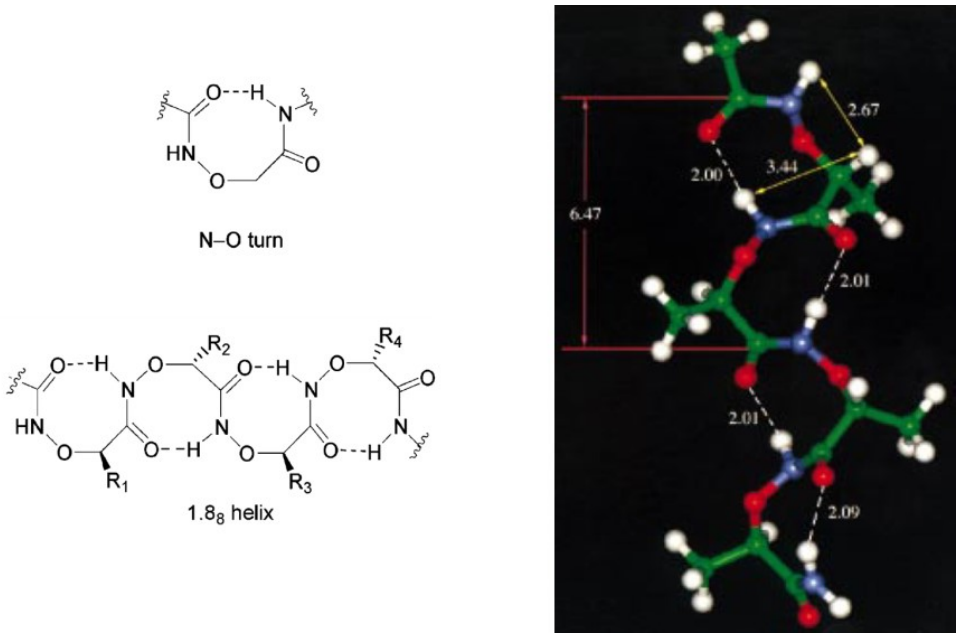

Figure 12. The 8-helix structure calculated at the HF/6-31G* level for R_i = Me.

Mimetics of β-peptides based on the insertion of a sp^3 nitrogen atom in the place of the Cβ atom, that is α-hydrazino-peptides, were also synthesized (Figure 13). Even though the secondary structures adopted in solution strongly vary depending on the particular substitution, and they are sometimes random coils, the presence of the basic and pyramidalized nitrogen atom led to the discovery of a peculiar folding, that is a new type of 8-helix.[10]

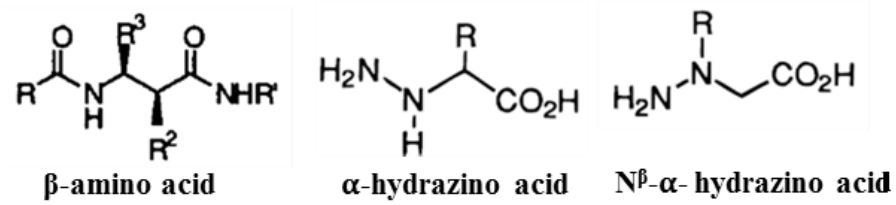

Figure 13. α-Hydrazino acids with Cα- and Nβ-substitutions.

In fact, at least in the crystalline state or in absence of acid and competing solvents, secondary structures consisting of a series of "hydrazino-turns" were obtained. Such structures show both the 8-helix H-bonding pattern, that is CO(*i-2*)-NH(*i*), and the additional N(*i-1*)-NH(*i*) H-bonds enclosed in the 8-membered cycles (Figure 14).

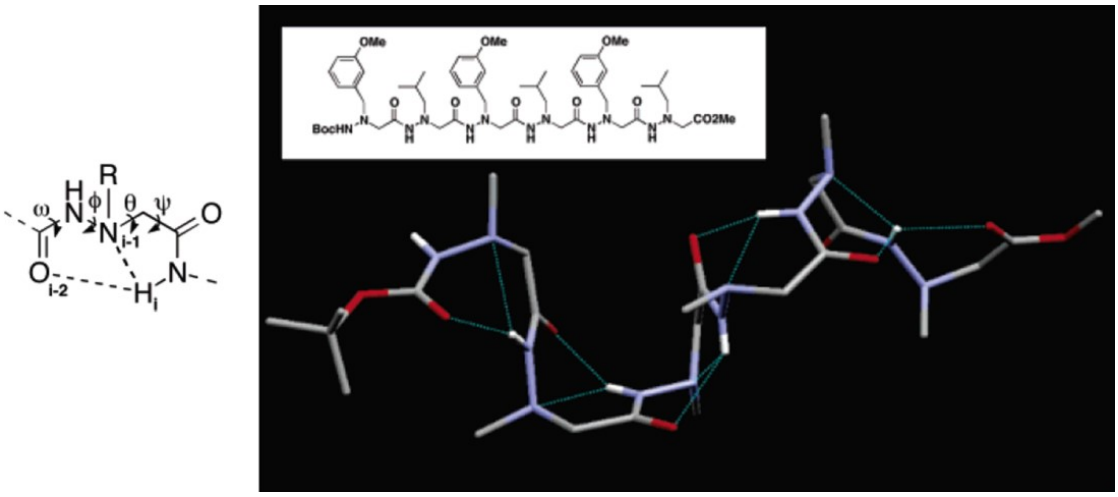

Figure 14. Left: general structure of a hydrazino-turn. Right: X-rays structure of the 8-helix composed of a hydrazino-turns series, obtained from the crystal of the hexamer shown (side chains and unnecessary hydrogens were omitted for clarity).

CHAPTER 2:

Imidazolidinone-based α-hydrazidopeptides

2. IMIDAZOLIDINONE-BASED α-HYDRAZIDOPEPTIDES

2.1 Introduction

As reported in the previous chapter, β-peptides are probably the most widely investigated peptide mimics and promising candidates for drug design, due to their protease resistance and their ability to adopt stable secondary structures with as few as six residues or less. In the framework of the synthesis of oligomers with a predictable folding, we have already reported the synthesis of hexamers based on conformationally constrained β-amino acids, in which the Cα and Cβ atoms are tethered in a pirrolidin-2-one ring (Figure 15).[11] NMR studies and molecular dynamics simulations showed the ability of *trans*-AOMPC ((3*R*,4*S*)-4-amino-5-oxo-1-((*S*)-1-(4-methoxyphenyl)ethyl)pyrrolidine-3-carboxylic acid) hexamer to fold into a 12-helix when R^1 = H,[11a] similarly to others cyclic β-peptides based on *trans* 2-aminocyclopentane or 2-aminopyrrolidine carboxylic acids.[8]

The systematic methylation of the Cα atoms along the backbone induced a gradual transition from the 12-helix to the 8-helix, due to the steric hindrance of the methyl groups and their effect on ψ dihedrals. In fact, when the third AOMPC residue was changed for AMOMPC (R^1 = Me, (3*R*,4*S*)-4-amino-3-methyl-5-oxo-1-((*S*)-1-(4-methoxyphenyl)ethyl)pyrrolidine-3-carboxylic acid), local 8-helix structures perturbed the predominant 12-helix in the most stable conformers, while when two AMOMPC were inserted as the second and fourth residues, only local 12-helices were present in the predominant 8-helix. Finally, the AMOMPC hexamer showed a stable 8-helix,[11b] which is a rare structure for β-peptides and has been so far observed only employing peculiar conformationally constrained monomers (Figure 15).[12,13]

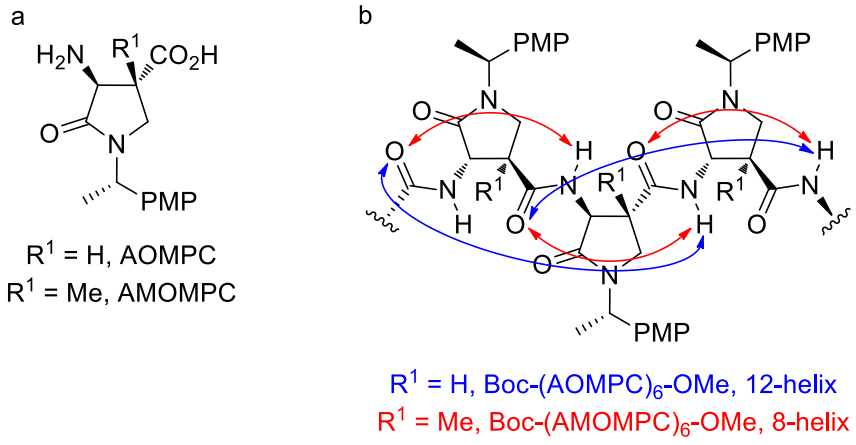

Figure 15. (a) Pyrrolidinone-based β-amino acids used as monomers in the previous works. (b) Secondary structures assumed by AOMPC and AMOMPC hexamers.

In an effort to expand the field of peptide mimics and explore more folding properties, the synthesis of new scaffolds is required. For instance, the replacement of the Cα and Cβ atoms of the β-amino acid residues by heteroatoms is an attractive design strategy. The substitution of the Cβ atom with nitrogen leads to hydrazino peptides, also called aza-β^3-peptides, composed of α-hydrazino acids. As a result, additional H-bonds via the basic sp^3 Nβ are possible, thus originating secondary structures made of 8-membered pseudocycles whit internal 5-membered cycles ("hydrazino turns") that cannot be formed by "normal" β-peptides.[10]

The overall effect can be so strong that a single residue prone to form such a structure can direct the switch from the natural 12-helix of *trans*-2-aminocyclobutanecarboxylic acid oligomers to the 8-helix, at least up to a length of 6 residues.[14]

2.2 Results and Discussion

2.2.1 Synthesis of New Imidazolidinone-based α-Hydrazidopeptides

In this contest, we designed a cyclic α-hydrazido acid by substituting the stereogenic Cβ atom on our previous β-amino acid monomer with nitrogen, switching from a pirrolidin-2-one-tethered β-amino acid (AOMPC) to an imidazolidin-2-one-tethered α-hydrazino acid, AOPIC ((*R*)-3-amino-2-oxo-1-((*S*)-1-phenylethyl)imidazolidine-4-carboxylic acid). It should be noted that, despite the structural resemblance with the α-hydrazino acids already reported in literature, in this case the Nβ atom should be much less basic, due to its delocalization onto the imidazolidinone carbonyl, thus AOPIC has to be considered more appropriately as a Nβ-acylated α-hydrazino acid, or a α-hydrazido acid (Figure 16).

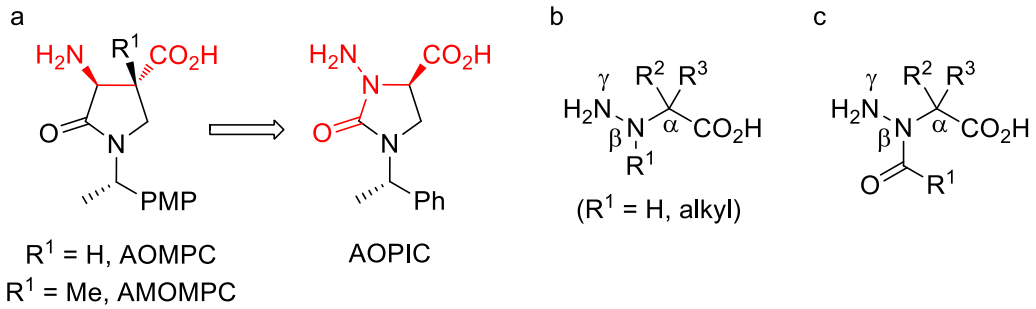

Figure 16. (a) Switch from pyrrolidinone-based monomers (AOMPC and AMOMPC) to the imidazolidinone-based monomers (AOPIC) by formal C-H → N substitution. The red color highlights the β-amino acid and α-hydrazido acid moieties in AOMPC and AOPIC, respectively. (b) A generic α-hydrazino acid, with a basic sp^3 Nβ atom. (c) A generic α-hydrazido acid, with a non-basic sp^2 Nβ atom.

We therefore synthesized conformationally constrained $\beta^{2,3}$-oligoazapeptides of different lengths, with the aim to investigate their folding patterns.

All the synthetic procedures reported here refers to previous works carried in our research group.[15] Anyway, in this thesis, all the methodologies were deeply reviewed and optimized, with the aim of obtaining the oligomers with high purity and better yields. Most importantly, a complete spectroscopic and computational investigation was performed in order to ascertain the preferred folding.

Methyl aziridine-2-carboxylate **1** was the readily available starting material[16] for the synthesis of Boc-AOPIC-OMe monomer used in the oligomers' synthesis. To introduce the hydrazine functionality, **1** was ring-opened by nucleophilic addition of *t*-butyl carbazate, catalysed by boron trifluoride etherate. This reaction proceeded with a complete conversion but low regioselectivity towards **2**, probably due to steric hindrance effects. Finally, the imidazolidinone ring in the monomer, Boc-AOPIC-OMe **3**, was created by a high-yielding cyclization of **2** with phosgene.

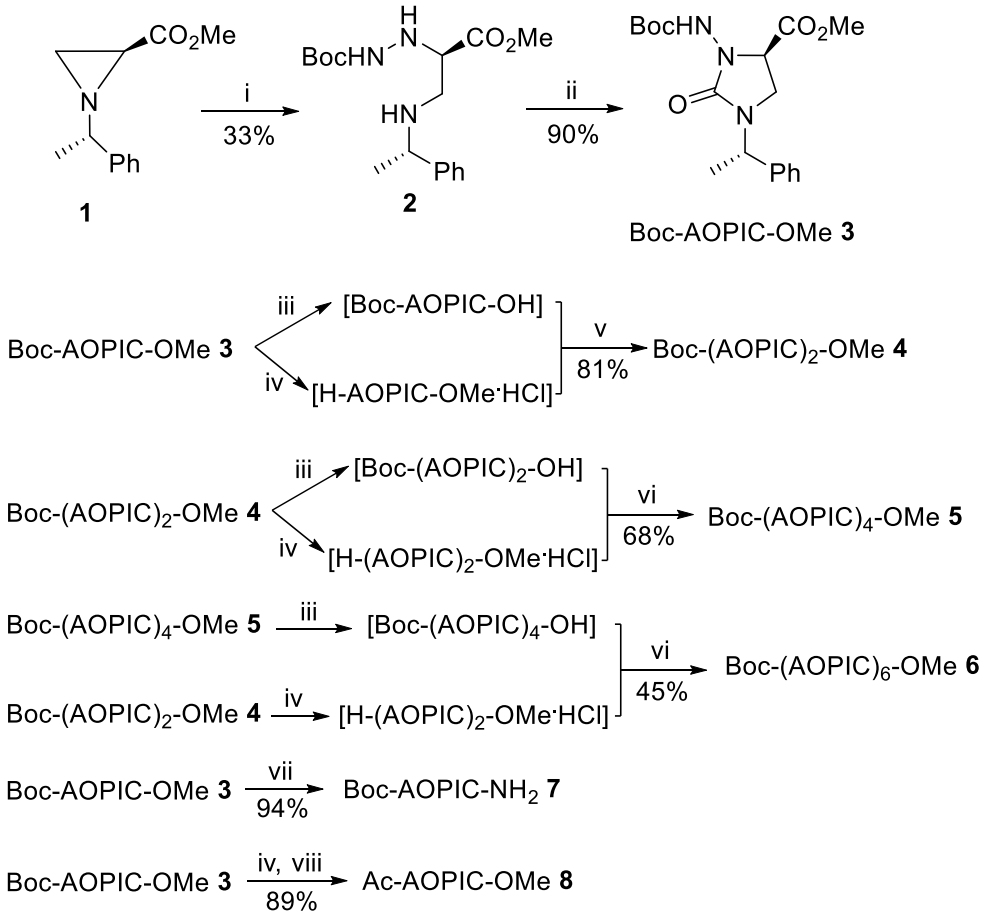

Scheme 1. Reagents and conditions: (i) *t*-butyl carbazate, $BF_3 \cdot Et_2O$, dry THF, reflux; (ii) $COCl_2$, aqueous saturated $NaHCO_3$, DCM, 0 °C; (iii) aqueous NaOH, MeOH, DCM; (iv) dry HCl in

MeOH, DCM, rt; (v) EDC, TEA, dry DCM, 0 °C; (vi) PyBroP, DIPEA, dry DCM, -18 °C to rt; (vii) NH_3/NH_4Cl, dry MeOH, rt; (viii) CH_3COCl, pyridine, dry DCM, rt; THF = tetrahydrofuran, DCM = dichloromethane, EDC = 1-ethyl-3-(3-dimethylaminopropyl)carbodiimmide hydrochloride, TEA = triethylamine, PyBroP = bromotripyrrolidinophosphonium hexafluorophosphate, DIPEA = diisopropylethylamine.

All the oligomers were synthesized exploiting the usual Boc removal/ester hydrolysis/peptide coupling sequence in liquid phase (Scheme 1), but the Boc-deprotected intermediates showed a somewhat unexpected behaviour. In fact, while they demonstrated a reduced nucleophilicity, in comparison to common amino acids, during the peptide couplings, they also gave traces of the corresponding Nγ-trifluoroacetylated products when submitted to Boc removal, using both commercial and redistilled trifluoroacetic acid. Thus, in order to obtain quantitatively the almost pure Boc-deprotected intermediates, suitable to be used in the following coupling without any purification, all the Boc removals were carried out using anhydrous HCl in MeOH/DCM mixtures. Moreover, the coupling reactions had to be carried out in quite concentrated solutions, using 1 mL or less of dichloromethane per mmol of N-deprotected intermediate, to achieve good (Boc-$(AOPIC)_2$-OMe **4**) or moderate yields (Boc-$(AOPIC)_4$-OMe **5** and Boc-$(AOPIC)_6$-OMe **6**) (Scheme 1). C-terminal amide monomer Boc-AOPIC-NH_2 **7** was synthesized to test the possible subsistence of an inherent tendency towards the formation of 8-membered H-bonded cycles, as evidenced by related α-aminoxy acids.[9]

Eventually, N-acetyl monomer Ac-AOPIC-OMe **8** was synthesized because its NH, which was further demonstrated to be intramolecularly non-H-bonded, should be the right reference for any hydrogen atoms belonging to peptide bonds in oligomers **4**, **5** and **6** that do not participate in hydrogen bonding. In the same way, the NH of Boc-AOPIC-OMe **3** should be the right reference to which compare the Boc-NHs belonging to monomer **7** and to the first residues of oligomers **4**-**6**.

2.2.1 Investigation by NMR and CD Spectra

Although the complete assignment of δ_{NH} resonances was possible only for monomers and oligomers up to tetramer **5**, due to broad peaks with an extended overlap in hexamer **6**, the simple analysis of their values in diluted solutions gave some important indications (Figure 17 and starting points in Figure 18 and Figure 19). In fact, the simple C-terminal amide monomer **7** showed a striking difference, about 2.7 ppm, between the intramolecularly bonded and unbonded amide hydrogens. This demonstrates the same inherent tendency to the formation of

8-membered H-bonded cycles reported for a monomeric C-terminal amide derivative of an α-aminoxy acid, that lead to 8-helix structures in oligomers.[9] Moreover, a similar difference between bonded and unbonded hydrogens was also observed for a closely related C-terminal amide α-hydrazino acid,[10c] which actually showed the proclivity to form an 8-membered pseudocycle with an enclosed additional 5-membered cycle, that is a hydrazino turn, in which the sp^3 basic hydrazinic nitrogen acts as an acceptor.

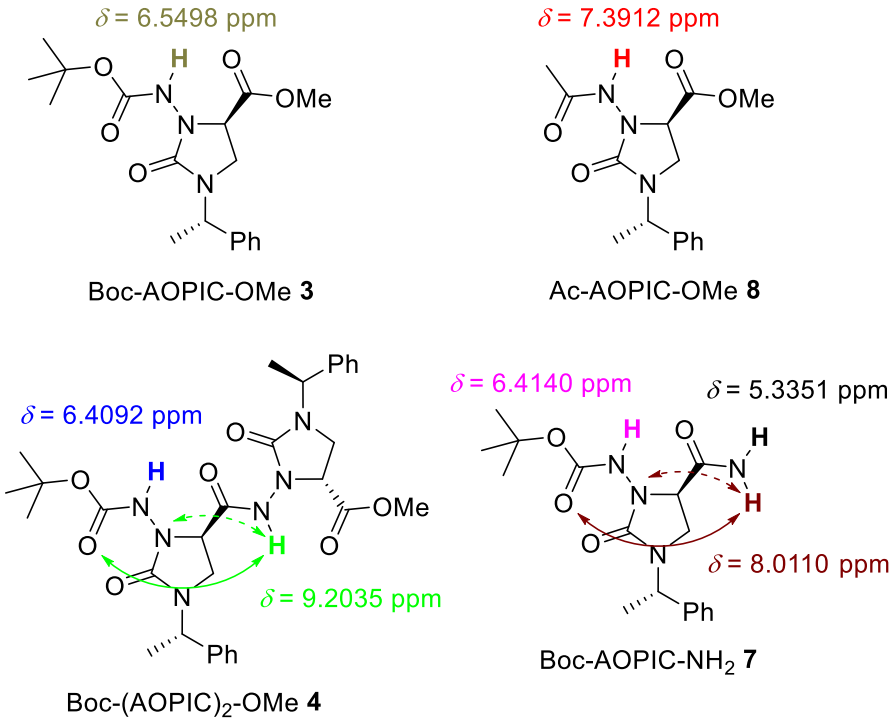

Figure 17. Chemical shifts for hydrazidic protons of Boc-AOPIC-OMe 3, Boc-(AOPIC)$_2$-OMe 4, Boc-AOPIC-NH$_2$ 7 and Ac-AOPIC-OMe 8 (1 mM solutions in dry $CDCl_3$ at 25 °C). The 8-membered H-bonded cycles are reported with continuous lines, the possible additional 5-membered cycles with dashed lines.

Taking into account oligomers **4-6**, the NH chemical shifts in diluted $CDCl_3$ solutions evidence the possibility for a reinforcing, cooperative effect as the length increases. Starting from 9.20 ppm for second residue of dimer **4**, the δ_{NHs} for the three intramolecularly H-bonded NHs become 9.11, 9.31 and 9.56 ppm for tetramer **5**, with values raising from the second to the fourth residue. The strengthening effect is even larger for hexamer **6**, with δ_{NH} = 9.24-9.62 ppm for the five H-bonding NHs (residues 2-6, values not assigned).

Moreover, in all compounds, hydrazidic Boc- or Ac-derivatized NHs belonging to the first residues are not involved even in weak intramolecular H-bonds, neither by a 6-membered cycle with the intraresidue carbonyl oxygen of the α-hydrazido acid moiety, nor by a 5-membered

cycle with the imidazolidinonic carbonyl. This can be easily inferred by the comparison of values obtained for all the first residue hydrazidic hydrogens in Figures 17-19, especially the N-acetyl derivative **8** (7.39 ppm), with the ones reported for the simple N,N′-dibenzoyl-hydrazide, whose 5-membered H-bonds lead to δ_{NH} = 9.23 ppm, or other symmetric and asymmetric benzohydrazides, where the intervention of additional (bifurcated) 6-membered H-bonds gives δ_{NH} up to 11.25 ppm.[17] This is very likely due to the possible repulsive interactions that could arise between the carbonyl oxygen onto Nγ and the imidazolidinonic urea moiety, or the substituted Cα, if the hydrazidic NH was H-bonded to the α-hydrazido acid carbonyl or the imidazolidinone carbonyl, respectively.

It should be noted at this point that such a H-bonding pattern, where the first residue NHs are always non-H-bonded and the number of intramolecular hydrogen-bonds is in any cases equal to the number of residues minus one, rules out from a logical point of view the most common structures obtained for the related β-peptides, the 12- and 14-helices,[1] as well as the uncommon 10/12-[7] and 10-helices.[18] In fact, from a logical point of view, in the case of a homogeneous secondary structure these first experimental observations point strongly towards the 8-helix folding, or its variant made of bifurcated H-bonds that form contemporaneously 8-terms cycles with enclosed 5-terms cycles (see the detailed discussion in Paragraph 2.5.1 Logical Analysis of Possible H-bonding Patterns for α-hydrazidopeptides).

Anyway, it was evident from NMR experiments with more concentrated solutions that, even in the case of the intramolecularly H-bonded NHs, a contribution originating from self-association was also present in all cases. Then, before proceeding with all the other structural investigations, it was necessary to safely determine if the intermolecular H-bonding was reasonably negligible at the concentrations used. In fact, in an effort devoted to the synthesis of self-assembling hydrazides, Zhao et al. obtained an equilibrium constant K_{inter} of 112 M^{-1} for a weak H-bond-driven intermolecular homodimerization, when just two reciprocal C=O···H-N interactions arranged in a β-sheet-like disposition were present between the molecules, but values up to 4.7×10^4 M^{-1} for quadruply H-bonding heterodimers.[19] Thus, due to the fact that, in line of principle, our compounds could behave as multiply hydrogen-bonding structures and dimerize, or even oligomerize, the tendency to the intermolecular H-bonding was quantitatively evaluated by dilution experiments in dry $CDCl_3$ on the reference monomer Ac-AOPIC-OMe **8** and the simplest oligomer, dimer Boc-$(AOPIC)_2$-OMe **4** (Figure 18). Anhydrous $CDCl_3$ was chosen to determine rigorously only the self-association, eliminating the effect of residual monomeric water, because a comparison with a 1 mM solution of **4** in wet deuterochloroform

furnished a negligible increase in chemical shift for the intramolecularly H-bonded NH belonging to the second residue (+0.01 ppm), but a quite pronounced increment for the BocNH (+0.06 ppm). The non-linear regression of the observed chemical shift (δ_{obs}) *vs* the total substrate concentration data for **8** allowed to obtain an intermolecular association constant K_{inter} = 4.7±0.6 M^{-1}, which is in agreement with just a weak tendency to the homodimerization by formation of intermolecular H-bonds (for a detailed discussion see Paragraph 2.5.2 Determination of Intermolecular H-bonding from Dilution Experiments).

In effect, this value is very small if compared to the ones reported by Zhao, while it is identical to the one obtained for *N*-methylacetamide in the less polar CCl_4, which becomes only 0.8 M^{-1} in the more polar CD_2Cl_2 (dielectric constants: carbon tetrachloride, 2.24; chloroform 4.81; methylene chloride, 8.93).[20,21] The computed percent molar fractions for the intermolecularly H-bonded homodimer of compound **8**, f_D, are 0.93%, 7.99% and 37.2% at a total substrate concentration of 1 mM, 10 mM, and 0.1 M, respectively (Table 6 in Paragraph 2.5.2 Determination of Intermolecular H-bonding from Dilution Experiments), indicating that, even for such a weak intermolecularly H-bonding substrate, the self-association becomes no more negligible if experiments are not carried out in very diluted solutions. Using the data for the first residue NH (Boc-NH) of Boc-$(AOPIC)_2$-OMe **4**, a larger intermolecular association constant K_{inter} of 8.1±0.6 M^{-1} was calculated, with percent molar fractions for the homodimer due to intermolecular H-bonding of Boc-NH, f_D, that raise to 1.57%, 12.4% and 46.5% at a total substrate concentration of 1 mM, 10 mM, and 0.1 M, respectively.

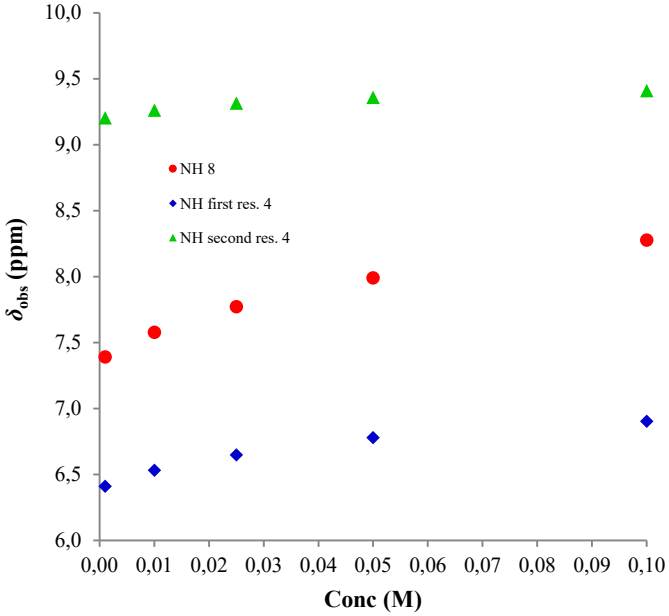

Figure 18. Variation of NH proton chemical shifts of reference monomer Ac-AOPIC-OMe 8 and dimer Boc-$(AOPIC)_2$-OMe 4 as a function of total substrate concentration from dilution experiments in dry $CDCl_3$ at 25 °C.

Using the same approach, but taking also into account the presence of the intramolecular H-bond for the second residue NH of compound **4**, the equilibrium constants for both the intermolecular and the intramolecular hydrogen-bonded species could not be computed exactly, because it is impossible to know precisely the limiting chemical shifts for the completely non-H-bonded (δ_M) and the completely intramolecularly H-bonded NH (δ_{intra}). Anyway, a limiting δ_D = 9.6017 ppm could be safely extrapolated for the completely intermolecularly H-bonded **4**, while the chemical shift of 7.3742 ppm obtained for the non-hydrogen-bonded reference compound **8**, where the NH is acylated as in the second residue of Boc-(AOPIC)$_2$-OMe **4**, can represent a good approximation for δ_M. Thus, we used the highest values available for intramolecularly hydrogen-bonded NHs in tetramer Boc-(AOPIC)$_4$-OMe **5** (9.5553 ppm) and hexamer Boc-(AOPIC)$_6$-OMe **6** (9.6148 ppm), in diluted solutions of anhydrous $CDCl_3$, as estimates for δ_{intra}, and then calculated approximate intramolecular and intermolecular association constants, K_{intra} and K_{inter}, of the second residue NH in Boc-(AOPIC)$_2$-OMe **4** (see detailed discussion in 2.5.2 Determination of Intermolecular H-bonding from Dilution Experiments). The plausible ranges for the equilibrium constants related to the NH belonging to the second residue of compound **4** were estimated as K_{intra} = 4.3-5.0 and K_{inter} = 18-21 M^{-1}, thus indicating a quite strong tendency to the intramolecular hydrogen-bonding, even in a simple dimer without the possibility for a cooperative effect, and again a weak, but not negligible, propensity to the intermolecular self-association, at least in a non-hydrogen-bonding solvent. In fact, in this case the percent molar fractions for the homodimer are 2.24%, 16.4% and 52.6% at a total substrate concentration of 1 mM, 10 mM, and 0.1 M, respectively, then we preferred to carry out all the subsequent NMR and CD analysis at concentrations lesser than 2 mM, with the exception of bidimensional NMR spectra, without extending the analysis of the competition between intra- and intermolecular H-bonding to longer oligomers.

The titration with DMSO-*d*$_6$, which is a strong H-bond acceptor, of diluted solutions of reference monomer Ac-AOPIC-OMe **8**, dimer Boc-(AOPIC)$_2$-OMe **4**, tetramer Boc-(AOPIC)$_4$-OMe **5** and hexamer Boc-(AOPIC)$_6$-OMe **6** in $CDCl_3$, is coherent with a progressive unfolding as the percentage of DMSO-*d*$_6$ added increases. However, although the limiting values in only DMSO-*d*$_6$, which are always in the range 9.98-10.25 ppm for all the hydrazide NHs and 8.84-8.86 ppm for the carbazate Boc-NHs, are indicative of a probably complete disruption of the folding observed in chloroform, the ability to resist to unfolding is strikingly different among oligomers **4-6** (Figure 19 and Tables 3-6 in Paragraph 2.5.3 Titrations with DMSO-d6.).

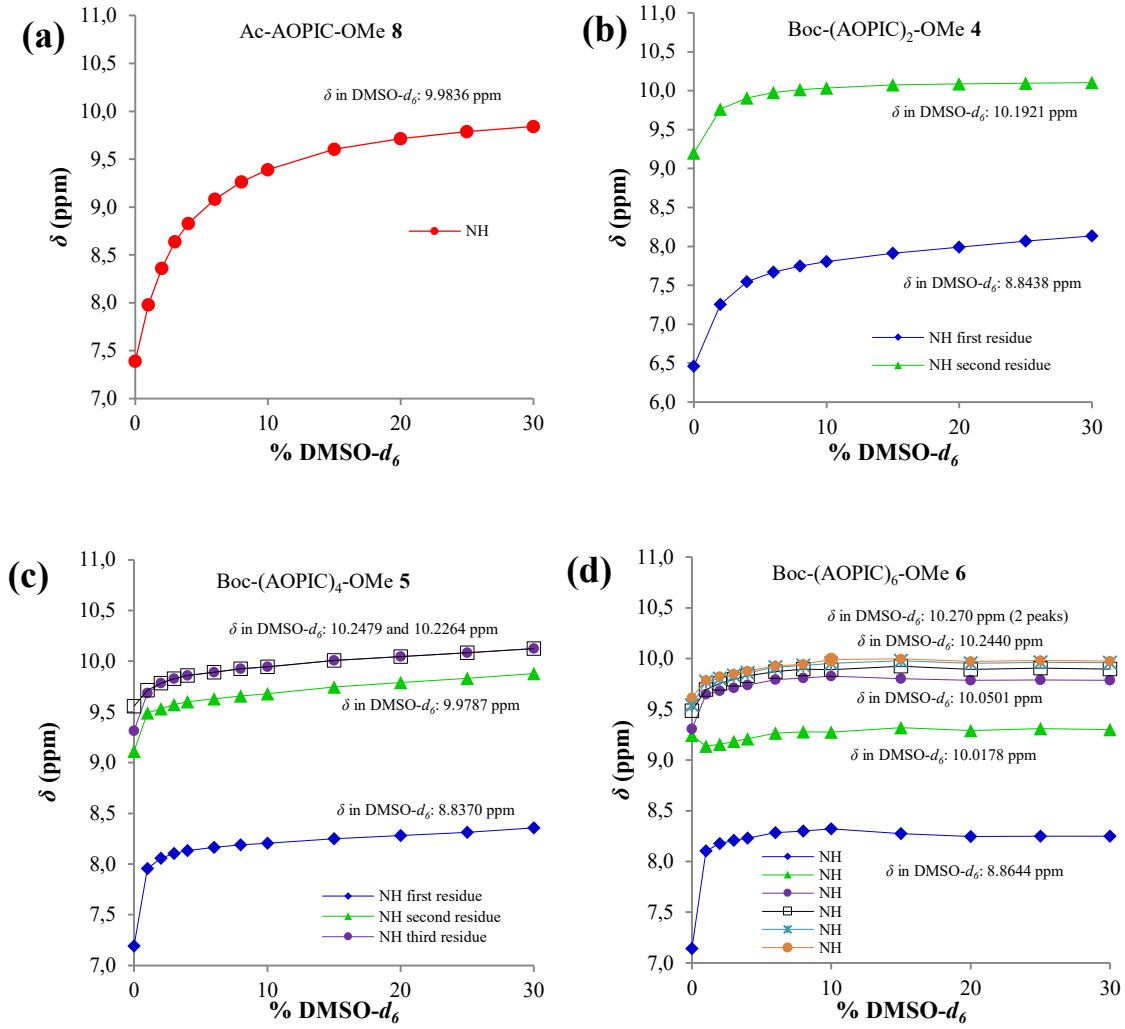

Figure 19. Variation of NH proton chemical shifts (ppm) of (a) reference monomer Ac-AOPIC-OMe 8, (b) dimer Boc-(AOPIC)$_2$-OMe 4, (c) tetramer Boc-(AOPIC)$_4$-OMe 5 and (d) hexamer Boc-(AOPIC)$_6$-OMe 6 as a function of increasing percentages of DMSO-d_6 added (v/v) to 1 mM (4 and 8) or 2 mM solutions (5 and 6) in $CDCl_3$ at 25 °C.

As it can be easily deduced by inspection of Figure 19b, the unfolding process of dimer is already almost complete at 10% added DMSO-d_6. In fact, for the NH of second residue in dimer Boc-(AOPIC)$_2$-OMe **4**, the observed chemical shift at 10% DMSO-d_6, $\delta_{10\%\text{DMSO-}d6}$ = 10.04 ppm, is very close to the value observed in only DMSO-d_6, $\delta_{\text{DMSO-}d6}$ = 10.19 ppm, the difference being only 0.15 ppm. The same difference become 0.30, 0.28 and 0.30 ppm for the second, third and fourth residues NHs, respectively, of tetramer Boc-(AOPIC)$_4$-OMe **5**, indicating an increased resistance to unfolding, which is apparent even by the monotonic increase of chemical shifts up to 30% added DMSO-d_6 (Figure 19c). The behaviour of hexamer **6** deserves a careful analysis because, even if δ values are almost constant for percentages of added DMSO-d_6 between 10% and 30% (Figure 19d), they are not indicative of a complete unfolding. This can

be inferred by the differences between $\delta_{10\%DMSO\text{-}d6}$ and $\delta_{DMSO\text{-}d6}$ values, which range from 0.22 to 0.74 ppm (Table 9), indicating that the secondary structure maintains some stability at least up to a 30% added DMSO-d_6, and that the complete unfolding must occur at higher percentages.

The reduced temperature coefficient of chemical shift, Δδ/ΔT, is a parameter commonly used in the conformational analysis of proteins in solution,[22] although its predictive use as an H-bond indicator gave many times poor or unreliable results.[23] Anyway, for many oligopeptides and their mimics, Δδ/ΔT values more negative than -2.6 ppb/K have been associated to a dynamic equilibration between an H-bonded and a non-H-bonded structure.[24] Conversely, smaller values have been generally interpreted as a completely H-bonded or a completely non-H-bonded NH, even if simple diamides have shown that small values can also derive from a complex balance among the many factors affecting the difference in stability between intramolecularly bonded and unbonded NHs.[21]

In the present case, the BocNHs of dimer **4** and tetramer **5** and the AcNH of monomer **8**, which have been previously proven to be intramolecularly non-H-bonded, show Δδ/ΔT values of -1.1, -2.1 and -2.0 ppb/K, respectively (Figure 20). On the contrary, the second residue NH of dimer **4** has a Δδ/ΔT = -4.0 ppb/K, and the second, third and fourth residue NHs of tetramer **5** have, respectively, values of -3.8, -4.7 and -4.9 ppb/K, which reflect the cooperativity of H-bonds and their order of strength revealed by chemical shifts.

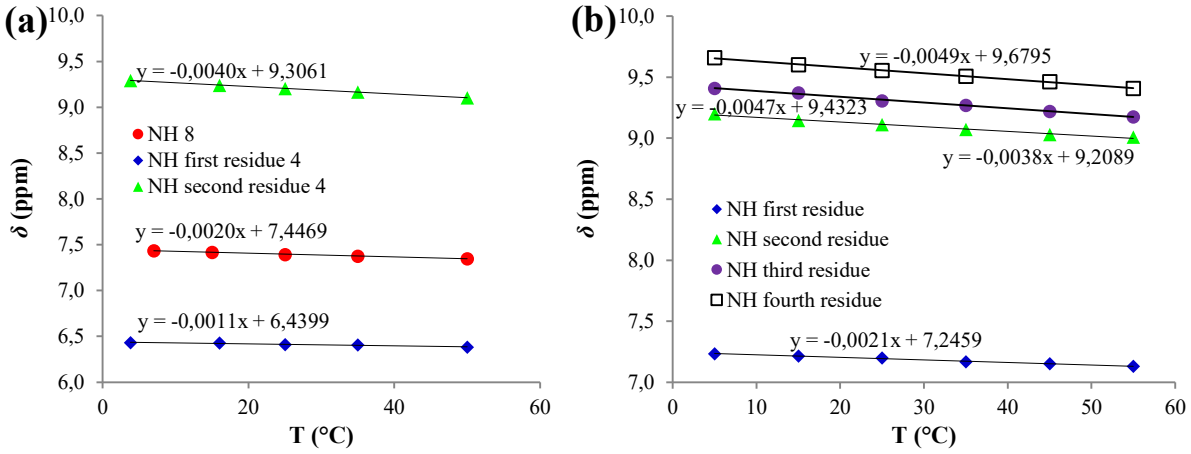

Figure 20. Variation of NH proton chemical shifts as a function of temperature. (a) Ac-AOPIC-OMe, 8 and Boc-(AOPIC)$_2$-OMe, 4 (1 mM solutions in dry $CDCl_3$). (b) Boc-(AOPIC)$_4$-OMe, 5 (2 mM solution in dry $CDCl_3$).

A further indication about the existence of a H-bonded-driven secondary structure and the possibility for a reinforcing cooperative effect due to elongation was obtained from analysis of CD spectra (Figure 21). Oligomers **4-6** were dissolved in methanol at concentrations where

self-association was previously demonstrated to be negligible by NMR, even in a much less hydrogen-donating/accepting solvent ($CDCl_3$). We did not undertake a comparison between experimental and theoretically computed spectra, although CD spectra were sometimes successfully used to determine the preferred conformation, or the equilibration between different folding patterns.[25] In fact, it was demonstrated that it can sometimes be difficult, or at least misleading, to derive the secondary structure from CD spectra, even in the case of much more extensively studied foldamers, such as the β-peptidic ones.[26]

The per-residue molar ellipticity of monomer Boc-AOPIC-OMe **5** differs not only quantitatively, but also qualitatively, from the ones of oligomers, in that the intensity increases up to 195 nm, with the exception of a secondary maximum at 220 nm, while for the oligomers there is a main peak at 202 nm (Figure 6). The CD spectra of dimer **4**, tetramer **5** and hexamer **6** are similar to the ones of the robust 8-helix structures formed by related α-aminoxy acids,[27] although they also resemble the one of a disordered hexapeptide made of Nβ-benzylated-α-hydrazino acids,[10a] both in the peak at about 200 nm and in the lack of a significant Cotton effect. It is noteworthy that, contrarily to this latter case, where the corresponding trimer had a different maximum and an increased intensity compared to the hexamer, in the present case there is no change in λ_{max} passing from the dimer to the hexamer, while there is an evident increase in per-residue molar ellipticity as the length increases. Moreover, the unfolded structure of those benzylated α-hydrazino peptides was mainly deduced on the basis of the missing Cotton effect, but this was demonstrated to be not always true. In fact, despite the evident Cotton effect in the typical CD spectra of 14-helices formed by many β-peptides,[28] the same feature is not present in the highly stable 14-helix formed by *trans*-2-aminocyclohexanecarboxylic acid (ACHC) oligomers,[29] and it is also absent in the case of the 10/12-helix exhibited by β^2/β^3-oligopeptides with an alternating substitution pattern.[7a]

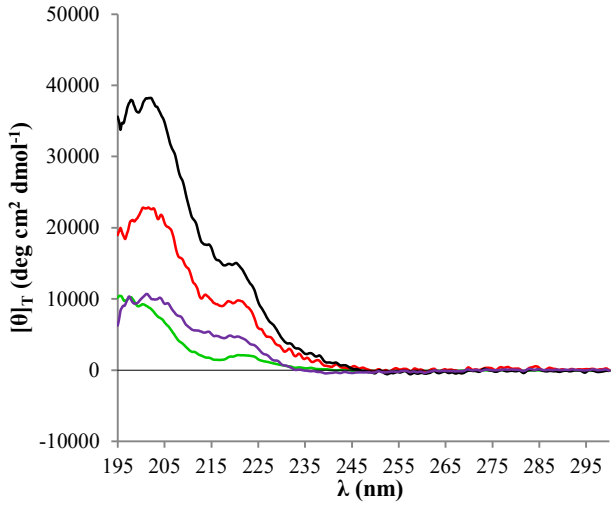

Figure 21. CD spectra of 1 mM Boc-AOPIC-OMe 3 (green line), 1 mM Boc-(AOPIC)$_2$-OMe 4 (purple line), 0.1 mM Boc-(AOPIC)$_4$-OMe 5 (red line) and 0.1 mM Boc-(AOPIC)$_6$-OMe 6 (black line) solutions in MeOH at 25 °C. Data normalized for concentration and number of residues.

The analysis of CD spectra in methanol, which is a much stronger H-bond donor/acceptor in comparison to chloroform, makes the gain in stability of the ordered secondary structure as the length increases even more evident than it could be derived from NMR spectra. In fact, it is obvious from the appearance of the maximum at 202 nm that dimer **4** is already partly folded, while the continuous increase in intensity passing from dimer to hexamer shows that the proportion of ordered conformation enlarges simultaneously with the elongation, thus proving the cooperativity in the folding stabilization.

2.2.2 Computational Investigation

Our experimental findings were plenty confirmed by an extensive molecular dynamics simulation on the hexamer, followed by cluster analysis and hydrogen bond lifetimes analysis.

This computational approach gave also additional information and shed some light on the preference between the two variant of the preferred structure, namely the "pure" 8-helix and its counterpart where there is an additional 5-terms cycle inside every 8-membered cycle, that is to say a sequence of the so-called hydrazino turns (note: in this case they are actually hydrazido turns).

MD simulations were carried out with the AMBER 11.0 suite of programs.[30] The peptide is parametrized using GAFF (general AMBER force field) force field.[31] The standard RESP procedure is carried out to assign charges to atoms by Antechamber.[32] The peptide was built and immersed in a solvent box of explicit chloroform molecules, reproducing the conditions in

which NMR spectra were registered. Periodic boundary conditions were used (see Paragraph 2.5.4 Computational for more details)

The molecular dynamics simulation for 100 ns highlighted the existence of an 8-helix-type folding as the sole stable secondary structure, as it is readily apparent from the results of the principal component analysis (PCA) (Figure 22).[33] The right-handed helix has a pitch of ≈6.3 Å and 1.9 residues per turn then, using the more complete helix nomenclature, it can be named as a (*P*)-1.9$_8$-helix. Moreover, the same results indicate that the preferred folding is very stiff, whit backbone dihedral angles poorly dispersed around the mean values and the phenylethyl chains always alternatively directed towards opposite sides with respect to the helix axis, in a β-strand-like fashion (Figure 22).

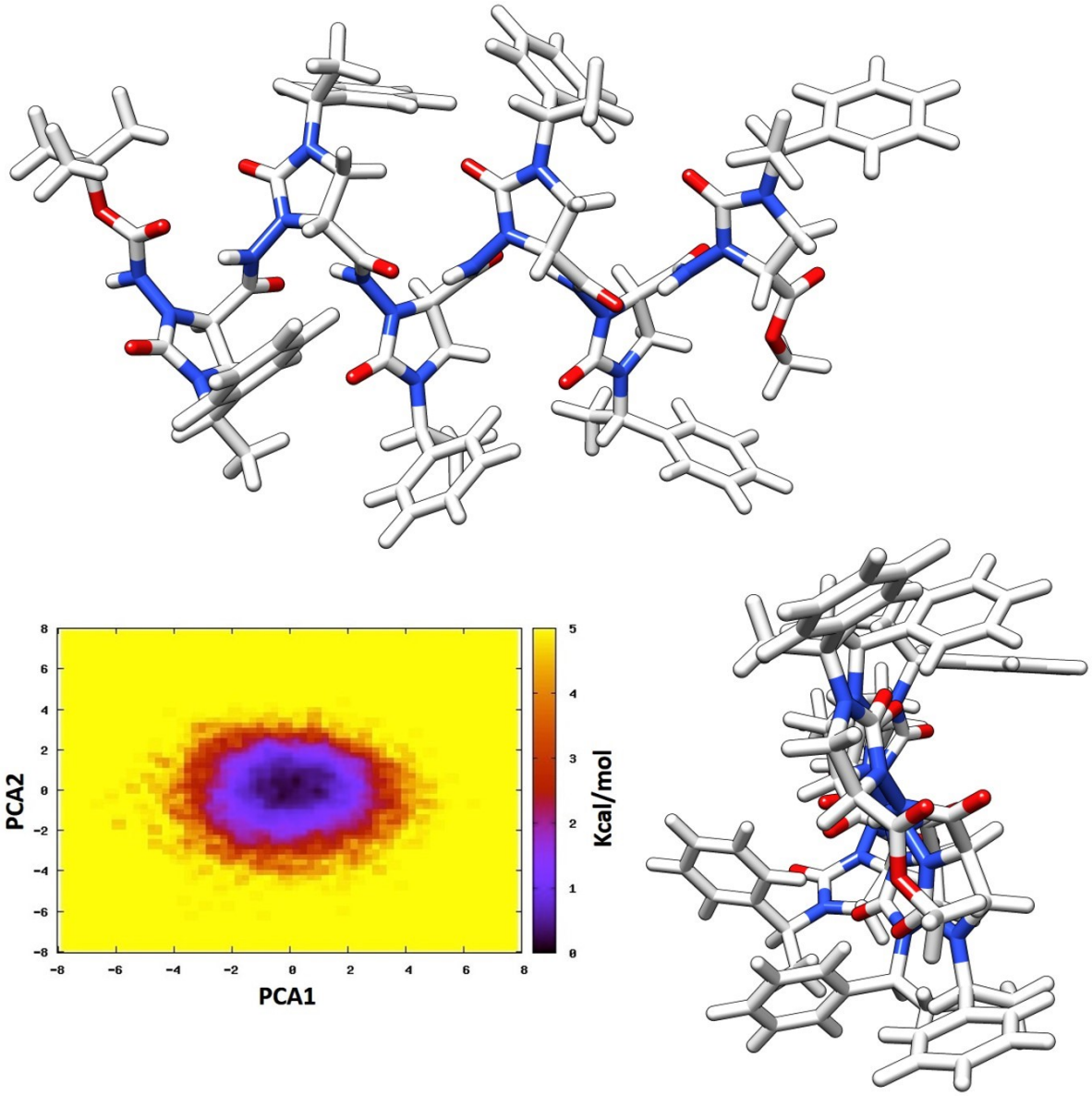

Figure 22. Results of conformational analysis of Boc-(AOPIC)$_6$-OMe 6. Representative views of the absolute minimum and two-dimensional free-energy landscape (the values are in kcal/mol).

PCA1 and PCA2 are the two eigenvectors with the lowest eigenvalues of the principal component analysis calculated from the analysis of the MD trajectory.

A deeper insight is necessary to establish, at least from a computational point of view, the preference between the "pure" and the "hydrazido-turn-series" variants of 8-helix, which relies on subtle geometric difference. As depicted in Figure 23 for the global minimum structure, the hydrazidic nitrogen atoms in the imidazolidinone rings are slightly pyramidalized and participate to 5-membered H-bonded cycles. Their arrangement is similar to the one reported for many non-conformationally constrained α-hydrazino-peptides,[10] and even closer to the one evidenced for an Nβ-acylated aza-β^3-cyclohexapeptide.[10f]

The H-bonds lifetime analysis furnished other important indications. In fact, in the system taken in consideration (room temperature and chloroform as the solvent), the great contribution from the C=O(i)•••H-N(i+2) and the Nβ(i)•••H-N(i+1) is strikingly evident, these H-bonds being occupied for 98.4-99.9% of the time (Figure 23). This also means that the computational results strongly corroborate the experimental deduction of an almost completely H-bonded folding of hexamer in chloroform at room temperature.

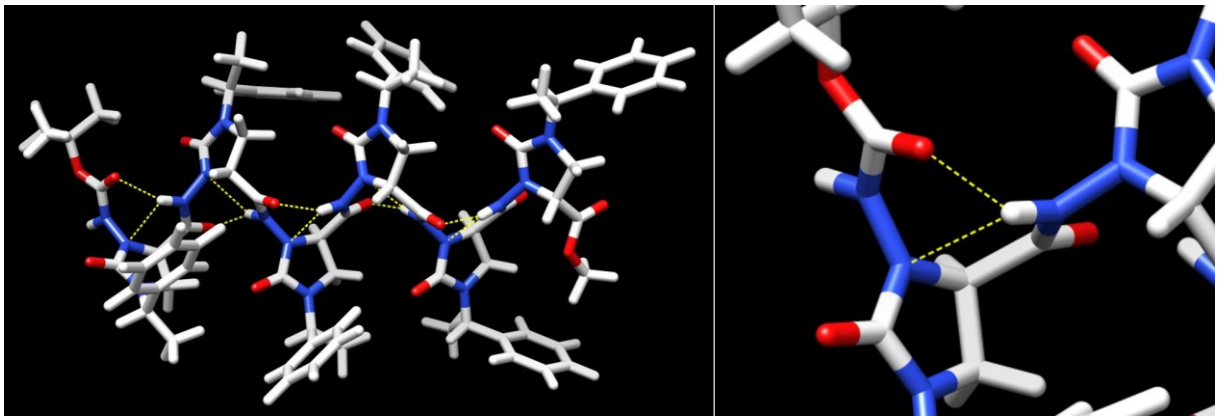

HBOND SUMMARY:

Distance cutoff is 3.60 angstroms, angle cutoff is 120.00 degrees
Hydrogen bond information dumped for occupancies > 2.00

DONOR		ACCEPTORH		ACCEPTOR				
atom#	:res@atom	atom#	:res@atom	atom#	:res@atom	%occupied	distance	angle
131	:1@O10	192	:1@H84	171	:1@N17	99.86	2.881 (0.12)	19.92 (10.88)
71	:1@O6	132	:1@H58	111	:1@N11	99.56	2.858 (0.11)	24.54 (12.17)
41	:1@O4	102	:1@H45	81	:1@N8	99.35	2.861 (0.12)	26.31 (12.21)
101	:1@O8	162	:1@H71	141	:1@N14	99.07	2.854 (0.11)	25.14 (12.40)
2	:1@O1	72	:1@H32	51	:1@N5	98.36	2.909 (0.14)	29.78 (12.59)
82	:1@O7	32	:1@H10	19	:1@C7	45.65	3.414 (0.13)	28.17 (14.46)
112	:1@O9	62	:1@H23	49	:1@C19	41.68	3.419 (0.13)	28.48 (14.73)
142	:1@O11	92	:1@H36	79	:1@C31	40.95	3.432 (0.12)	25.87 (14.06)
172	:1@O13	122	:1@H49	109	:1@C43	37.94	3.425 (0.12)	29.19 (14.50)
52	:1@O5	16	:1@H9	7	:1@C5	5.97	3.411 (0.12)	47.91 (9.84)
52	:1@O5	15	:1@H8	7	:1@C5	5.78	3.399 (0.13)	48.89 (9.15)
52	:1@O5	14	:1@H7	7	:1@C5	5.41	3.417 (0.12)	48.47 (9.91)
52	:1@O5	13	:1@H6	6	:1@C4	2.39	3.420 (0.11)	49.10 (8.71)
52	:1@O5	12	:1@H5	6	:1@C4	2.37	3.404 (0.13)	48.01 (10.47)
52	:1@O5	11	:1@H4	6	:1@C4	2.06	3.412 (0.13)	48.10 (10.70)

Figure 23. Conventional H-bonds (heteroatom•••H-N) characterizing the hydrazido-turn series in Boc-(AOPIC)$_6$-OMe 6, depicted in the global minimum structure. The inset is a close view of the H-bonded cycles formed by the NH of the second residue.

Moreover, an additional stabilization comes from unconventional (non-standard) H-bonds (Figure 24). Among all the contributions, the four C=O•••H-C bonds between imidazolidinone carbonyl of residue i and phenyl *orto*-hydrogen of residue i-2 are, by far, the most energetically important and are occupied for a substantial percent of time. Eventually, a minor contribution comes also from the C=O•••H-C bonds between the second residue imidazolidinone carbonyl and the *t*-butyl hydrogens of the N-terminal Boc protecting group.

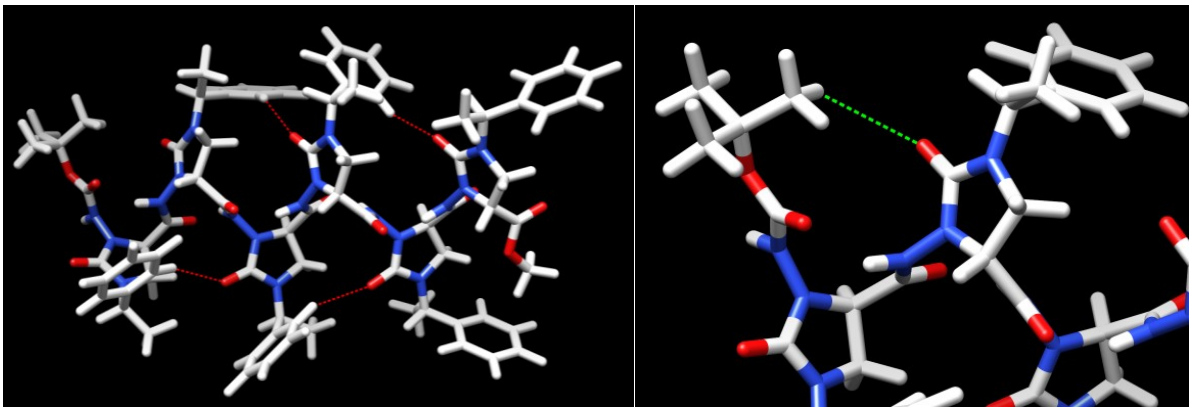

HBOND SUMMARY:

Distance cutoff is 3.60 angstroms, angle cutoff is 120.00 degrees
Hydrogen bond information dumped for occupancies > 2.00

DONOR		ACCEPTORH		ACCEPTOR				
atom#	:res@atom	atom#	:res@atom	atom#	:res@atom	%occupied	distance	angle
131	:1@O10	192	:1@H84	171	:1@N17	99.86	2.881 (0.12)	19.92 (10.88)
71	:1@O6	132	:1@H58	111	:1@N11	99.56	2.858 (0.11)	24.54 (12.17)
41	:1@O4	102	:1@H45	81	:1@N8	99.35	2.861 (0.12)	26.31 (12.21)
101	:1@O8	162	:1@H71	141	:1@N14	99.07	2.854 (0.11)	25.14 (12.40)
2	:1@O1	72	:1@H32	51	:1@N5	98.36	2.909 (0.14)	29.78 (12.59)
82	:1@O7	32	:1@H10	19	:1@C7	45.65	3.414 (0.13)	28.17 (14.46)
112	:1@O9	62	:1@H23	49	:1@C19	41.68	3.419 (0.13)	28.48 (14.73)
142	:1@O11	92	:1@H36	79	:1@C31	40.95	3.432 (0.12)	25.87 (14.06)
172	:1@O13	122	:1@H49	109	:1@C43	37.94	3.425 (0.12)	29.19 (14.50)
52	:1@O5	16	:1@H9	7	:1@C5	5.97	3.411 (0.12)	47.91 (9.84)
52	:1@O5	15	:1@H8	7	:1@C5	5.78	3.399 (0.13)	48.89 (9.15)
52	:1@O5	14	:1@H7	7	:1@C5	5.41	3.417 (0.12)	48.47 (9.91)
52	:1@O5	13	:1@H6	6	:1@C4	2.39	3.420 (0.11)	49.10 (8.71)
52	:1@O5	12	:1@H5	6	:1@C4	2.37	3.404 (0.13)	48.01 (10.47)
52	:1@O5	11	:1@H4	6	:1@C4	2.06	3.412 (0.13)	48.10 (10.70)

Figure 24. Unconventional H-bonds (C=O•••H-C) in Boc-(AOPIC)$_6$-OMe 6, depicted in the global minimum structure. In red: C=O•••H-C bonds between imidazolidinone carbonyls and phenyl *orto*-hydrogens. In green: C=O•••H-C bonds between imidazolidinone carbonyl of second residue and *t*-butyl hydrogens.

At this point,some peculiar features of the preferred folding should be emphasized. First, as it is evident from the inspection of Figure 22-Figure 24, due to the directionalities of H-bond donors and acceptors, the hydrogen-bonding functionalities are solvent-exposed and they also appear to be available for bimolecular interactions leading to self-association. This could partly explain, at least in a qualitative way, the fact that even in presence of strong intramolecular hydrogen bonds (evidenced for all the oligomers), some tendency to both bimolecular association and competition by DMSO was experimentally ascertained by NMR analysis (see Paragraph 2.2.1 Investigation by NMR and CD Spectra). Moreover, both these proclivities were almost completely absent in the structurally related 8-helix-forming pyrrolidinone-based β-hexapeptide already synthesized in our laboratory, Boc-(AMOMPC)$_6$-OMe (see Paragraph

2.1 Introduction).[11b] Anyway, obviously hydrogen bonds non-shielded from the solvent, or from bimolecular association, are not *per s*e sufficient to explain the above reported experimental findings, which must be related to some energetic factor leading to a little destabilization in comparison to the very stable and stiff 8-helix of pyrrolidinone-based β-peptide parent compounds. Unfortunately, at the moment no compelling hypothesis can be made about the reason(s) of the observed behaviour, but these explanations are beyond the scope of this thesis and will be the topic of a future study. Anyway, on the basis of the impressive amount of studies available on foldamers, a general observation can at least be made.

In fact, among the many factors that can affect the stability of an oligomer, the most important was demonstrated to be by far the preorganization of the monomers, that is the inherent tendency to arrange firmly the H-bonding functionalities in the proper positions and with the correct directionalities.[1] Thus, the little instability in comparison with the 8-helix formed by our previously reported β-peptide hexamer, Boc-(AMOMPC)$_6$-OMe, which was based on a pyrrolidinone-tethered monomer, could be tentatively ascribed to a generic "less than optimal" preorganization of the imidazolidinone-tethered α-hydrazido acids, which would lead to some tensions during the formation of H-bonds.

In this regard, another interesting feature of the computed 8-helix folding of the hexamer Boc-(AOPIC)$_6$-OMe deserve some comments. Using the more precise conformer-based nomenclature of Perczel,[6] the close inspection of the 8-helices reported in literature for β-peptides reveals that the most part of the 8-helices obtained so far, based on *trans*-β-amino acids tethered on peculiar cycles,[11b,12b-d,14] exists in the helical (H8) conformation (Figure 25). The only exception are the 8-helices show by oligopeptides derived from the achiral 1-(aminomethyl)cyclopropanecarboxylic acid[12a] and the *cis*-aminocyclobutane-1-carboxylic acid (ACBA), the latter being actually able to form both the zigzag structures Z8, leading to the 8-helix, and Z6, leading to another β-strand-like secondary structure (Figure 25).[12e]

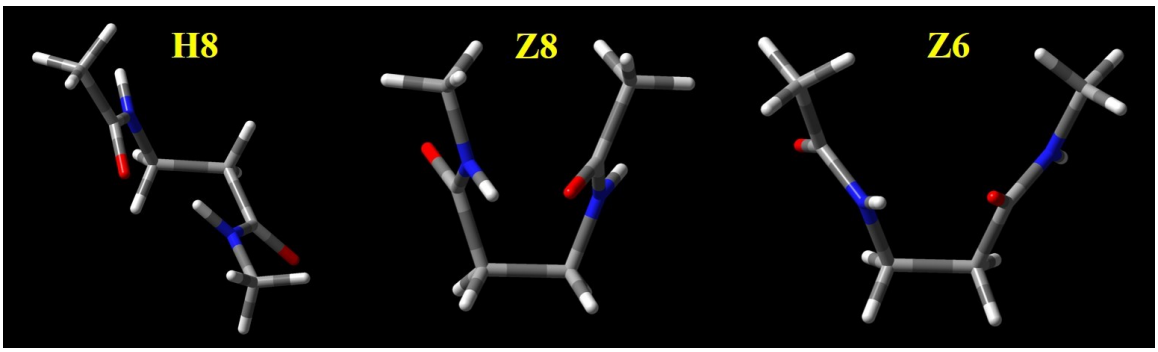

Figure 25. Conformer-based description of the two types of arrangements leading to an 8-helix folding (H8 and Z8) and another arrangement (Z6) leading to a strand-like structure, reported for a generic β-amino acid diamide.

On the contrary, considering the 8-helices formed by α-aminoxy-peptides[9] and properly derivatized α-hydrazino-peptides,[10b] it is easy to deduce that, even if they are not in a "perfect" Z8 conformation, their folding is much more similar to a zigzag disposition than to an helical (H8) one. Moreover, the average backbone torsional angles for the computed Z8-like minimum energy conformation of α-aminoxy-tetramer[9] reported in Figure 26 (ϕ = -125°, θ = 80°, ψ = 25°), and for the crystal structure of α-hydrazino-pentamer in Figure 27 (ϕ = -120°, θ = 75°, ψ = 15°),[10b] are the only ones quite close to the values of backbone dihedrals computed for the global minimum of our hexamer Boc-(AOPIC)$_6$-OMe, **6** (Table 1). The close inspection of global minimum structure for hexamer Boc-(AOPIC)$_6$-OMe and α-hydrazino acid pentamer crystal structure highlights also the expected differences in H-bonds lengths and in pyramidalizations of nitrogen atoms participating to the 5-membered cycles, which are both due to the reduced basicity of sp^2 nitrogens in hydrazido-turns, compared to sp^3 nitrogens in hydrazino-turns. In fact, while for α-hydrazino-pentamer the C=O•••H-N (2.03-2.44 Å) and the Nβ•••H-N (2.18-2.39 Å) distances are in all cases quite close, for Boc-(AOPIC)$_6$-OMe the computed C=O•••H-N lengths (1.89-2.00 Å) are always much shorter than the Nβ•••H-N ones (2.38-2.43 Å). Furthermore, the analysis of improper dihedrals angles confirms that all Nγ atoms are strongly out-of-plane (54-62°) when they are attached to sp^3 Nβ atoms in α-hydrazino-pentamer, but they are in a quasi-planar arrangement (5-16° out-of-plane bending) when they are bonded to sp^2 Nβ atoms in Boc-(AOPIC)$_6$-OMe. These observations confirm that the overall contribution of the additional 5-membered cycles to the hydrazido-turn stability is much lesser than the same contribution in the case of hydrazino-turns.

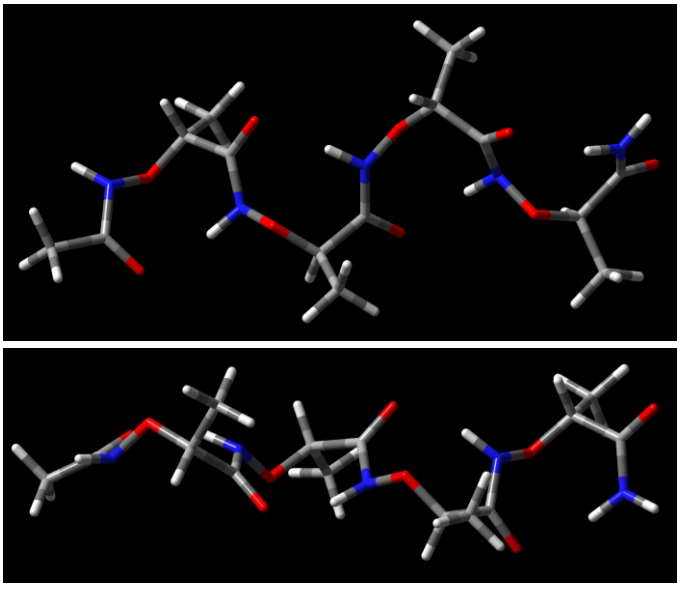

Figure 26. Minimum energy conformer computed at HF/6-31G* level for an α-aminoxy acid tetramer (taken from Ref. 9).

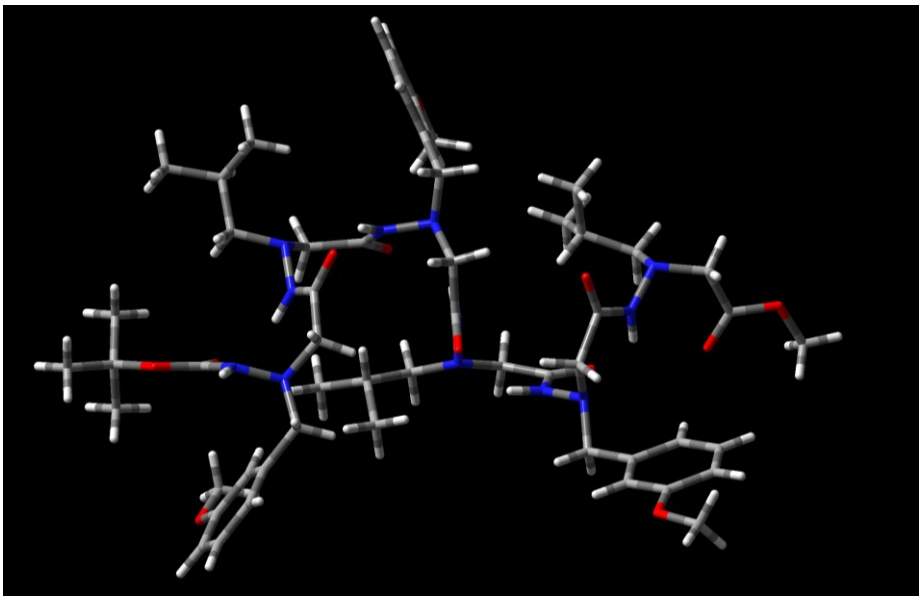

Figure 27. X-ray crystal structure of an α-hydrazino acid pentamer (taken from Ref. 10b).

Thus, as reported above, there are completely different backbone conformations that can lead to 8-helices, even if they have always the same strand-like global structure and arrangement of side chains.

This is even more evident comparing the two 8-helices obtained from the present hexamer, Boc-(AOPIC)$_6$-OMe **6**, and its formal parent compound, that is our previously synthesized pyrrolidinone-based hexamer, Boc-(AMOMPC)$_6$-OMe, [11b] (Figure 28 e Table 1). Due to the fact that Boc-(AMOMPC)$_6$-OMe was constructed starting from a monomer having an opposite absolute configuration at Cα, thus leading to a secondary structure with opposite helicity, during the comparison the signs of dihedral angles in Table 1 must be inverted.

It is evident from data in Table 1 that, despite the illusory resemblance of the two 8-helices, the in-depth analysis confirms that Boc-(AMOMPC)$_6$-OMe is well described as a H8 conformation. On the contrary, the arrangement of Boc-(AOPIC)$_6$-OMe is more resembling to a Z8 conformation, even if the values of backbone torsional angles are not in a perfect agreement with the ones computed by Perczel for β-peptides.[6]

Table 1. Comparison of dihedral angles in minimum energy conformers of 8-helices of imidazolidinone-based Boc-(AOPIC)$_6$-OMe and pyrrolidinone-based Boc-(AMOMPC)$_6$-OMe.[a]

Residue number	Boc-(AOPIC)$_6$-OMe			Boc-(AMOMPC)$_6$-OMe[a]		
	ϕ	θ	ψ	ϕ	θ	ψ
1	-108.5	68.4	18.4	89.9	-104.4	45.5
2	-109.4	68.5	15.1	90.9	-101.4	46.7
3	-107.9	68.4	14.5	95.8	-98.3	48.7
4	-110.5	62.3	11.1	96.5	-101.9	49.3
5	-111.8	65.0	7.9	91.7	-101.3	49.3
6	-99.4	61.0	-88.8	88.8	-99.1	-50.8

[a] Taken from Ref. 11b.

Eventually, the striking differences between the two 8-helices of Boc-(AOPIC)$_6$-OMe and Boc-(AMOMPC)$_6$-OMe can be better evidenced by the visual inspection of both backbone conformations in the global minima, using the mirror image in the case of Boc-(AMOMPC)$_6$-OMe (Figure 28).

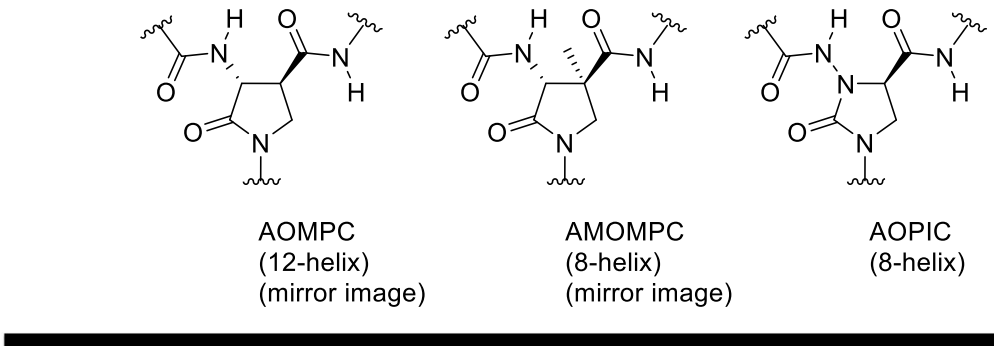

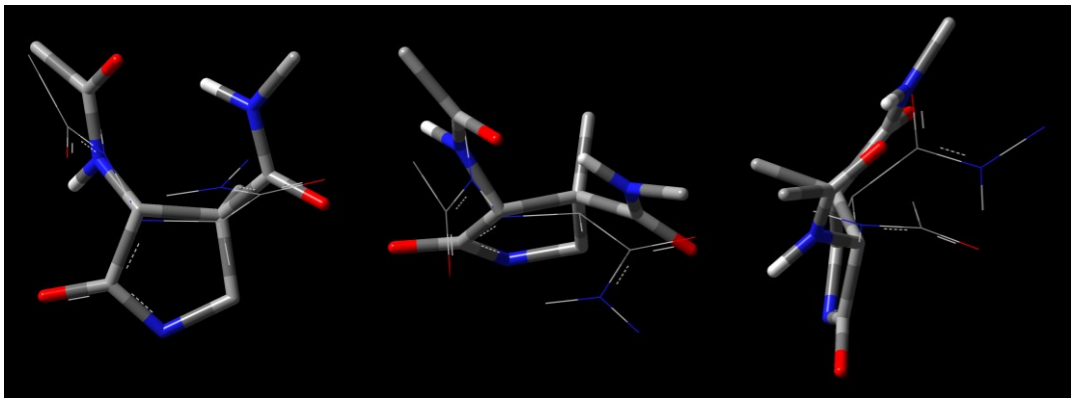

Figure 28. Top: fragments of structures of Boc-(AOPIC)$_6$-OMe and mirror images of Boc-(AOMPC)$_6$-OMe and Boc-(AMOMPC)$_6$-OMe considered in the comparison. Middle: H8 structure of Boc-(AOMPC)$_6$-OMe (left), H8 structure of Boc-(AMOMPC)$_6$-OMe (centre) and Z8-like structure of Boc-(AOPIC)$_6$-OMe (right). Bottom: three different views of the superimposed structures of Boc-(AOPIC)$_6$-OMe and Boc-(AMOMPC)$_6$-OMe (wireframe = Boc-(AOPIC)$_6$-OMe, stick = Boc-(AMOMPC)$_6$-OMe). Unnecessary hydrogens and phenylethyl side chains omitted for clarity.

In Figure 28, it is also evident the even more remarkable difference between the folding of the present imidazolidinone-based hexamer, Boc-(AOPIC)$_6$-OMe, and its closer analogue, the Cα-unmethylated version of the previous pyrrolidinone-tethered hexamer, Boc-(AOMPC)$_6$-OMe.[11a] Although the different conformation of H-bonding functionalities is obvious, due to the fact that the secondary structure of Boc-(AOMPC)$_6$-OMe was ascertained to be a 12-helix, it is very interesting to note how dramatically the formal change C → N affects the disposition of the groups involved, even if the cyclic fragments have very similar structures. Anyway, the elucidation of the deep reasons, that is to say the energetic factors related to all the possible intra- and inter-residue interactions, are beyond the scope of this work and will be analysed further.

2.2.3 ROESY analysis

In the case of hexamer Boc-(AOPIC)$_6$-OMe **6**, the extensive overlap and the broad peaks prevented the residue-specific assignment of ^{1}H and ^{13}C backbone resonances, even after many attempts with prolonged acquisition times, different solvent mixtures and temperatures.

On the contrary, ^{1}H and ^{13}C resonances could be assigned for dimer Boc-(AOPIC)$_2$-OMe **4** and tetramer Boc-(AOPIC)$_4$-OMe **5**, with the exception of phenylethyl side chains. In particular, for dimer **4** the analysis of a concentrated sample (0.1 M) in $CDCl_3$ at 35 °C allowed us to obtain resolved ^{1}H and ^{13}C signals and easily detectable HSQC and HMBC crosspeaks, while for tetramer **5** it was necessary to use an anhydrous $CDCl_3$:DMSO-d_6 9:1 solvent system

at 19 °C, in order to narrow ^{1}H and ^{13}C resonances and then detect the requested heteronuclear couplings. The assignments for dimer **4** (Table 2) and tetramer **5** (Table 3) were obtained as follows:

- from the ^{t}Bu protons, the Boc carbonyl group resonance was identified by HMBC spectrum;
- from the Boc carbonyl carbon, the NH(A) was assigned by HMBC correlation;
- NH(A) did not show the expected crosspeak with C4(A), but furnished an evident ^{3}J coupling with the imidazolidinonic carbonyl C2(A);
- from C2(A), both H_5 and H_5' of residue A were assigned by HMBC correlation;
- from H_5(A) and H_5'(A), C5(A) was identified by HSQC spectrum;
- from C5(A), ^{2}J coupling allowed to assign H_4(A) resonance;
- from H_4(A), the resonances of C4(A) and carbonyl group (peptidic CO) of residue A were assigned by HSQC and HMBC correlations, respectively;
- from the peptidic CO(A), HMBC spectrum revealed the ^{2}J coupling with the NH(B) resonance;
- from NH(B), continuing to exploit the same step-by-step approach, all the backbone resonances were sequentially assigned.

Table 2. Assignment of ^{1}H and ^{13}C backbone resonances of compound Boc-(AOPIC)$_2$-OMe 4 (0.1 M in $CDCl_3$ at 35 °C).

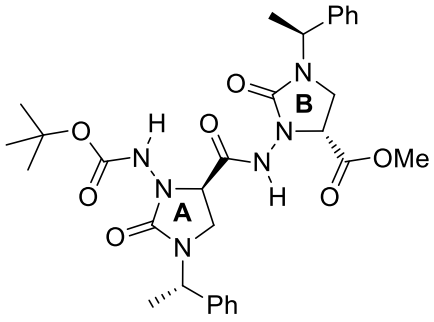

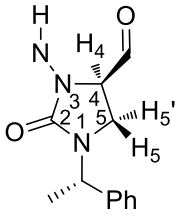

Boc-(AOIPC)$_2$-OMe **4**

	A	B
Peptidic CO	169.7	---
C4	59.3	57.4
NHCO-O^{t}Bu	156.3	---
NHCO$_2$-C(CH$_3$)$_3$	82.6	---
NHCO$_2$-C(CH$_3$)$_3$	28.2	---

C5	41.1	39.9
Imidazolidinone N1-(CO)-N3 (C2)	158.9	157.7
CO_2CH_3	---	52.7
CO_2CH_3	---	170.1
NH	6.90	9.41
H_4	4.17	4.47
$H_5 + H_5'$	3.44-3.46	3.27-3.29
$NHCO_2$-$C(CH_3)_3$	1.50	---
CO_2CH_3	---	3.75

Table 3. Assignment of ^{1}H and ^{13}C backbone resonances of compound Boc-(AOPIC)$_4$-OMe, 5 (20 mM in $CDCl_3$:DMSO-*d*$_6$ 9:1 at 19 °C, with powdered 4 Å m.s.).

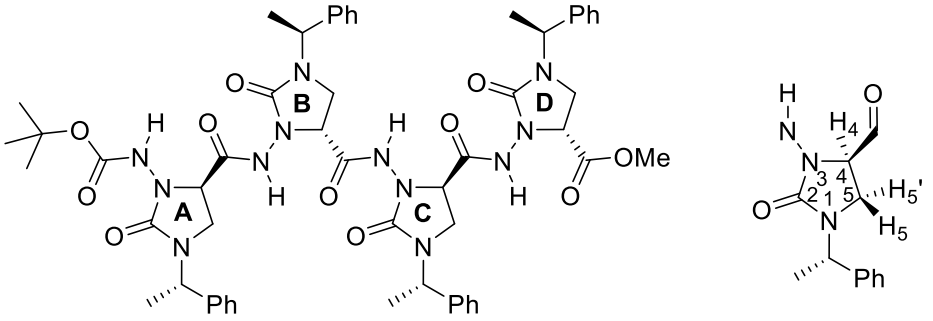

Boc-(AOPIC)$_4$-OMe **5**

	A	B	C	D
Peptidic CO	169.95	170.66	168.54	---
C4	58.46	58.07	58.76	56.77
NHCO-O^{t}Bu	154.74	---	---	---
$NHCO_2$-C$(CH_3)_3$	81.04	---	---	---
$NHCO_2$-C$(CH_3)_3$	28.11	---	---	---
C-5	41.02	40.70	41.22	39.39

Imidazolidinone N1-(CO)-N3 (C2)	158.40	157.36	157.82	157.50
$CO_2\underline{C}H_3$	---	---	---	52.17
$\underline{C}O_2CH_3$	---	---	---	169.00
N$\underline{H}$	8.18	9.48	9.90	9.92
H_4	4.44	4.45	4.17	4.30
H_5	3.25	3.17	3.06	2.93
H_5'	3.83	3.76	3.70	3.54
$NHCO_2$-C($C\underline{H}_3$)$_3$	1.42	---	---	---
$CO_2C\underline{H}_3$	---	---	---	3.40

Some portions of the ROESY spectrum are reported in Figure 29, while a full correlation table is reported in Table 4.

In particular, the portions in Figure 29 are related to the cross-peaks which are decisive in order to determine the precise folding, that is to distinguish between the two variants of the 8-helix folding.

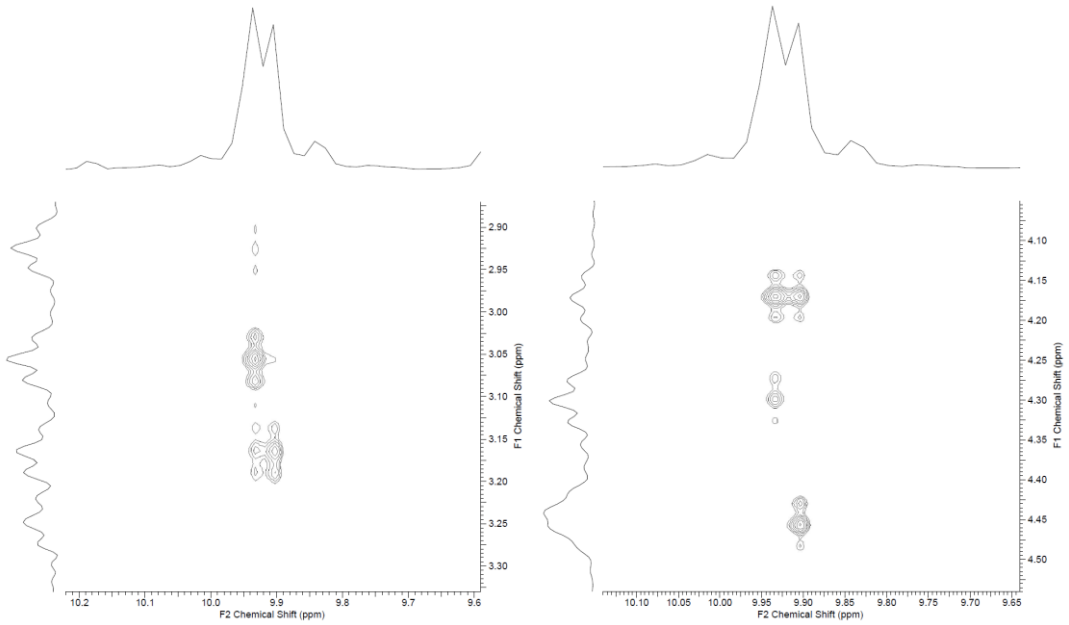

Figure 29. Representative portions of the ROESY spectrum of Boc-(AOPIC)$_4$-OMe, 5, showing the crucial cross-peaks related to NHs of residues C and D.

Table 4. Intensities of ROESY peaks (arbitrary units) of tetramer Boc-(AOPIC)$_4$-OMe, 5 (20 mM in CDCl$_3$:DMSO-*d*$_6$ 9:1 at 19 °C, with powdered 4 Å m.s.).

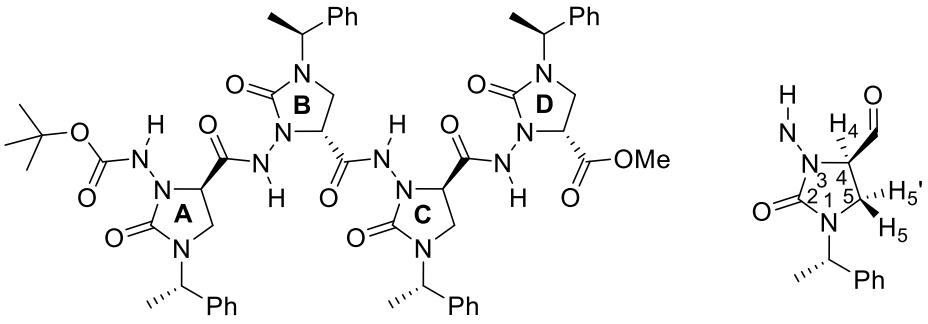

Boc-(AOPIC)$_4$-OMe **5**

			Residue A				Residue B				Residue C				Residue D			
			NH	H4	H5	H5'	NH	H4	H5	H5'	NH	H4	H5	H5'	NH	H4	H5	H5'
			8.18	4.44	3.25	3.83	9.48	4.45	3.17	3.76	9.90	4.17	3.06	3.70	9.92	4.30	2.93	3.54
A	NH	8.18																
	H4	4.44																
	H5	3.25																
	H5'	3.83																
B	NH	9.48																
	H4	4.45																
	H5	3.17																
	H5'	3.76																
C	NH	9.90																
	H4	4.17																
	H5	3.06																
	H5'	3.70																
D	NH	9.92																
	H4	4.30																
	H5	2.93																
	H5'	3.54																

very strong (intra-CH_2) (I>10000)
strong (10000>I>2000)
medium (2000>I>1000)
weak (1000>I>200)
very weak (I<200)

With the aim to confirm the computationally evident preference for the zig-zag 8-helix (Z8) over its helical (H8) counterpart, the experimental intensities of ROESY cross-peaks obtained for tetramer Boc-(AOPIC)$_4$-OMe, **5**, were compared to the theoretically expected ones for both

the variants of the 8-helix secondary structure (Table 5and Figure 30). In the case of Z8 secondary structure, the average backbone dihedrals computed for the lowest energy conformer of hexamer Boc-(AOPIC)$_6$-OMe, **6**, were used in order to determine the relevant interatomic distances and then the expected ROESY cross-peaks. Due to the fact that no H8 folding was evidenced for Boc-(AOPIC)$_6$-OMe during molecular dynamics simulation, the backbone was forced to take such a conformation. To this end, we used the average dihedrals computed for the minimum energy conformer of the related pyrrolidinone analogue Boc-(AMOMPC)$_6$-OMe, which was demonstrated to fold into a very stable H8 8-helix.[11b] Even if all the other secondary structures were already discarded, the expected cross-peaks for the 12- and 14-helices, obtained again imposing the suitable backbone torsional angles to our imidazolidinonic structure, were also added in Table 5 in order to better appreciate the striking difference in the expected ROESY signals.

Table 5. Comparison between experimental and theoretically expected cross-peaks intensities for various secondary structures of tetramer Boc-(AOPIC)$_4$-OMe, 5.

	Theoretically expected				Experimental
	Z8 8-helix[a]	H8 8-helix[b]	12-helix[c]	14-helix[d]	
NH(i)-H$_4$(i)	medium/weak	medium/weak	medium	medium/strong	weak
NH(i)-H$_5$(i)	no	no	no	no	no
NH(i)-H$_5$'(i)	no	no	no	no	no
NH(i+1)-H$_4$(i)	weak	medium/strong	strong	strong	weak
NH(i+1)-H$_5$(i)	weak	no/very weak	no	no/very weak	weak
NH(i+1)-H$_5$'(i)	no	no	no/very weak	weak	no
NH(i+1)-NH(i)	weak/very weak	very weak	no/very weak	no	very weak[e]
H$_4$(i+1)-H$_4$(i)	no	no	no	no	no
H$_4$(i+1)-H$_5$(i)	no	no	no	no	no
H$_4$(i+1)-H$_5$'(i)	no	no	no	no	no
H$_5$(i+1)-H$_4$(i)	no	no	no	no	no
H$_5$(i+1)-H$_5$(i)	no	no	no	no	no
H$_5$(i+1)-H$_5$'(i)	no	no	no	no	no
H$_5$'(i+1)-H$_4$(i)	no	no	no	no	no

H_5'(i+1)-H_5(i)	no	no	no	no	no
H_5'(i+1)-H_5'(i)	no	no	no	no	no
NH(i+2)-H_4(i)	no	no	no	no	no
NH(i+2)-H_5(i)	weak	medium/strong	no	no	weak
NH(i+2)-H_5'(i)	no	no	no	no	no
H_4(i+2)-H_4(i)	no	no	no	no	no
H_4(i+2)-H_5(i)	no	no	very weak	no	no
H_4(i+2)-H_5'(i)	no	no	no	no	no
H_5(i+2)-H_4(i)	no	no	no	no	no
H_5(i+2)-H_5(i)	no	no	no	no	no
H_5(i+2)-H_5'(i)	no	no	no	no	no
H_5'(i+2)-H_4(i)	no	no	no	no	no
H_5'(i+2)-H_5(i)	no	no	no	no	no
H_5'(i+2)-H_5'(i)	no	no	no	no	no
NH(i+3)-H_4(i)	no	no	no	no	no
NH(i+3)-H_5(i)	no	no	very weak/no	no	no
NH(i+3)-H_5'(i)	no	no	no	no	no
H_4(i+3)-H_4(i)	no	no	no	no	no
H_4(i+3)-H_5(i)	no	no	no	no	no
H_4(i+3)-H_5'(i)	no	no	no	no	no
H_5(i+3)-H_4(i)	no	no	no	no	no
H_5(i+3)-H_5(i)	no	no	no	no	no
H_5(i+3)-H_5'(i)	no	no	no	no	no
H_5'(i+3)-H_4(i)	no	no	no	no	no
H_5'(i+3)-H_5(i)	no	no	no	no	no
H_5'(i+3)-H_5'(i)	no	no	no	no	no

[a] Evaluated considering the most stable conformers computed in molecular dynamics simulations. [b] Evaluated considering the hypothetical H8 structure obtained by using the backbone torsional angles of the H8 folding computed for the absolute minimum of the related pyrrolidinone analogue Boc-(AMOMPC)$_6$-OMe (Ref. 11b). [c] Evaluated considering the hypothetical 12-helix structure obtained by using the backbone torsional angles of the folding computed for the absolute minimum of the related pyrrolidinone analogue Boc-(AOMPC)$_6$-OMe (Ref. 11a). [d] Evaluated considering the hypothetical 14-helix structure obtained by using the typical backbone torsional angles for β-peptides (Ref. 34). [e] NHs of residues C and D are too close each other to show off-diagonal cross-peaks.

Although the overall arrangement of both Z8 and H8 variants is very similar, the close inspection of interatomic nearest-neighbor distances involving NH(i+1) and either H_4(i) or H_5(i), as well as distances between NH(i+2) and H_5(i), rules out the helical (H8) conformation (Figure 30). In fact, in the case of the H8 folding, medium/strong intensities are expected for both the NH(i+1)-H_4(i) and NH(i+2)-H_5(i) through-space couplings, while only extremely weak (or no) cross-peaks should be visible for the NH(i+1)-H_5(i) interactions. On the contrary, in the case of the zig-zag (Z8) folding, all the NH(i+1)-H_4(i), NH(i+1)-H_5(i) and NH(i+2)-H_5(i) cross-peaks should be weak and of comparable intensities, exactly as determined experimentally.

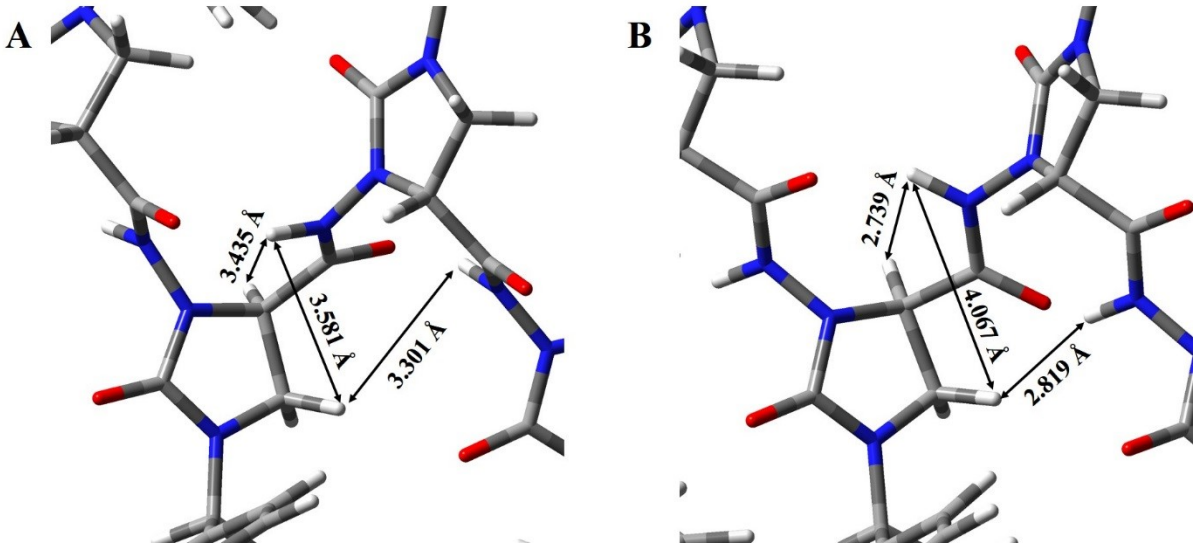

Figure 30. Representative views of crucial NH(i+1)-H_4(i), NH(i+1)-H_5(i) and NH(i+2)-H_5(i) distances in (A) the minimum energy Z8 8-helix structure computed for hexamer Boc-(AOPIC)$_6$-OMe, 6, and (B) the hypothetical H8 8-helix structure obtained for the same compound by using the backbone torsional angles computed for the minimum energy H8 8-helix structure of the related pyrrolidinone analogue Boc-(AMOMPC)$_6$-OMe (Ref. 11b).

2.3 Conclusions

In searching for new foldamers, novel mimics of β-peptides based on the formal substitution Cβ → Nβ(acyl) have been synthesized. Thus, starting from our previously reported hexamers based on pirrolidin-2-one-tethered *trans*-β-amino acids, namely AOMPC and its Cα-methylated counterpart AMOMPC, the dimer, tetramer and hexamer based on a new imidazolidinone-tethered α-hydrazido acid (3-amino-2-oxo-imidazolidine-4-carboxylic acid

(AOPIC) were constructed and analysed using spectroscopic (NMR and CD) and computational (MD) techniques.

The formal C → N substitution changed dramatically the folding in comparison to the parent AOMPC hexamer, which showed a stable 12-helix in chloroform. In fact, all the oligomers formed 8-helices, with as few as two residues, and even a simple C-terminal-amide monomer highlighted the same pronounced tendency. The stability of the secondary structure was demonstrated to be a function of the length, thus proving the existence of a synergistic effect, and of the presence of hydrogen-bond-accepting/donating solvents, the effect being more pronounced for shorter oligomers.

The computational analysis, besides furnishing the theoretical proof of the 8-helix as the only stable structure, allowed to distinguish between the two possible variants of such a folding, strongly pointing towards the "hydrazido-turn" sequence, where additional 5-membered H-bonded cycles are enclosed within the 8-membered ones. Molecular dynamics simulations also underlined the substantial participation of unconventional hydrogen-bonds, involving imidazolidinone carbonyls and C-H belonging to phenyl and *t*-butyl groups. Moreover, the in-depth analysis of the backbone conformation pointed out that the arrangement of H-bond-donating and accepting functionalities is strikingly different from the H8 structure observed predominantly in literature for the 8-helices, and assumed by our previously reported hexamer of a pyrrolidinone-based Cα-methylated *trans*-β-amino acid, AMOMPC. Indeed, it is more resembling to a Z8 conformation, as plenty confirmed by the ROESY spectrum, even if the backbone torsional angles are distorted in comparison to the preferred values for such a conformation in β-peptides. The sole Z8-like structures described with quite similar values are the Z8 8-helices of α-aminoxy- and α-hydrazino-peptides but, in spite of the likeness in backbone dihedrals between the latter and our AOPIC foldamers, the sequences of hydrazino- and hydrazido-turns evidenced important differences in terms of relative contributions from the 8-membered C=O•••H-N and the 5-membered Nβ•••H-N H-bonds, due to differences in both basicity and geometrical arrangements between sp^2 and sp^3 Nβ nitrogens.

These results contribute to our knowledge and understanding of the growing family of foldamers, especially the ones based on peptide mimics. A series of studies, which will be devoted to investigate deeply all the factors that may govern the conformational preferences for both the imidazolidinone-tethered α-hydrazido-peptides and their acyclic versions, will be reported in due course.

2.4 Experimental

2.4.1 Materials and methods

Melting points were obtained on an Electrothermal apparatus IA 9000 and are uncorrected. ^{1}H and ^{13}C-NMR spectra were determined at 25 °C on a Varian MR400 spectrometer, at 400 and 100 MHz for ^{1}H and ^{13}C, respectively, in $CDCl_3$ unless otherwise reported. Chemical shifts are reported in ppm relative to residual solvent signals (δ = 7.26 and 77.16 ppm for ^{1}H and ^{13}C NMR, respectively), and coupling constants (J) are given in Hz. Stock 0.1 M solutions of pure **4** and **8** for dilution experiments were obtained diluting 0.2 mmol of compounds in 2 mL graduated flasks, using $CDCl_3$ dried over activated molecular sieves, then all the other concentrations (0.05, 0.025, 0.01 and 0.001 M) were obtained by serial dilutions with dry $CDCl_3$. Titrations with DMSO-d_6 were carried out at 25 °C by careful sequential additions of suitable volumes of DMSO-d_6 to NMR tubes filled with exactly 0.7 mL of 1 mM (compounds **4** and **8**) or 2 mM solutions (compound **5**) in $CDCl_3$. Chemical shifts are reported in ppm relative to TMS. The CD spectra were recorded between 195 and 300 nm on a Jasco J-710 spectropolarimeter using a 1mm path length fused quartz cuvette. The values are expressed in terms of $[\theta]_T$, the total molar ellipticity (deg cm^2 $dmol^{-1}$). High-resolution electrospray ionization mass spectrometry was performed on a Finnigan MAT 95 XP double-focusing magnetic sector mass spectrometer. Column chromatography was performed using Kieselgel 60 Merck (230-400 mesh ASTM). Tetrahydrofuran and DMF were distilled from sodium-benzophenone and P_4O_{10}, respectively, under an argon atmosphere. The TLC analysis was performed with sheets of silica gel Fluka TLC-PET, using exposure to UV light and immersion in aqueous $KMnO_4$, followed by heating and by possible immersion in H_2SO_4 9 M. Compound **1** was synthesized from methyl 2,3-dibromopropionate[35] with a previously described procedure.[36] Compounds not appearing in the main text are numbered separately, with the letter "S" preceding the numbering of these compounds.

2.4.2 Synthetic procedures and characterizations

Procedure for nucleophilic ring opening of aziridine aziridine-2-carboxylate 1

To a solution of aziridine **1** (40 mmol, 8.21 g) and *t*-butyl carbazate (60 mmol, 7.93 g) in dry THF (60 mL) under inert atmosphere, $BF_3 \cdot Et_2O$ (20 mmol, 3.15 mL) was added. The solution was refluxed for 6 hours and then cooled down. After quenching with a phosphate buffer solution at pH 12 (200 mL), the product was extracted with ethyl acetate (3 × 200 mL), then the organic layers were dried over anhydrous Na_2SO_4 and the solvent evaporated under reduced

pressure. The two regioisomers **S1** and **2** were purified by silica gel chromatography (CH_2Cl_2/MeOH = 99:1-95:5) and collected as pure compounds.

***tert*-butyl 2-((*S*)-3-methoxy-3-oxo-2-(((*S*)-1-phenylethyl)amino)propyl)hydrazinecarboxylate (S1)**

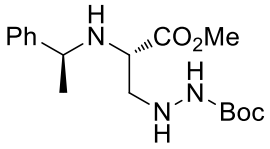

Colourless oil, 51% yield (6.89 g). ^{1}H NMR (400 MHz, $CDCl_3$): δ 1.36 (d, *J* = 6.8 Hz, 3H), 1.46 (s, 9H), 1.61 (bs, 1NH), 2.94 (dd, *J* = 4.8, 12.0 Hz, 1H), 3.01 (dd, *J* = 7.6, 12.0 Hz, 1H), 3.15 (dd, *J* = 4.8, 7.6 Hz, 1H), 3.72 (s, 3H), 3.75 (q, *J* = 6.8 Hz, 1H), 5.83 (bs, 1NH), 7.22-7.27 (m, 1ArH), 7.29-7.34 (m, 4ArH). ^{13}C NMR (100 MHz, $CDCl_3$): δ 25.2, 28.4, 52.0, 54.1, 56.8, 57.6, 80.5, 127.0, 127.3, 128.6, 144.9, 156.5, 175.0. HRMS (ESI): *m/z* calc. for $[C_{17}H_{27}N_3NaO_4]^+$ ($[M+Na]^+$) 360.1899, found 360.1903.

***tert*-butyl 2-((*R*)-1-methoxy-1-oxo-3-(((*S*)-1-phenylethyl)amino)propan-2-yl)hydrazinecarboxylate (2)**

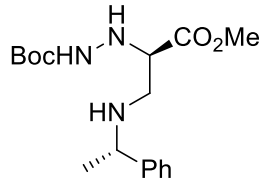

Colourless oil, 33% yield (4.45 g). ^{1}H NMR (400 MHz, $CDCl_3$): δ 1.39 (d, *J* = 6.4 Hz, 3H), 1.45 (s, 9H), 2.34 (bs, 1NH), 2.69 (dd, *J* = 8.4, 12.4 Hz, 1H), 2.83 (dd, *J* = 4.0, 12.4 Hz, 1H), 3.71 (s, 3H), 3.69-3.76 (m, 2H), 4.53 (bs, 1NH), 6.26 (bs, 1NH), 7.24-7.27 (m, 1ArH), 7.31-7.36 (m, 4ArH). ^{13}C NMR (100 MHz, $CDCl_3$): δ 23.6, 28.2, 46.4, 52.1, 58.6, 62.4, 80.6, 126.6, 127.2, 128.5, 144.3, 156.7, 172.5. HRMS (ESI): *m/z* calc. for $[C_{17}H_{27}N_3NaO_4]^+$ ($[M+Na]^+$) 360.1899, found 360.1902.

Synthesis of (*R*)-methyl 3-(*tert*-butoxycarbonylamino)-2-oxo-1-((*S*)-1-phenylethyl)imidazolidine-4-carboxylate, Boc-AOPIC-OMe 3

The hydrazine derivative **2** (13 mmol, 4.39 g) was dissolved in DCM (65 mL), then saturated aqueous $NaHCO_3$ (65 mL) was added and the biphasic system was thermostated at 0°C without stirring. A solution of phosgene in toluene (1.9 M, 15.6 mmol, 8.21 mL) was rapidly added directly in the organic phase and the mixture was stirred vigorously for 20 min at 0°C, then the

two phases were separated and the aqueous layer was extracted with DCM (2 × 20 mL). The reunited organic phases were dried over anhydrous Na_2SO_4 and the solvent was evaporated under reduced pressure, then compound **3** was obtained pure by silica gel chromatography (cyclohexane/ethyl acetate = 90:10-60:40).

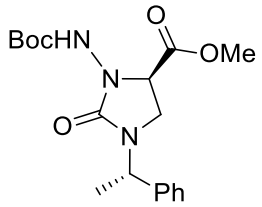

Amorphous white solid, 90% (11.7 mmol, 4.25 g). mp = 162-164 °C. ^{1}H NMR (400 MHz, $CDCl_3$): δ 1.48 (s, 9H), 1.58 (d, *J* = 7.4 Hz, 3H), 2.91 (t, *J* = 8.2 Hz, 1H), 3.62 (t, *J* = 9.0 Hz, 1H), 3.70 (s, 3H), 4.48 (t, *J* = 8.0 Hz, 1H), 5.32 (q, *J* = 7.2 Hz, 1H), 6.62 (bs, 1NH), 7.25-7.35 (m, 5ArH). ^{13}C NMR (100 MHz, $CDCl_3$): δ 16.3, 28.3, 39.9, 50.8, 52.8, 57.3, 82.0, 127.2, 127.8, 128.8, 139.6, 154.7, 158.3, 170.7. HRMS (ESI): *m/z* calc. for $[C_{18}H_{25}N_3NaO_5]^+$ ($[M+Na]^+$) 386.1692, found 386.1694.

Synthesis of (*R*)-methyl 3-((*R*)-3-(*tert*-butoxycarbonylamino)-2-oxo-1-((*S*)-1-phenylethyl)imidazolidine-4-carboxamido)-2-oxo-1-((*S*)-1-phenylethyl)imidazolidine-4-carboxylate, Boc-(AOPIC)$_2$-OMe 4

To a solution of Boc-AOPIC-OMe **3** (2 mmol, 727 mg) in MeOH (4 mL) and DCM (2 mL), aqueous NaOH 1 M (2.4 mL) was added at room temperature. The mixture was stirred for 20 min, then it was cooled down at 0 °C and HCl 1 M was added dropwise until pH 3. Volatiles were eliminated under reduced pressure and the product was extracted with ethyl acetate (3 × 30 mL). The reunited organic phases were dried over anhydrous Na_2SO_4 and evaporated under reduced pressure. The product (C-terminal acid) was azeotropically dried by dissolution in dry THF followed by rotary evaporation (2 times), repeating the procedure with dry DCM, and then used in the next synthetic step without further purifications.

Meanwhile, a solution of anhydrous HCl in MeOH (about 2.5 M, 12.5 mL) was rapidly added to a solution of Boc-AOPIC-OMe **3** (2.5 mmol, 909 mg) in DCM (1.25 mL). The solution was stirred for 3 hours, then all the volatiles were evaporated under reduced pressure. Residual traces of methanol were azeotropically eliminated by dissolution in dry DCM followed by rotary evaporation (2 times). The product (the hydrochloride of the N-terminal hydrazide) was used in the next synthetic step without further purifications.

The two intermediates, obtained as described above, were taken in the same flask using dry DCM, and then dissolved in dry DCM (1.5 mL) at 0 °C under an Ar atmosphere. TEA (2.5 mmol, 350 μL) and EDC hydrochloride (3 mmol, 575 mg) were sequentially added. The solution was stirred at 0 °C for 5 hours, then water (20 mL) was added and the mixture was extracted with ethyl acetate (2 × 50 mL). The organic layers were dried over anhydrous Na_2SO_4 and the solvent evaporated under reduced pressure. The residue was purified by silica gel chromatography (cyclohexane/ethyl acetate 90:10-60:40) to give the pure dimer Boc-(AOPIC)$_2$-OMe **4**.

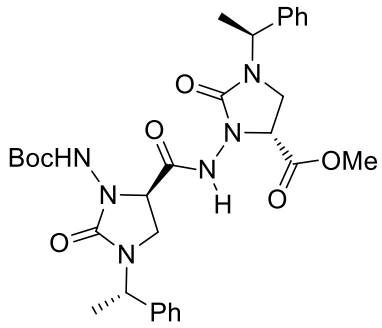

Colourless oil, 81% (1.61 mmol, 958 mg). ^{1}H NMR (400 MHz, $CDCl_3$): δ 1.47 (s, 9H), 1.54 (d, *J* = 7.2 Hz, 3H), 1.56 (d, *J* = 7.2 Hz, 3H), 2.93 (t, *J* = 9.6 Hz, 1H), 3.17 (t, *J* = 9.4 Hz, 1H), 3.60 (s, 3H), 3.60 (t, *J* = 9.4 Hz, 1H), 3.71 (t, *J* = 9.6 Hz, 1H), 4.30 (t, *J* = 9.6 Hz, 1H), 4.45 (t, *J* = 9.4 Hz, 1H), 5.18 (q, *J* = 7.2 Hz, 1H), 5.24 (q, *J* = 7.2 Hz, 1H), 6.92 (bs, NH), 7.18-7.38 (m, 10ArH), 9.36 (bs, 1NH). ^{13}C NMR (100 MHz, $CDCl_3$): δ 16.3, 16.9, 28.2, 39.8, 41.4, 50.9, 51.6, 52.6, 57.1, 59.0, 82.5, 127.0, 127.1, 127.8, 127.8, 128.7, 128.8, 139.3, 156.0, 157.7, 159.0, 169.7, 170.0. HRMS (ESI): *m/z* calc. for $[C_{30}H_{38}N_6NaO_7]^+$ ($[M+Na]^+$) 617.2700, found 617.2704.

Synthesis of (*R*)-methyl 3-((*R*)-3-((*R*)-3-((*R*)-3-((*tert*-butoxycarbonyl)amino)-2-oxo-1-((*S*)-1-phenylethyl)imidazolidine-4-carboxamido)-2-oxo-1-((*S*)-1-phenylethyl)imidazolidine-4-carboxamido)-2-oxo-1-((*S*)-1-phenylethyl)imidazolidine-4-carboxamido)-2-oxo-1-((*S*)-1-phenylethyl)imidazolidine-4-carboxylate, Boc-(AOPIC)$_4$-OMe 5

To a solution of Boc-(AOPIC)$_2$-OMe **4** (0.5 mmol, 297 mg) in MeOH (1 mL) and DCM (0.5 mL), aqueous NaOH 1 M (0.6 mL) was added at room temperature. The mixture was stirred for 20 min, then the C-terminal acid was obtained as reported above for the hydrolysis of compound **3** and used in the next synthetic step without further purifications.

Meanwhile, a solution of anhydrous HCl in MeOH (about 2.5 M, 3 mL) was rapidly added to a solution of Boc-(AOPIC)$_2$-OMe **4** (0.6 mmol, 357 mg) in DCM (0.3 mL). The solution was

stirred for 3 hours, then the hydrochloride of the N-terminal hydrazide was obtained as reported above for the N-Boc deprotection of compound **3** and used in the next synthetic step without further purifications.

The two intermediates, obtained as described above, were taken in the same flask using dry DCM, and then dissolved in dry DCM (0.5 mL) at -18 °C under an Ar atmosphere. DIPEA (1.75 mmol, 305 μL) and PyBroP (0.6 mmol, 280 mg) were sequentially added and the solution was stirred at -18 °C for 1 hour, then at 0 °C for 5 hours. The mixture was diluted with ethyl acetate (20 mL) and water (5 mL) and the two phases were separated. The organic phase was washed with HCl 0.5 M (2 × 2 mL) and NaOH 0.1 M (2 × 2 mL), then the aqueous phases were extracted again with ethyl acetate (20 mL) and the new organic phase was washed with HCl 0.5 M (2 × 2 mL) and NaOH 0.1 M (2 × 2 mL). The reunited organic layers were dried over anhydrous Na_2SO_4 and the solvent evaporated under reduced pressure. The residue was purified by silica gel chromatography (diethyl ether/ethyl acetate 100:0-40:60) to give the pure tetramer Boc-(AOPIC)$_4$-OMe **5**.

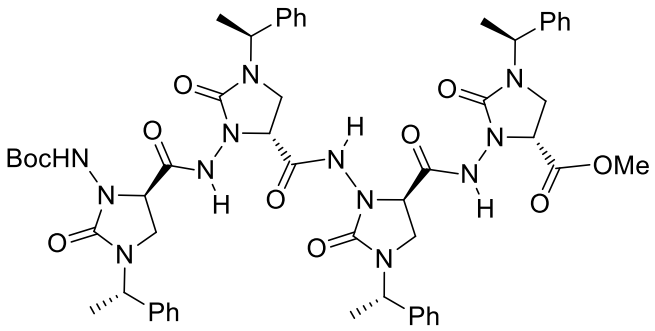

Colourless wax, 68% (338 μmol, 357 mg). ^{1}H NMR (400 MHz, $CDCl_3$): δ 1.46 (s, 9H), 1.52-1.56 (m, 12H), 2.93 (t, *J* = 8.8 Hz, 1H), 3.09 (t, *J* = 8.8 Hz, 1H), 3.11 (t, *J* = 8.8 Hz, 1H), 3.27 (t, *J* = 8.8 Hz, 1H), 3.43 (s, 3H), 3.52 (t, *J* = 9.2 Hz, 1H), 3.64 (t, *J* = 9.6 Hz, 2H), 3.67 (t, *J* = 9.2 Hz, 1H), 3.72 (t, *J* = 9.6 Hz, 1H), 3.98 (t, *J* = 9.2 Hz, 1H), 4.28 (t, *J* = 9.2 Hz, 1H), 4.31 (t, *J* = 9.2 Hz, 1H), 4.33 (t, *J* = 9.6 Hz, 1H), 5.05 (q, *J* = 7.2 Hz, 1H), 5.13-5.24 (m, 3H), 7.15 (bs, 1NH), 7.19-7.36 (m, 20 ArH), 9.07 (bs, 1NH), 9.35 (bs, 1NH), 9.58 (bs, 1NH). ^{13}C NMR (100 MHz, $CDCl_3$): δ 16.5, 17.0, 17.1, 17.2, 28.3, 39.8, 41.3, 41.4, 41.6, 51.1, 51.8, 52.0, 52.6, 57.2, 59.4, 82.6, 127.1, 127.3, 127.9, 128.0, 128.1, 128.8, 128.9, 129.0, 139.1, 139.3, 139.4, 140.0, 156.5, 157.4, 157.6, 158.5, 168.7, 169.5, 171.2, 171.6. HRMS (ESI): *m/z* calc. for $[C_{54}H_{64}N_{12}NaO_{11}]^+$ ($[M+Na]^+$) 1079.4715, found 1079.4720.

Synthesis of (*R*)-methyl 3-((*R*)-3-((*R*)-3-((*R*)-3-((*R*)-3-((*tert*-butoxycarbonyl)amino)-2-oxo-1-((*S*)-1-phenylethyl)imidazolidine-4-carboxamido)-2-oxo-1-((*S*)-1-phenylethyl)imidazolidine-4-carboxamido)-2-oxo-1-((*S*)-1-phenylethyl)imidazolidine-4-carboxamido)-2-oxo-1-((*S*)-1-phenylethyl)imidazolidine-4-carboxamido)-2-oxo-1-((*S*)-1-phenylethyl)imidazolidine-4-carboxamido)-2-oxo-1-((*S*)-1-phenylethyl)imidazolidine-4-carboxylate, Boc-(AOPIC)$_6$-OMe 6

To a solution of Boc-(AOPIC)$_4$-OMe **5** (150 μmol, 159 mg) in MeOH (1 mL) and DCM (0.5 mL), aqueous NaOH 1 M (0.3 mL) was added at room temperature. The mixture was stirred for 2 hours, then the C-terminal acid was obtained as reported above for the hydrolysis of compound **3** and used in the next synthetic step without further purifications. Meanwhile, 0.2 mmol of Boc-(AOPIC)$_2$-OMe **4** (119 mg) were N-Boc deprotected as reported above for the synthesis of compound **5**. The C-terminal acid and the hydrochloride of the N-terminal hydrazide were taken in the same flask using dry DCM, and then dissolved in dry DCM (200 μL) at 0 °C under an Ar atmosphere. DIPEA (475 μmol, 83 μL) and PyBroP (165 μmol, 77 mg) were sequentially added and the solution was stirred at 0 °C overnight. The mixture was diluted with ethyl acetate (20 mL) and water (5 mL) and the two phases were separated. The organic phase was washed with HCl 0.5 M (2 × 1 mL) and NaOH 0.1 M (2 × 1 mL), then the aqueous phases were extracted again with ethyl acetate (10 mL) and the new organic phase was washed with HCl 0.5 M (2 × 1 mL) and NaOH 0.1 M (2 × 1 mL). The reunited organic layers were dried over anhydrous Na_2SO_4 and the solvent evaporated under reduced pressure. The residue was purified by silica gel chromatography (dichloromethane/methanol 100:0-95:5) to give the pure hexamer Boc-(AOPIC)$_6$-OMe **6**.

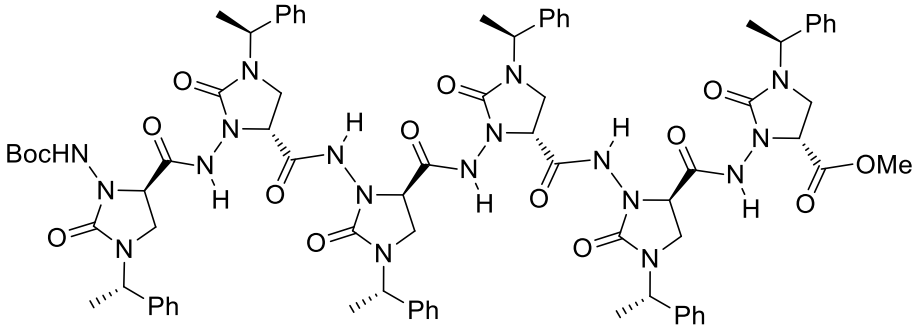

Colourless wax, 45% (67.7 μmol, 103 mg). ^{1}H NMR (600 MHz, DMSO-*d*$_6$, 35 °C): δ 1.40 (s, 9H), 1.47-1.53 (m, 18H), 2.81-3.01 (m, 6H), 3.53-3.75 (m, 9H), 4.27-4.45 (m, 6H), 4.96-5.07 (m, 6H), 7.11-7.35 (m, 30ArH), 8.81 (bs, 1NH), 9.97 (bs, 1NH, major conformer), 10.00 (bs, 1NH, minor conformer), 10.02 (bs, 1NH), 10.20 (bs, 1NH + 1NH, minor conformer), 10.23 (bs, 1NH + 1NH, major conformer). ^{13}C NMR (150 MHz, DMSO-*d*$_6$, 35 °C): δ 16.5, 16.62, 16.67,

16.72, 16.9, 17.0, 28.0, 40.06, 40.14, 40.2, 40.3, 40.4, 40.5, 50.65, 50.69, 50.77, 50.81, 52.3, 55.8, 56.06, 56.11, 56.2, 56.9, 79.8, 126.66, 126.73, 126.77, 126.81, 126.9, 127.1, 127.2, 127.26, 127.33, 127.37, 127.44, 128.2, 128.4, 128.5, 139.75, 139.77, 140.1, 140.15, 140.24, 140.4, 154.8, 157.1, 157.29, 157.31, 158.2, 168.2, 168.4, 168.5, 168.8, 169.5. HRMS (ESI): *m/z* calc. for $[C_{78}H_{90}N_{18}NaO_{15}]^+$ ($[M+Na]^+$) 1541.6731, found 1541.6735.

Synthesis of *tert*-butyl ((*R*)-5-carbamoyl-2-oxo-3-((*S*)-1-phenylethyl)imidazolidin-1-yl)carbamate, Boc-AOPIC-NH$_2$ 7

Boc-AOPIC-OMe **3** (0.3 mmol, 109 mg) was dissolved in dry MeOH (3 mL) at 0 °C, then NH_4Cl (0.6 mmol, 32 mg) was added and dry gaseous ammonia was gently bubbled into the stirring solution for 10 min. The flask was tightly capped and the cooling bath was removed, then after 1 hour all the volatiles were evaporated under reduced pressure and the residue was diluted with ethyl acetate (20 mL) and water (5 mL). After separation, the organic phase was washed with water (2 × 1 mL) and the aqueous phase was extracted with ethyl acetate (10 mL), then the second organic phase was washed with water (2 × 1 mL). The reunited organic phases were dried over anhydrous Na_2SO_4 and evaporated under reduced pressure to give directly the pure C-terminal amide Boc-AOPIC-NH$_2$ **7**.

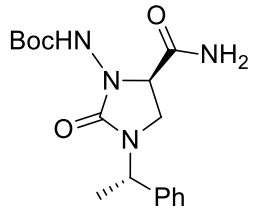

Colourless wax, 94% (281 μmol, 98 mg). ^{1}H NMR (400 MHz, $CDCl_3$): δ 1.50 (s, 9H), 1.57 (d, *J* = 7.4, 3H), 2.93 (t, *J* = 9.4 Hz, 1H), 3.68-3.73 (m, 1H), 4.05 (t, *J* = 9.4 Hz, 1H), 5.24 (q, *J* = 7.4 Hz, 1H), 5.34 (bs, 1NH), 6.41 (bs, 1NH), 7.27-7.36 (m, 5ArH), 8.01 (bs, 1NH). ^{13}C NMR (100 MHz, $CDCl_3$): δ 16.4, 28.3, 40.5, 51.3, 57.9, 82.8, 127.1, 128.0, 128.9, 139.0, 156.2, 158.9, 172.3. HRMS (ESI): *m/z* calc. for $[C_{17}H_{24}N_4NaO_4]^+$ ($[M+Na]^+$) 371.1695, found 371.1697.

Synthesis of (*R*)-methyl 3-acetamido-2-oxo-1-((*S*)-1-phenylethyl)imidazolidine-4-carboxylate, Ac-AOPIC-OMe 8

Boc-AOPIC-OMe **3** (0.3 mmol, 109 mg) was submitted to Boc removal as reported above for the synthesis of compound **4**, then the hydrochloride of the N-terminal hydrazide was dissolved in dry DCM (1 mL) at room temperature. After sequential addition of pyridine (0.75 mmol, 61 μL) and acetyl chloride (0.31 mmol, 22 μL), the reaction mixture was stirred for 30 min and

then diluted with ethyl acetate (20 mL) and water (5 mL). After separation, the organic phase was washed sequentially with water (2 × 1 mL), HCl 1 M (2 × 1 mL) and aqueous saturated Na_2CO_3 (2 mL). The neutral aqueous phases were extracted with ethyl acetate (10 mL), then the second organic phase was washed with water (2 × 1 mL), HCl 1 M (2 × 1 mL) and aqueous saturated Na_2CO_3 (2 mL). The reunited organic phases were dried over anhydrous Na_2SO_4 and evaporated under reduced pressure, then the residue was purified by silica gel chromatography (cyclohexane/ethyl acetate 50:50-0:100) to give the pure Ac-AOPIC-OMe **8**.

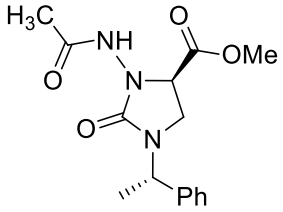

Colourless oil, 89% (266 μmol, 81 mg). ^{1}H NMR (400 MHz, $CDCl_3$): δ 1.58 (d, *J* = 7.0, 3H), 2.04 (s, 3H), 2.95 (d, *J* = 7.0, *J* = 9.4 Hz, 1H), 3.64-3.69 (m, 4H), 4.55 (d, *J* = 7.4, *J* = 9.4 Hz, 1H), 5.30 (q, *J* = 7.0 Hz, 1H), 7.27-7.35 (m, 5ArH), 7.58 (bs, 1NH). ^{13}C NMR (100 MHz, $CDCl_3$): δ 16.3, 21.1, 40.2, 50.9, 52.7, 57.0, 127.2, 127.8, 128.8, 139.6, 158.3, 169.8, 170.7. HRMS (ESI): *m/z* calc. for $[C_{15}H_{19}N_3NaO_4]^+$ ($[M+Na]^+$) 328.1273, found 328.1271.

2.5 Supplementary session

2.5.1 Logical Analysis of Possible H-bonding Patterns for α-hydrazidopeptides

The following logical analysis of H-bonding patterns applies to homogeneous secondary structures and is valid for the imidazolidinone-based α-hydrazidopeptides, but it can also be extended to any other oligomer constructed from monomers where the NH and C=O functionalities are separated by two atoms (e.g. β-amino acids and α-aminoxy acids). As reported above (Paragraph 2.2 Results and Discussion), NMR experiments clearly demonstrated that in all the oligomers the number of intramolecular hydrogen bonds is equal to the number of residues minus one ($n_{H\text{-}bonds} = n_{residues} - 1$), the first residue NH (BocNH) being the only one non-hydrogen-bonded. Using the hexamer schematized in Figure 31 as an example, it can be easily seen that the most common structures for β-peptides, the 12- and 14-helices,[1] are ruled out by logic, because they cannot form more than 4 hydrogen bonds, or in general a number equal to the number of residues minus two ($n_{H\text{-}bonds} = n_{residues} - 2$). In addition, in the 12-helix the BocNH should participate to an intramolecular H-bond, contrarily to the experimental results. The same observation rules out the 10-helix, which could form, at least in

line of principle, $n_{H\text{-}bonds} = n_{residues} - 1$ intramolecular H-bonds. The 10-helix was observed only employing β-amino acids tethered on a four-membered oxetane ring, with a *cis* relative stereochemistry of amine and acid groups, and using in the first residue an azido group instead of an amine protected as a carbamate or amide.[18] Both the possibility for the 10/12-helix, a peculiar structure of β-peptides that has been obtained so far only with an alternate placement of monosubstituted β^2- and β^3-amino acids,[7] can be also eliminated. In this structure, the alternating substitution in the monomers triggers the existence of two different amide bond orientations, in sharp contrast to all the other helices (8-, 10-, 12- and 14-helices) based on the repetition of homosubstituted and homochiral monomers. The first 10/12-helix in Figure 31 can be excluded because it has 5 H-bonds, as detected by NMR experiments, but the BocNH acts as the H-bond donor, while the second 10/12-helix presents only 4 hydrogen bonds.

Eventually, sheet-like conformations are extremely unlikely in the present case. In fact, even if they were initially proposed for some high molecular weight poly-β-amino acids, especially in crystal phase, they were subsequently demonstrated to be disordered structures or helices in solution. On the other hand, oligomeric sheet secondary structures could be prepared using *syn*-2,3-disubstituted β-amino acids for the linear strands, due to the fact that such a relative configuration strongly favours the *trans* conformation of NH and CO groups, and employing different central dimeric sequences to induce the turn.[1d] Anyway, our oligomers are homomonomeric and made of conformationally constrained units that are constitutionally unable to place the NH and CO groups in the required antiperiplanar conformation. Moreover, the simple visual inspection highlight that a sheet-like conformation should show a very limited number of intramolecular H-bonds, compared to all the helical structures theoretically possible for a given oligomer,[1d] and this is in obvious contradiction with our experimental observations.

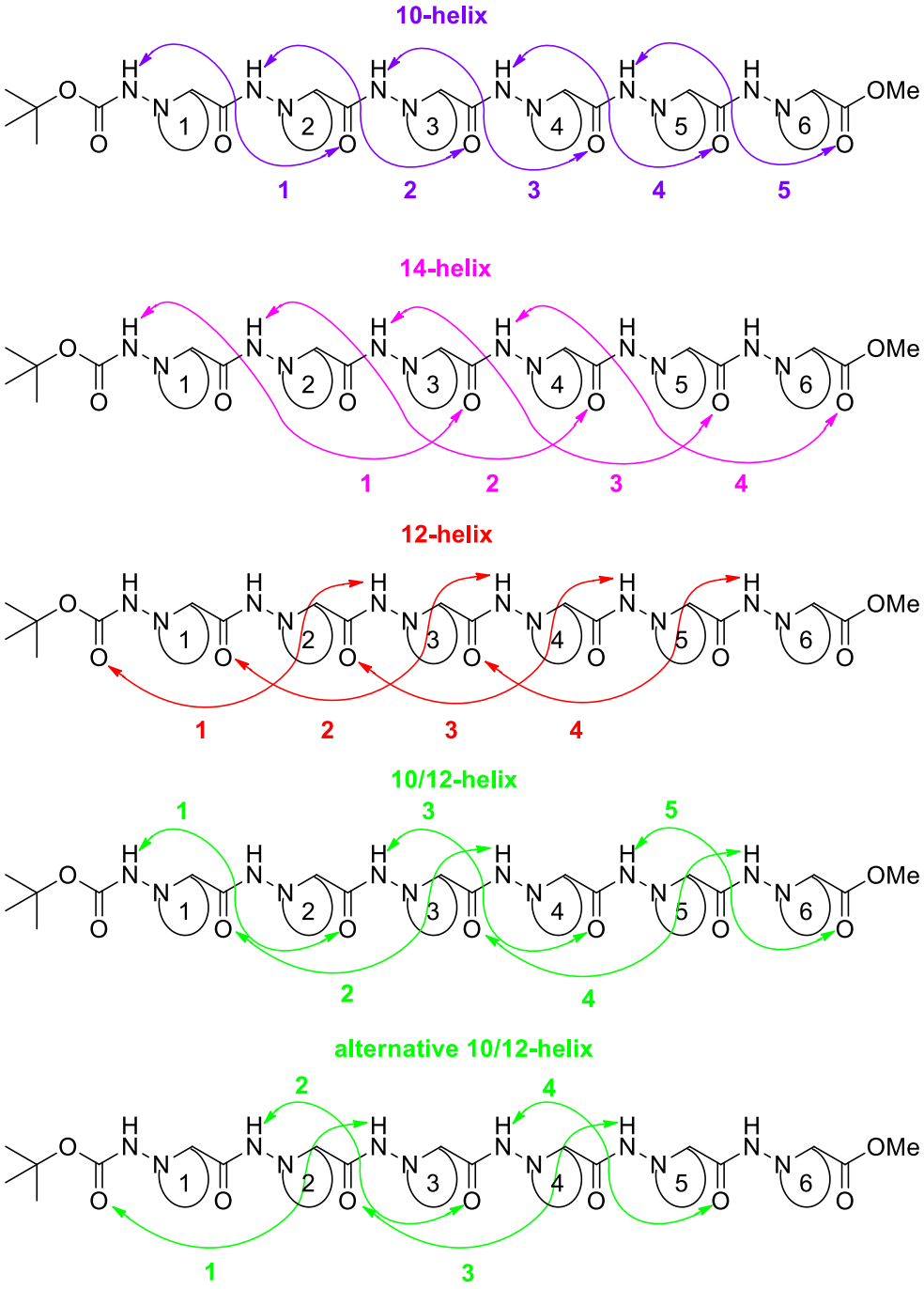

Figure 31. Theoretically possible H-bonding patterns for α-hydrazidopeptides that are ruled out by the experimental observations.

As reported in Figure 32, there are only two possibilities complying with the experimentally observed number of intramolecular H-bonds. The first is the 8-helix, where the $N^{\gamma}H_{(i)}\cdots CO_{(i-2)}$ pattern lead in any oligomers to $n_{H\text{-}bonds} = n_{residues} - 1$. This folding is quite rare for β-peptides, requiring peculiar monomers to be formed[11b,12] but it was also evidenced for α-aminoxy-peptides[9] and some α-hydrazino-peptides.[10]

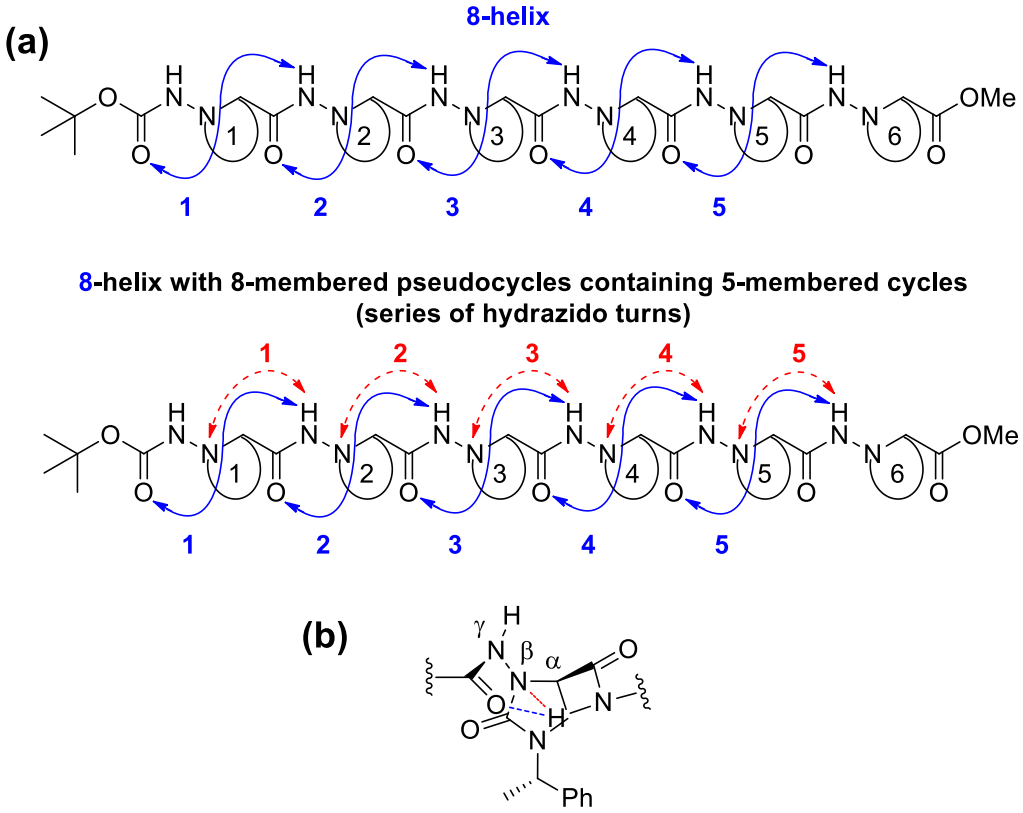

Figure 32. (a) Theoretically possible H-bonding patterns for α-hydrazidopeptides that are coherent with the experimental observations. (b) Schematic representation of the $N^{\gamma}H_{(i)}\cdots CO_{(i-2)}$ H-bond (blue dashed line) present in both 8-helices, and the $N^{\gamma}H_{(i)}\cdots N^{\beta}_{(i-1)}$ H-bond (red dashed line) present only in the 8-helix variant made of pseudocycles.

The other possibility is the helical structure typically formed by α-hydrazinopeptides, which is a variant of the above reported β-peptide 8-helix, and is due to the formal replacement of the C^{β} atom with a basic sp^3 N^{β} atom. In such a variant, there are bifurcated H-bonds in which $N^{\gamma}H_{(i)}$ acts as an H-bond donor towards both the $CO_{(i-2)}$, exactly as in the 8-helix, and the basic $N^{\beta}_{(i-1)}$ atom, then forming additional 5-membered cycles that are internal to the 8-membered ones ("hydrazino turns") (Figure 32).[11b,12] This peculiar secondary structure rely on the basic sp^3 hydrazinic N^{β} atoms, but in a macrocyclic derivative it was demonstrated to resist even when the N^{β} atoms were transformed in sp^2 nitrogens of ureic derivatives by reaction with isocyanates,[37] thus transforming the residues in α-hydrazido acids. Then, in the present case, where there are only N^{β}-acylated α-hydrazino acids (α-hydrazido acids), the corresponding structure should be more properly named "hydrazido turn".

2.5.2 Determination of Intermolecular H-bonding from Dilution Experiments

The determination of the amount of self-association, due to the intermolecular H-bonding of NHs in the N-acetyl monomer, Ac-AOPIC-OMe **8**, and in the first residue of Boc-(AOPIC)$_2$-OMe **4**, was carried out using the observed chemical shift *vs* concentration data. We exploited a slight variation of the iterative method reported by Chen and Shirts,[38] which is based on the assumption that only one rapid dimerization equilibrium exists, that is the one between the monomer M and its intermolecularly H-bonded dimer D (Scheme 1). It should be noted that the following analysis will apply in both cases of a symmetric dimer (two NHs with identical chemical shift δ_D) and an asymmetric dimer with two NHs with different chemical shifts δ_D and δ_D', which is equivalent to two NHs with two identical average chemical shifts $\delta_{Daverage} = (\delta_D + \delta_D')/2$.

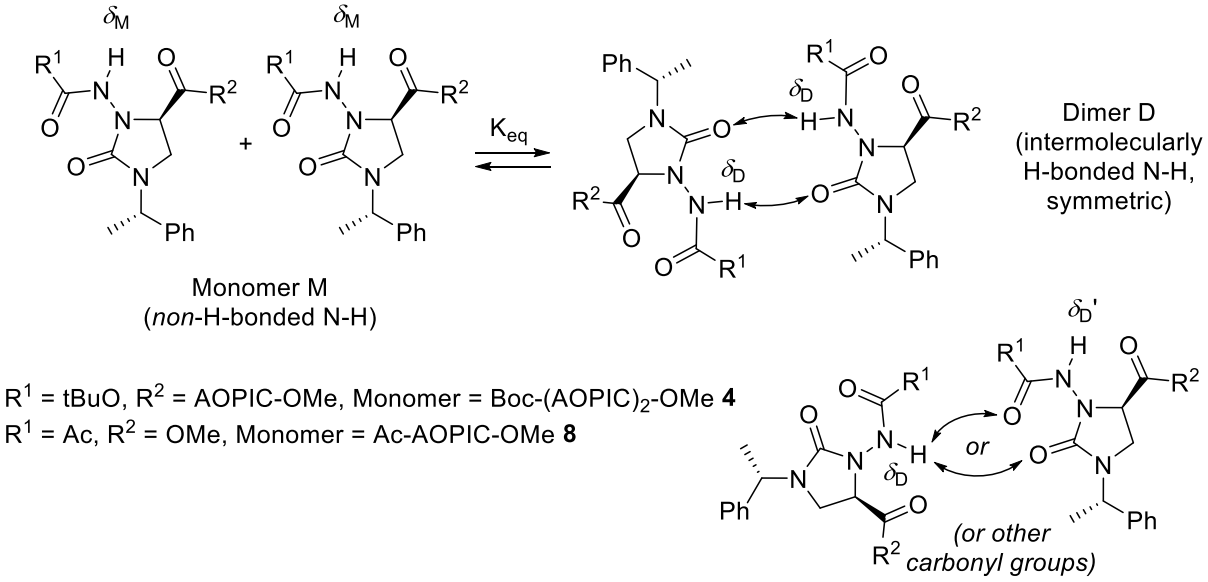

Scheme 1. Intermolecular H-bonding equilibria of Boc-(AOPIC)$_2$-OMe 4 and Ac-AOPIC-OMe 8.

If the previous assumption is valid, then the actual (equilibrium) monomer concentration [M], and the dimer concentration [D] can be related to the total (initial) monomer concentration [M_0] by eq 1.

eq 1 $$[\mathbf{M_0}] = [\mathbf{M}] + \mathbf{2}[\mathbf{D}]$$

The observed chemical shift (δ_{obs}) for the partly intermolecularly H-bonded NH is the weighted average of monomer (δ_M) and dimer (δ_D) chemical shifts.[39] The mole fractions for monomer M (f_M) and dimer D (f_D) can also be written as a function of [M_0], [M] and [D] eq 2.

eq 2
$$\boldsymbol{\delta_{obs} = \delta_M f_M + \delta_D f_D = \delta_M \frac{[M]}{[M_0]} + \delta_D \frac{2[D]}{[M_0]}}$$

The equilibrium constant for the formation of the H-bonded dimer, K_{eq}, can be written as a function of molar fractions (eq 3).

eq 3
$$\boldsymbol{K_{eq} = \frac{[D]}{[M]^2} = \frac{f_D}{2[M_0]f_M{}^2}}$$

Then, substituting $f_M = 1 - f_D$ in eq 3, the dimer molar fraction can be expressed as in eq 4:

eq 4
$$\boldsymbol{f_D = \frac{(1+8K_{eq}[M_0])^{\frac{1}{2}}-1}{(1+8K_{eq}[M_0])^{\frac{1}{2}}+1}}$$

If $f_M = 1 - f_D$ is used in eq 2, δ_{obs} can be expressed as a function of δ_M, δ_D and f_D (eq 5).

eq 5
$$\boldsymbol{\delta_{obs} = \delta_M f_M + \delta_D f_D = \delta_M + f_D(\delta_D - \delta_M)}$$

Then, substituting f_D eq 4 in eq 5, δ_{obs} can be conveniently expressed as a function of δ_M, δ_D, [M_0] and K_{eq} (eq 6).

eq 6
$$\boldsymbol{\delta_{obs} = \delta_M + (\delta_D - \delta_M)\frac{(1+8K_{eq}[M_0])^{\frac{1}{2}}-1}{(1+8K_{eq}[M_0])^{\frac{1}{2}}+1}}$$

Now, in the place of using iteratively eq 6 and the *X* parameter, as reported in the original manuscript,[38] we tried two different approaches for finding the three unknown constants δ_M, δ_D and K_{eq} from the interpolation of δobs *vs* [M_0] data.

The first method is iterative and formally equivalent to the one used by Chen and Shirts. It is based on the cyclic fitting of eq 6 by non-linear regression, carried out as follows: in the first iteration, it is easy to suppose a good approximated value for δ_M, which is used to find the first values for δ_D and K_{eq} by non-linear regression of eq 6. Then, in the second iteration, these values

are exploited in another non-linear regression of eq 6 to find a new value for δ_M, which in turn is used to find the second values for δ_D and K_{eq}, and so on. Starting from a reasonable δ_M generally ensures the convergence in 10-15 iterations, if just four decimal places are used for both the chemical shifts and the equilibrium constant. Anyway, it should be noted that at least five decimal places must be used in this iterative approach in order to prevent a premature convergence and obtain values that are very similar to the ones computed whit the second (direct) method, mainly because δ_D and K_{eq} demonstrated to be extremely sensitive even to very slight changes in δ_M. Thus, we used the first (iterative) method with five decimal places for both Ac-AOPIC-OMe **8** and Boc-(AOPIC)$_2$-OMe **4**, starting from different δ_M values and carrying out 30-45 iterations to reach the convergence, just to check the exactness of the δ_M, δ_D and K_{eq} values found with the second (direct) method. In an extended iterative trial with Ac-AOPIC-OMe **8**, we verified that using six decimal places gives exactly the same results, in terms of both values and standard errors, as the direct computation with the second method.

The second method is much less tedious and time-consuming, being based on the direct and contemporary interpolation by non-linear regression of δ_M, δ_D and K_{eq} values, but requires at least reasonable starting values for all the parameters and the constraints $\delta_D > \delta_M$ and $K_{eq} > 0$ to give always the exact solutions.

The calculated δ_M, δ_D and K_{eq}, as well as the f_D computed for the five total substrate concentrations [M_0], are reported in Table 6 for both the reference N-acetylated compound Ac-AOPIC-OMe **8**, in which the NH should likely be intramolecularly non-H-bonded, and the shortest oligomer, Boc-(AOPIC)$_2$-OMe **4**, in which even at the lowest concentration (10^{-3} M) there is the evidence of a strongly H-bonded second residue NH (δ_{obs} = 9.2035 ppm).

Table 6. Evaluation of δ_M, δ_D, K_{eq} and f_D from dilution experiments in anhydrous $CDCl_3$ at 25 °C.

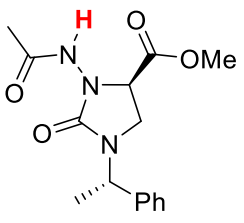

Ac-AOPIC-OMe **8**

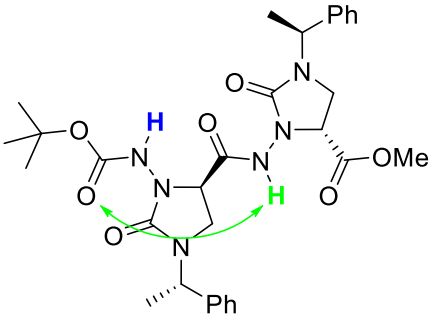

Boc-(AOPIC)$_2$-OMe **4**

	$[M_0]$ (M)	δ_{obs} (ppm)	δ_M (ppm) [δ_M±std. err. (ppm)][a]	δ_D (ppm) [δ_D±std. err. (ppm)][a]	K_{eq} (M^{-1}) [K_{eq}±std. err. (M^{-1})][a]	R^{2a}	f_D [f_D±std. err.][b]
NH	0.001	7.3912	7.37419 [7.374±0.010]	9.78524 [9.79±0.13]	4.71799 [4.7±0.6]	0.9995	$9.262*10^{-3}$ [$9.26±0.04*10^{-3}$]
	0.010	7.5763					0.07989 [0.080±0.004]
	0.025	7.7721					0.16462 [0.165±0.018]
	0.050	7.9894					0.25903 [0.26±0.06]
	0.100	8.2754					0.37206 [0.37±0.16]
NH	0.001	6.4092	6.39186 [6.392±0.005]	7.49586 [7.50±0.03]	8.11742 [8.1±0.6]	0.9997	$1.5728*10^{-2}$ [$1.573±0.008*10^{-2}$]
	0.010	6.5306					0.12445 [0.124±0.006]
	0.025	6.6488					0.23656 [0.24±0.03]
	0.050	6.7789					0.34658 [0.35±0.09]
	0.100	6.9036					0.46488 [0.5±0.2]
NH	0.001	9.2035	9.19432[c] [9.194±0.002]	9.60169[c] [9.602±0.011]	11.70637[c] [11.7±0.9]	0.9997[c]	$2.2377*10^{-2}$ [$2.238±0.016*10^{-2}$]
	0.010	9.2603					0.16373 [0.164±0.012]
	0.025	9.3154					0.29277 [0.29±0.05]
	0.050	9.3591					0.40895 [0.41±0.15]
	0.100	9.4092					0.52601 [0.5±0.4]

[a] Calculated by non-linear regression of eq 6, using the second (direct) method. [b] H-bonded dimer molar fractions calculated for the total substrate concentrations $[M_0]$ reported in the second column. Five significant figures for K_{eq} were used in eq 4 in order to minimize rounding errors during f_D calculations and during intermediate calculations for the propagation of errors in the calculation of f_D standard error. [c] Calculated by non-linear regression of eq 6, intentionally assuming that the equilibrium in Scheme 1 is valid instead of the equilibrium in Scheme 2.

From the data in Table 6, some considerations can be easily drawn. NHs in **8** and in the first residue of **4** (NHBoc) are substantially intermolecularly non-H-bonded at 10^{-3} M, the dimer percent molar fractions being about 1% ($f_D = 9.26*10^{-3}$ for **8** and $1.573*10^{-2}$ for NHBoc of **4**), but the tendency to self-association is quite evident from K_{eq} values. In fact, the f_D values computed at the highest concentrations used, that is 0.1 M, highlight that for Boc-$(AOPIC)_2$-OMe **4** (NHBoc) and Ac-AOPIC-OMe **8** the percent molar fractions of dimers are about 46% and 37%, respectively.

The parameters computed for the second residue NH of **4**, in light green in Table 6, deserved a deeper investigation, because such an observed chemical shift at 10^{-3} M (9.2035 ppm) is not coherent with a completely non-H-bonded NH bearing an acyl group, the corresponding value in reference monomer Ac-AOPIC-OMe **8** being only 7.3912 ppm. Moreover, in **8** the δ_{obs} raises to 8.2754 ppm at 0.1 M, when the percent molar fraction of intermolecularly H-bonded Ac-AOPIC-OMe is about 37%, so that the relevant δ_{obs} observed at 10^{-3} M for the second residue NH of Boc-$(AOPIC)_2$-OMe **4** must be essentially due to a large extent of intramolecular H-bonding.

Then, even if non-linear regressions for both NHs of Boc-$(AOPIC)_2$-OMe **4** are apparently perfectly describing a simple monomer/dimer equilibrium (Table 6 and Figure 33), in the case of the second residue NH the increase of δ_{obs} with the concentration must be due to the intermolecular H-bonding of the residual amount of intramolecularly non-H-bonded **4**, while the extrapolated chemical shift at infinite dilution must be the weighted average of non-H-bonded and intramolecularly H-bonded **4** (Scheme 2).

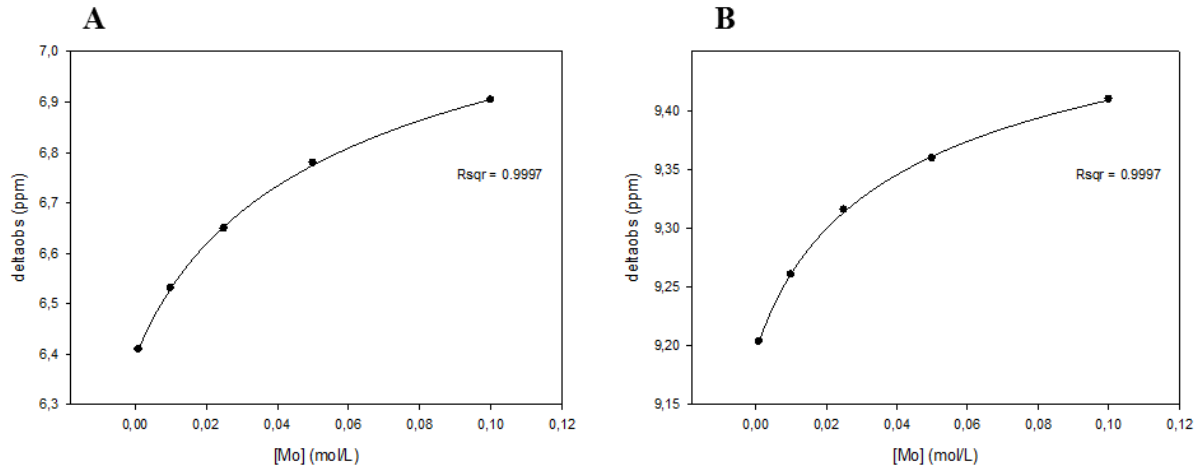

Figure 33. Non-linear regressions for dilution experiments data of Boc-$(AOPIC)_2$-OMe (eq 6). (A) Intramolecularly non-H-bonded first residue NHBoc. (B) Intramolecularly H-bonded second residue NHBoc.

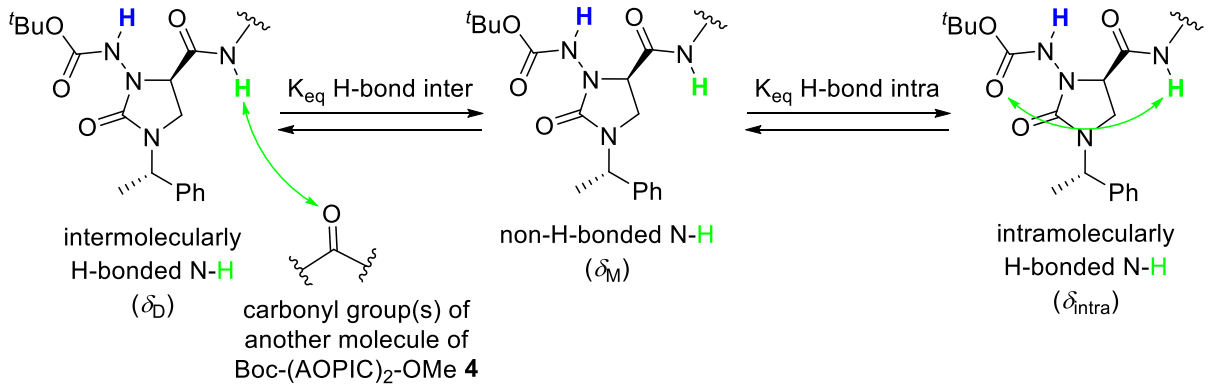

Scheme 2. H-bonding equilibria of second residue NH of Boc-(AOPIC)$_2$-OMe 4.

In this case, the actual (equilibrium) non-H-bonded monomer concentration [M], the intramolecularly H-bonded monomer concentration [M_{intra}] and the intermolecularly H-bonded dimer concentration [D] can be related to the total (initial) substrate concentration [M_0] by eq 7.

eq 7 $$[\mathbf{M_0}] = [\mathbf{M}] + [\mathbf{M_{intra}}] + \mathbf{2}[\mathbf{D}]$$

The observed chemical shift (δ_{obs}) is obtained weighting the non-H-bonded monomer (δ_M), intramolecularly H-bonded monomer (δ_{intra}) and intermolecularly H-bonded dimer (δ_D) chemical shifts by the respective mole fractions f_M, f_{intra} and f_D eq 8).

eq 8 $$\boldsymbol{\delta_{obs} = \delta_M f_M + \delta_{intra} f_{intra} + \delta_D f_D}$$

The equilibrium constants for the formation of the intermolecularly H-bonded dimer, K_{inter}, and the intramolecularly H-bonded monomer, K_{intra}, can be written as a function of molar fractions eq 9 and eq 10):

eq 9 $$\mathbf{K_{inter}} = \frac{\sqrt{[\mathbf{D}]}}{[\mathbf{M}]} = \frac{\sqrt{f_D}}{f_M\sqrt{2[\mathbf{M_0}]}}$$

eq 10 $$\mathbf{K_{intra}} = \frac{[\mathbf{M_{intra}}]}{[\mathbf{M}]} = \frac{f_{intra}}{f_M}$$

Then, the molar fractions of dimer and intramolecularly H-bonded monomer can be written as in eq 11 and eq 12:

eq 11 $$\boldsymbol{f_D = 2K_{inter}^2[M_0]f_M^2}$$

eq 12 $$\boldsymbol{f_{intra} = K_{intra}f_M}$$

Substituting eq 12 in $f_D = 1 - f_M + f_{intra}$, we can easily see in eq 13 that the equilibria in Scheme 2 behave exactly as the simple monomer/dimer equilibrium used for the previous calculation reported in Table 6. Thus, the relationship between the dimer molar fraction and the "apparent" monomer molar fraction (f_M*(1+K_{intra})) must be at the basis of the excellent non-linear regression obtained even in the case of the largely intramolecularly H-bonded proton in Boc-(AOPIC)$_2$-OMe **4**.

eq 13 $$\boldsymbol{f_D = 1 - f_M(1 + K_{intra})}$$

Then, substituting eq 13 in eq 11 and rearranging, the quadratic equation eq 14 can be easily obtained.

eq 14 $$\boldsymbol{2K_{inter}^2[M_0]f_M^2 + (1 + K_{intra})f_M - 1 = 0}$$

The two solutions for f_M are in eq 15, but the only one with a physical sense is that one with the plus sign, because f_M must be a positive number.

eq 15 $$\boldsymbol{f_M = \frac{-(1+K_{intra}) \pm \sqrt{(1+K_{intra})^2 + 8K_{inter}^2[M_0]}}{4K_{inter}^2[M_0]}}$$

The substitution of eq 12 and eq 13 in eq 8 and some rearrangements give eq 16, where f_M is as reported above, thus offering the equation to be interpolated by non-linear regression of δ_{obs} *vs* [M_0] data reported in Table 6 for the partly intramolecularly H-bonded NH of Boc-(AOPIC)$_2$-OMe **4**.

eq 16 $$\boldsymbol{\delta_{obs} = \delta_D - f_M[\delta_D(1 + K_{intra}) - \delta_M - \delta_{intra}K_{intra}]}$$

Unfortunately, no reliable δ_M, δ_{intra}, K_{inter} and K_{intra} values could be obtained due to solving problems (numerically singular arrays occurred in the Marquardt algorithm), using both approaches, iterative and direct, as explained above. This is simply due to the fact that there are

infinite solutions, because the constant term in square parentheses is undetermined. Ultimately, this situation is due to the impossibility to determine independently δ_M, δ_{intra} and K_{intra}. In effect, only δ_D can be determined using eq 16, and its value is exactly the same as the one reported in Table 6 using eq 6. In fact, δ_D obtained using both eq 6 (for the monomer/dimer equilibrium) and eq 16 (for the non-H-bonded monomer/intramolecularly H-bonded monomer/dimer equilibrium) must be the same, because in both cases when $[M_0]$ raises δ_{obs} tends to δ_D.

Anyway, some extremely useful deductions can be obtained by simple considerations. If we use the highest chemical shifts obtained for tetramer Boc-(AOPIC)$_4$-OMe **5** (9.5553 ppm) or hexamer Boc-(AOPIC)$_6$-OMe **6** (9.6148 ppm) in diluted solutions of anhydrous $CDCl_3$ as approximate values for an almost completely intramolecularly H-bonded NH, and δ_M computed for the reference monomer Ac-AOPIC-OMe **8** as (7.3742 ppm) as an approximate value for the non-H-bonded NH of Boc-(AOPIC)$_2$-OMe **4**, then an approximate range for the molar fraction of intramolecularly H-bonded f_{intra} can be computed as follows. In an infinitely diluted solution, when self-association is null, the "apparent" δ_M computed using eq 6 and reported in Table 6 must be equal to $\delta_{inf.dil.}$ (δ at infinite dilution) in eq 17, easily obtained from eq 8 and eq 12 with a little algebra and $f_D = 0$, thus the value extrapolated supposing the simple equilibria in Scheme 1 is just the expected weighted average of the unknown δ_{intra} and "true" δ_M values.

eq 17 $$\boldsymbol{\delta_{inf.dil.} = \delta_M f_{M\ inf.dil.} + \delta_{intra} f_{intra\ inf.dil.} = f_{M\ inf.dil.}(\delta_M + \delta_{intra} K_{intra})}$$

The useful eq 18 can be easily derived from eq 17 and $f_{M\ inf.dil.} = 1 - f_{intra\ inf.dil.}$ ($f_{D\ inf.dil.} = 0$).

eq 18 $$\boldsymbol{f_{intra\ inf.dil.} = \frac{\delta_{infinite\ dilution} - \delta_M}{\delta_{intra} - \delta_M}}$$

Once $f_{intra\ inf.dil.}$ and $f_{M\ inf.dil.} = 1 - f_{intra\ inf.dil.}$ for an infinite dilution are computed using suitable values for δ_{intra} and δ_M, K_{intra} can be computed with eq 10. Eventually, inserting δ_{intra}, δ_M and K_{intra} in eq 16, K_{inter} can be obtained by non-linear regression.

Using the $\delta_{inf.dil.} = 9.1943$ ppm obtained previously, the approximate $\delta_M = 7.3742$ ppm (taken from the reference compound **8**), and the two values reported above for δ_{intra}, a 83.4% (using $\delta_{intra} = 9.5553$ ppm) or 81.2% (using $\delta_{intra} = 9.6148$ ppm) intramolecularly H-bonded conformer can be evaluated at infinite dilution, that is $K_{intra} = 5.042$ ($\delta_{intra} = 9.5553$ ppm) or 4.329 ($\delta_{intra} = 9.6148$ ppm) (Table 7). Inserting these values, together with the computed δ_D, the δ_M for the reference monomer and the appropriate δ_{intra} in eq 16, gives by non-linear regression a K_{inter} =

20.67 (for K_{intra} = 5.042 and δ_{intra} = 9.5553 ppm) or 18.23 (for K_{intra} = 4.329 and δ_{intra} = 9.6148 ppm), always with R^2 = 0.9997.

Table 7. Evaluation of K_{intra}, K_{inter} and f_D for the second residue NH of compound 4, using δ_M of compound 8 and approximate values for δ_{intra}.

Approximate δ_{intra} (ppm)	K_{intra} (M^{-1})[a]	K_{inter} (M^{-1})[b]	f_D[c] at various [M_0]
9.5553	5.0419	20.672	0.0224 (0.001 M) 0.0429 (0.002 M) 0.0618 (0.003 M) 0.0794 (0.004 M) 0.0957 (0.005 M) 0.1110 (0.006 M) 0.1254 (0.007 M) 0.1389 (0.008 M) 0.1516 (0.009 M) 0.1637 (0.010 M) 0.2928 (0.025 M) 0.4089 (0.050 M) 0.5260 (0.100 M)
9.6148	4.3285	18.231	0.0224 (0.001 M) 0.0429 (0.002 M) 0.0618 (0.003 M) 0.0794 (0.004 M) 0.0957 (0.005 M) 0.1110 (0.006 M) 0.1254 (0.007 M) 0.1389 (0.008 M) 0.1516 (0.009 M) 0.1637 (0.010 M) 0.2928 (0.025 M) 0.4089 (0.050 M) 0.5260 (0.100 M)

[a] Calculated as described in the text, for both the approximated δ_{intra} values reported in Column 1 and using for δ_M the limiting value computed for compound **8**. [b] Calculated by non-linear regression of eq 16, as described in the text. [c] H-bonded dimer molar fractions calculated for the total substrate concentrations [M_0] indicated, using eq 15 and then eq 13.

Finally, it is interesting to note that the molar fractions of H-bonded dimer f_D at various total substrate concentrations [M_0] reported in Table 7 are independent from the choice of δ_{intra} and are also identical to the ones in Table 6.

2.5.3 Titrations with DMSO-d_6.

Table 8. Chemical shifts *vs* added DMSO-d_6 data for compounds 8, 4 and 5 in $CDCl_3$ at 25 °C[a].

Compound	% DMSO-d_6 added (v/v)	$\Delta\delta_{\text{first residue}}$ (ppm)	$\delta_{\text{second residue}}$ (ppm)	$\delta_{\text{third residue}}$ (ppm)	$\delta_{\text{fourth residue}}$ (ppm)
8	0	7.391	---	---	---
	1	7.980			
	2	8.360			
	3	8.637			
	4	8.827			
	6	9.084			
	8	9.263			
	10	9.390			
	15	9.603			
	20	9.715			
	25	9.789			
	30	9.843			
	only DMSO-d_6[b]	9.984			
4	0	6.459	9.201	---	---
	2	7.254	9.764		
	4	7.546	9.907		
	6	7.670	9.976		
	8	7.746	10.014		
	10	7.803	10.036		
	15	7.912	10.074		
	20	7.991	10.087		
	25	8.069	10.098		
	30	8.134	10.105		
	only DMSO-d_6[b]	8.845	10.192		
5	0	7.192	9.111	9.312	9.555
	1	7.955	9.489	9.686	9.714
	2	8.057	9.532	9.784[c]	9.784[c]
	3	8.104	9.573	9.827[c]	9.827[c]
	4	8.133	9.600	9.859[c]	9.859[c]
	6	8.163	9.628	9.892[c]	9.892[c]
	8	8.188	9.659	9.925[c]	9.925[c]
	10	8.204	9.678	9.945[c]	9.945[c]
	15	8.249	9.747	10.007[c]	10.007[c]
	20	8.282	9.791	10.046[c]	10.046[c]
	25	8.314	9.832	10.083[c]	10.083[c]
	30	8.356	9.878	10.124[c]	10.124[c]
	only DMSO-d_6[b]	8.837	9.979	10.226	10.248

[a] 1 mM (**4** and **8**) or 2 mM (**5**) solutions in $CDCl_3$. [b] 1 mM (**4** and **8**) or 2 mM (**5**) solutions in DMSO-d_6. [c] Completely superimposed peaks (no detectable shoulders).

Table 9. Chemical shifts *vs* added DMSO-d_6 data for compound 6 (2 mM solution in $CDCl_3$ at 25 °C).

% DMSO-d_6 added (v/v)	$\delta_{\text{first residue}}$ [b] (ppm)	δ 2 [b] (ppm)	δ 3 [b] (ppm)	δ 4 [b] (ppm)	δ 5 [b] (ppm)	δ 6 [b] (ppm)
0	7.143	9.243	9.306	9.487	9.541	9.615
1	8.104	9.136	9.647	9.694	9.774	9.787
2	8.177	9.154	9.683	9.753	9.803	9.823
3	8.207	9.184	9.711	9.794	9.834	9.849
4	8.232	9.208	9.739	9.830	9.859	9.877
6	8.283	9.265	9.793	9.873	9.915	9.928
8	8.301	9.279	9.808	9.895	9.931	9.945
10	8.323	9.275	9.828	9.889	9.952	9.990
15	8.275	9.319	9.801	9.925	9.979	9.998
20	8.245	9.292	9.788	9.894	9.953	9.972
25	8.248	9.310	9.788	9.906	9.963	9.982
30	8.250	9.299	9.787	9.896	9.959	9.976
only DMSO-d_6 [a]	8.864	10.018	10.050	10.244	10.270 [c]	10.270 [c]

[a] 2 mM solution in DMSO-d_6. [b] Only the resonance of first residue BocNH could be assigned by analogy with compounds **4** and **5**. The resonances 2-5 could not be assigned to the residues. The numbering indicates the ascending order of chemical shifts. [c] Completely superimposed peaks (no detectable shoulders).

Table 10. Increments in chemical shift passing from only $CDCl_3$ to 10% added DMSO-d_6 ($\Delta\delta_{10\%}$) and from only $CDCl_3$ to only DMSO-d_6 for compounds 8, 4 and 5 at 25 °C[a].

Compound	$\Delta\delta_{10\%}$ (ppm) [$\Delta\delta_{100\%}$ (ppm)] [b]			
	first residue	second residue	third residue	fourth residue
8	1.999 [2.593]	---	---	---
4	1.344 [2.386]	0.835 [0.991]	---	---
5	1.012 [1.645]	0.567 [0.868]	0.633 [0.914]	0.390 [0.693]

[a] Computed using values in Table 8. [b] $\Delta\delta_{10\%} = \delta_{10\%\ \text{DMSO-}d6\ \text{added}} - \delta_{CDCl3}$, $\Delta\delta_{100\%} = \delta_{\text{DMSO-}d6} - \delta_{CDCl3}$.

Table 11. Increments in chemical shift passing from only $CDCl_3$ to 10% added DMSO-d_6 ($\Delta\delta_{10\%}$) and from only $CDCl_3$ to only DMSO-d_6 for compound 6 at 25 °C[a].

$\Delta\delta_{10\%}$ (ppm) [$\Delta\delta_{100\%}$ (ppm)] [b]					
first residue [c]	NH 2 [c]	NH 3 [c]	NH 4 [c]	NH 5 [c]	NH 6 [c]
1.180 [1.721]	0.032 [0.775]	0.522 [0.744]	0.402 [0.757]	0.411 [0.729]	0.375 [0.655]

[a] Computed using values in Table 9. [b] $\Delta\delta_{10\%} = \delta_{10\%\ \text{DMSO-}d6\ \text{added}} - \delta_{CDCl3}$, $\Delta\delta_{100\%} = \delta_{\text{DMSO-}d6} - \delta_{CDCl3}$. [c] Only the resonance of first residue BocNH could be assigned by analogy with compounds **4** and **5**. The resonances 2-5 could not be assigned to the residues. The numbering indicates the ascending order of chemical shifts.

2.5.4 Computational details

MD simulations were carried out with the AMBER 11.0 suite of programs. The peptide is parametrized using GAFF (general AMBER force field) force field. The standard RESP procedure is carried out to assign charges to atoms by Antechamber.

The peptide was built and immersed in a solvent box of explicit chloroform molecules. Periodic boundary conditions were used. An equilibration protocol consisting of four individual steps was applied, resulting in an unconstrained well-tempered NPT ensemble at target conditions. A Langevin thermostat was used to set a constant temperature at 300 K and 1 atm. Particle Mesh Ewald summation was used throughout (cut off radius of 10 Å for the direct space sum). Bonds involving H atoms were constrained using the SHAKE algorithm, and a time step of 2 fs was applied in all runs. Overall sampling time for MD production was 100 ns.

Snapshot structures were saved into individual trajectory files every 5000 time steps, that is, every 10 ps of molecular dynamics, for a total of 10000 snapshots. MD simulations were carried out using pmemd.

FES building

Two-dimensional free-energy profiles for the peptide in explicit solvent were obtained as a function of PCA1 and PCA2. The program **"**ptraj**"** in the AMBER package was used in the PCA. The values are given in kcal mol^{-1}. The energy landscape of the peptide is visualized by means of free-energy functions, which are projected as contour lines onto a two-dimensional space formed by the PCA1/PCA2 axes. These coordinates are derived from a principal component analysis. The free-energy change associated with the passage between two different states of a system in thermodynamic equilibrium is given by $\Delta G = -RT (\ln p1/p2)$. Here, R is the ideal gas constant, T is the absolute temperature, and p_i is the probability of finding the system in state i. The two-dimensional space defined by the PCA1 and PCA2 axes has been divided into a grid and the free energy has been calculated for each bin of the grid on the basis of the previous equation. The whole set of G values was shifted in such a way that the lowest value of the free energy surface corresponds to zero. Thus, the reported ΔG values represent the transfer free energies with respect to the bin that has been set to zero. To obtain the p values, the trajectory at ambient temperature was projected onto the PCA1/PCA2 space, and p corresponds to the number of times the trajectory "visits" a given bin.

H-bond lifetimes

Hydrogen bonds are detected based on a geometric criterion:

i) The distance between acceptor and hydrogen is less than or equal to distance (default is 3.6 Å).

ii) The angle between donor-hydrogen-acceptor is greater than or equal to angle (default is 120º).

All the snapshot of the MD trajectory is analyzed and the existence of the hydrogen bond is calculated every snapshot, so to determine the percentage of occupation time.

*2.5.5 Backbone Resonances Assignment for Compounds **4** and **5***

In the case of hexamer Boc-(AOPIC)$_6$-OMe **6**, the extensive overlap and the broad peaks prevented the residue-specific assignment of ^{1}H and ^{13}C backbone resonances, even after many attempts with prolonged acquisition times, different solvent mixtures and temperatures. On the contrary, ^{1}H and ^{13}C resonances could be assigned for dimer Boc-(AOPIC)$_2$-OMe **4** and tetramer Boc-(AOPIC)$_4$-OMe **5**, with the exception of phenylethyl side chains. In particular, for dimer **4** the analysis of a concentrated sample (0.1 M) in $CDCl_3$ at 35 °C allowed us to obtain resolved ^{1}H and ^{13}C signals and easily detectable HSQC and HMBC crosspeaks, while for tetramer **5** it was necessary to use an anhydrous $CDCl_3$:DMSO-d_6 9:1 solvent system at 19 °C, in order to narrow ^{1}H and ^{13}C resonances and then detect the requested heteronuclear couplings. The assignments for dimer **4** (Table 12) and tetramer **5** (Table 13) were obtained as follows:

- from the ^{t}Bu protons, the Boc carbonyl group resonance was identified by HMBC spectrum;
- from the Boc carbonyl carbon, the NH(A) was assigned by HMBC correlation;
- NH(A) did not show the expected crosspeak with C4(A), but furnished an evident ^3J coupling with the imidazolidinonic carbonyl C2(A);
- from C2(A), both H_5 and H_5' of residue A were assigned by HMBC correlation;
- from H_5(A) and H_5'(A), C5(A) was identified by HSQC spectrum;
- from C5(A), ^2J coupling allowed to assign H_4(A) resonance;
- from H_4(A), the resonances of C4(A) and carbonyl group (peptidic CO) of residue A were assigned by HSQC and HMBC correlations, respectively;
- from the peptidic CO(A), HMBC spectrum revealed the ^2J coupling with the NH(B) resonance;

- from NH(B), continuing to exploit the same step-by-step approach, all the backbone resonances were sequentially assigned.

Table 12. Assignment of ^{1}H and ^{13}C backbone resonances of compound Boc-$(AOPIC)_2$-OMe 4 (0.1 M in $CDCl_3$ at 35 °C).

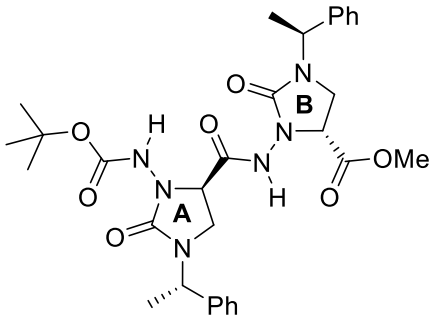

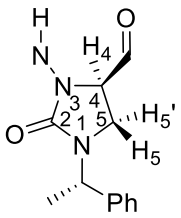

Boc-$(AOPIC)_2$-OMe **4**

	A	B
Peptidic CO	169.7	---
C4	59.3	57.4
NHCO-O^{t}Bu	156.3	---
$NHCO_2$-$C(CH_3)_3$	82.6	---
$NHCO_2$-$C(CH_3)_3$	28.2	---
C5	41.1	39.9
Imidazolidinone N1-(CO)-N3 (C2)	158.9	157.7
CO_2CH_3	---	52.7
CO_2CH_3	---	170.1
NH	6.90	9.41
H_4	4.17	4.47
$H_5 + H_5'$	3.44-3.46	3.27-3.29

$NHCO_2$-C($C\underline{H}_3$)$_3$	1.50	---
$CO_2C\underline{H}_3$	---	3.75

Table 13. Assignment of ^{1}H and ^{13}C backbone resonances of compound Boc-(AOPIC)$_4$-OMe 5 (20 mM in $CDCl_3$:DMSO-d_6 9:1 at 19 °C, with powdered 4 Å m.s.)

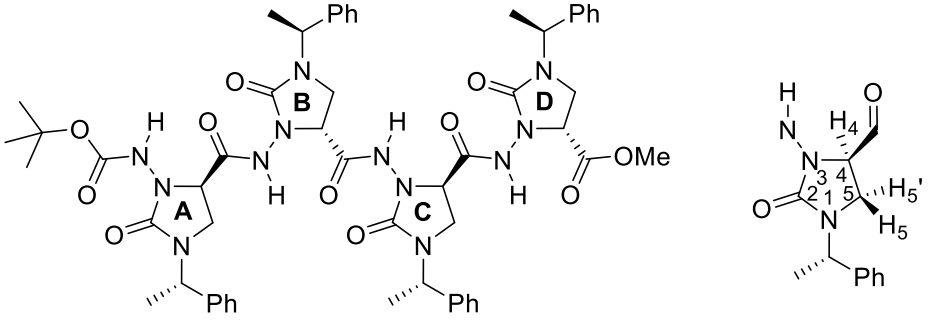

Boc-(AOPIC)$_4$-OMe **5**

	A	B	C	D
Peptidic $\underline{C}O$	169.95	170.66	168.54	---
$\underline{C}4$	58.46	58.07	58.76	56.77
$NH\underline{C}O$-O^{t}Bu	154.74	---	---	---
$NHCO_2$-$\underline{C}(CH_3)_3$	81.04	---	---	---
$NHCO_2$-C($\underline{C}H_3$)$_3$	28.11	---	---	---
$\underline{C}$-5	41.02	40.70	41.22	39.39
Imidazolidinone N1-($\underline{C}O$)-N3 ($\underline{C}2$)	158.40	157.36	157.82	157.50
$CO_2\underline{C}H_3$	---	---	---	52.17
$\underline{C}O_2CH_3$	---	---	---	169.00
$N\underline{H}$	8.16	9.49	9.90	9.91
H_4	4.44	4.45	4.17	4.30

H_5	3.25	3.17	3.06	2.93
H_5'	3.83	3.76	3.70	3.54
$NHCO_2$-C($C\underline{H}_3$)$_3$	1.42	---	---	---
$CO_2C\underline{H}_3$	---	---	---	3.40

CHAPTER 2:

Achiral α-hydrazidopeptides

3. ACHIRAL α-HYDRAZIDOPEPTIDES

3.1 Introduction

As seen in the previous chapters, foldamers based on α-hydrazido acids tethered into an imidazolidinonic ring fold into one of the two variant of the 8-helix secondary structure: the "pure" 8-helix, which is a quite rare conformation shown by α-aminoxy-peptides[9] and peculiar β-peptides,[11,12] or, most probably, its variant made of consecutive hydrazino turns, found so far only in α-hydrazino-peptides,[10] where the NHs participate to bifurcated H-bonds and each 8-membered cycle include an additional 5-membered cycle involving the sp^3 hydrazinic nitrogen. Both of these structures allow the substituents of the various residues to be arranged alternately on opposite sides along the helix axis.

With the aim of devising simpler and cheaper analogues, we focused our attention on the synthesis of the unconstrained and achiral version of the previous oligomers (Figure 34). In fact, besides the improvement in our understanding of the factors governing the folding of both conformationally constrained and unconstrained α-hydrazido-peptides, our target is to obtain the same secondary structure with much less synthetic effort and to increase the ease of side chains substitution. This is due to the fact that such a disposition of side chains could also be a good starting point for a practical purpose, that is the synthesis of amphiphilic foldamers to be tested as antibacterial agents.

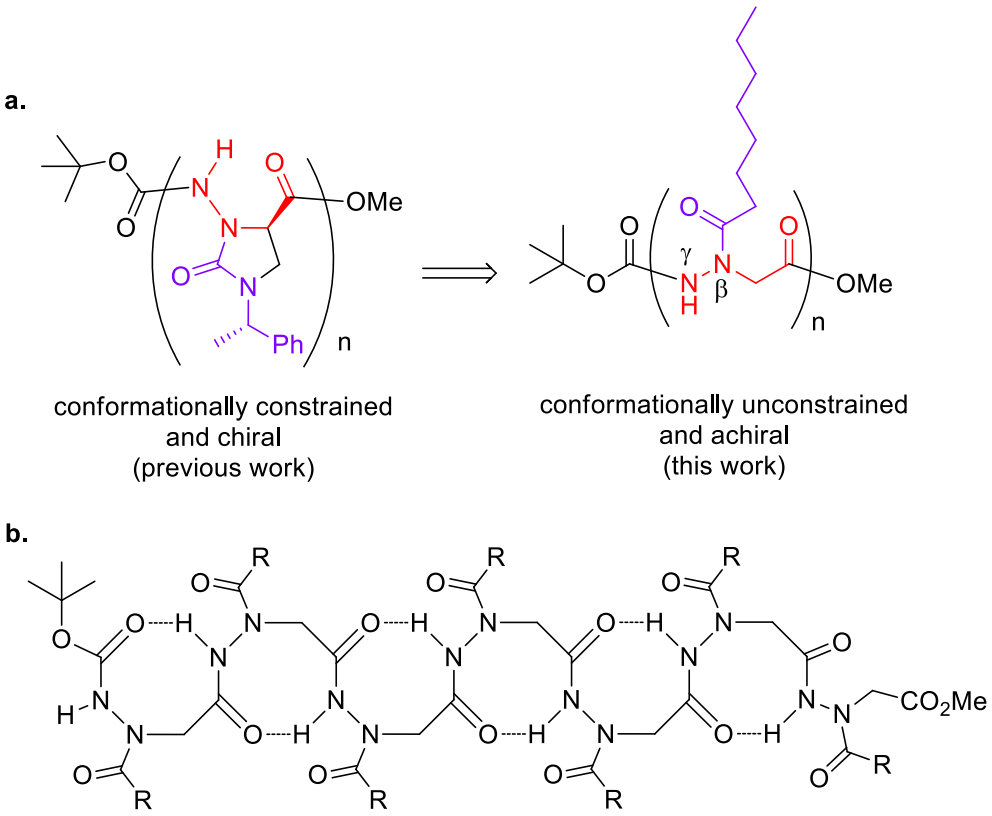

Figure 34. a) Variation of the synthetic target from the imidazolidinone-constrained oligo-α-hydrazido-peptides to the conformationally unconstrained and achiral oligo-α-hydrazido-peptides. b) Exemplification of the desired 8-helix structure with the alternate disposition of the substituents (the "pure" 8-helix folding was depicted for convenience).

To this end, we envisaged that it would be easier to perform the synthesis of new foldamers exploiting easily obtainable achiral monomers as building blocks for the usual peptide synthesis in homogeneous phase. The N-octanoyl hydrazido acid derivatives reported in Figure 34 were chosen on the basis of their solubility in the most common organic solvents, with the aim of carrying out - as usual in the foldamers' field - a complete structural determination in a non-aqueous environment, before undertaking the synthesis and the following elucidation of folding for a water-soluble analogue.

3.2 Results and Discussion

3.2.1 Synthesis of α-hydrazido acid monomers and oligomers

The synthesis of the N-Boc-protected monomer turned out to be unexpectedly challenging. It was optimized starting from *t*-butyl carbazate **9**, and methyl bromoacetate **10**, and a lot of solvents, bases and temperatures were employed in order to find the best experimental

conditions and to attain the highest possible yield (Scheme 3). In fact, due to the poor nucleophilicity of *t*-butyl carbazate, even slightly nucleophilic amines, such as TEA (triethylamine), gave a competitive S_N2 reaction onto bromoacetate, leading to extremely low yields of the alkylated carbazate **11**. Using an insoluble base (anhydrous K_2CO_3) in dichloromethane (DCM) or 1,2-dichloroethane (DCE) at reflux, lead to moderate yields in reasonable reaction times, but substantial amounts of dialkylated carbazate were invariably recovered, probably due to the deprotonation of BocNH in compound **11** caused by the excessive basicity of K_2CO_3.

Therefore, we devised to use a weaker base, diisopropylethylamine (DIPEA), which is also strongly hindered and non-nucleophilic, to remove the hydrobromic acid formed by the slow S_N2 reaction between *t*-butyl carbazate and methyl bromoacetate. Moreover, the reaction was carried out at room temperature, but using a very little amount of solvent (DCM, 0.5 mL/mmol carbazate) to compensate for the low reactivity of carbazate **9**. Under these conditions, the intermediate product **11** was finally obtained in an excellent yield on a multigram scale (Scheme 3) and used directly in the following reaction.

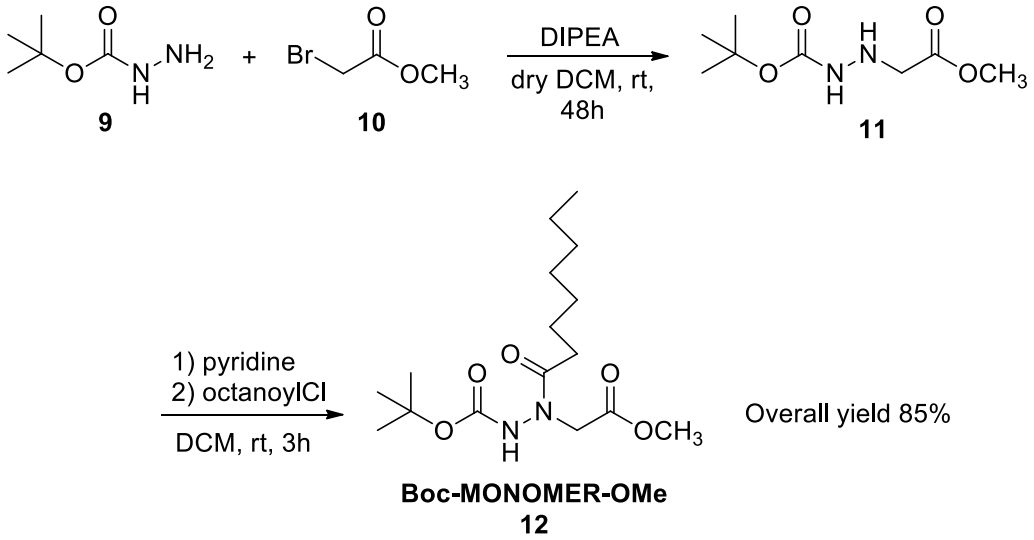

Scheme 3. Synthesis of Boc-MONOMER-OMe 12.

The subsequent acylation reaction of intermediate **11** with octanoyl chloride was optimized in DCM at room temperature, using different tertiary bases and stoichiometries. In fact, the commonly used bases TEA and DIPEA turned out to be excessively basic, leading to the further octanoylation at the Boc-protected nitrogen, while the less basic pyridine furnished the most selective reaction, giving the desired product **12** in an excellent overall yield.

The nomenclature reported in Scheme 3 for compound **12**, and used hereafter to describe all the monomers and oligomers throughout the discussion, relies on a simple description of the number of hydrazidic ("mer") units and of the type of N- and C-terminal derivatization, *N-terminalGroup-NumberOfResidues-CterminalGroup*: e.g. compound 12 is Boc-MONOMER-OMe = Boc protecting group at N-terminal – one hydrazidic residue – methyl ester derivatization at C-terminal).

Following the same approach already reported for the imidazolidinone-constrained hydrazido-peptides, other suitable monomeric compounds were also synthesized in order to be used as references in the spectroscopic evaluation of the presence and the strength of intramolecular hydrogen bonds. Indeed, even in this "unconstrained" case, all the NHs belonging to the various residues in all the synthesized oligomers, except the N-terminus, are not derivatized as carbazates, O-CO-NH-N, as in **Boc-MONOMER-OMe 12**, but as hydrazides, CH_2-CO-NH-N. To this purpose, the reference monomer **Ac-MONOMER-OMe 14**, was easily obtained from **12** by acidic removal of the Boc protecting group, followed by an extractive work-up under basic conditions that afforded the crude free hydrazide **13**, which was directly acetylated to give the desired **Ac-MONOMER-OMe 14** in very good overall yield (Scheme 4).

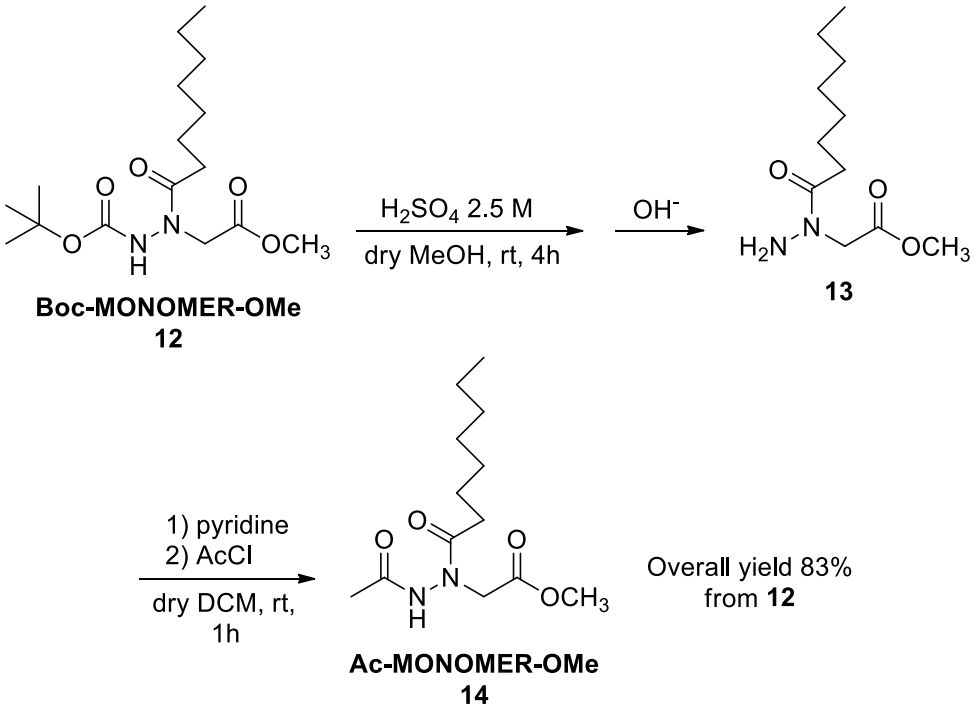

Scheme 4. Synthesis of the reference monomer Ac-MONOMER-OMe 14.

In addition, the C-terminal amide derivative **Boc-MONOMER-NH$_2$ 15**, was synthesized to verify the possible inherent tendency to form 8-membered H-bonded cycles, which was demonstrated to be typical for α-aminoxy[9] and α-hydrazino acid amide derivatives,[10] as well as for our imidazolidinone-tethered α-hydrazido acids (Paragraph 2.2 Results and Discussion).

Thus, starting compound **12** was submitted to ammonolysis in a buffer system, in order to minimize hydrolysis, and **Boc-MONOMER-NH$_2$** was obtained in excellent yield (Scheme 5).

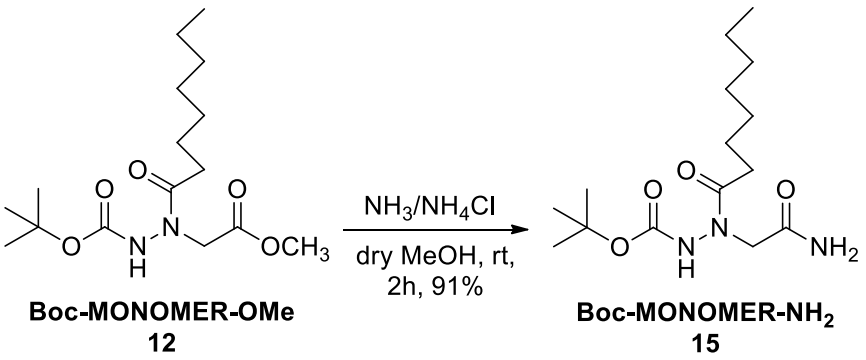

Scheme 5. Synthesis of the reference monomer Boc-MONOMER-NH$_2$ 15.

Starting from **Boc-MONOMER-OMe 12**, the C-terminal acid derivative **16**, suitable for the peptide coupling with compound **13**, was obtained in quantitative yield by hydrolysis (Scheme 6). Unfortunately, despite the numerous attempts carried out using different coupling agents (EDCI, PyBrOP, DCC) and reaction conditions, only traces of the highly impure dimer **Boc-DIMER-OMe**, **17**, were invariably obtained (Scheme 6). In fact, as expected from the experimental observation reported above for the synthesis of intermediate compound **11**, the desired reaction is very slow, due to very poor nucleophilicity of hydrazide **13**, which is further reduced in comparison to *t*-butyl carbazate. Even if the side reactions were not deeply investigated, they should likely involve the intramolecular cleavage of the activated derivatives of acid **16**, as supported by mass spectra indicating the formation of a byproduct deriving by cyclization followed by loss of *t*-butyl group.

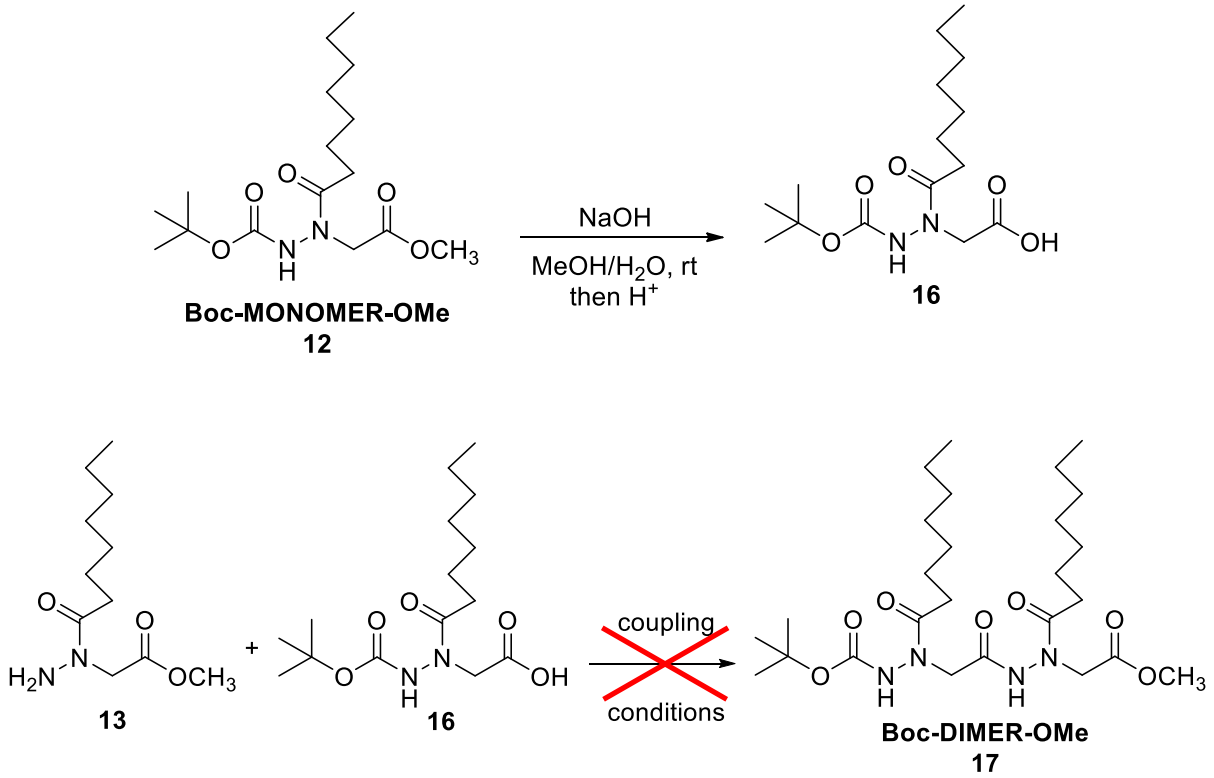

Scheme 6. Attempted synthesis of Boc-DIMER-OMe 17, by peptide coupling.

Once the unpracticality of the usual peptide coupling in solution phase was verified, we preferred not to try the oligomers synthesis in solid phase, but to use the same synthetic strategy already employed for the monomer, instead. To this end, the free hydrazide **13**, obtained from monomer **12** as described above, was transformed into the N-bromoacetyl derivative **18** in very good yield, by reaction with bromoacetyl bromide in the presence of pyridine (Scheme 7).

Then, exploiting again a S_N2 reaction in concentrated solution with DIPEA as the base, compound **18** was transformed into the intermediate **19**, which in turn was submitted to the acylation reaction with octanoyl chloride and pyridine, furnishing the desired dimer **17** in a good overall yield (Scheme 7).

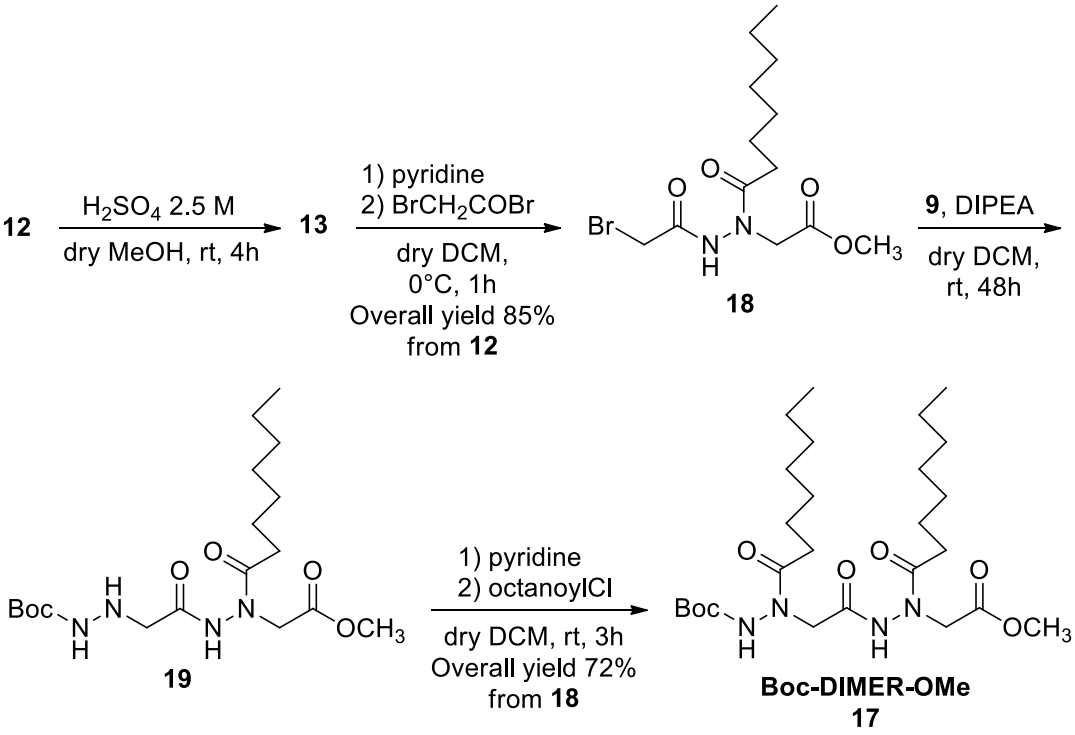

Scheme 7. Synthesis of Boc-DIMER-OMe 17.

The trimer was synthesized carrying out again a substitution reaction onto the N-terminal bromoacetyl derivative **18**, but exploiting the C-terminal hydrazide derivative **20** as the electrophile, instead of carbazate **9**. The hydrazidic derivative was obtained in high purity and in almost quantitative yield by the simple treatment of monomer **12** with hydrazinic buffer in a methanol/dichloromethane mixture, followed by the extractive work-up (Scheme 8). Thus, the crude compound **20** and the bromoacetyl derivative **18** were submitted to the S_N2 reaction in dry DCM, with DIPEA as the base to remove the hydrobromic acid. Eventually, the crude product **21** was rapidly purified by silica gel chromatography and then immediately treated with octanoyl chloride and pyridine, as previously described, to give **Boc-TRIMER-OMe 22**, in fairly good overall yield (Scheme 8).

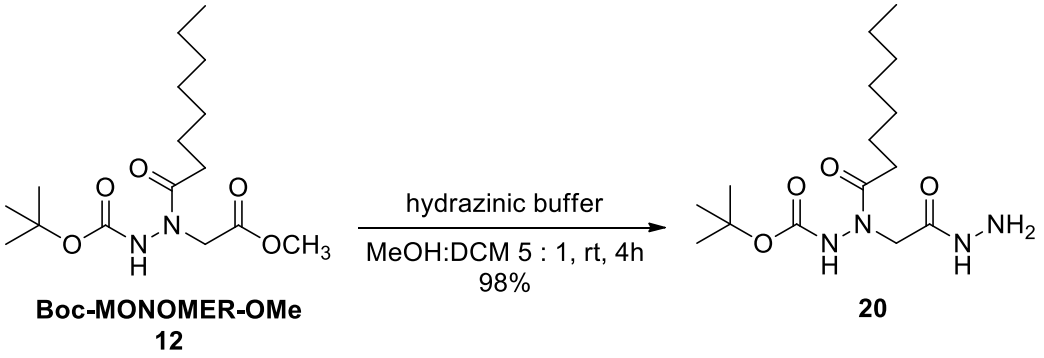

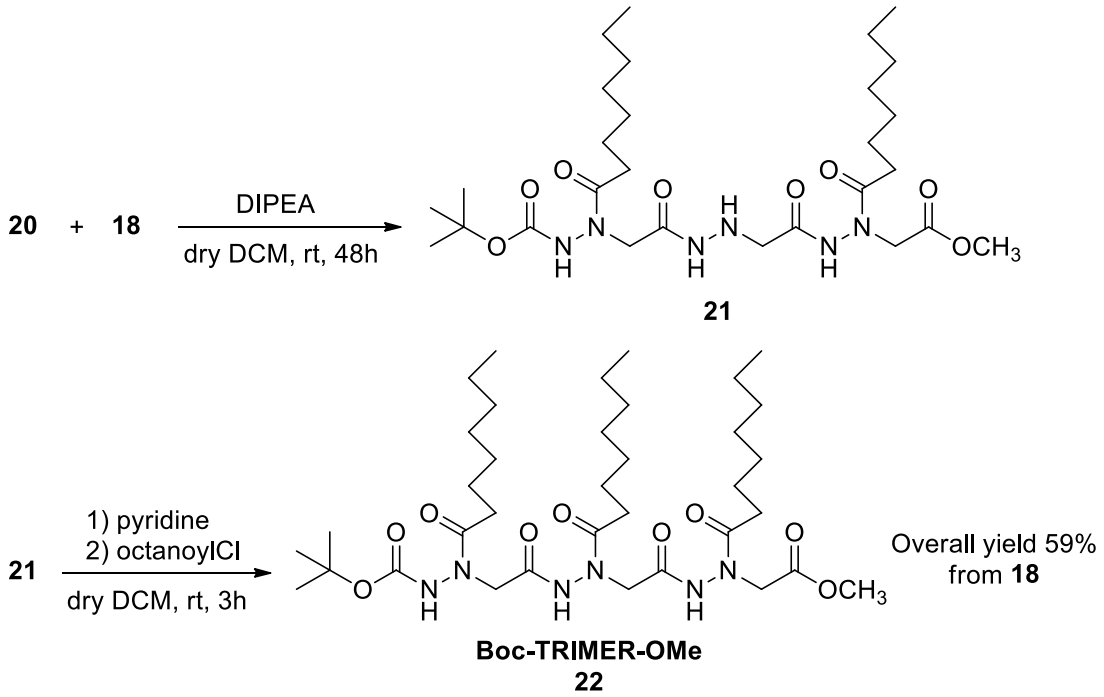

Scheme 8. Synthesis of Boc-TRIMER-OMe 22.

Starting from dimer **17**, and following the same synthetic approach, the bromoacetyl derivative **24** was obtained in good yield. Compound **24** was reacted with C-terminal hydrazide **20**, furnishing intermediate **25** that, after a rapid chromatographic purification, was octanoylated as already reported, then obtaining the desired **Boc-TETRAMER-OMe 26**, in satisfactory yield (Scheme 9).

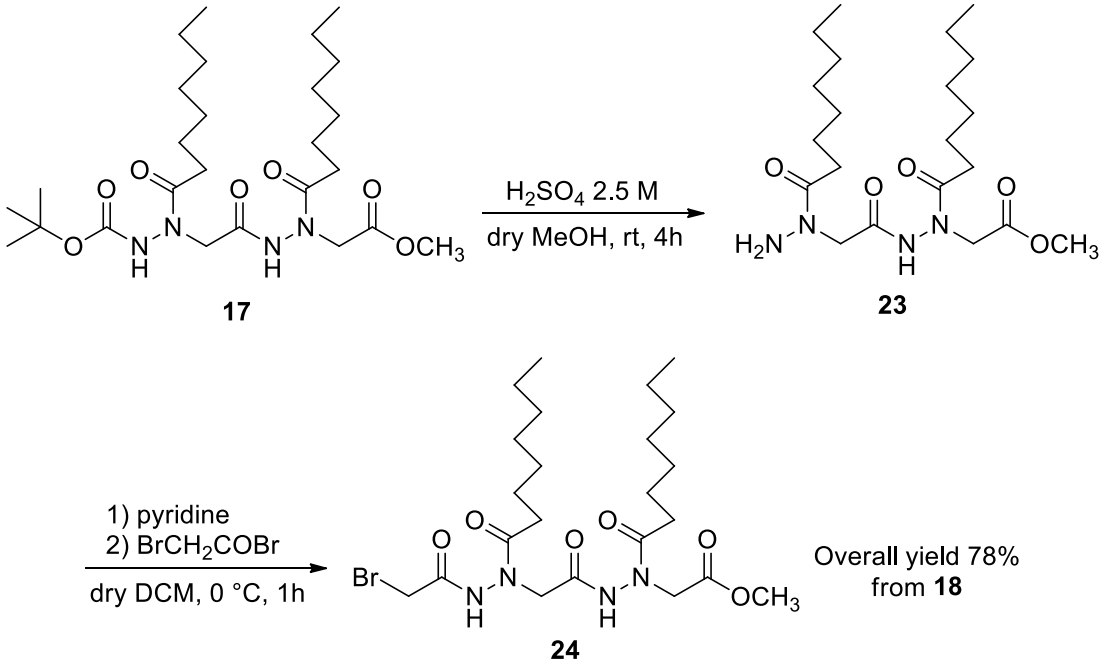

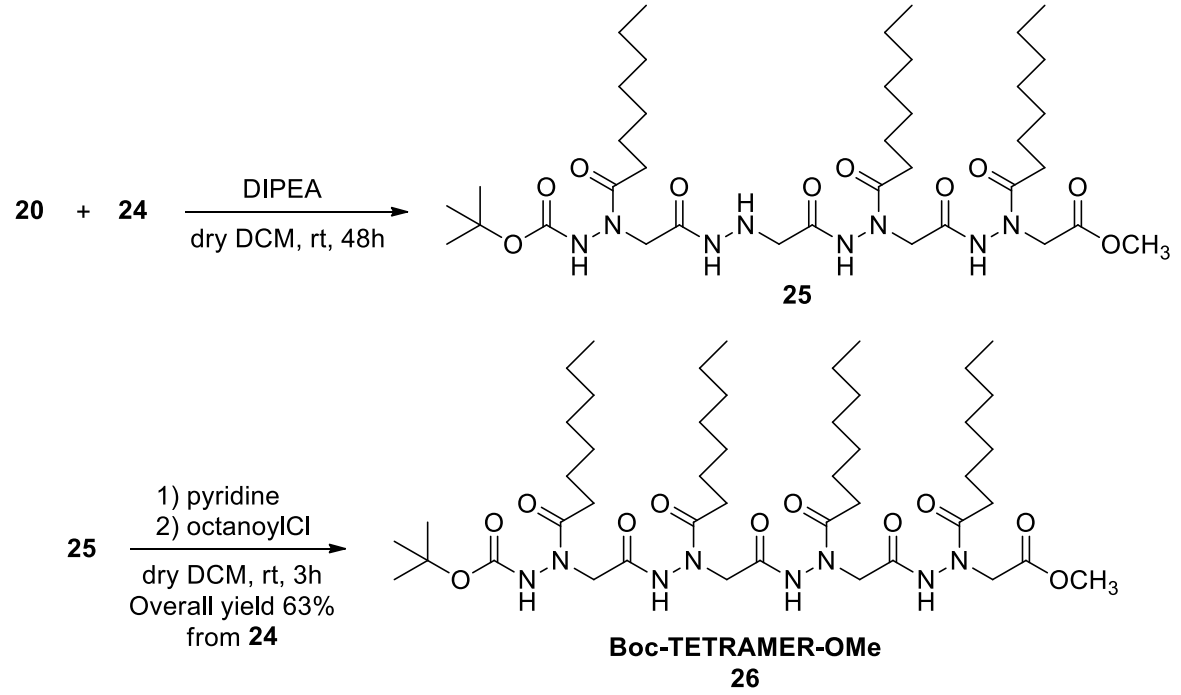

Scheme 9. Synthesis of Boc-TETRAMER-OMe 26.

The longest oligomer, heptamer **Boc-HEPTAMER-OMe 31**, was synthesized using only **Boc-TRIMER-OMe 22**, as the starting material. Thus, treatment of **22** with hydrazinic buffer gave in almost quantitative yield the C-terminal hydrazide **27**, while removal of Boc functionality, followed by acylation with bromoacetyl bromide, gave in fairly good yield the bromoacetyl derivative **29**. The reaction of compounds **27** and **29** was carried out according to the conditions described above, to give compound **30**, which after rapid purification by silica gel chromatography was eventually octanoylated to give the heptamer **31** (**Boc-EPTAMER-OMe**) in moderate overall yield (Scheme 10).

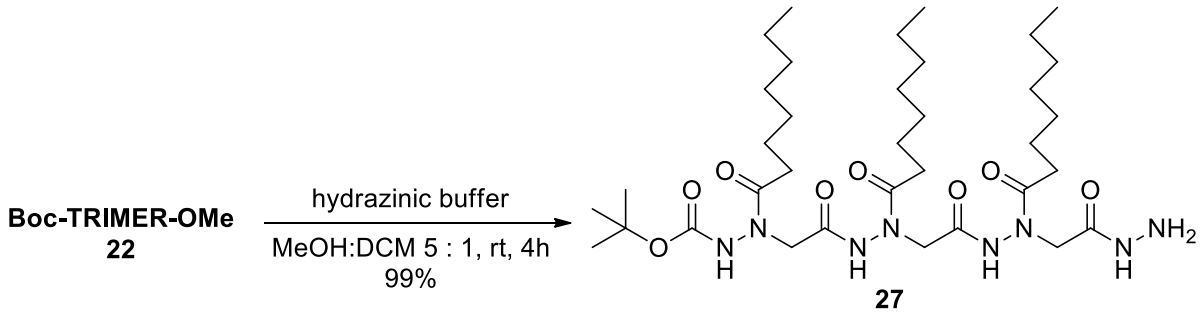

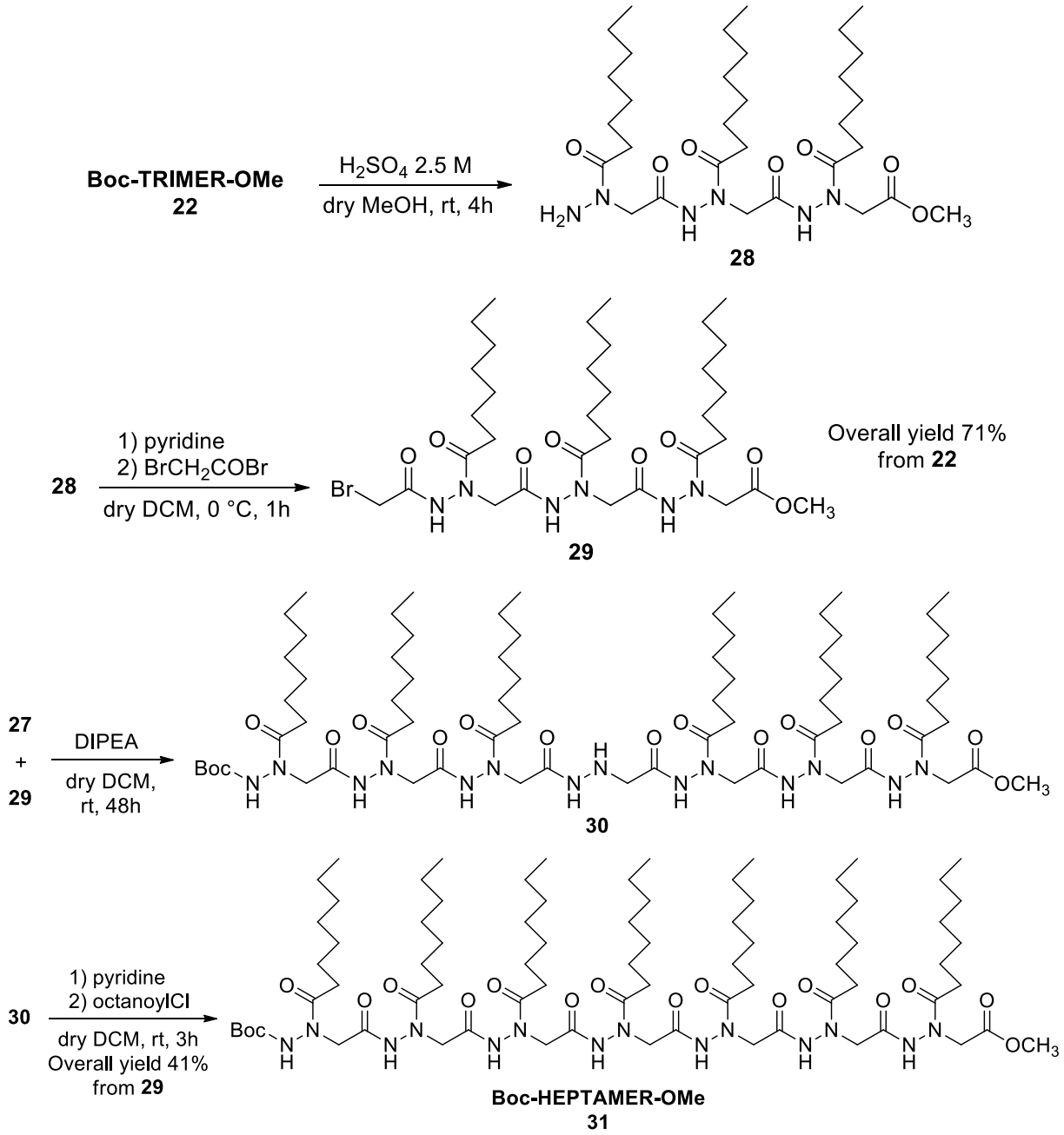

Scheme 10. Synthesis of Boc-HEPTAMER-OMe 31.

3.2.2 Preliminary assignment of secondary structure of oligomers

Although only the preliminary ^{1}H NMR spectra for compounds characterization were recorded so far in order to ascertain the structure of the synthesized compounds, some important indications can be drawn. Anyway, it should be noted that no bidimensional spectra have been recorded, yet. Thus, the assignment of NHs resonances, especially for the reference monomer Boc-MONOMER-NH_2 **15**, which will be used throughout the following discussion, is based only on the comparison of δ values, and the same apply to the intramolecular H-bonds, assigned only on a logical basis.

First of all, from the analysis of ^{1}H NMR spectrum of Boc-MONOMER-OMe **12**, it is evident that, in analogy with the imidazolidinone-tethered counterpart Boc-AOPIC-OMe **3**, its NH is not involved in any intramolecular hydrogen bond or, at the best, it is involved only in a very weak H-bond. Indeed, its chemical shift in 1 mM $CDCl_3$ solution (6.94 ppm) is typical of an isolated carbazate, and a similar value (6.83 ppm) was obtained for the BocNH of monomer **15** (Boc-MONOMER-NH_2), while 7.81 ppm for the AcNH of compound **14**, as reported in Figure 35.

In compound **15**, the amide proton shown in black is not involved in any hydrogen bond, displaying a chemical shift which is typical for free terminal amides (5.40 ppm), while the H in green is more deshielded (7.02 ppm, +1.63 ppm). This demonstrates the same inherent tendency to the formation of 8-membered H-bonded cycles reported for imidazolidinone based α-hydrazidopeptides (Paragraph 2.2 Results and Discussion)and for monomeric C-terminal amide derivative of an α-aminoxy acid, that lead to 8-helix structures in oligomers,[9] and also for a closely related C-terminal amide α-hydrazino acid,[10c] which actually showed the proclivity to form an 8-membered pseudocycle with an enclosed additional 5-membered cycle (see Paragraph 2.5 Supplementary session).

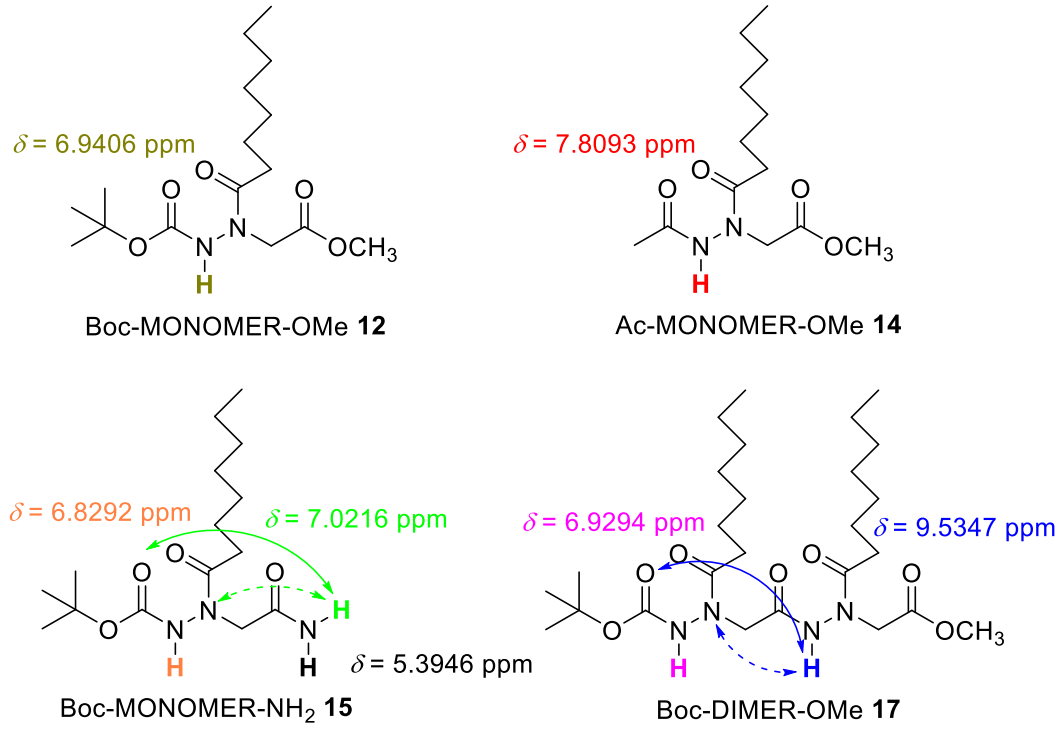

Figure 35. Chemical shifts for hydrazidic protons of Boc-MONOMER-OMe 12, Ac-MONOMER-OMe 14, Boc-MONOMER-NH_2 15 and Boc-DIMER-OMe 17 (10 mM solutions in $CDCl_3$ at 25 °C). The 8-membered H-bonded cycles are reported with continuous lines, the possible additional 5-membered cycles with dashed lines.

Another interesting feature of Boc-MONOMER-NH_2 is the existence of a series of signals due to a minor conformer, which is slowly interconverting with the predominating one, at least on the NMR time-scale. Such a feature is much less pronounced in the case of Boc-MONOMER-OMe **12**, where the resonances possibly due to partly locked conformers have low intensities (Figure 36).

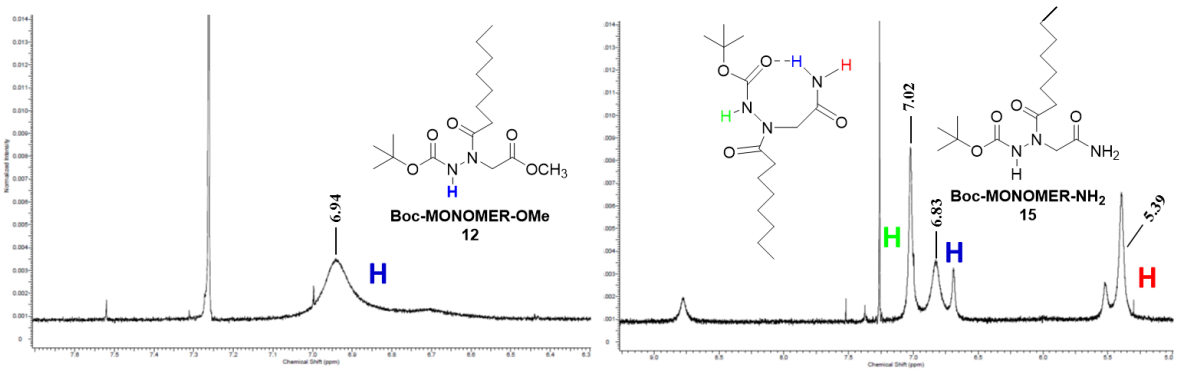

Figure 36. Comparison between the chemical shifts of the NHs of Boc-MONOMER-OMe, 12, and Boc-MONOMER-NH_2, 15, in which the presence of conformers is much more evident (10 mM solutions in $CDCl_3$ at 25 °C).

The comparison of the ^{1}H-NMR spectra of all synthesized oligomers (17, 22, 26 and 31) with the reference N-terminal acetylated monomer, Ac-MONOMER-OMe 14, further support the possibility for an 8-helix folding made of a series of hydrazido-turns as the preferred secondary structure even for this achiral and unconstrained version of the imidazolidinonic of α-hydrazidopeptides seen above (Chapter 2. Imidazolidinone-based α-Hydrazidopeptides).

As reported in Table 14, the chemical shift for the (very likely) non-hydrogen-bonded AcNH (7.81 ppm) in Ac-MONOMER-OMe 14 is much lower than the value observed for the NH belonging to the second residue in dimer 17 (9.53 ppm, +1.72 ppm). The NHs chemical shifts raise in a monotonic way through the series of oligomers, up to impressive values for Boc-HEPTAMER-OMe 31 (10.56-11.10 ppm, from +2.75 to +3.29 ppm), indicating a cooperative effect as the length increases. In addition, the number of H-bonded NHs is always equal to the number of residues minus one. Both the latter observations appear to indicate strongly that the behaviour of these oligomers is qualitatively identical, or at least very similar, to the one reported earlier for their imidazolidinone-tethered counterparts (Chapter 2. Imidazolidinone-based α-Hydrazidopeptides).

Table 14. NHs chemical shift values of monomer Ac-MONOMER-OMe 14 and oligomers Boc-DIMER-OMe 17, Boc-TRIMER-OMe 22, Boc-TETRAMER-OMe 26 and Boc-HEPTAMER-OMe 31 in 10 mM $CDCl_3$ solutions at 25 °C.

	δ BocNH (ppm)	δ NHs (ppm)
Ac-MONOMER-OMe	---	7.81
Boc-DIMER-OMe	6.93	9.53
Boc-TRIMER-OMe	7.62	10.25, 10.55
Boc-TETRAMER-OMe	7.88	10.20, 10.72, 10.81
Boc-HEPTAMER-OMe	8.29	10.56-11.10 (6 NHs)

It should also be noted that the minor conformers evidenced for the intramolecularly hydrogen-bonded Boc-MONOMER-NH_2 **15**, and to a smaller extent for Boc-MONOMER-OMe **12**, are observed in an even smaller ratio in dimer **17**, and are almost no longer present in trimer **22** (Figure 37). The same applies to tetramer **26** and heptamer **31** (not shown), thus highlighting that the preference for a unique folding, without the intervention of other competitive long-living conformers, parallels the reinforcing effect of the increase in length onto the H-bond strength.

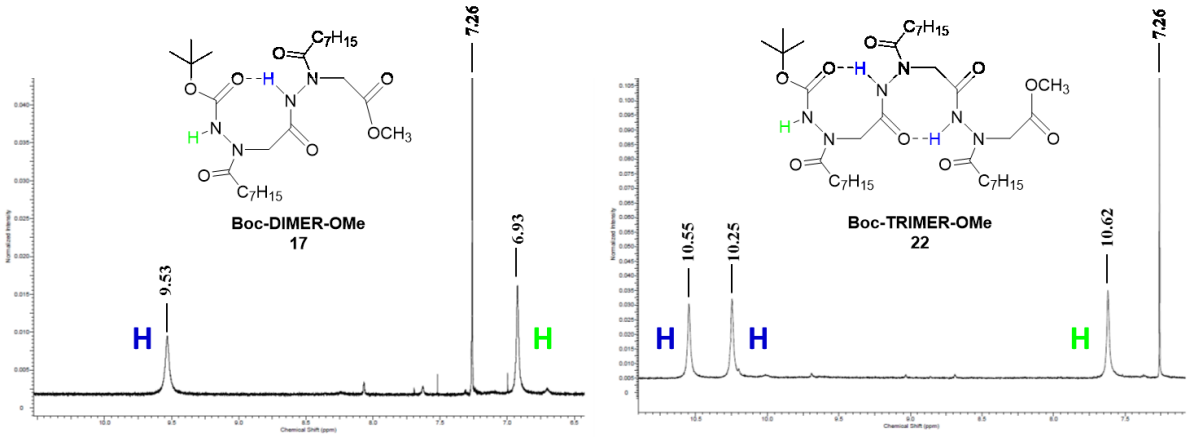

Figure 37. NHs resonances of Boc-DIMER-OMe and Boc-TRIMER-OMe, with the putative 8-helix H-bonding patterns (10 mM samples in $CDCl_3$ at 25 °C).

All the previous reasoning were made on the basis of a supposed low intermolecular-H-bonds-driven self-association in the 10 mM samples considered so far. With the aim to better investigate the tendency to dimerization in solution, the competitive formation of intermolecular H-bonds was quantitatively evaluated by dilution experiments in $CDCl_3$ on the

reference monomers, Boc-MONOMER-OMe **12** and Ac-MONOMER-OMe **14**, as well on the simplest oligomer, dimer Boc-DIMER-OMe **17** (Figure 38).

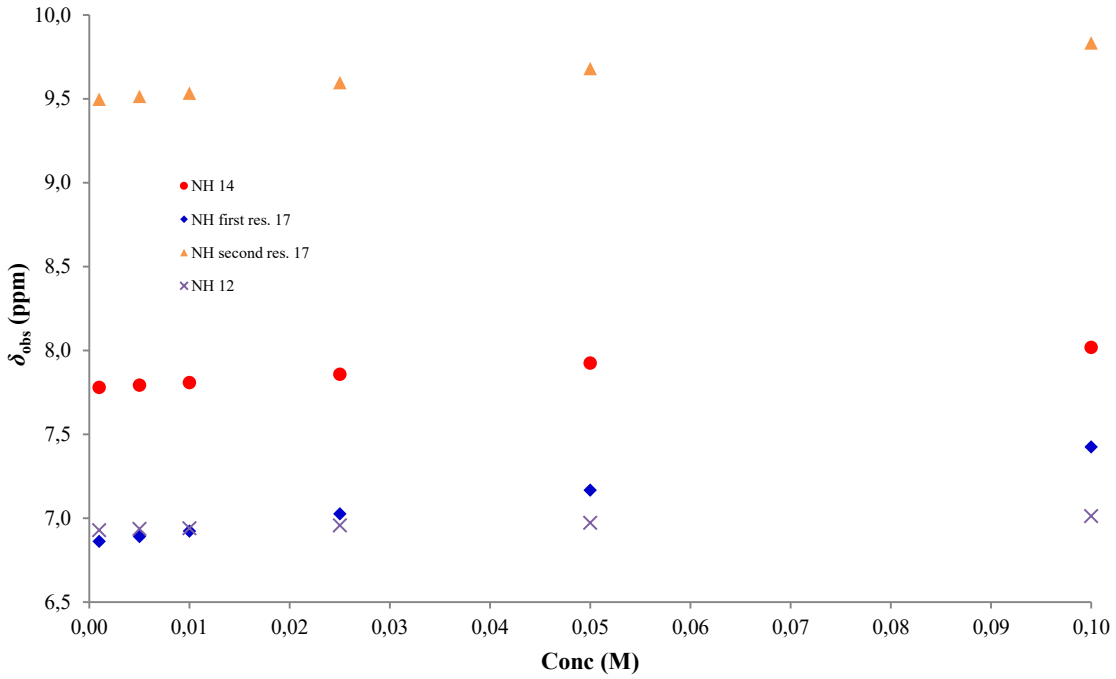

Figure 38. Variation of NH proton chemical shifts of reference monomers Boc-MONOMER-OMe 12 and Ac-MONOMER-OMe 14, and dimer Boc-DIMER-OMe 17, as a function of total substrate concentration from dilution experiments in $CDCl_3$ at 25 °C.

The non-linear regressions of the observed chemical shifts (δ_{obs}) *vs* the total substrate concentration data, which were done using the previously reported equation (eq.6), furnished the values reported in Table 15, where the ones previously obtained for AOPIC-based compounds are also reported.

It is evident from the comparison of intermolecular association constants, K_{inter}, that the tendency to H-bond-driven self-association in solution showed by the achiral and unconstrained α-hydrazidopeptides is much lower in comparison to the one calculated for the AOPIC analogues. Examples of this are the K_{inter} computed for N-acetyl derivatized monomers **8** and **14**, which are 4.7±0.6 M^{-1} and 1.6±0.2 M^{-1}, respectively, while the related percent molar fractions for the intermolecularly H-bonded homodimers, f_D, are about 0.9%, 8% and 37% at a total substrate concentration of 1 mM, 10 mM, and 0.1 M, for compound **8**, and about 0.3%, 3% and 20% at the same concentrations for compound **14**. The difference between the values computed for dimers **4** and **17** is even larger (Table 15), thus demonstrating that the tendency

to homodimerization by formation of intermolecular H-bonds in the case of unconstrained α-hydrazidopeptides is even weaker, in comparison to the AOPIC-based monomers and oligomers. Then, it can be safely assumed that, in the present cases, the self-association remains negligible for concentrations up to 10-25 mM.

Table 15. Comparison of K_{inter} and f_D for the self-association of constrained and unconstrained versions of α-hydrazidopeptides monomers and dimers.[a]

MONOMERS	INTERMOLECULAR ASSOCIATION CONSTANT (K_{inter})		f_D (%) for representative sample concentrations					
			1 mM		10 mM		100 mM	
8	4.7±0.6 M^{-1}		0.9%		8.0%		37.2%	
12	0.6±0.5 M^{-1}		0.1%		1.2%		9.7%	
14	1.6±0.2 M^{-1}		0.3%		3.0%		20.3%	
DIMERS	**1st residue**	**2nd residue**	**1st residue**	**2nd residue**	**1st residue**	**2nd residue**	**1st residue**	**2nd residue**
4	8.1±0.6 M^{-1}	11.7±0.9 M^{-1}	1.5%	2.2%	12.4%	16.3%	46.5%	52.6%
17	0.67±0.07 M^{-1}	0.72±0.09 M^{-1}	0.1%	0.1%	1.3%	1.4%	10.7%	11.3%

[a] Values for AOPIC-based structures taken from Table 6 and Table 7.

A tentative explanation for the observed decrease in the H-bonded-driven self-association, passing from the previously reported AOPIC derivatives to the present oligomers, rely on the electronic factors related to the change in derivatization of Nβ. The achiral α-hydrazidopeptides present both a better H-bond donor and a worst H-bond acceptor, in comparison to the AOPIC-based compounds, due to the lack of the imidazolidinone ring, thus there are two opposite effects. In fact, due to its powerful +M mesomeric effect onto the imidazolidinone carbonyl, the N of the imidazolidinone ring highlighted in bold in Figure 39 slightly decreases the overall electronwithdrawing effect onto the NH of the same residue, thus reducing its electrophilicity by a little extent. On the contrary, due to the same mesomeric effect, the imidazolidinone carbonyl is by far the most powerful H-bond acceptor among all the electrondonating groups in Figure 39. The observed behaviour could then be easily explained assuming the predominance of the latter effect over the former, then promoting a stronger intramolecular H-bond in the case of imidazolidinone-tethered compounds.

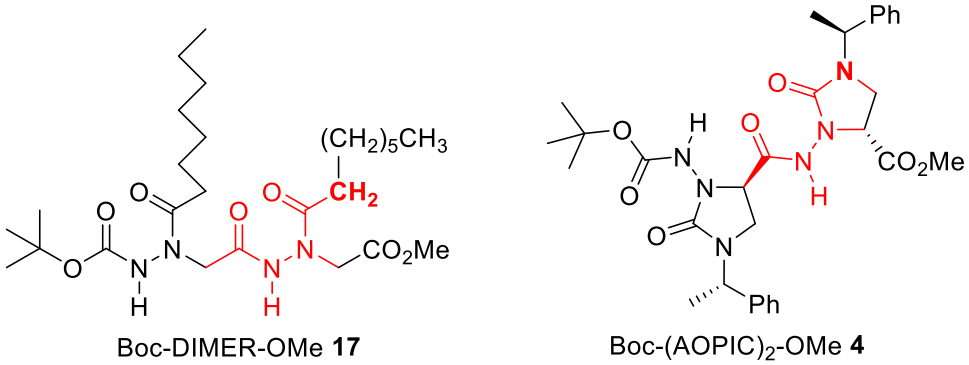

Figure 39. Similarities (in red) and differences (highlighted in bold) between the two dimeric α-hydrazidopeptides 17 and 4.

Using the same approach reported in Paragraph 1.2.6.2, we decided also to evaluate the strength of the intramolecular H-bond for the second residue NH of compound **17**. As reported above (Paragraph 2.5.2 Determination of Intermolecular H-bonding from Dilution Experiments), the equilibrium constants for the intramolecularly hydrogen-bonded species cannot be computed exactly, due the unknown values for chemical shifts of both intramolecularly H-bonded and non-H-bonded NHs. Indeed, the only experimental value available for this purpose is the limiting chemical shift extrapolated at infinite dilution for the NH of second residue in compound **17**, $\delta_{inf.dil.}$ = 9.4936 ppm (Table 17), which is the weighted average between the chemical shift for the H-bonded case, δ_{intra}, and the chemical shift for the unbonded case, δ_M. Anyway, it is easy to suppose quite reliable values for these two limiting situations. In fact, the chemical shift of 7.7757 ppm, extrapolated at infinite dilution for the essentially non-hydrogen-bonded reference compound **14** (Table 17), where the NH is acylated as in the second residue of Boc-DIMER-OMe **17**, can represent a good approximation for δ_M, whereas the highest value available for intramolecularly hydrogen-bonded NHs in heptamer Boc-HEPTAMER-OMe **31** (11.10 ppm, Table 14), can be considered as a good estimate for the limiting value of a completely intramolecularly H-bonded NH, δ_{intra}. Then, using eq 18, an approximate percent molar fraction of intramolecularly H-bonded conformer of 51.7% can be derived, then leading to an intramolecular association constant K_{intra} of 1.07 for the NH of second residue in Boc-DIMER-OMe **17**. These values are lower than the ones for the AOPIC-based dimer **4**, that showed a 81.2-83.4% percent molar fraction of intramolecularly H-bonded conformer and K_{intra} = 4.33-5.04.

A possible qualitative explanation for this decrease in the value of K_{inter} could be based on the lack of conformational restrictions in comparison to the imidazolidinone-tethered

counterparts. Obviously, the use of a non-preorganized monomer lead to an increased conformational entropy, thus eliciting an entropically less favourable formation of the intramolecular H-bond. On the other hand, a non-preorganized monomer could also suffer from enthalpically less favourable steric interactions in the backbone and/or side chains during the reorganization process necessary for the hydrogen-bond formation. Anyway, the observed tendency to the formation of less stable secondary structures, when non-preorganized and non-conformationally constrained residues are employed, is a common feature of almost every type of foldamer.[1]

The titrations with DMSO-d_6 of diluted solutions of reference monomers Ac-MONOMER-OMe **14** and Boc-MONOMER-OMe **12**, as well as dimer Boc-DIMER-OMe **17** in $CDCl_3$ confirm the previous finding (Figure 40). In fact, the observed change in NH chemical shift for the second residue of dimer **17** is coherent with a progressive and rapid unfolding due to the strong intermolecular hydrogen-bond formed between a good H-bond acceptor (DMSO) and a good H-bond donor (the second residue NH in **17**). The comparison with the (very likely) non-intramolecularly H-bonded reference monomers **12** and **14** suggests that, when the percentage of DMSO-d_6 reaches about10%, the unfolding process seems to be almost complete, coherently with Boc-$(AOPIC)_2$-OMe **4** (Figure 19b). In fact, even in the present case, the chemical shift observed at 10% DMSO-d_6 for the NH of second residue in dimer Boc-DIMER-OMe **17**, $\delta_{10\%\text{DMSO-}d6}$ = 10.33 ppm, is very close to the value observed in only DMSO-d_6, $\delta_{\text{DMSO-}d6}$ = 10.58 ppm, the difference being only 0.25 ppm. In addition, the deep comparison of DMSO titrations experiments for dimers **4** (AOPIC-based) and **17** (unconstrained) underline again that the intramolecular H-bonds for these unconstrained α-hydrazido acids is slightly less robust than in the case of AOPIC-based compounds (see Paragraph 2.5.3 Titrations with DMSO-d6.). Unfortunately, a complete series of titration experiments for oligomers **22** (trimer), **26** (tetramer), and **31** (heptamer) has not been carried out yet, so we cannot ascertain the resistance to unfolding of longer oligomers.

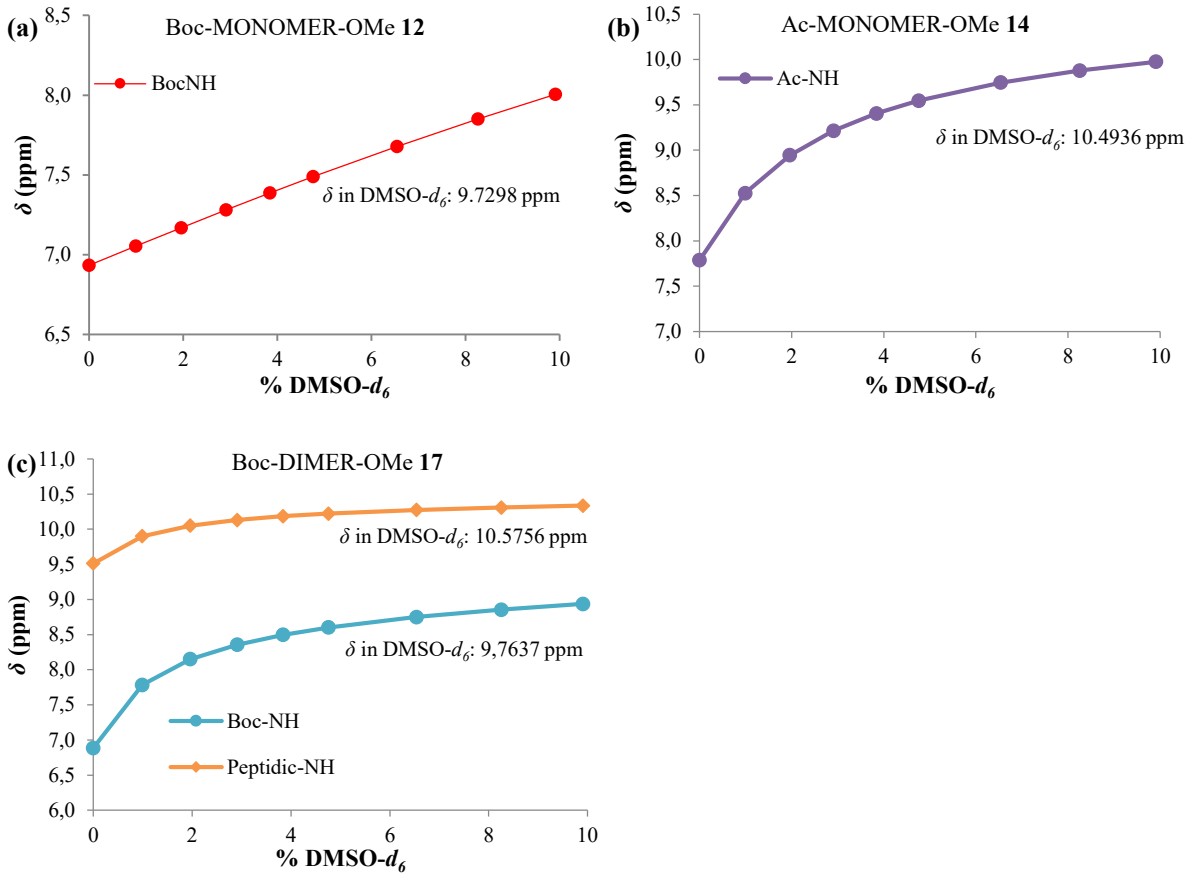

Figure 40. Variation of NHs chemical shifts (ppm) as a function of increasing percentages of DMSO-d_6 added (v/v) to 5 mM solutions in $CDCl_3$ at 25 °C. (a) Boc-MONOMER-OMe 12; (b) Ac-MONOMER-OMe 14; (c) Boc-DIMER-OMe 17.

Variable temperature experiments (VT) were also carried out with the aim of calculating the reduced temperature coefficient of chemical shift, Δδ/ΔT, that is commonly used in order to evaluate the strength of intramolecular H-bonds. It is mainly used in the conformational analysis of proteins in solution,[22] even though its predictive power as an H-bond indicator was sometimes questioned.[23] Usually, Δδ/ΔT values more negative than -2.6 ppb/K have been associated, for many oligopeptides and their mimics, to a dynamic equilibration between an H-bonded and a non-H-bonded structure.[24] On the contrary, smaller values have been associated to either a completely H-bonded or a completely non-H-bonded NH, even if small values can also result from the competition among the many factors affecting the difference in stability between intramolecularly bonded and unbonded NHs, as found for simple diamides.[21]

It is very interesting to note that the values obtained for the BocNH of monomer **12** (Δδ/ΔT = -2.7 ppb/K) and the AcNH of monomer **14** (Δδ/ΔT = -3.6 ppb/K) appear to indicate the presence of a dynamic equilibration between intramolecularly H-bonded and unbonded

conformers, and the same is valid for the BocNH belonging to the first residue of dimer **17**, even if they were previously assumed to be almost completely unbonded on the basis of their chemical shifts (Figure 41). This logical assumption was demonstrated to be valid for AOPIC derivatives, where hydrazidic Boc- or Ac-derivatized NHs belonging to the first residues were not involved even in weak intramolecular H-bonds, neither by a 6-membered cycle with the intraresidue carbonyl oxygen of the α-hydrazido acid moiety, nor by a 5-membered cycle with the imidazolidinonic carbonyl. This contradiction cannot be safely explained at the moment, but the partial intervention of a conformation similar to the zig-zag Z6 H-bonded structure (see Figure 25) between the BocNH (or the AcNH) and the ester carbonyl could be at the basis of the observed discrepancy. Anyway, it was demonstrated in literature that some hydrazido-derivatives can form strong 5-terms and also bifurcated 5-term plus 6-terms H-bonded pseudocycles.[17]

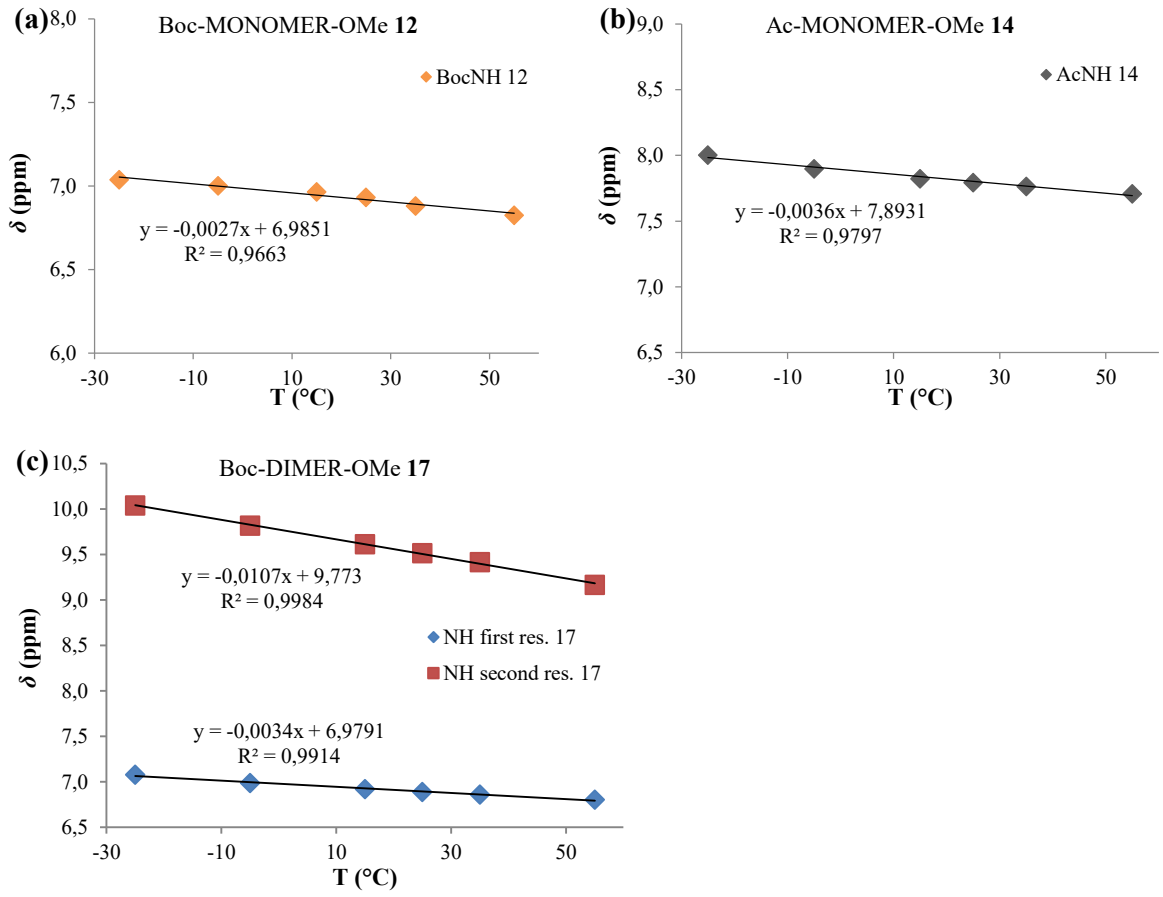

Figure 41. Variation of NH proton chemical shifts as a function of temperature (5 mM solutions in $CDCl_3$). (a) Boc-MONOMER-OMe 12; (b) Ac-MONOMER-OMe 14; (c) Boc-DIMER-OMe 17.

Eventually, the second residue NH of dimer **17** has a remarkable $\Delta\delta/\Delta T$ = -10.7 ppb/K, which is coherent with the presence of a dynamic equilibration between its intramolecularly H-bonded structure and the unbonded one.

3.2.3 Preliminary NMR and DFT analysis of Boc-MONOMER-NH$_2$ conformers

In light of the inconsistency reported above, we have started an in-depth analysis of Boc-MONOMER-NH$_2$ **15**, the simplest member of our α-hydrazido acid derivatives that, in theory, is constitutionally able to form both 8-membered and 6-membered intramolecular hydrogen-bonds. This compound highlighted the presence of a non-negligible amount of a slowly interconverting minor conformer, which showed a very deshielded NH signal (Figure 36).

Even if a rigorous resonances assignment has not been accomplished yet, both variable temperature and DMSO titration experiments were carried out in order to ascertain which of the observed signals belong to the intramolecularly H-bonded conformer(s) (Figure 42). Anyway, although the resonance assignment used throughout this discussion could be wrong, the qualitative analysis reported here and the conclusions that will be drawn after the computational section are reliable (*vide infra*).

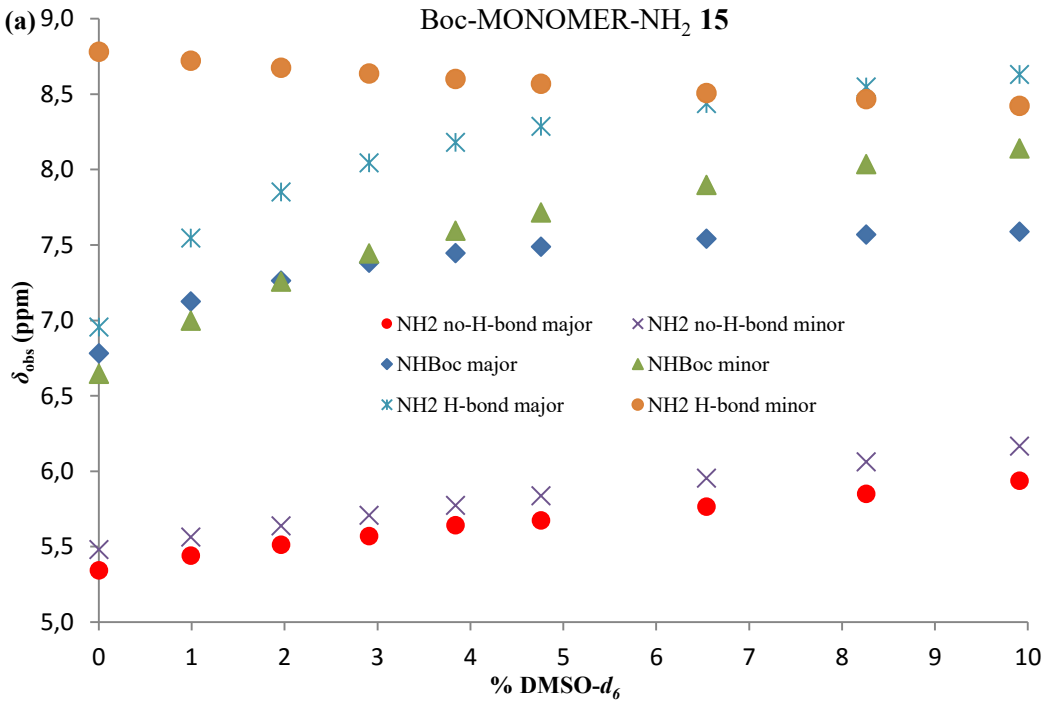

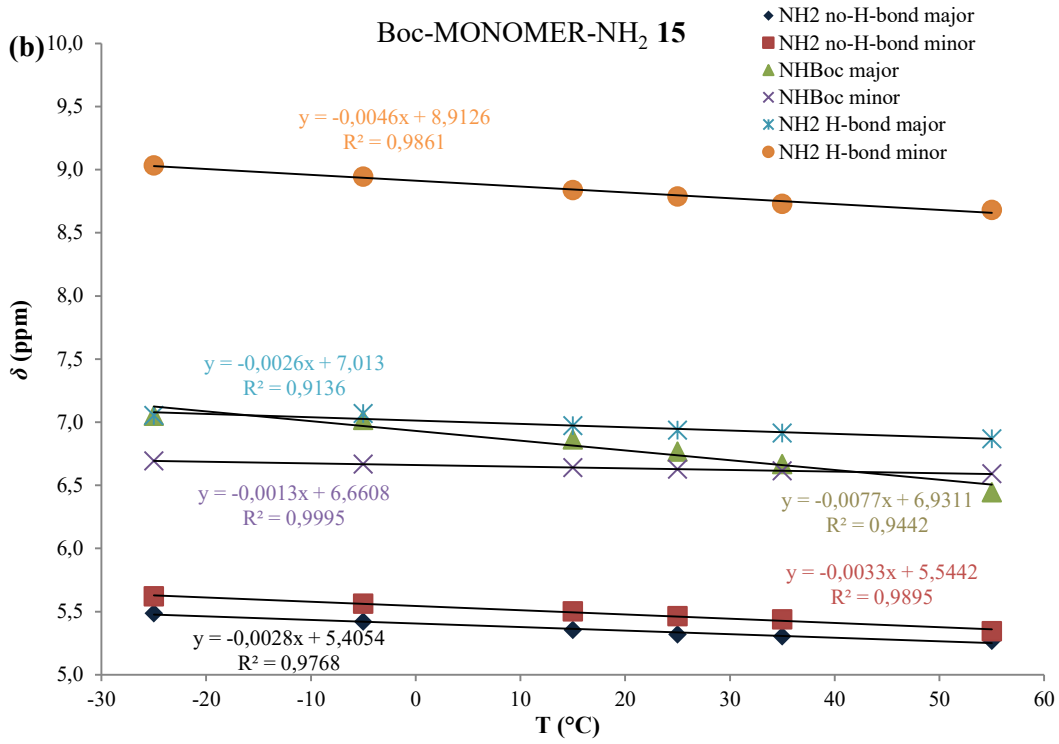

Figure 42. Variation of NH proton chemical shifts of Boc-MONOMER-NH$_2$ 15 (a) as a function of increasing percentages of DMSO-d_6 added (5 mM solution in $CDCl_3$), and (b) as a function of temperature (1 mM solution in $CDCl_3$). Note: the putative assignment reported here has not been confirmed by bidimensional NMR experiments, yet.

It is evident from the results reported in Figure 42 that both one of the two C-terminal NH and the BocNH are involved in two different types of intramolecular H-bonds, which conformers are slowly interconverting. Thus, the two sets of conformers probably differ each other by the arrangement of a carbonyl group conjugated with one of the hydrazidic nitrogens.

Obviously, a thorough *in silico* investigation should also include the computation of transition states, in order to find which is the slow movement leading to the observation of separate conformers on the NMR time-scale. Anyway, in this case our aim is simply to ascertain if there are energetically close conformers with different types of intramolecular H-bonds. To this purpose, the conformational space of Boc-MONOMER-NH$_2$ **15** was explored at the density functional theory (DFT) level, using the Becke's three-parameter exchange functional in conjunction with the Lee-Yang-Parr correlation functional (B3LYP).[40] For all the atoms, the 6-311+G(2d,p) basis set was used. To take into account bulk solvent effects, full geometry optimizations within a continuum solvent model (with chloroform as solvent) were carried out via the self-consistent reaction field (SCRF) approach, using the polarizable continuum model

method (IEF-PCM).[41] All calculations were performed with the Gaussian 09 suite of programmes (Gaussian, Inc., Pittsburgh, PA, USA).[42]

More than 40 different initial conformations were optimized, changing all the possible dihedral angles except for the Boc group and the octanoyl side chain, for which the minimum energy conformation was always used. Anyway, for the most stable conformer, three different conformations around the C(O)-Cα bond were computed to ensure the exactness of the assumption about the minimum energy conformation of the octanoyl side chain. The optimizations always converged to one of the 11 structures in Figure 43, reported in order of stability (note: **1b** and **1c** are the two conformers of the absolute minimum, **1a**, with less stable dispositions of the octanoyl side-chain).

1a	**2**	**3**
E = -1054.61536800 au	E = -1054.61512304 au	E = -1054.61497780 au
0.00 Kcal/mol	+0.15 Kcal/mol	+0.24 Kcal/mol

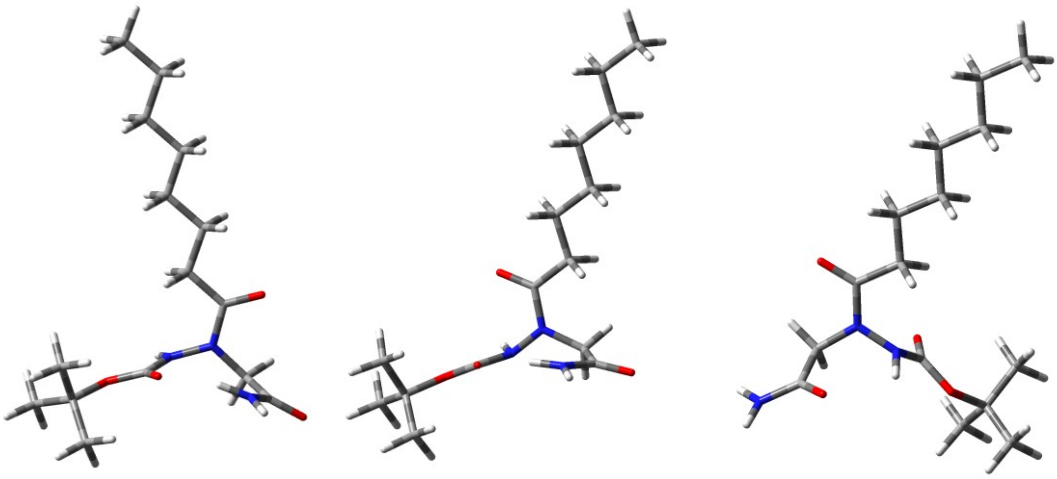

1b

E = -1054.61425565 au

+0.70 Kcal/mol

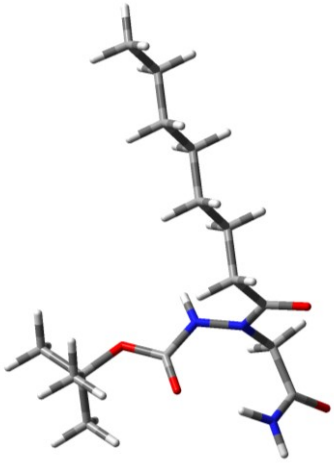

1c

E = -1054.61388967 au

+0.93 Kcal/mol

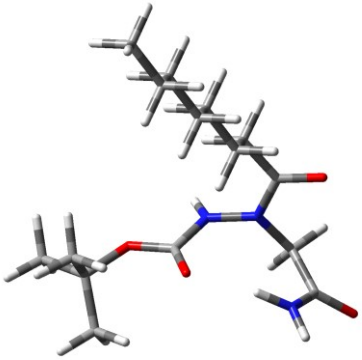

4

E = -1054.61366744 au

+1.07 Kcal/mol

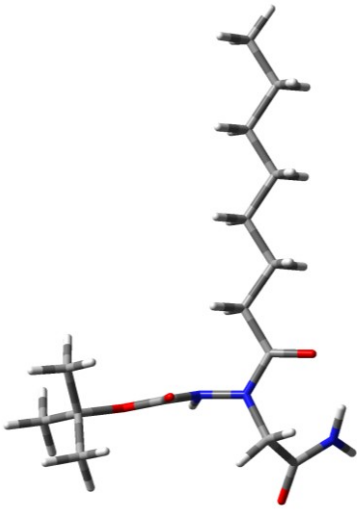

5

E = -1054.61251817 au

+1.79 Kcal/mol

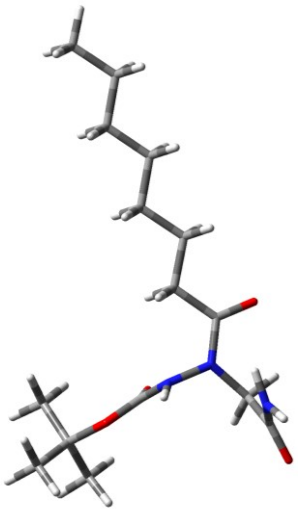

6

E = -1054.61239551 au

+1.87 Kcal/mol

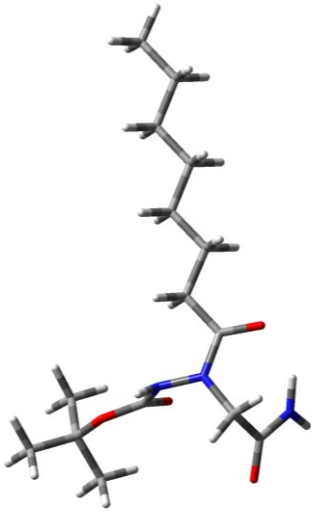

7

E = -1054.61060907 au

+2.99 Kcal/mol

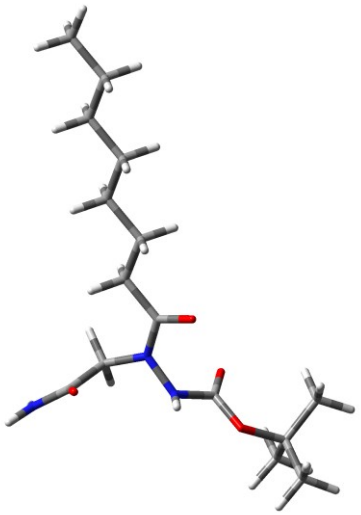

8

E = -1054.60987498 au

+3.45 Kcal/mol

9

E = -1054.60872338 au

+4.17 Kcal/mol

10

E = -1054.60581351 au

+6.00 Kcal/mol

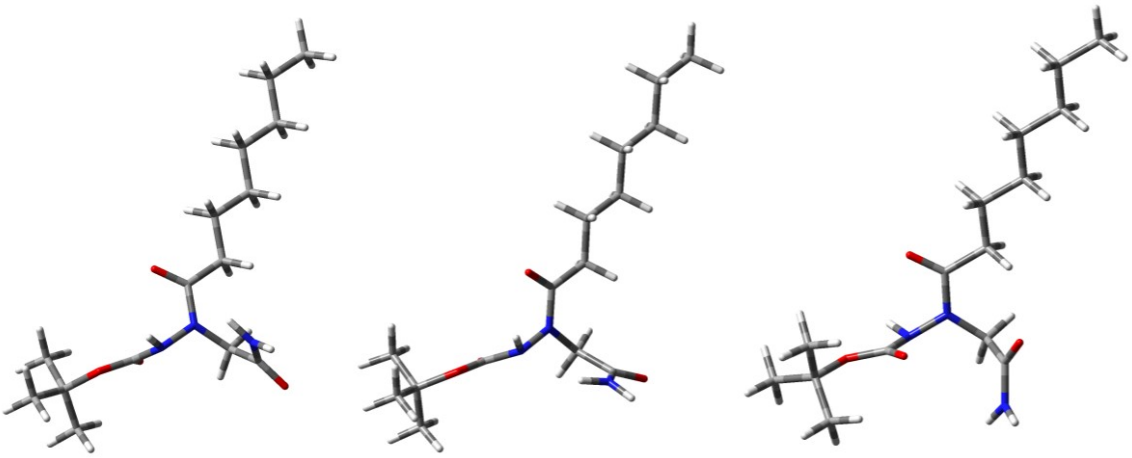

11

E = -1054.60554090 au

+6.17 Kcal/mol

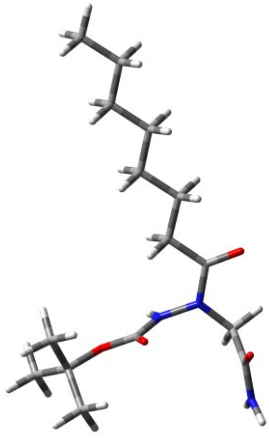

Figure 43. Absolute and relative energies computed for the conformers of Boc-MONOMER-NH_2.

Even if the results confirm the very variegated scenario of intramolecular H-bonding options, the two most stable conformations, **1a** and **2**, are very similar to the ones computed for the AOPIC-based foldamer reported in Paragraph 2.2.2 Computational Investigation. In fact, they are Z8 "hydrazido-turns" with the carbonyl group of the octanoyl side-chain having either a

syn- or an antiperiplanar arrangement with respect to the N-N single bond. Their overall geometries are quite similar (Table 16), the differences of few degrees in ϕ, θ, and ψ dihedrals being easily explained in terms of reduction of electronic repulsion in conformer **2**. Indeed, in structure **2**, an sp^2 electron pair of C=O in the octanoyl side-chain is pointed towards Nγ, and the pyramidalization adopted by Nγ itself (-24.6°) alleviates this effect. In the case of C=O•••H-N lengths in **1a** (1.973 Å) and **2** (1.924 Å), the sensible shortening in the latter case is indicative of a more robust H-bond, but this is balanced by the less favourable electronic interaction reported above, so that the two hydrazido-turns have almost the same stability. Nβ•••H-N distances in **1a** and **2** are very close each other, but their values are much larger than the C=O•••H-N ones, signalling that there is an evident preponderance in the stabilization due to hydrogen-bonding with the Boc carbonyl. The relative weakness of these Nβ•••H-N bonds is confirmed also by the very little pyramidalization of Nβ nitrogen in both conformers **1a** and **2**.

Table 16. Comparison of geometrical parameters in the most stable conformers computed for Boc-MONOMER-NH_2.

	1a	**2**	**3**
ϕ (°)	96.3	112.5	81.9
θ (°)	-107.0	-101.8	67.4
ψ (°)	17.6	13.8	172.4
C=O•••H-N (Å)	1.973	1.924	2.354
Nβ•••H-N (Å)	2.498	2.485	-
Nβ pyramidalization (°)	6.0	6.2	-4.9
Nγ pyramidalization (°)	2.8	-24.6	18.9

On the other hand, structure **3**, which is the only other local minimum with a stability comparable to hydrazido-turn conformers, is a completely different type of structure, due to its Z6 intraresidual hydrogen-bond between the hydrazidic NH and the C-terminal carbonyl oxygen (C=O•••H-N = 2.354 Å). The stability of such a structure relies on the good electrondonating ability of the amidic C-terminal carbonyl, which makes the 6-terms intramolecular H-bond with the partially positively charged hydrazidic NH quite stable.

It should be stressed here that, from an electronic point of view, the almost equal stability of the Z6 and Z8 structures found in the C-terminal amide monomer **15** should no longer be possible in oligomers, due to the very different electronic features of the acylhydrazide group, which is a stronger H-bond-donating and a weaker H-bond-accepting functionality in comparison to the amide group, thus favouring the Z8 folding.

3.3 Preliminary Conclusions

The analysis of the first NMR spectra, albeit non-conclusive, point towards the same folding observed for the conformationally constrained variants based on imidazolidinone-tethered α-hydrazido acids (AOPIC), that is to say the zig-zag 8-helix (Z8), although at the moment a competitive alternative H-bond pathway cannot be excluded (zig-zag 6-helix, Z6). The intramolecularly H-bonded conformers appear to be less stable than their AOPIC counterparts, probably due to the lack of any conformational constriction and preorganization, but also less prone to H-bond-driven self-association in solution. Anyway, even though the few experimental data available at the time seem to indicate that the synthesis of a simple and achiral foldamer with a β-sheet-like disposition of side-chains has been reached, they cannot be considered conclusive, yet. Then, the entire set of experiments with variable concentrations, variable temperature, and dimethyl sulfoxide titrations will be extended to the longer oligomers.

Moreover, as reported for the previous AOPIC derivatives, a thorough resonance assignment will be carried out on all the molecules synthesized by means of ^{1}H-^{13}C heteronuclear correlation experiments, followed by ROESY experiments, with the aim of precisely ascertaining the folding. Eventually, a complete computational analysis with an extended molecular dynamics simulation will be used to confirm and integrate the experimental findings.

3.4 Experimental

3.4.1 Materials and methods

^{1}H and ^{13}C-NMR spectra reported in the characterization section were recorded at 25 °C at 400 and 100 MHz, respectively, using 10mM samples for ^{1}H and 100 mM samples for ^{13}C-NMR spectra in $CDCl_3$ as solvent, on a Varian MR 400 spectrometer equipped with an indirect probe. Chemical shifts are reported in ppm relative to TMS for ^{1}H-NMR spectra and in ppm relative to residual solvent signals (77.16 ppm) for ^{13}C-NMR. Coupling constants (*J*) are given in Hz. Abbreviations for multiplicity are: s, singlet; bs, broad singlet; d, doublet; dd, doublet of doublets; t, triplet; q, quartet; m, multiplet. The prefix "p" (pseudo) will be used when needed. Stock 0.1 M solutions of pure **12**, **14**, **15** and **17** for dilution experiments were obtained diluting 0.2 mmol of compounds in 2 mL graduated flasks, using $CDCl_3$, then all the other concentrations (0.05, 0.025, 0.01, 0.005 and 0.001 M) were obtained by serial dilutions with $CDCl_3$. Titrations with DMSO-d_6 were carried out at 25 °C, by careful sequential additions of

suitable volumes of DMSO-d_6 to NMR tubes filled with exactly 0.7 mL of 5 mM solutions of compounds in $CDCl_3$. Chemical shifts are reported in ppm relative to TMS.

LC electrospray ionization mass spectra were obtained with a Finnigan Navigator LC/MS single-quadrupole mass spectrometer, cone voltage 25 V and capillary voltage 3.5 kV, injecting samples dissolved in methanol, acetonitrile or $CH_3CO_2NH_4$ 0.1 M in acetonitrile. Melting points were measured on an Electrothermal IA 9100 apparatus and are uncorrected. All reagents and solvents were used as received, except in cases of anhydrous solvents. Anhydrous DCM and methanol were obtained, respectively, by distillation on calcium hydride and sodium, respectively, immediately prior to use. Column chromatography was performed with silica gel 60 (230-400 mesh ASTM). The TLC analysis was performed with sheets of silica gel Fluka TLC-PET, using exposure to UV light and immersion in aqueous KMnO4, followed by heating and by possible immersion in H_2SO_4 9 M. The hydrazine buffer (3 M hydrazine/0.3 M hydrazine dihydrochloride) was obtained by mixing 14.7 mL of hydrazine monohydrate and 3.18 g of hydrazine dihydrochloride, and then bringing to a final volume of 100 mL with a mixture of MeOH/DCM 5:1.

3.4.2 Synthetic procedures and characterizations

tert-Butyl 2-(2-methoxy-2-oxoethyl)-2-octanoylhydrazine-1-carboxylate, Boc-MONOMER-OMe 12

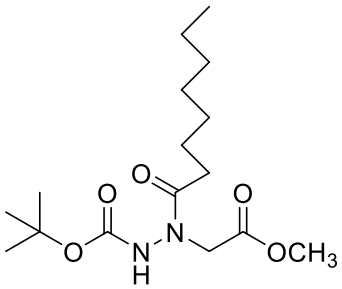

To a solution of *t*-butyl carbazate (52.5 mmol, 7.0 g) and methyl bromoacetate (50 mmol, 4.88 mL) in anhydrous DCM (25 mL) at room temperature, DIPEA (52.5 mmol, 9.15 mL) was added and the reaction was vigorously stirred under inert atmosphere for 48 hours at room temperature. After evaporation under vacuum, the residue was extracted using a mixture of cyclohexane/ethyl acetate 1:1 (200 mL) as the organic phase and water (50 mL). The organic phase was washed with HCl 1 M (2 × 5 mL) and water (5 mL), then the aqueous phases were sequentially extracted with additional 200 mL of *c*-Ex/AcOEt 1:1. The second organic phase was washed with HCl 1 M (2 × 5 mL) and water (5 mL), then the reunited organic phases were dried over anhydrous sodium sulphate. After evaporation under vacuum, the crude product was

directly used in the following reaction without any further purification. To the crude product **11** dissolved in dry DCM (240 mL) at room temperature, pyridine (72 mmol, 5.82 mL) was added, followed by dropwise addition of octanoyl chloride (62.4 mmol, 10.65 mL). The reaction was stirred under inert atmosphere for 3 hours, then DCM was evaporated under vacuum at room temperature and the residue was diluted with ethyl acetate (200 mL) water (50 mL). After separation, the organic phase was washed with HCl 1 M (2 × 5 mL), saturated aqueous sodium carbonate (5 mL) and water (5 mL). The aqueous phases were sequentially extracted with additional 200 mL of ethyl acetate, then the second organic phase was washed with HCl 1 M (2 × 5 mL), saturated aqueous sodium carbonate (5 mL) and water (5 mL). The reunited organic phases were dried over anhydrous sodium sulphate and evaporated under vacuum, then the crude product was purified by flash column chromatography on silica gel (cyclohexane/ethyl acetate), obtaining the pure compound **12** as a colourless oil with an overall yield of 85% (42.5 mmol, 14.04 g).

R_f = 0.41 (*c*-Ex/AcOEt = 1:1). ^{1}H NMR (400 MHz, $CDCl_3$): δ 0.87 (t, *J* = 6.9 Hz, 3H), 1.26-1.33 (m, 8H), 1.48 (s, 9H), 1.58-1.65 (m, 2H), 2.41 (t, *J* =7.2 Hz, 2H), 3.60 (bs, 1H), 3.75 (s, 3H), 5.10 (bs, 1H), 6.94 (bs, NH). ^{13}C NMR (100 MHz, $CDCl_3$): δ 14.2, 22.7, 24.7, 28.3, 29.1, 29.3, 31.8, 32.0, 48.3, 52.4, 82.3, 154.0, 170.2, 176.3. MS (ESI): *m/z* = 331.2 $[M+H]^+$, 348.3 $[M+NH_4]^+$.

Methyl *N*-acetamido-*N*-octanoylglycinate, Ac-MONOMER-OMe 14

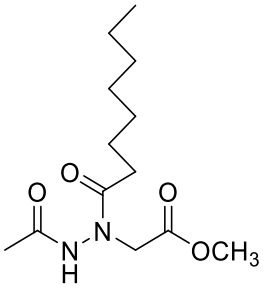

To a solution of compound **12** (1 mmol, 331 mg) dissolved in anhydrous MeOH (2 mL) and anhydrous DCM (0.5 mL) at room temperature, concentrated H_2SO_4 (347 μL) was added dropwise. After 4 hours under stirring, anhydrous Na_2CO_3 was added in aliquots until effervescence ceased, then the solution was diluted with Et_2O (30 mL) and water (30 mL). After separation, the organic phase was washed with a saturated aqueous solution of Na_2CO_3 (2 × 2 mL), then the aqueous phases were extracted again with Et_2O (30 mL). The second organic phase was washed with saturated Na_2CO_3 (2 x 2 mL), then the combined organic phases were dried with anhydrous Na_2SO_4 and the solvent was eliminated under vacuum. To the obtained

crude product, dissolved in anhydrous DCM (5 mL) at room temperature, pyridine (1.5 mmol, 121 μL) and AcCl (1.3 mmol, 93 μL) were sequentially added. After 1 h under stirring, all the volatiles were evaporated under vacuum at room temperature and the residue was diluted with AcOEt (30 mL) and water (5 mL). After separation, the organic phase was washed with HCl 1 M (2 × 3 mL), saturated aqueous sodium carbonate (5 mL) and water (5 mL). The aqueous phases were sequentially extracted with additional 30 mL of ethyl acetate, then the second organic phase was washed with HCl 1 M (2 × 3 mL), saturated aqueous sodium carbonate (5 mL) and water (5 mL). The combined organic phases were dried over anhydrous sodium sulphate and evaporated under vacuum and the crude product was purified by column chromatography on silica gel (*c*-Ex/AcOEt), obtaining the pure product **14** with a 83% yield (0.83 mmol, 226 mg) as a colourless oil.

R_f = 0.20 (*c*-Ex/AcOEt = 4:6). ^{1}H NMR (400 MHz, $CDCl_3$): δ 0.87 (t, *J* = 6.9 Hz, 3H), 1.26-1.31 (m, 8H), 1.59-1.64 (m, 2H), 2.03 (s, 3H), 2.35 (t, *J* = 7.7 Hz, 2H), 3.75 (s, 3H), 4.42 (bs, 2H), 7.81 (bs, NH). ^{13}C NMR (100 MHz, $CDCl_3$): δ 14.2, 21.0, 22.7, 24.6, 29.2 ,29.3, 31.8, 31.9, 48.1, 52.5, 168.7, 170.6, 175.5. MS (ESI): *m/z* = 273.2 $[M+H]^+$, 295.1 $[M+Na]^+$.

tert-Butyl 2-(2-amino-2-oxoethyl)-2-octanoylhydrazine-1-carboxylate, Boc-MONOMER-NH_2 15

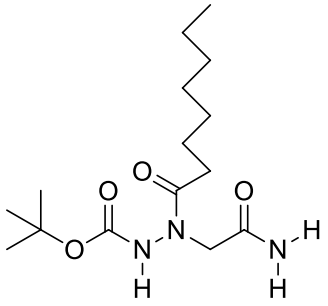

To a solution of compound **12** (1 mmol) in anhydrous MeOH (5 mL) under inert atmosphere at room temperature, ammonium chloride (2 mmol, 107 mg) was added and then dry gaseous ammonia was slowly bubbled for 10 minutes. The flask was tightly capped and the reaction was stirred for 2 hours, then all the volatiles were evaporated under vacuum at room temperature and the residue was dissolved in AcOEt (20 mL) and water (5 mL). After separation, the organic phase was washed with water (2 × 2 mL), then the aqueous phases were extracted with additional AcOEt (20 mL). After separation, the second organic phase was washed with water (2 × 2 mL) and the combined organic phases were dried with anhydrous Na_2SO_4, then the solvent was eliminated at reduced pressure. The crude product was purified by flash

chromatography on silica gel (AcOEt/MeOH), obtaining the pure product **15** with a 91% yield (0.91 mmol, 301 mg) as a white crystalline solid.

R_f = 0.43 (AcOEt). m.p. = 123-124 °C. ^{1}H NMR (400 MHz, $CDCl_3$, major conformer): δ 0.88 (t, *J* = 6.9 Hz, 3H), 1.26-1.33 (m, 8H), 1.49 (s, 9H), 1.60-1.65 (m, 2H), 2.37-2.41 (m, 2H), 4.21 (bs, 2H), 5.39 (bs, NH), 6.83 (bs, NH), 7.02 (bs, NH). ^{13}C NMR (100 MHz, $CDCl_3$, major conformer): δ 14.2, 22.7, 24.6, 28.3, 29.1, 29.4, 31.8, 32.0, 52.3, 82.6, 155.1, 171.4, 176.7. MS (ESI): *m/z* = 316.3 $[M+H]^+$, 338.2 $[M+Na]^+$.

N-((*tert*-Butoxycarbonyl)amino)-N-octanoylglycine 16

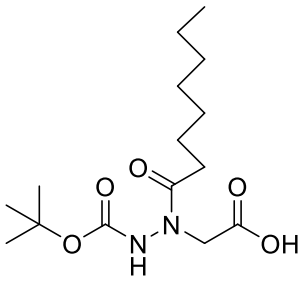

To a solution of compound **12** (0.3 mmol, 99 mg) in MeOH (0.9 mL) at room temperature, NaOH 1 M (0.45 mL) was added. The reaction was stirred for 30 minutes, then was cooled at 0 °C before the dropwise addition of HCl 1 M (0.5 mL). Thus all the volatiles were evaporated under vacuum at room temperature and the residue was dissolved in AcOEt (10 mL). After separation, the organic phase was washed with water (2 × 2 mL), then the aqueous phases were extracted with additional AcOEt (10 mL). After separation, the second organic phase was washed with brine (2 × 2 mL) and the combined organic phases were dried with anhydrous Na_2SO_4, then the solvent was eliminated at reduced pressure, directly furnishing the pure product **16** with a 98% yield (0.18 mmol, 57 mg) as a colourless oil.

R_f = 0.57 (DCM/MeOH = 9:1). ^{1}H NMR (400 MHz, $CDCl_3$): δ 0.88 (t, *J* = 6.9 Hz, 3H), 1.26-1.33 (m, 8H), 1.50 (s, 9H), 1.56-1.68 (m, 2H), 2.27-2.59 (m, 2H), 3.30-5.23 (bs, 3H), 7.12 (bs, NH) ^{13}C NMR (100 MHz, $CDCl_3$, major conformer): δ 14.2, 22.7, 24.6, 28.3, 29.2, 29.3, 31.8, 32.0, 49.4, 82.9, 154.8, 169.3, 172.8. MS (ESI): *m/z* = 317.3 $[M+H]^+$, 339.2 $[M+Na]^+$.

General procedure for the synthesis of the N-terminal bromoacetyl derivatives and their characterization.

Note: representative procedure referred to 1 mmol of starting compound; the actual amounts of starting compounds used in the reactions are reported case by case.

To a solution of 1 mmol of the starting compound (**12**, **17** or **22**) in a mixture of anhydrous MeOH (2 mL) and anhydrous DCM (0.5 mL) at room temperature, concentrated H_2SO_4 was added dropwise (347 µL). After 4 hours under stirring, anhydrous Na_2CO_3 was added in aliquots until effervescence ceased, then the solution was diluted with Et_2O (40 mL) and water (30 mL). After separation, the organic phase was washed with a saturated aqueous solution of Na_2CO_3 (2 × 2 mL), then the aqueous phases were sequentially extracted with additional Et_2O (30 mL). The second organic phase was washed with saturated Na_2CO_3 (2 × 2 mL/mmol) and water (2 mL), then the combined organic phases were dried with anhydrous Na_2SO_4 and the solvent was eliminated at reduced pressure. The crude product was dissolved in anhydrous DCM (5 mL), pyridine (1.2 mmol, 97 µL) was added and the mixture was brought to 0 °C, then bromoacetyl bromide (1.1 mmol, 96 µL) was added dropwise. The reaction was stirred at 0 °C for 1 hour, then all the volatiles were evaporated under vacuum without using the thermostating bath and the residue was diluted with AcOEt (30 mL) and water (5 mL). After separation, the organic phase was washed with HCl 1 M (2 × 3 mL), saturated aqueous sodium carbonate (5 mL) and water (5 mL). The aqueous phases were sequentially extracted with additional 30 mL of ethyl acetate, then the second organic phase was washed with HCl 1 M (2 × 3 mL), saturated aqueous sodium carbonate (5 mL) and water (5 mL). The combined organic phases were dried over anhydrous sodium sulphate and evaporated under vacuum, then the crude product was purified by flash column chromatography on silica gel (cyclohexane/ethyl acetate), obtaining the pure products **18**, **24** and **29**.

Methyl *N*-(2-bromoacetamido)-*N*-octanoylglycinate, 18

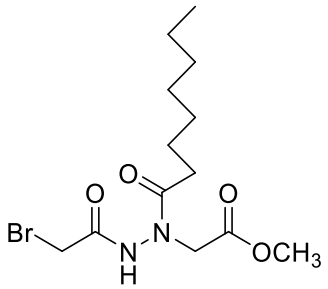

Starting from compound **12** (18 mmol, 5.95 g), product **18** was obtained as a white crystalline solid (15.83 mmol, 5.56 g, yield 88%).

R_f = 0.47 (*c*-Ex/AcOEt = 3:7). m.p. = 111-112 °C. ^{1}H NMR (400 MHz, $CDCl_3$): δ 0.87 (t, *J* = 6.9 Hz, 3H), 1.26-1.33 (m, 8H), 1.59-1.65 (m, 2H), 2.35 (t, *J* = 7.4 Hz, 2H), 3.77 (s, 3H), 3.88 (s, 2H), 4.42 (bs, 2H), 8.58 (bs, NH). ^{13}C NMR (100 MHz, $CDCl_3$): δ 14.0, 22.6, 24.4, 25.9,

29.0, 29.1, 31.6, 31.8, 47.8, 52.5, 164.6, 170.1, 175.2. MS (ESI): *m/z* = 351.1 [M(^{79}Br)+H]$^+$, 353.1 [M(^{81}Br)+H]$^+$, 373.0 [M(^{79}Br)+Na]$^+$, 375.1 [M(^{81}Br)+Na]$^+$.

Methyl *N*-(2-(2-(2-bromoacetyl)-1-octanoylhydrazinyl)acetamido)-*N*-octanoylglycinate, 24

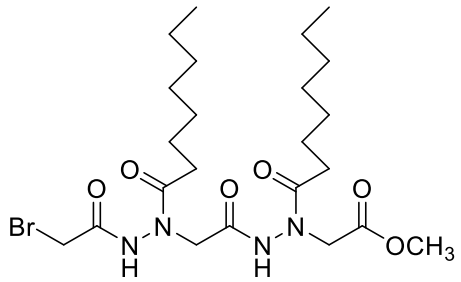

Starting from compound **17** (2.5 mmol, 1.32 g), product **24** (1.95 mmol, 1.16 g, yield 78%) was obtained as a colourless wax.

R_f = 0.16 (*c*-Ex/AcOEt = 3:7). ^{1}H NMR (400 MHz, $CDCl_3$): δ 0.86-0.89 (m, 6H), 1.26-1.29 (m, 16H), 1.54-1.62 (m, 4H), 2.30-2.35 (m, 4H), 3.74 (s, 3H), 3.93 (s, 2H), 4.19 (bs, 2H), 4.37 (bs, 2H), 8.90 (bs, NH), 9.33 (bs, NH). MS (ESI): *m/z* = 549.2 [M(^{79}Br)+H]$^+$, 551.2 [M(^{81}Br)+H]$^+$, 571.2 [M(^{79}Br)+Na]$^+$, 573.3 [M(^{81}Br)+Na]$^+$.

Methyl *N*-(2-(2-(*N*-(2-bromoacetamido)-*N*-octanoylglycyl)-1-octanoylhydrazinyl)acetamido)-*N*-octanoylglycinate, 29

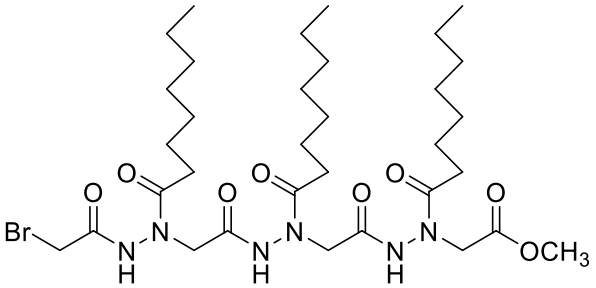

Starting from compound **22** (300 μmol, 218 mg), product **29** (213 μmol, 159 mg, yield 71%) was obtained as a colourless wax.

R_f = 0.06 (*c*-Ex/AcOEt = 3:7). ^{1}H NMR (400 MHz, $CDCl_3$): δ 0.87 (ps, 9H), 1.27 (ps, 24H), 1.56 (ps, 6H), 2.25-2.35 (m, 6H), 3.72 (s, 3H), 3.94 (s, 2H), 3.99-4.50 (bs, 6H), 9.62 (bs, NH), 10.02 (bs, NH), 10.24 (bs, NH). ^{13}C NMR (100 MHz, $CDCl_3$): δ 14.11, 14.13, 14.15, 22.67, 22.69 24.3, 24.5, 24.8, 25.1, 29.14, 29.20, 29.24, 29.28, 29.7, 31.73, 31.78, 31.81, 31.85, 31.90, 32.1, 48.8, 52.5, 53.3, 54.3, 168.1, 168.7, 169.5, 169.9, 175.5, 175.8, 176.4. MS (ESI): *m/z* = 747.4 [M(^{79}Br)+H]$^+$, 749.3 [M(^{81}Br)+H]$^+$, 769.3 [M(^{79}Br)+Na]$^+$, 771.4 [M(^{81}Br)+Na]$^+$.

General procedure for the synthesis of the C-terminal hydrazidic derivatives and their characterization.

Note: representative procedure referred to 1 mmol of starting compound; the actual amounts of starting compounds used in the reactions are reported case by case.

To a solution of the starting compound (**12** or **22**, 1 mmol) in DCM (0.2 mL), the hydrazine buffer in methanol (1 mL) was added and the reaction was stirred for 4 hours at room temperature. All the volatiles were evaporated under vacuum, without using the thermostating bath, and the residue was diluted with Et_2O (30 mL) and water (10 mL). After separation, the organic phase was washed water (2 × 3 mL), then the combined aqueous phases were extracted with additional Et_2O (30 mL) and, after separation, the second organic phase was washed with water (2 × 3 mL). The combined organic phases were dried over anhydrous Na_2SO_4 and the solvent was eliminated under reduced pressure, without using the thermostating bath. Compound **20** was almost pure and did not need any further purification, while compound **27** was purified by flash chromatography on a short column of silica gel (Et_2O/MeOH). The collected fractions were evaporated under reduced pressure, without using the thermostating bath. Pure compounds **20** and **27** were stored at -18 °C and used within a month.

***tert*-Butyl 2-(2-hydrazinyl-2-oxoethyl)-2-octanoylhydrazine-1-carboxylate, 20**

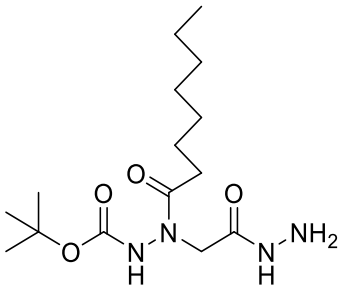

Starting from compound **12** (9 mmol, 2.97 g), product **20** (8.82 mmol, 2.91 g, yield 98%) was obtained as a colourless oil.

R_f = 0.19 (AcOEt). ^{1}H NMR (400 MHz, $CDCl_3$): δ 0.85-0.88 (m, 3H), 1.26 (bs, 8H), 1.48 (s, major conformer, 9H), 1.49 (s, minor conformer, 9H), 1.54-1.63 (m, 2H), 2.39-2.45 (m, 2H), 3.85 (bs, 1H), 5.00 (bs, 1H), 7.10 (bs, 2NH), 8.56 (bs, NH), 10.66 (bs, NH). ^{13}C NMR (100 MHz, $CDCl_3$): δ 14.2, 22.7, 24.6, 28.3, 29.2, 29.4, 31.8, 32.0, 51.5, 82.7, 155.0, 169.2, 176.8. MS (ESI): *m/z* = 331.2 $[M+H]^+$, 353.2 $[M+Na]^+$.

***tert*-Butyl 2-(2-(2-(2-(2-(2-hydrazinyl-2-oxoethyl)-2-octanoylhydrazinyl)-2-oxoethyl)-2-octanoylhydrazinyl)-2-oxoethyl)-2-octanoylhydrazine-1-carboxylate, 27**

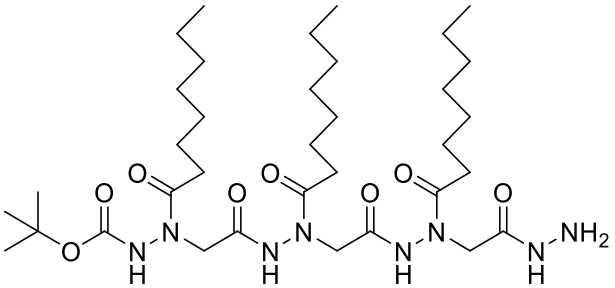

Starting from compound **22** (300 μmol, 218 mg), product **27** (297 μmol, 216 mg, yield 98%) was obtained as a colourless oil.

R_f = 0.16 (Et_2O/MeOH = 9:1). ^{1}H NMR (400 MHz, $CDCl_3$): δ 0.83-0.86 (m, 9H), 1.24 (ps, 24H), 1.49 (s, 9H), 1.45-1.57 (m, 6H), 2.25-2.35 (m, 6H), 4.20 (bs, 6H+2NH), 8.73 (bs, 1NH), 9.15 (bs, 1NH), 10.72 (bs, 1NH), 10.91 (bs, 3NH). ^{13}C NMR (100 MHz, $CDCl_3$): δ 14.14, 14.15, 14.18, 22.7, 24.46, 24.47, 24.57, 28.3, 29.1, 29.23, 29.25, 29.31, 29.4, 31.78, 31.81, 31.83, 32.0, 52.3, 53.5, 53.9, 83.6, 156.8, 168.8, 169.3, 170.8, 175.5, 176.1, 176.6. MS (ESI): *m/z* = 727.5 $[M+H]^+$, 749.5 $[M+Na]^+$.

General procedure for the synthesis of the oligomers and their characterization.

Note: representative procedure referred to 1 mmol of starting N-terminal bromoacetyl derivative; the actual amounts of starting compounds used in the reactions are reported case by case.

In a pear-shaped two-necked flask, the suitable N-terminal bromoacetyl derivatives (**18**, **24** or **29**, 1 mmol) and C-terminal hydrazides (**20**, **27** or *t*-butyl carbazate, **9**, 1.05 mmol) were dissolved in anhydrous DCM (0.5 mL) under inert atmosphere (Note: compounds **20** and **27** were brought in the flask by dilution, using the necessary amounts of anhydrous DCM, then the solvent was removed by evaporation under vacuum at room temperature). DIPEA (1.05 mmol, 183 μL) was added, the reaction was stirred for 48 hours at room temperature, and then the volatile species were eliminated under vacuum at room temperature. The crude mixture was submitted to a partial purification by flash chromatography on silica gel (*c*-Ex/AcOEt), obtaining the corresponding intermediate (**19**, **21**, **25** or **30**), impure of a little trace of C-terminal hydrazide (**20** or **27**), as a colourless oil. The intermediate was diluted in DCM (5 mL), then pyridine (1.2 mmol, 97 μL) and octanoyl chloride (1.1 mmol, 188 μL) were sequentially added. The reaction was stirred for 3 hours, then all the volatiles were evaporated under vacuum without using the thermostating bath. The residue was diluted with Et_2O (30 mL) and water (10

mL), the phases were separated and the organic one was washed with HCl 0.5 M (2 × 3 mL), NaOH 0.1 M (2 × 3 mL) and water (3 mL). The aqueous phases were sequentially extracted with additional Et_2O (30 mL), then the second organic phase was washed with water (5 mL), HCl 0.5 M (3 mL), NaOH 0.1 M (3 mL) and water (3 mL). The combined organic phases were dried over anhydrous Na_2SO_4 and the solvent was eliminated under reduced pressure. The crude product was purified by silica gel flash chromatography, obtaining the pure compound (**17**, **22**, **26** or **31**).

***tert*-Butyl 2-(2-(2-(2-methoxy-2-oxoethyl)-2-octanoylhydrazinyl)-2-oxoethyl)-2-octanoylhydrazine-1-carboxylate, Boc-DIMER-OMe 17**

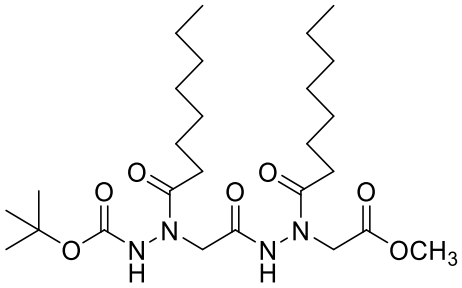

Starting from compounds **18** (3 mmol, 1.06 g) and **9** (3.15 mmol, 417 mg), product **17** (2.17 mmol, 1.15 g, yield 72%) was obtained as a colourless oil.

R_f = 0.35 (*c*-Ex/AcOEt = 1:1). ^{1}H NMR (400 MHz, $CDCl_3$, major conformer): δ 0.87 (t, *J* = 6.9 Hz, 3H), 0.88 (t, *J* = 6.9 Hz, 3H), 1.24-1.33 (m, 16H), 1.51 (s, 9H), 1.55-1.67 (m, 4H), 2.31-2.42 (m, 4H), 3.72 (s, 3H), 4.16 (bs, 2H), 4.39 (bs, 2H), 6.92 (bs, NH), 9.53 (bs, NH). ^{13}C NMR (100 MHz, $CDCl_3$, major conformer): δ 14.16, 14.2, 22.73, 22.74, 24.5, 24.7, 28.2, 29.17, 29.25, 29.31, 29.38, 31.78, 31.86, 31.88, 32.0, 48.2, 52.3, 53.9, 83.4, 155.5, 167.6, 169.6, 175.7, 176.4. MS (ESI): *m/z* = 529.4 $[M+H]^+$, 551.3 $[M+Na]^+$.

***tert*-Butyl 2-(2-(2-(2-(2-(2-methoxy-2-oxoethyl)-2-octanoylhydrazinyl)-2-oxoethyl)-2-octanoylhydrazinyl)-2-oxoethyl)-2-octanoylhydrazine-1-carboxylate, Boc-TRIMER-OMe 22**

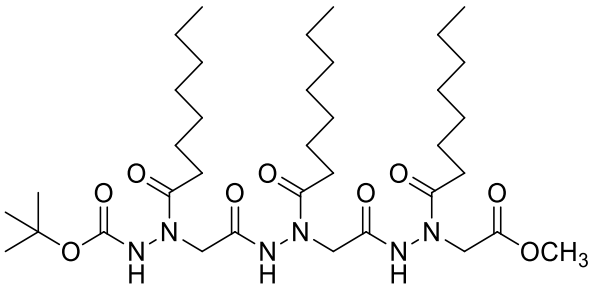

Starting from compounds **18** (1.5 mmol, 527 mg) and **20** (1.58 mmol, 522 mg), product **22** (886 μmol, 644 mg, yield 59%) was obtained as a colourless oil.

R_f = 0.45 (AcOEt). ^{1}H NMR (400 MHz, $CDCl_3$): δ 0.84-0.87 (m, 9H), 1.26 (bs, 24H), 1.51 (s, 9H), 1.54-1.61 (m, 6H), 2.25-2.34 (m, 6H), 3.71 (s, 3H), 3.70-4.60 (m, 6H), 7.62 (bs, NH), 10.25 (bs, NH), 10.55 (bs, NH). MS (ESI): *m/z* = 727.5 $[M+H]^+$, 749.4 $[M+Na]^+$.

1-(*tert*-Butyl) 17-methyl 3,7,11,15-tetraoctanoyl-5,9,13-trioxo-2,3,6,7,10,11,14,15-octaazaheptadecanedioate, Boc-TETRAMER-OMe 26

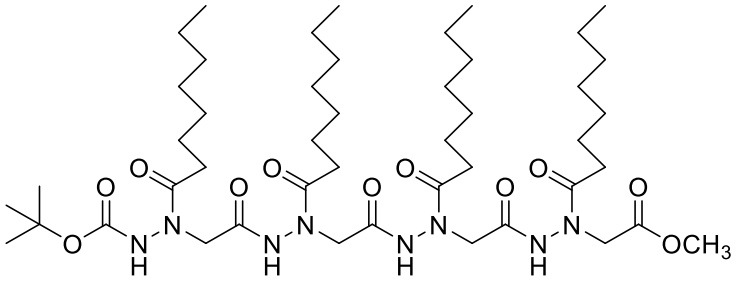

Starting from compounds **24** (1 mmol, 550 mg) and **20** (1.05 mmol, 347 mg), product **26** (628 μmol, 581 mg, yield 63%) was obtained as a colourless oil.

R_f = 0.33 (AcOEt). ^{1}H NMR (400 MHz, $CDCl_3$): δ 0.85-0.88 (m, 12H), 1.27-1.29 (m, 32H), 1.53 (s, 9H), 1.54-1.62 (m, 8H), 2.22-2.36 (m, 8H), 3.50-4.70 (m, 8H), 3.72 (s, 3H), 7.88 (bs, NH), 10.20 (bs, NH), 10.72 (bs, NH), 10.81 (bs, NH). MS (ESI): *m/z* = 925.6 $[M+H]^+$, 947.6 $[M+Na]^+$.

1-(*tert*-Butyl) 29-methyl 3,7,11,15,19,23,27-heptaoctanoyl-5,9,13,17,21,25-hexaoxo-2,3,6,7,10,11,14,15,18,19,22,23,26,27-tetradecaazanonacosanedioate, Boc-HEPTAMPER-OMe 31

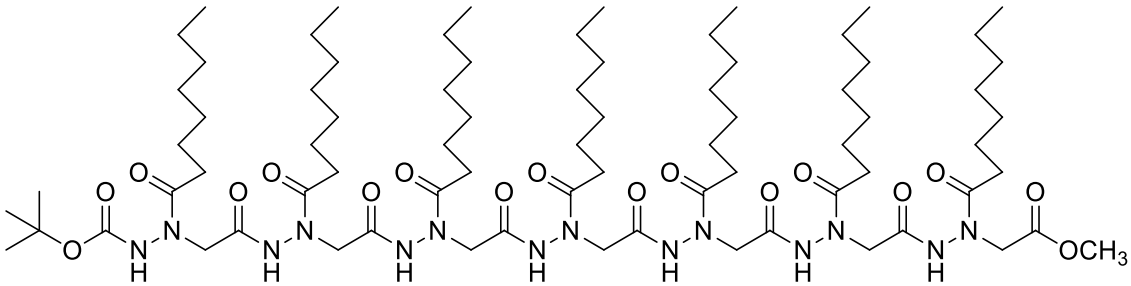

Starting from compounds **29** (200 μmol, 150 mg) and **27** (210 μmol, 153 mg), product **31** (82 μmol, 125 mg, yield 41%) was obtained as a colourless wax.

R_f = 0.14 (AcOEt/MeOH = 98:2). ^{1}H NMR (400 MHz, $CDCl_3$): δ 0.85-0.87 (m, 21H), 1.26 (bs, 56H), 1.52 (s, 9H), 1.54-1.57 (m, 14H), 2.29-2.34 (m, 14H), 3.40-4.80 (m, 8H), 3.71 (s, 3H),

8.29 (bs, 1NH), 10.25 (bs, 2NH), 10.98 (bs, 3NH), 11.13 (bs, 1NH). MS (ESI): *m/z* = 1520.1 $[M+H]^+$, 1521.0 $[M(1\ ^{13}C)+H]^+$, 1542.1 $[M+Na]^+$, 1543.1 $[M(1\ ^{13}C)+Na]^+$.

3.5 Supplementary session

Table 17. Evaluation of δ_M, δ_D, K_{eq} and f_D from dilution experiments in $CDCl_3$ at 25 °C.

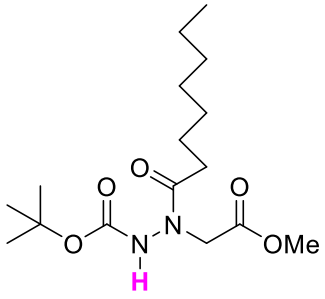

Boc-MONOMER-OMe **12**

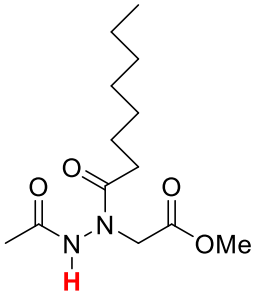

Ac-MONOMER-OMe **14**

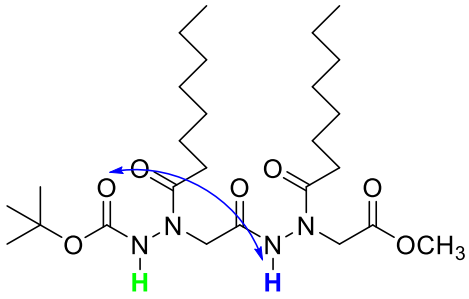

Boc-DIMER-OMe **17**

	$[M_0]$ (M)	δ_{obs} (ppm)	δ_M (ppm) [δ_M±std. err. (ppm)][a]	δ_D (ppm) [δ_D±std. err. (ppm)][a]	K_{eq} (M^{-1}) [K_{eq}±std. err. (M^{-1})][a]	R^{2a}	f_D [f_D±std. err.][b]
NH	0.001 0.005 0.010 0.025 0.050 0.100	6.9301 6.9367 6.9406 6.9577 6.9738 7.0143	6.93077 [6.931±0.002]	7.79021 [7.8±0.6]	0.59149 [0.6±0.5]	0.9962	$1.1802*10^{-3}$ $[1.180±0.004*10^{-3}]$ $5.8460*10^{-3}$ $[5.85±0.11*10^{-3}]$ $1.156*10^{-2}$ $[1.16±0.04*10^{-2}]$ $2.795*10^{-2}$ $[2.8±0.3*10^{-2}]$ $5.304*10^{-2}$ $[5±1*10^{-2}]$ 0.09656 $[1.0±0.4*10^{-1}]$
NH	0.001 0.005 0.010 0.025 0.050 0.100	7.7813 7.7945 7.8093 7.8589 7.9258 8.0200	7.77569 [7.776±0.002]	8.97853 [9.0±0.1]	1.6049 [1.6±0.2]	0.9997	$3.1894*10^{-3}$ $[3.189±0.005*10^{-3}]$ $1.5554*10^{-2}$ $[1.555±0.013*10^{-2}]$ $3.0189*10^{-2}$ $[3.02±0.05*10^{-2}]$ 0.069481 $[6.9±0.3*10^{-2}]$ 0.12334 $[1.2±0.1*10^{-1}]$ 0.20359 $[2.0±0.3*10^{-1}]$
NH	0.001 0.005 0.010 0.025 0.050 0.100	6.8634 6.8915 6.9244 7.0270 7.1693 7.4251	6.85641 [6.856±0.002]	12.1678 [12.2±0.5]	0.6708 [0.67±0.07]	0.9999	$1.3380*10^{-3}$ $[1.3380±0.0008*10^{-3}]$ $6.6195*10^{-3}$ $[6.62±0.02*10^{-3}]$ $1.3068*10^{-2}$ $[1.307±0.008*10^{-2}]$ $3.1463*10^{-2}$ $[3.15±0.05*10^{-2}]$ $5.9353*10^{-2}$ $[5.94±0.17*10^{-2}]$ $1.0699*10^{-1}$ $[1.07±0.06*10^{-1}]$
NH	0.001 0.005	9.4976 9.5152	9.49358[c] [9.494±0.001]	12.5136[c] [12.5±0.3]	0.7177[c] [0.72±0.09]	0.9998[c]	$1.4312*10^{-3}$ $[1.431±0.001*10^{-3}]$ $7.0758*10^{-3}$ $[7.08±0.02*10^{-3}]$

	0.010	9.5347					$1.3956*10^{-2}$ $[1.40\pm0.01*10^{-2}]$
	0.025	9.5972					$3.3520*10^{-2}$ $[3.35\pm0.06*10^{-2}]$
	0.050	9.6822					$6.3010*10^{-2}$ $[6.3\pm0.2*10^{-2}]$
	0.100	9.8350					$1.1295*10^{-1}$ $[1.13\pm0.08*10^{-1}]$

[a] Calculated by non-linear regression of eq 6. [b] H-bonded dimer molar fractions calculated for the total substrate concentrations [M_0] reported in the second column. Five significant figures for K_{eq} were used in eq 4in order to minimize rounding errors during f_D calculations and during intermediate calculations for the propagation of errors in the calculation of f_D standard error. [c] Calculated by non-linear regression of eq 6, intentionally assuming that the equilibrium in Scheme 1is valid instead of the equilibrium Scheme 2

Table 18. Chemical shifts *vs* added DMSO-d_6 data for compounds 12, 14, 17 and 15 in $CDCl_3$ at 25 °C.[a]

Compound	% DMSO-d_6 added (v/v)	$\delta_{\text{first residue}}$ (ppm)	$\delta_{\text{second residue}}$ (ppm)
12	0	6.933	---
	0.99	7.054	
	1.96	7.169	
	2.91	7.281	
	3.84	7.388	
	4.76	7.490	
	6.54	7.678	
	8.26	7.850	
	9.91	8.005	
	only DMSO-d_6[a]	9.730	
14	0	7.788	---
	0.99	8.525	
	1.96	8.944	
	2.91	9.214	
	3.84	9.406	
	4.76	9.546	
	6.54	9.745	
	8.26	9.877	
	9.91	9.974	
	only DMSO-d_6[b]	10.494	
17	0	6.886	9.513
	0.99	7.785	9.901
	1.96	8.151	10.050
	2.91	8.357	10.131
	3.84	8.497	10.185
	4.76	8.602	10.222
	6.54	8.750	10.274
	8.26	8.856	10.309
	9.91	8.937	10.335
	only DMSO-d_6[b]	9.764	10.576

Compound	% DMSO-d_6 added (v/v)	$\delta_{\text{first residue}}$ (ppm)	$\delta_{\text{second residue}}$ (ppm)	$\delta_{\text{first residue}}$ (minor conformer) (ppm)	δ_{NH_2} H-bonded major conformer (ppm)	δ_{NH_2} H-bonded minor conformer (ppm)	δ_{NH_2} NO H-bonded major conformer (ppm)	δ_{NH_2} NO H-bonded minor conformer (ppm)
15[c]	0	6,956	---	6.647	6.784	8.783	5.344	5.481
	0.99	7.547		6.999	7.125	8.724	5.442	5.564
	1.96	7.852		7.264	7.265[d]	8.676	5.514	5.639
	2.91	8.045		7.450	7.382	8.637	5.570	5.710
	3.84	8.181		7.596	7.447	8.601	5.622	5.774
	4.76	8.285		7.716	7.490	8.573	5.672	5.839
	6.54	8.437		7.899	7.542	8.508	5.766	5.953
	8.26	8.548		8.036	7.571	8.461	5.853	6.064
	9.91	8.633		8.144	7.588	8.422	5.937	6.166
	only DMSO-d_6[b]	9.585		9.028	7.373	6.514	7.115	6.635

[a] 5 mM solutions in $CDCl_3$. [b] 5 mM solutions in DMSO-d_6. [c] Compound **15** presents several conformers. [d] Approximated value due to extended overlaps among NHs and residual solvent peak.

CHAPTER 4:

α-Hydrazido acids as small synthetic mimics of antimicrobial peptides

4. THE NEED FOR NEW ANTIBACTERIAL AGENTS: AN OVERVIEW

4.1 Introduction: *The "Post-Antibiotic Era"*

The development of resistance to first-line antibiotics is a natural biological phenomenon that can be amplified by several factors.[43] Some bacteria are naturally resistant to certain classes of antibiotics, due to different mechanisms such as: production of specific enzymes, release of antibacterial agents through a system of efflux pumps, modification of the antibacterial targets and presence of alternative metabolic pathways. Other bacteria may spontaneously develop resistance due to genetic mutations. These genes can also be transferred by conjugation, transduction or transformation to other strains of the same bacterium, or also to different species (Figure 44).

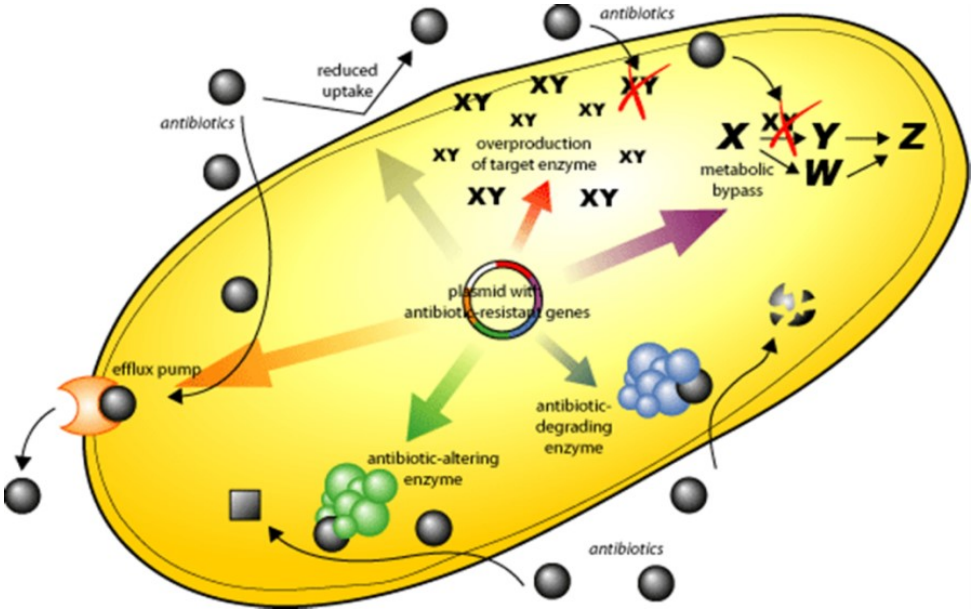

Figure 44. Bacterial resistance mechanisms.

Therefore, mutations and selection, together with the genetic exchange mechanisms, make many bacterial species able to adapt quickly to new antibacterial agents, facilitating the development of drug resistance, as exemplified by the sharp rise in strains of *S. aureus* resistant to methicillin (MRSA), multidrug-resistant *K. pneumoniae* (MDRKP), vancomycin-resistant *Enterococci* (VRE), and multidrug-resistant *P. aeruginosa* (MDRPA) in Europe in 2014 (Figure 45). Given these premises, it is therefore evident the need to find new classes of antimicrobial agents with new mechanisms of action, or that have as targets bacterial structures or molecules that are difficult to change, making these new drugs much less susceptible to the development of resistance.

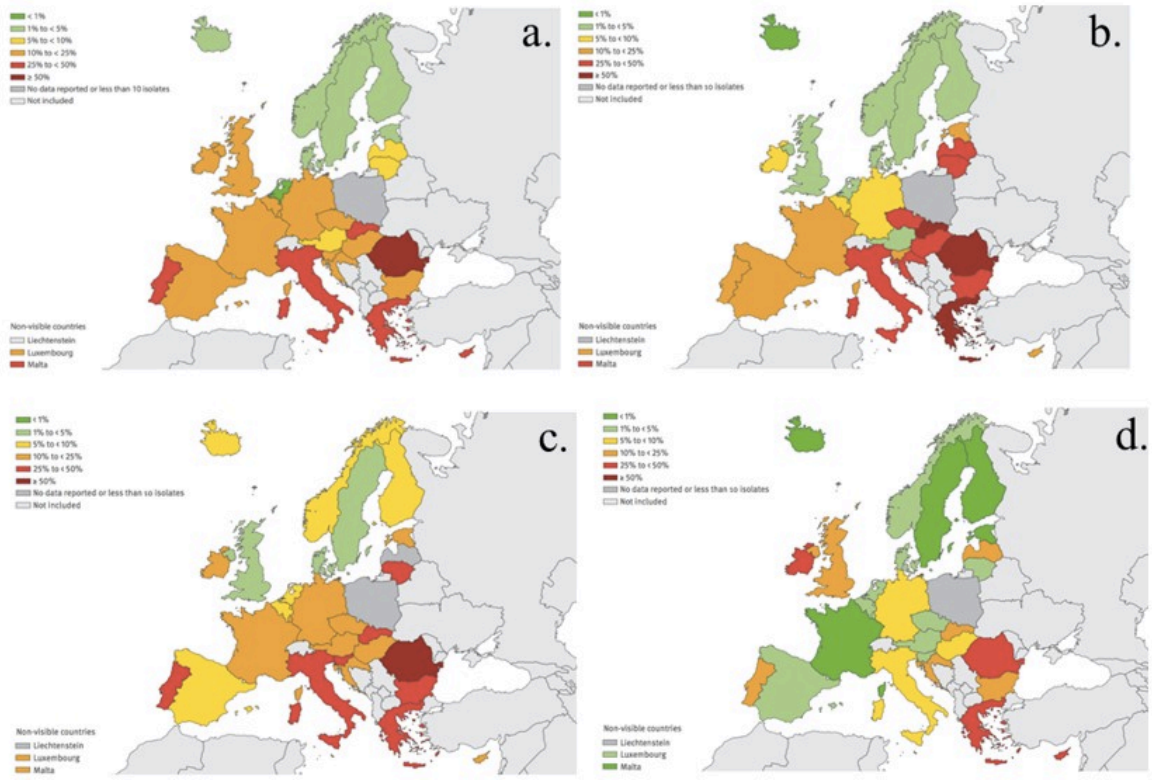

Figure 45. Percentage (%) of invasive isolates with resistance to several drugs by country (EU/EEA countries, 2014). (a) *S. aureus* isolates with resistance to meticillin (MRSA); (b) *K. pneumoniae* isolates with combined resistance to fluoroquinolones, third-generation cephalosporins and aminoglycosides; (c) *P. aeruginosa* isolates with resistance to piperacillin + tazobactam; (d) *Enterococci* isolates with resistance to vancomycin (VRE). Data from European Centre for Disease Prevention and Control (ECDC).

4.2 Natural AntiMicrobial Peptides (AMPs): are they promising candidates?

Since 1970, when the first antimicrobial and hemolytic peptide, *mellitin*, was isolated from bee venom, hundreds of cationic antimicrobial peptides (AMPs, AntiMicrobial Peptides, also known as Host-Defense Peptides) were found in all classes of life, including humans (Figure 46).[44]

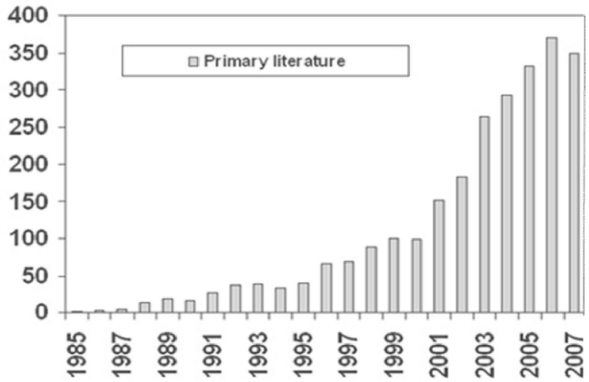

Figure 46. New AMPs isolated per year.

Despite the variety in primary and secondary structure (Figure 47), AMPs have some common features. They are relatively small (12-50 amino acids), with the 50% of hydrophilic residues and a net positive charge (+2 to +5) due to an excess of Arg and Lys.[45] They can show either amphiphilic or random structures in solution but, even in the latter case, during the interaction with the cell membrane they completely reorganize their conformation, so that they have an amphiphilic folding, with a well defined segregation of the lipophilic and hydrophilic moieties.[46]

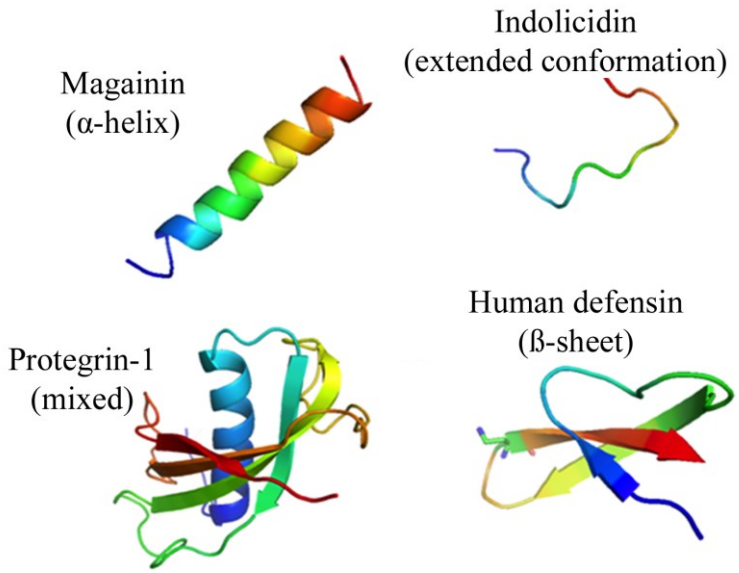

Figure 47. Principal structural classes of AMPs.

The cationic and amphiphilic nature of AMPs is essential for their action, but their mechanism of action is still unclear. They are generally considered to act mainly on the cellular membrane, even if some recent evidences have suggested that some of them can also act onto intracellular targets.[47] To carry out their function, antimicrobial peptides must first be attracted onto the cell surface (Figure 48). One clue to the potential specificity of killing by membrane disruption is that there are significant differences in the lipid composition of bacterial and eukaryotic cell membranes.[48] Bacterial membranes are negatively charged, due to the presence of anionic phospholipids, such as phosphatidylserine (PS), phosphatidylglycerol (PG), or cardiolipin (CL).

For this reason, the cationic antimicrobial peptides are electrostatically attracted to these membranes. On the other hand, the mammalian membrane is neutral, due to the presence of zwitterionic phospholipids, such as phosphatidylethanolamine (PE), phosphatidylcholine (PC) or sphingomyelin (SM). Moreover, the presence of cholesterol stabilizes the phospholipid

bilayer. Due to these differences on the composition of the membranes, AMPs can selectively act against bacterial targets (Figure 48).[44,49]

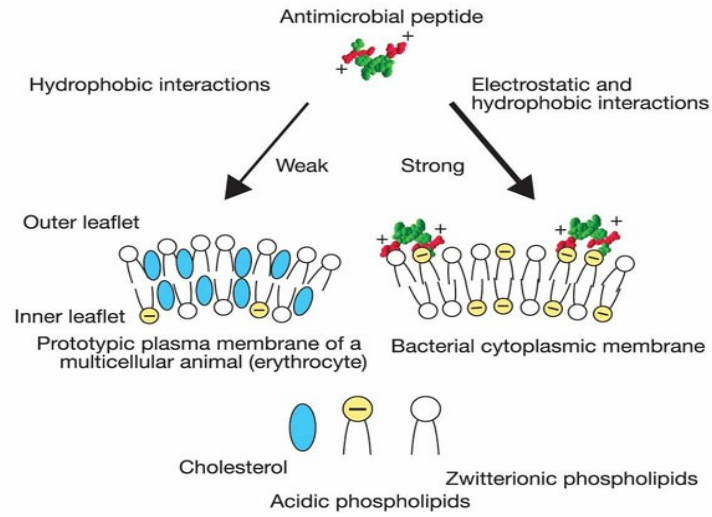

Figure 48. Bases of specificity of AMPs' action.

During the interaction with the membrane of Gram-negative bacteria, AMPs must first pass through the outer membrane, which is essentially composed of anionic lipopolysaccharide (LPS), associated with divalent cations such as Mg^{2+} and Ca^{2+} (Figure 49).

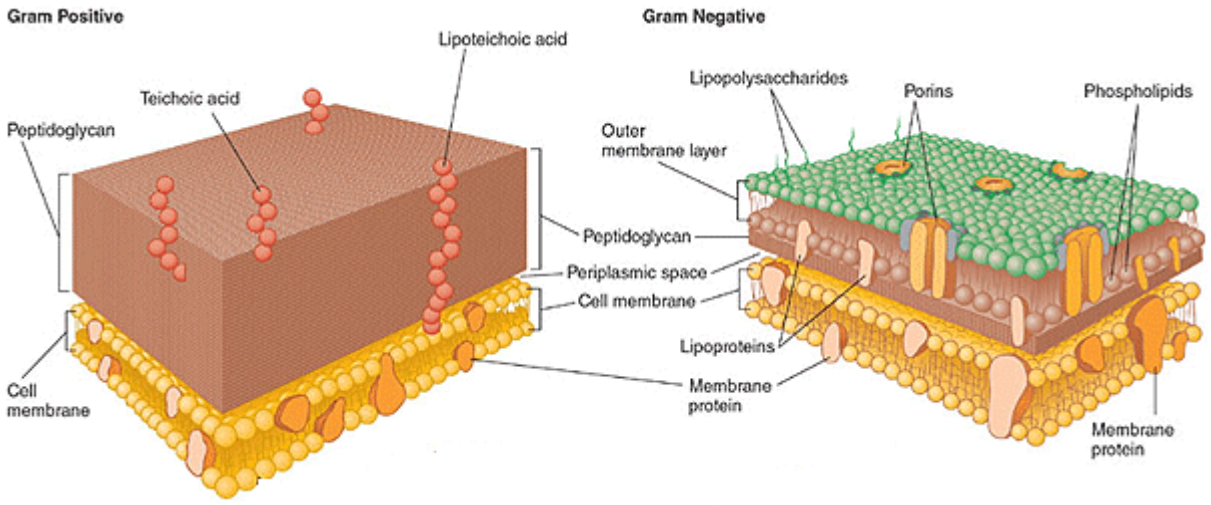

Figure 49. Membrane composition of the Gram-positive and Gram-negative bacteria.

According to the *self-promoted uptake* process,[50] the cationic nature of the natural antimicrobial peptides leads them to replace these ions by electrostatically interaction with lipopolysaccharides. This interaction causes a destabilization of the area through which the peptides reach the periplasmic space. In a similar manner, by interacting with the teichoic acid and lipoteichoic acids, these molecules can cross the thick wall of Gram-positive bacteria, made

of peptidoglycan. At this point, AMPs can interact with the phospholipid bilayer of the cytoplasmic membrane and give rise to their action according to various models (Figure 7).[44,49,50,51]

In the *carpet model* (Figure 50A), cationic peptides bind to the membrane by means of electrostatic interactions and accumulate themselves on the outer surface. Then, when they reach a critical density, the curvature strain to which the membrane is subjected leads to the disruption of the membrane itself. In the *barrel-stave model* (Figure 50B), after the electrostatic interaction, the peptides insert perpendicularly in the membrane and form transmembrane pores. The amphiphilic conformation plays a central role in this mechanism, since the hydrophobic surface of AMPs interacts with the lipophilic chains of the membrane, while their hydrophilic surface forms the central lumen of the channel. Alamethicin is a well-studied example of this type of mechanism.[52] In the *toroidal-pore model* (Figure 50C), the introduction of antimicrobial peptides inside the membrane causes the bending of the layers through the pores, so that the water-exposed core is composed of both the hydrophilic portions of the antimicrobial peptides and the negatively charged phospholipid heads. This mechanism appears to be exploited by magainin, protegrin and mellitin.[53]

In all the previous models, the resulting effects are the membrane destabilization and the increase of permeability, which lead both to a loss of ions and metabolites, and to depolarization with the lysis and bacterial death. Anyway, not all antimicrobial peptides have this disruptive effect on the membrane. In fact, some of them can also penetrate inside the cell and act on intracellular targets (Figure 50D). These non-membrane active peptides are able to translocate across the membrane without disrupting its integrity, accumulating within the target cells, and inhibiting essential cellular processes, such as DNA or RNA synthesis, protein folding or expression of the enzymes crucial for metabolism, biosynthesis of the cell wall components, and proliferation of pathogens.[44,49,54] It should be mentioned that some membranolytic peptides were also found to be able to interact with intracellular targets when used in sub-minimal inhibitory concentrations, thus showing the possibility for multiple mechanisms of action.[55]

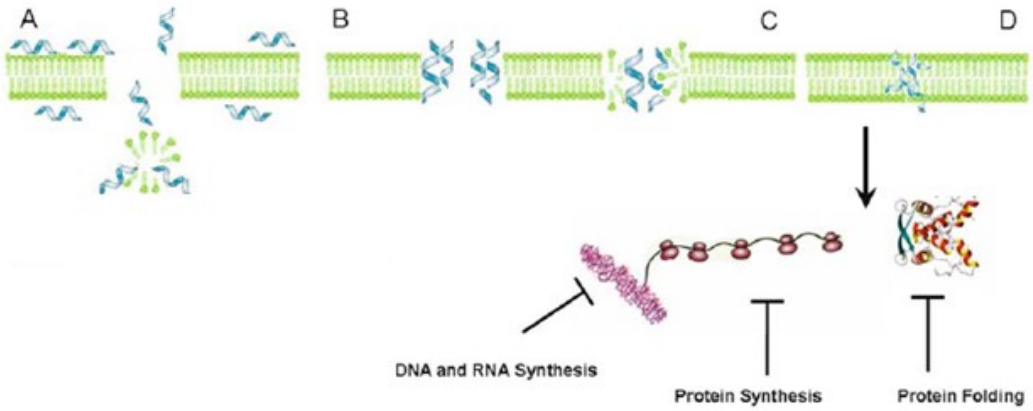

Figure 50. Possible mechanisms of action for AMPs. A) *carpet model*, B) *barrel-stave model*, C) *toroidal-pore model*, D) *Intra*cellular targets.

Thus, due to the fact that the activity of AMPs is not based on a specific target, at least in the most part of cases, it is unlikely for bacteria to develop resistance according to one of the mutations described above. To prevent the action of cationic peptides, the bacteria should massively modify their membrane structure, which is a very unlikely process, although some cases of resistance have been detected.[56] Therefore, it is generally accepted that AMPs have a quite low propensity to develop resistance, and this is confirmed by the fact that they have remained effective for billions of years against bacterial infections.

These features, together with their broad spectrum of activity against microbes and their selective activity against the bacterial cells rather than the human cells, have recently made AMPs promising candidates for the "post-antibiotic era".

4.2.1 Problems related to the use of natural antimicrobial peptides

Since pathogenic bacteria constantly meet AMPs during infections, they have developed several mechanisms which confer intrinsic or inducible resistance.[57]

One of the most characterized resistance to AMPs is the one to polymyxin B (PXB, Figure 51) mediated by lipopolysaccharide (LPS). PXB is a cyclic lipopeptide that binds to lipid A, lethal for some Gram-negative bacteria, and has long been used as a model to define both the mechanisms by which AMPs kill bacteria and the ways in which bacteria may develop resistance to AMPs.

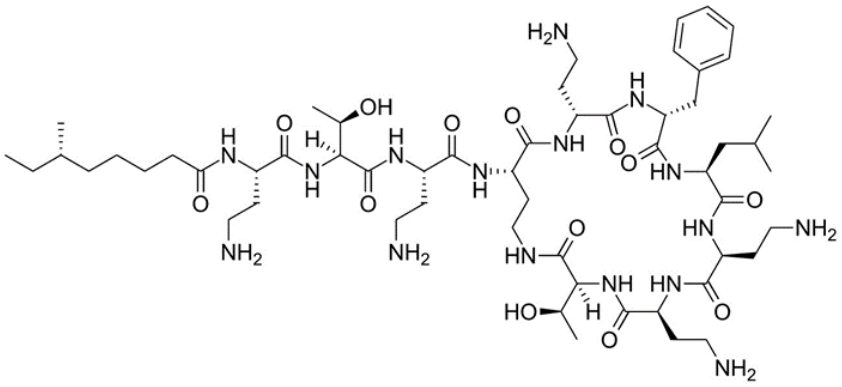

Figure 51. Structure of polymyxin B.

Resistance mechanisms include the use of membrane-associated proteases that degrade the peptides, efflux pumps and transport systems that export AMPs from the periplasmic and intracellular compartment, the modulation of the permeability of the outer membrane by the proteins of the latter, and structural changes in the lipopolysaccharide (LPS) and lipooligosaccharides (LOS) (Figure 52).

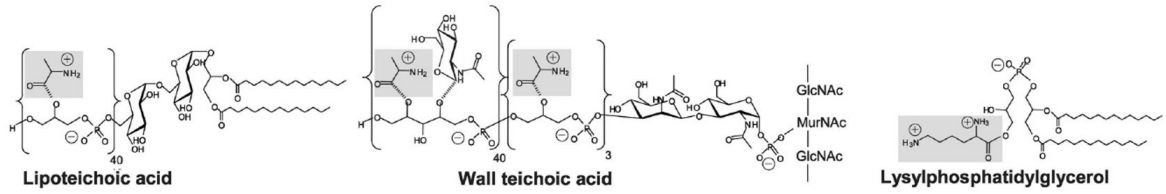

Figure 52. Modifications of the staphylococcal wall components involved in resistance towards antimicrobial cationic molecules. Highlighted in grey are the esters of *D*-alanine in teichoic acids and the esters of *L*-lysine in L-PG.

Studies on the acquired resistance against the antimicrobial peptides have identified genes that, when broken, make certain microorganisms more susceptible to a particular antimicrobial peptide and, in fact, these genes seem to have specific roles in virulence (Table 19).[57]

Table 19. Summary of known mechanisms of acquired resistance to antimicrobial peptides.

ORGANISM	METHOD FOR ISOLATION	AMP RESISTANCE	GENES INVOLVED IN AMP RESISTANCE	PROPOSED MECHANISM
Staphylococcus aureus	Clinical isolates	LL-37, human β-defensin 2, human β-defensin 3, lactoferricin B	*hemB*	Inactivation results in small colony variant (SCV) phenotype with reduced AMP binding/uptake
Escherichia coli, Klebsiella pneumoniae	Clinical isolates	Colistin, polymyxin B	*mcr-1*	Encodes a PEtN transferase modifies lipid A to reduce anionic charge
Listeria monocytogenes	Direct plating with leucocin A	Leucocin A	*mptACD*	Unknown

Acinetobacter baumannii	Direct plating with colistin	Colistin, polymyxin B	*lpxA, lpxD, or lpxC*	Inactivation results in complete loss of LPS production, reduced AMP binding
Salmonella typhimurium	DES mutagenesis	Polymyxin, CAP37, CAP57, protamine, polylysine	*phoQ*	Constitutive activation in low Mg^{2+} of phoP-regulated LPS modifications reduce anionic charge
	Direct plating with colistin	Colistin, polymyxin B	*pmrA, pmrB*	Constitutive activation of pmrAB-regulated Ara4N and PEtN LPS modification reduce anionic charge
	Direct plating with PR-39	PR-39	*sbmA*	Inactivation reduces AMP uptake
	Direct plating with protamine	Protamine, colistin, lactoferricin, human α-defensin 1	*hemA, hemB, hemC, hemL*	Inactivation results in small colony variant (SCV) phenotype with reduced AMP binding/uptake
	Serial passage with LL-37 or CNY100HL	LL-37, CNY100HL, wheat germ histones	pmrB, phoP	Constitutive activation of various LPS modifications reducing anionic charge

Ara4N, 4-aminoarabinose; PEtN, phosphoethanolamine.

Further investigations above resistance of Gram-negative bacteria have shown that some strains possess a resistance mechanism based on a membrane modification. The charge on the outer membrane is modulated by the regulon PhoPQ, a two-component system that uses a sensor (PhoQ) and an intracellular effector (PhoP) that, depending on the environmental changes, can change the external structure of the membrane, thus lending resistance to AMP.[58]

This system has not spread in all microbial species, since the modification and/or reorganization of membrane structure requires substantial metabolic costs. Most peptides, however, are created by sequences of amino acids devoid of epitopes that may serve as the recognition site for proteases. Moreover, multicellular organisms attack microbes with several peptides coming from different structural classes, and for this reason the destruction of a particular peptide may not be sufficient for the bacterial survival.

Furthermore, in addition to the limitations listed above, AMPs suffer from several limitations regarding safety, pharmacokinetics, metabolic stability and production costs. Although many of the natural peptides, such as magainins, show good *in vitro* activity, unfortunately they are effective *in vivo* only at high doses, next to the toxicity, and this lack in terms of safety often makes AMPs unacceptable as systemic therapeutic agents. In fact, to date only few classes of AMPs are in clinical development, and they are mainly used only for topical therapy (Table 20).[57]

Table 20. Antimicrobial peptides in clinical development.

Peptide	AMP source (host)	Status	Administration	Indication	Company
OP-145	LL-37 (human)	Phase I/II	Ear drops	Chronic bacterial ear infection	OctoPlus Inc.
hLF1–11 (Lactoferrin)	Lactoferrin 1–11 (human)	Not specified	Intravenous	Neutropenic stem cell transplantation patients	AM-Pharma B.V.
Pexiganan (MSI-78)	Magainin (frog)	Phase III	Topical cream	Diabetic foot infection	Dipexium Pharmaceuticals, Inc.
		Phase III	Topical cream	Diabetic foot ulcers	MacroChem Corporation
Iseganan (IB-367)	Protegrin-1 (porcine leukocytes)	Phase III	Mouth wash	Prevention of chemotherapy-induced mucositis	National Cancer Institute (NCI)
		Phase II/III	Mouth wash	Prevention of ventilator-associated pneumonia	IntraBiotics Pharmaceuticals
Omiganan (MBI 226, CLS001)	Indolicidin (bovine neutrophils)	Phase III	Topical cream	Topical skin antisepsis, prevention of catheter infections	Mallinckrodt
		Phase III	Topical cream	Rosacea	Cutanea Life Sciences, Inc.
		Phase II	Topical cream	Usual type vulvar intraepithelial neoplasia (uVIN)	Cutanea Life Sciences, Inc.
		Phase II	Topical cream	Moderate to severe inflammatory acne vulgaris	Cutanea Life Sciences, Inc.
		Phase II	Topical cream	Mild to moderate atopic dermatitis	Cutanea Life Sciences, Inc.
Lytixar (LTX-109)	Synthetic antimicrobial peptidomimetic	Phase II	Topical cream	Uncomplicated Gram-positive skin infections	Lytix Biopharma AS
		Phase I/IIa	Nasal	Nasal carriers of *Staphylococcus aureus*	Lytix Biopharma AS
C16G2	Synthetic specifically targeted antimicrobial peptide	Phase II	Mouth wash	Prevent tooth decay caused by *Streptococcus mutans*	C3 Jian, Inc.

Moreover, α-peptides are usually sensitive to proteases and other plasma components, lowering their bioavailability and therefore negatively affecting their pharmacokinetics. Eventually, the production cost of synthetic peptides is so high, compared to conventional antibiotics, that pharmaceutical industries are reluctant to put much effort into both the testing and developing of new variants.

Because of these drawbacks, several studies were conducted to obtain modified peptides (peptidomimetics) with the necessary biological activity and a higher resistance under physiological conditions.[59,60,61] Therefore, an important objective of today's pharmaceutical chemistry is to design and produce a new generation of effective peptide drugs, or their mimics, by chemical modification of lead compounds.

Since the antimicrobial activity of cationic peptides is not strictly dependent on a specific amino acid sequence, but only on specific physical and chemical properties (size, hydrophobicity, net positive charge, amphipathicity, proportion between the polar and apolar parts), it is possible to design and synthesize new active structures with the same properties and minor disadvantages.

4.3 Synthetic Mimics of AntiMicrobial Peptides (SMAMPs)

As reported above, the possible pharmacological use of AMPs as systemic drugs is prevented by many problems mainly inherent to the chemical nature of AMPs themselves. For these reasons, it is necessary to develop new generation drugs inspired by the mode of action of

AMPs, but without their negative features. These Synthetic Mimics of AMPs (SMAMPs) can be grouped in three major classes, depending on the size of the chemical species involved (small molecules, oligomers or polymers):

- Amphiphilic foldamers (Paragraph 4.3.1 Antimicrobial foldamers)
- Antimicrobial polymers (Paragraph 4.3.2 Antimicrobial polymers)
- Small Molecular Mimics of AntiMicrobial Peptides (SMMAMPs) (Paragraph 4.3.3 Small Molecular Mimics of AMPs: SMMAMPs)

4.3.1 Antimicrobial foldamers

As reported in the previous chapter, β-peptidic foldamers are the most widely investigated peptidomimetic oligomers. They are stable to proteases and peptidases, and usually fold into well-ordered secondary structures with as few as six amino acids, but sometimes even dimers or trimers can have a stable folding.

In this context, several research groups have developed β-peptidic amphiphilic foldamers with a 12- and 14-helix folding that are able to realize an antimicrobial action comparable to - or even better than - that of magainins, but with a lower haemolytic activity (Figure 53 and Figure 54).[62,63]

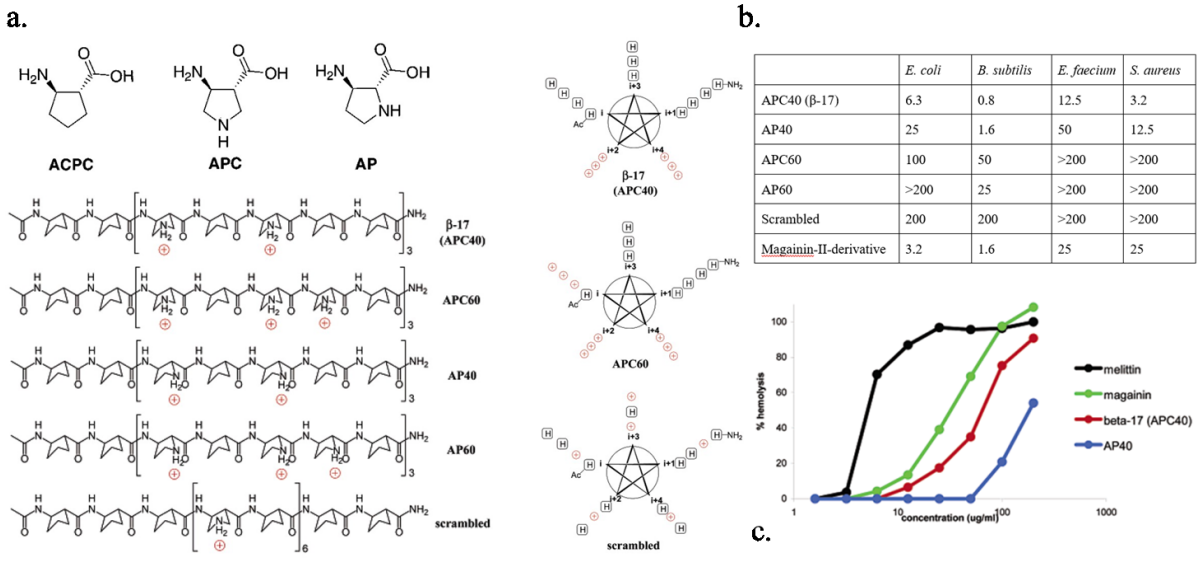

	E. coli	*B. subtilis*	*E. faecium*	*S. aureus*
APC40 (β-17)	6.3	0.8	12.5	3.2
AP40	25	1.6	50	12.5
APC60	100	50	>200	>200
AP60	>200	25	>200	>200
Scrambled	200	200	>200	>200
Magainin-II-derivative	3.2	1.6	25	25

Figure 53. (a) Structures of the 12-helix-forming antimicrobial derivatives tested; (b) bacteriostatic activity (MIC in μg/mL) of Ala[46,59,64]-magainin-II-amide and the 12-helix β-peptides; (c) haemolytic activity of the 12-helix β-peptides. Mellitin was used as the control for haemolytic activity (200 μg/mL as 100%). Taken from Ref. 62.

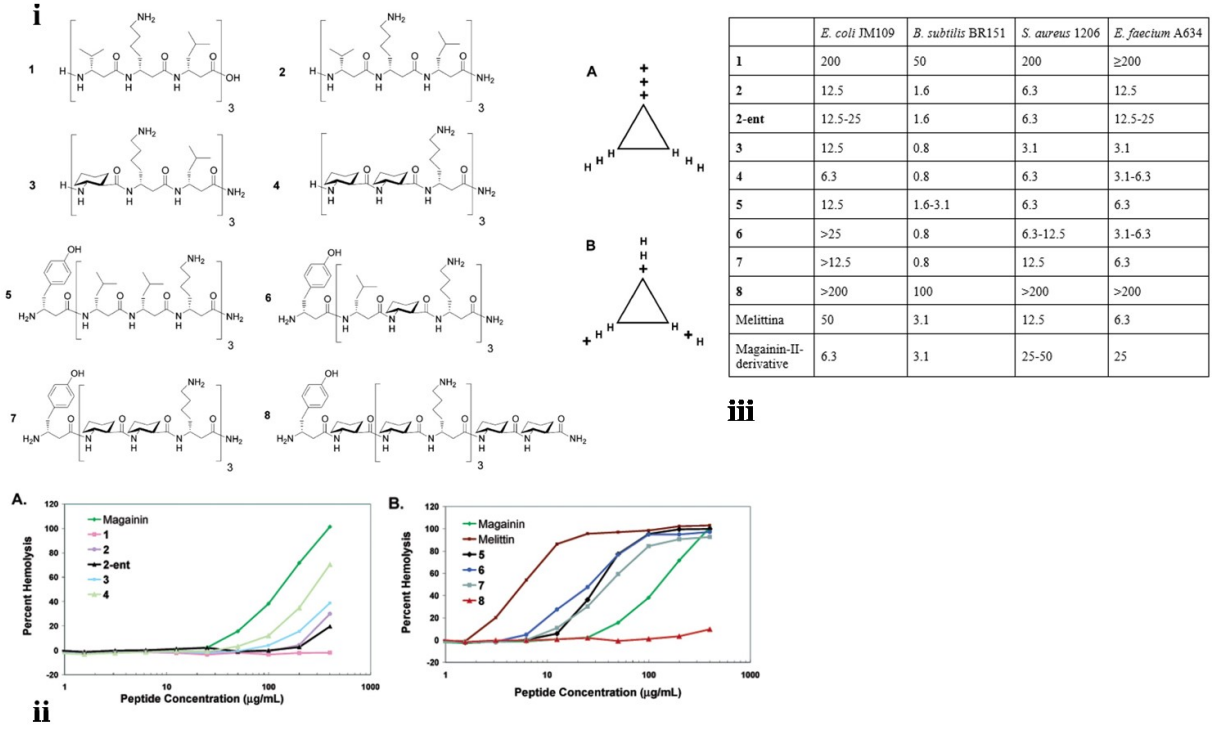

iii

	E. coli JM109	*B. subtilis* BR151	*S. aureus* 1206	*E. faecium* A634
1	200	50	200	≥200
2	12.5	1.6	6.3	12.5
2-ent	12.5-25	1.6	6.3	12.5-25
3	12.5	0.8	3.1	3.1
4	6.3	0.8	6.3	3.1-6.3
5	12.5	1.6-3.1	6.3	6.3
6	>25	0.8	6.3-12.5	3.1-6.3
7	>12.5	0.8	12.5	6.3
8	>200	100	>200	>200
Melittina	50	3.1	12.5	6.3
Magainin-II-derivative	6.3	3.1	25-50	25

Figure 54. (i) Structures of the 14-helix-forming antimicrobial derivatives tested and disposition of the hydrophobic (H) and charged (+) residues; (ii) haemolytic activity of the β-peptidic oligomers, mellitin and Ala[46,59,64] -magainin-II-amide; (iii) bacteriostatic activity (MIC in µg/mL) of Ala[46,59,64] -magainin-II-amide and 14-helix β-peptides. Taken from Ref. 63.

Other studies demonstrated how N,N'-oligoureas with length of eight residues are effective against both Gram-negative and Gram-positive bacteria (including methicillin-resistant *Staphylococcus aureus*) and show selectivity for bacterial cells compared to those of mammals and high resistance to proteolytic degradation (Figure 55).[65]

COMPOUND 10
***i*Pr-NHCO-β-HVal^{u}-β-HLys^{u}-β-HTrp^{u}-β-HVal^{u}-β-HLys^{u}-β-HTrp^{u}-β-HLys^{u}-β-HVal^{u}**

COMPOUND 15
Cyclo(^{D}Arg-Arg-^{D}Lys-Trp-^{D}Leu-Trp-^{D}Leu-Trp)

a.

	Compound	*E. coli* MIC	*E. coli* MBC	*P. aeruginosa* MIC	*P. aeruginosa* MBC	*S. aureus* MIC	*S. aureus* MBC	MRSA MIC	MRSA MBC
10	*i*Pr-NHCO-β-HVal^{U}-β-HLys^{U}-β-HTrp^{U}-β-HVal^{U}-β-HLys^{U}-β-HTrp^{U}-β-HLys^{U}-β-HVal^{U}	16	64	16	128	16	32	16	32
15	Cyclo((D)Arg-Arg-(D)Lys-Trp-(D)Leu-Trp-(D)Leu-Trp)	64	256	64	256	16	64	16	32
	Melittin	32	64	64	256	8	32	8	64

b.

Compound	HC_{50}	Selectivity (HC_{50}/MIC) *E. coli*	Selectivity (HC_{50}/MIC) *S. aureus*
Melittin	30	1.9	3.75
10	150	9.4	9.4
15	100	3.1	6.3

c.

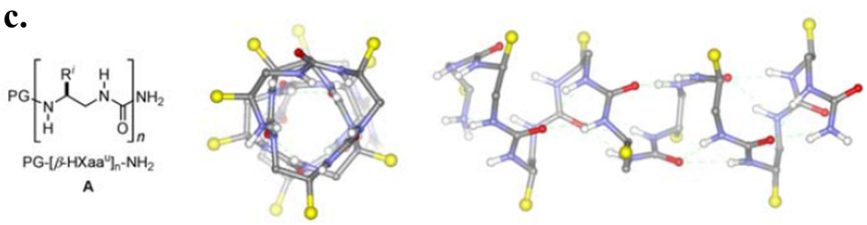

Figure 55. (a) Antimicrobial activities evaluated in Mueller-Hinton broth (MIC and MBC in μg/ml. MRSA: methicillin resistant *Staphylococcus aureus*); (b) Haemolytic activity and selectivity of mellitin and oligourea 10 (HC_{50} in mg/ml. MIC (in mg/ml). Compound 15 is a cyclic L-α-peptide not discussed in the text; (c) Generic structure of a N,N'-Oligourea and representation of the $2.5_{12,14}$ helix.

Moreover, several peptoids with antimicrobial activity were developed, as the first water-soluble antibacterial peptoids based on helical mimics of magainins (Figure 56).[66] Certain peptoids exhibited selective, potent antibacterial activity against both Gram-positive and Gram-negative bacteria.

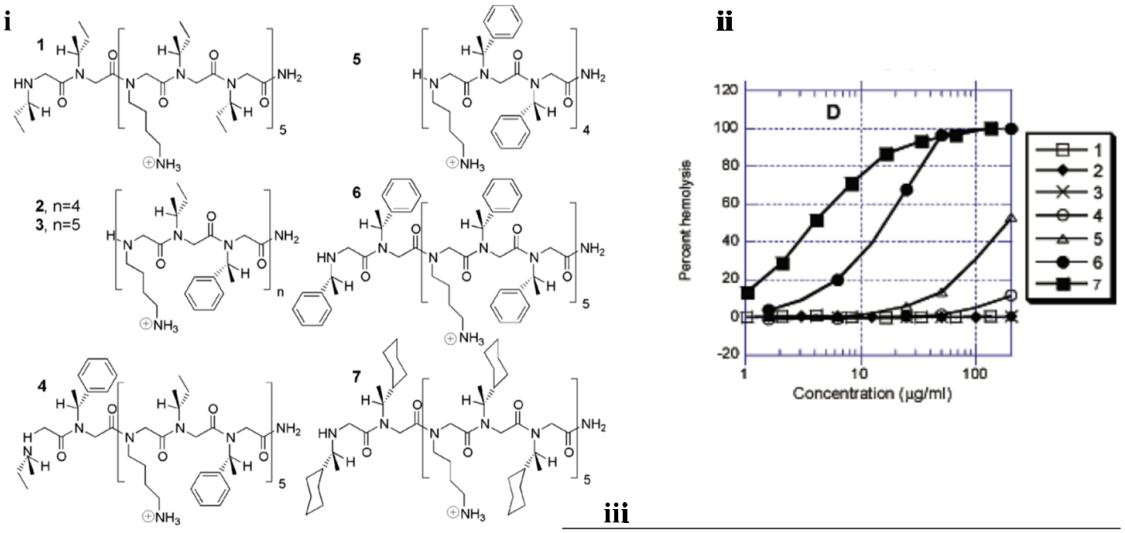

iii

	HPLC elution solvent[a]	*E. coli* MIC[b] μM (μg/mL)	*B. subtilis* MIC[b] μM (μg/mL)	hemolysis at *E. coli* MIC
1	38.9%	>100 (>200)	>100 (>200)	0%
2	39.2%	49 ± 8.3 (80)	7.8 ± 1.3 (13)	0%
3	42.0%	9.9 ± 2.5 (20)	4.4 ± 0.8 (8.9)	0%
4	45.5%	19 ± 4.9 (44)	1.4 ± 0.2 (3.2)	1.2%
5	46.2%	5.4 ± 0.9 (9.8)	0.82 ± 0.14 (1.5)	1.4%
6	57.5%	7.7 ± 1.3 (20)	1.2 ± 0.2 (3.1)	51%
7	83%	>75 (>200)	>75 (>200)	100%[c]

[a] Vydac C4 column. Percent solvent B in A. Solvent A: 0.1 vol % TFA in H_2O. Solvent B: 0.1% (v/v) TFA in CH_3CN. [b] With estimated uncertainty. [c] Reported at 200 μg/mL (~75 μM).

Figure 56. (i) Peptoid mimics of magainin-II-amide; (ii) Hemolytic activities of 1-7 as the percentage erythrocytes lysed following a 1 h peptoid incubation. The most lipophilic peptoids are also the most hemolytic. Conversely, the most hydrophilic peptoids 1-4 exhibit negligible hemolysis at concentrations as high as 200 μg/mL; (iii) Antibacterial and haemolytic activities of peptoids 1-7.

4.3.2 Antimicrobial polymers

The antimicrobial polymers can have extremely different features in terms of chemical structure, but they are all characterized by specific hydrophilic and lipophilic groups, which provide the antibacterial properties, linked to polymeric structures that can be of various sizes, in any case larger than the ones of foldamers. The antimicrobial polymers are mimetic of the action of natural peptides, with the ability to inhibit the growth of microorganisms such as bacteria, fungi or protozoa.[67] Many polymeric SMAMPs show an amphiphilic arrangement during the action but a disordered folding in solution, like some AMPs that fold into amphiphilic structures only when they interact with the bacterial cell membrane (Figure 57a).[68] Anyway, it was demonstrated that polymers containing both cationic and lipophilic side chains may also be induced to adopt a globally amphiphilic structure, but conformationally irregular in terms of backbone torsional angles, when they interact with the bacterial cell membrane, if the backbone is flexible enough (Figure 57b).[69] Indeed, the structural analysis showed that heterochiral polypeptides can be induced by the environment to adopt specific irregular conformations that

cause a global segregation of the hydrophilic and lipophilic moieties. This implies that random copolymers consisting in cationic and lipophilic monomers may be able to mimic the natural defence peptides.[70]

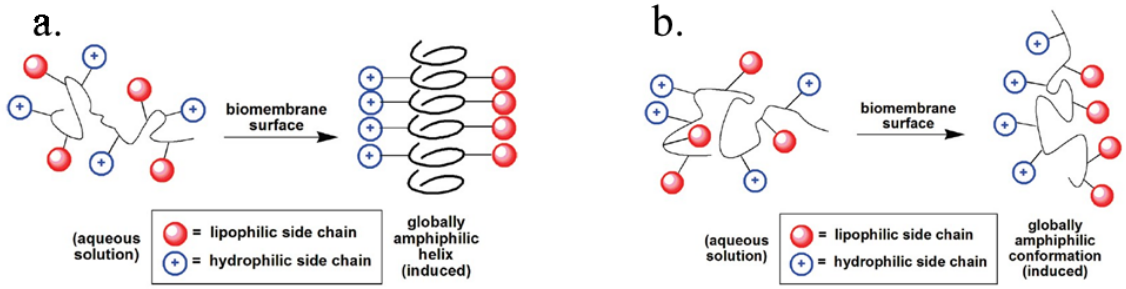

Figure 57. (a) Adoption of a globally amphiphilic ordered helix; (b) Adoption of a globally amphiphilic random conformation.

Usually, the antimicrobial polymers are produced by connecting or inserting an active antimicrobial agent on a polymeric structure *via* an alkyl or acyl linker, making those molecules ideal candidates for several applications: in medicine as "infection-fighters",[71] in the food industry to prevent bacterial contamination,[72] and for the sanitization of drinkable water.[73]

In this category, we can find the nylon-3 polymers, which have a β-peptidic backbone. They can be seen as the higher homologues of poly-α-amino acids and can be conveniently prepared by anionic polymerization, exploiting the ring opening of racemic β-lactams (Figure 58).[74] Despite the heterogeneity in terms of sequence of subunits and stereochemistry, the nylon-3 polymers family shows structure activity relationships (SARs) comparable to those of natural defence peptides and oligomeric analogues.

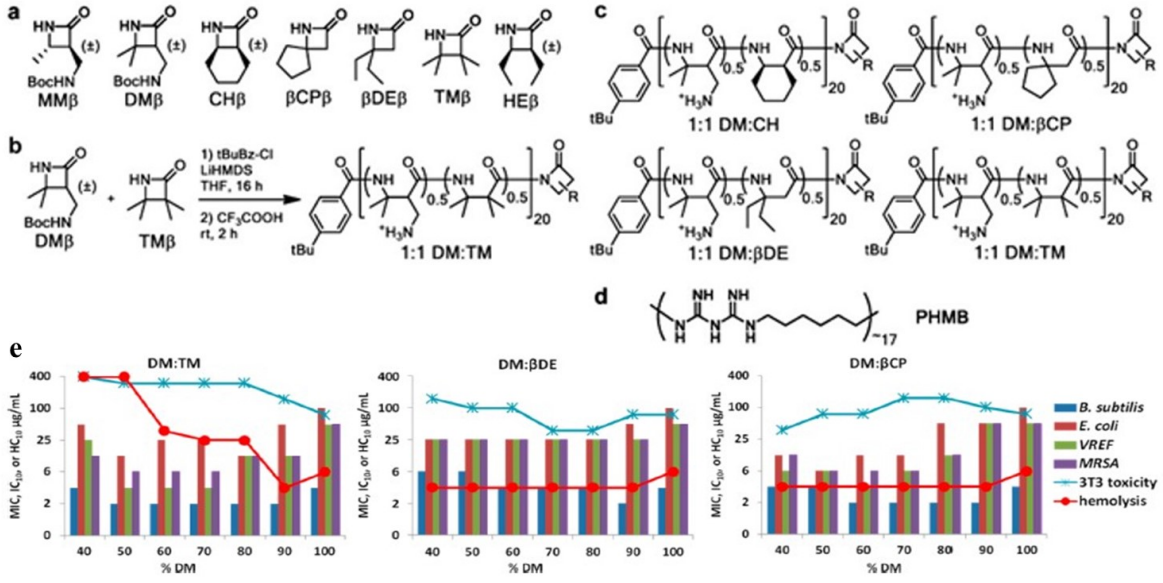

Figure 58. (a) structures of β-lactam monomers; (b) example of copolymer synthesis; (c) mixed polymeric structure made by equimolar mixtures of β-lactam monomers; (d) PHMB. Subunits DM and CP are racemic and all the polymers are heterochiral; (e) evaluation of biological activity.

There are other antimicrobial polymers with ammonium-based functionalities: styrene copolymers,[75] polymeric nanoparticles,[76,77] N,N-dodecyl-methyl polyethylenimine (PEIs),[78] and poly(isobutylene)maleimide with ammonium pendants.[79]

A certain number of polymeric disinfectants[80] were prepared using conventional synthetic polymers, including poly(vinylpyridine),[81] poly(vinyl alcohol),[82] and polyacrylates.[83] However, one of the main drawbacks is the lack of selectivity between human and bacterial cells, limiting their clinical usefulness. [84]

For pyridinium polymers with similar composition of the backbone and with similar charge/lipophilic tail ratio, it was demonstrated that the insertion of charges and lipophilic chains in spatially separated centres allows a greater efficiency in the interruption of the membrane, as evidenced by the greater antibacterial and haemolytic activities.[85] This lack of selectivity arises when the hydrophobic interactions exceed the electrostatic attraction to the surface of the bacterial cell. Furthermore, it was also shown that the spatial positioning of the positive charges and the type of the alkyl tails affects significantly the toxicity of the polymers. Figure 59 shows the series of amphiphilic pyridinium-methacrylate copolymers that were synthesized to establish these structure-activity relationships, the MIC against some Gram-positive and Gram-negative strains and the haemolytic activities.

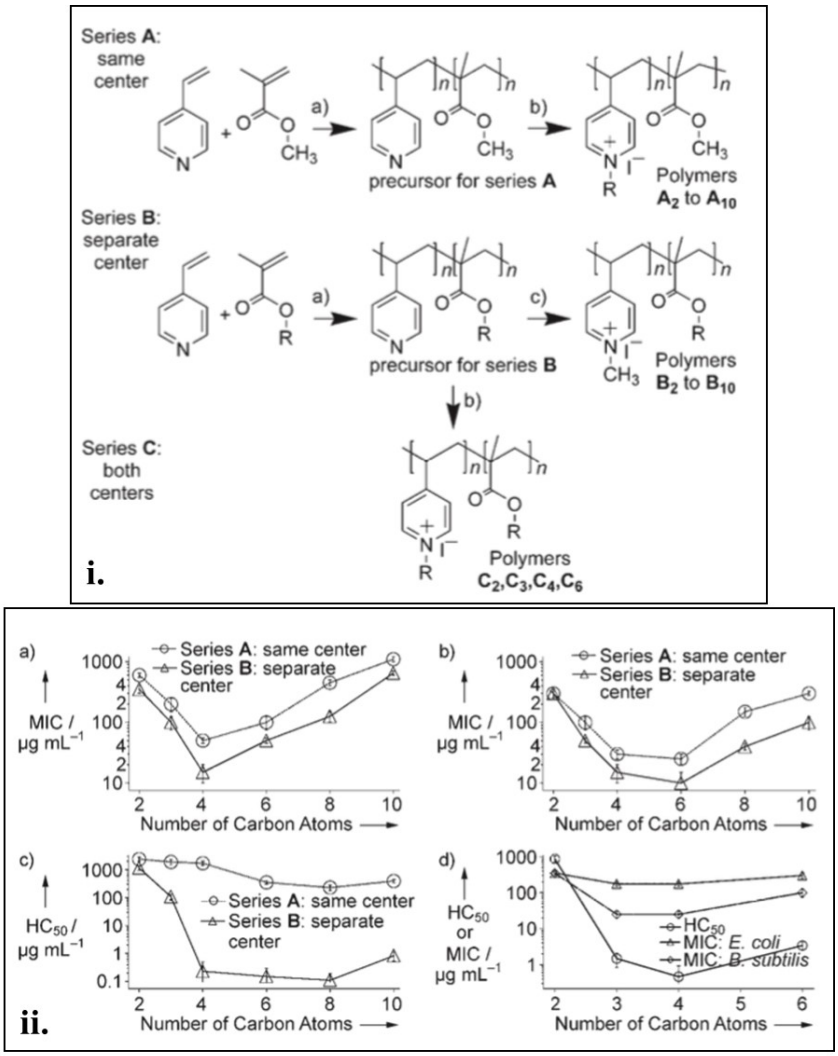

Figure 59. (i) Synthesis of three series of pyridinium–methacrylate copolymers differing in the spatial positioning of the charges and tails, as well as in the length of the alkyl tails. Subscripts denote the number of carbon atoms in the alkyl tail R. (ii) Average activities with error bars of pyridinium–methacrylate copolymers from series A, B, and C as a function of tail length: a) antibacterial activity (MIC) of series A and B towards Gram-negative *E. coli*; b) antibacterial activity (MIC) of series A and B towards Gram-positive *B. subtilis*; c) haemolytic activity (HC50) of series A and B towards human red blood cells; and d) antibacterial (MIC) and haemolytic (HC50) activity of polymers from series C.

During the last decade, the biological properties and the interaction mechanisms with membranes of a big number of polymeric SMAMPs obtained with the ring-opening metathesis polymerization (ROMP) of suitable alkenes were also well studied.[86] This is because ROMP is a polymerization technique that produces molecules with a low dispersion over a wide range of molecular weights, and it is highly tolerant for many functional groups. The structures of various compounds are summarized in Figure 60, which shows how a library of polymers with antibacterial properties and adjustable hemolytic activities were obtained with ROMP as a synthetic platform.

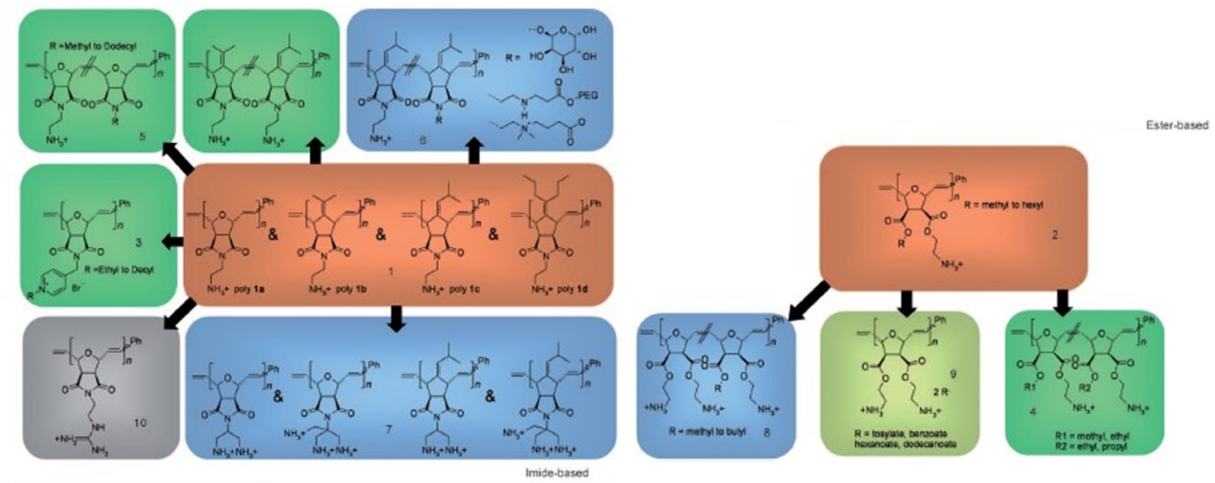

Figure 60. Library of SMAMPs synthesized by ROMP. The precursor is shown in red and the relative derivatizations are coloured in green (lipophilic) and blue (hydrophilic). The change of counterion is shown in light green. Furthermore, a SMAMP was modified with guanidinium groups (grey).

Lienkamp et *al*., reported a study[87] on the selectivity of antimicrobial polymers between Gram-positive and Gram-negative bacteria, using polymers obtained by ROMP with different monomer/initiator ratios (Figure 61a). These polymers have different sizes and the results show how the selectivity between bacteria and eukaryotic cells, and also the selectivity between Gram-positive and negative bacteria, varies as a function of molecular weight.

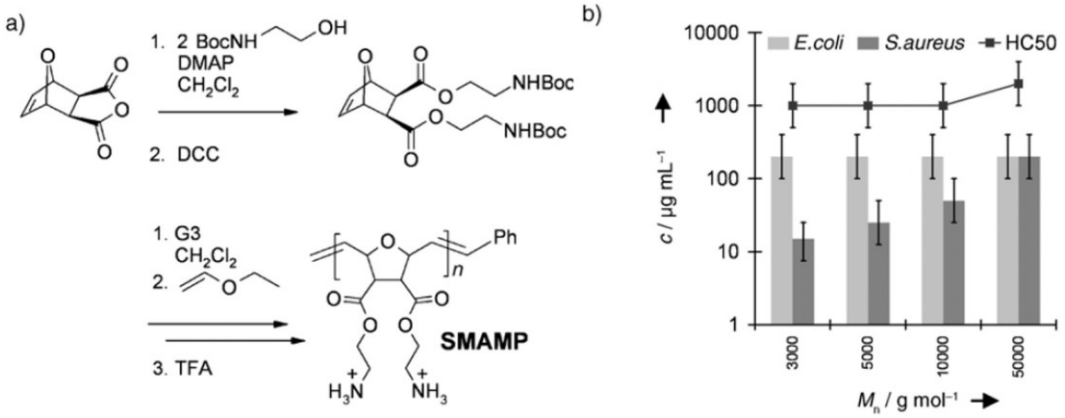

Figure 61. (a) Synthesis and structure of SMAMPs obtained by ROMP; (b) Antimicrobial assays (MIC) against *E. coli* (light grey) and *S. aureus* (dark grey), and haemolytic activity (black squares: HC_{50}).

4.3.3 Small Molecular Mimics of AMPs: SMMAMPs

There is a last possibility to obtain molecules capable of mimicking the behaviour of AMPs: the small SMAMPs or SMMAMPs. These *Small Molecular Mimics of AntiMicrobial Peptides* are simple amphiphilic molecules able to interact with the membranes, causing the damage that leads to the death of the bacterium. The mechanisms of action are generally not well

characterized and could also be different from the relatively ordered models (e.g. the barrel-stave or toroidal pore models seen above) often postulated for natural AMPs and amphiphilic foldamers.[88] Moreover, the precise mode of action could easily vary depending on the specific molecules involved.

Cationic antimicrobial agents differ greatly in their selectivity towards different bacteria. Some compounds show a broad antimicrobial spectrum, whereas different cationic peptides have a higher toxicity against Gram-positive bacteria than against the Gram-negative ones.[89]

However, there are agents, such as polymyxin, which are selective for Gram-negative bacteria because they have affinity for a component of the outer membrane.[90] The *ceragenins* are examples furnished by Nature.[91] They are derivatives of bile acids with amines attached covalently, and many of them have a lipophilic portion that facilitates the absorption into cells and their action onto bacterial membranes. Furthermore, the ceragenins are polycationic compounds, and this is an important feature for the selective toxicity against bacteria. The ceragenins differ significantly in their toxicity against various species of pathogenic bacteria, and some of the most important examples of structures are shown in Figure 62.

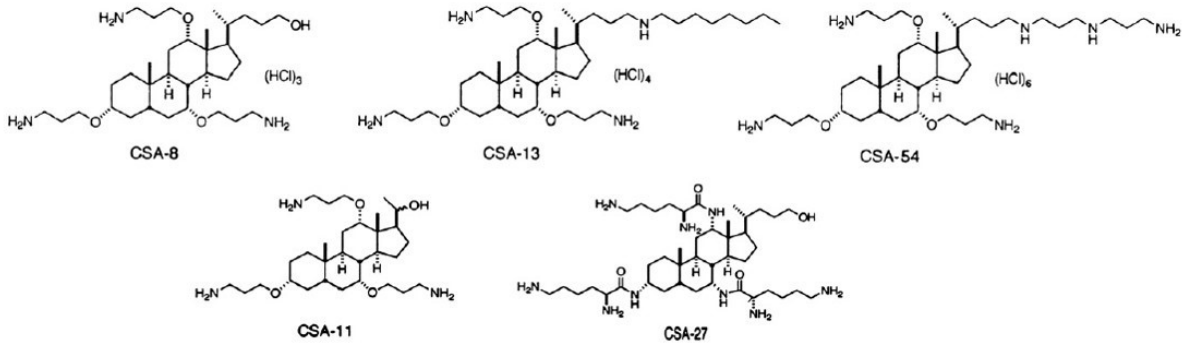

Figure 62. Structure of derivative compounds of the bile acids.

Often it is assumed that the outer membrane of Gram-negative bacteria offers an increased protection, preventing access of antimicrobial agents to the inner membrane. However, this is not the case of the CSA-8, since experiments on *-pss* mutant strain of *E. coli* (mutation that involves the lack of PE (phosphatidylethanolamine), led to an increase in sensitivity to this antimicrobial agent. Compared to the + *pss* strain, the *-pss* strain has a larger ratio of cardiolipin content, which might cause increased sensitivity to the toxic cationic agents.[92]

Typically, Gram-positive bacteria have a low content in PE in their membranes, contrarily to Gram-negative, except for some strains like *B. polymyxa*, *B. cereus* and *B. anthracis*, which have a relatively high PE content even if they are Gram-positive bacteria. On the other hand, *C. crescentus* is an example of Gram-negative bacteria with a low PE content. The MIC values

for CSA-8 appear to be more related to the content of PE of the bacteria than to the presence or absence of an outer membrane (Figure 63).

a.

Bacteria	MIC (μg/mL)	% PE
Gram negative bacteria		
Proteus mirabilis	500	80
Escherichia coli	36	80
Pseudomonas aeruginosa	20	60
Caulobacter crescentus	5	~0
Gram positive bacteria		
Bacillus polymyxa	35	60
B. anthracis	20	43
Bacillus cereus	50	43
Bacillus subtilis	0.5	12
S. aureus	2	~0
S. pyogenes	0.5	~0

b.

Organism	MIC Values (μg/mL) of Ceragenins[a]				
	CSA-13	CSA-54	CSA-8	CSA-11	CSA-27
Gram negative bacteria					
Proteus mirabilis	16	500	500	ND	ND
E. coli	3.0	7.0	36	80	85
P. aeruginosa	2.0	ND	20	85	ND
Gram positive bacteria					
B. anthracis	2.5	ND	20	ND	ND
S. aureus	0.4	2.0	2.0	9.0	ND
S. pyogenes	0.5	0.5	0.5	ND	ND
B. subtilis	0.5	1	0.5	ND	ND
Hemolysis					
Minimum hemolytic concentration	30	>100	100	>100	ND

ND = Not Determined.

Figure 63. (a) MICs of CSA-8 and %PE of different bacterial strains; (b) Evaluation of MICs and HC_{50} of ceragenins.

In the last decades, studies on monomeric and cationic amphiphilic compounds derived from quaternary ammonium compounds that show a good antimicrobial activity have been carried out. Their action is based on the ability to disrupt the bacterial membrane with a hydrophobic and electrostatic adsorption phenomenon at the membrane/water interface, followed by the rupture of the membrane.[93] To this regard, dimeric amphiphilic cationic compounds were developed, having different methylene spacers between the two head-groups (Figure 64).[94]

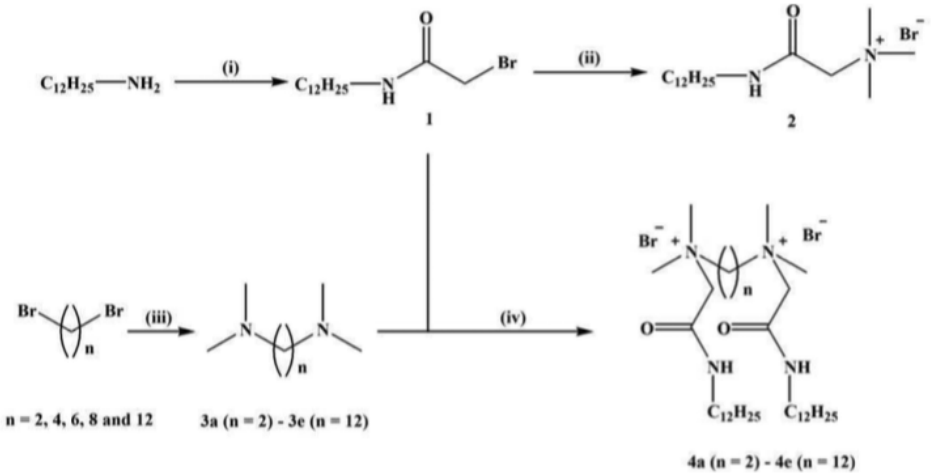

Figure 64. Synthesis of cationic monomeric and dimeric amphiphiles bearing amide linkages. Reagents, conditions, and yields: (i) $BrCH_2COBr$, K_2CO_3, DCM, H_2O; 5 °C, 30 min, rt, 2 h; 100%. (ii) NMe_3, acetone; pressure tube, rt, 12 h; 99%. (iii) $NHMe_2$, tetrahydrofuran; rt, 24 h; 100%. (iv) Acetonitrile; pressure tube, 85 °C, 12 h; 99%.

These compounds showed high antibacterial activity against human pathogenic bacteria (*E. coli* and *S. aureus*) and low cytotoxicity. The most active amphiphile (n = 6) had a 10-13-fold

higher HC_{50} than did the MIC. In addition, this amphiphile did not show any cytotoxicity against mammalian cells (HeLa cells) even at a concentration above the MIC (20 μM), as shown in Figure 65.

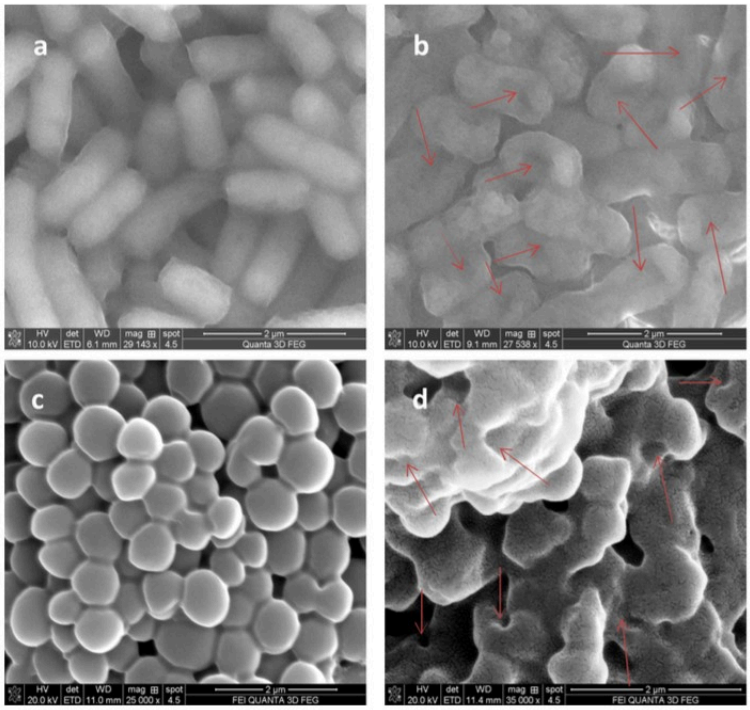

Figure 65. Scanning electron microscopy (SEM) images of (a) untreated *E. coli*; (b) *E. coli* treated with amphiphile 4c (100 μM); (c) untreated *S. aureus*; (d) *S. aureus* treated with amphiphile 4c (100 μM).

On the basis of recent discoveries on the structure and biological properties, aryl small SMAMPs (SMMAMPs) were studied to determine the role of the amphiphilicity on their antimicrobial activity against Gram-positive and Gram-negative bacteria.[95] The first set of SMAMPs was called "FA" (facially amphiphilic), and the second "DA" (disrupted amphiphilic), with a polar amide linkers incorporated into hydrophobic region in order to interrupt the amphiphilicity (Figure 66).

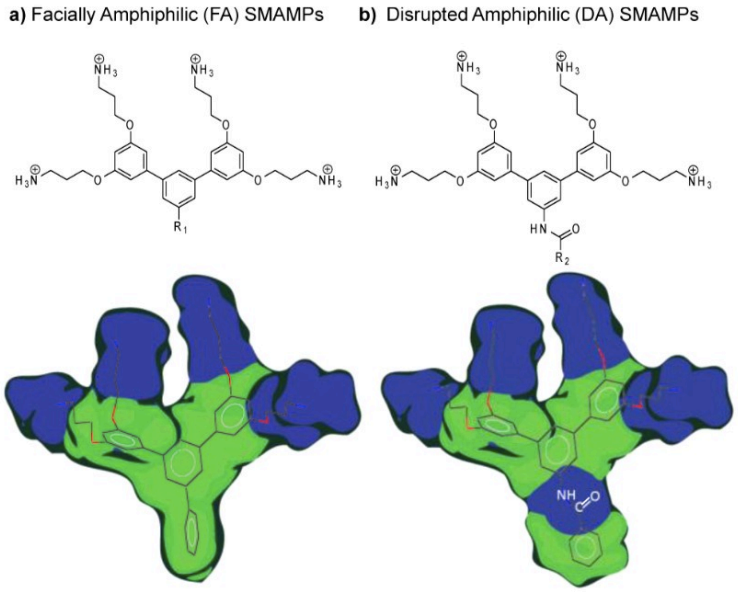

Figure 66. Design of aryl SMAMPs with pendant aromatic groups. (a) SMAMPs with a FA topology and (b) SMAMPs with a DA topology. R_1 and R_2 represent the pendant aromatic groups. Blue and green colours represent the hydrophilic and hydrophobic regions, respectively.

The FA SMAMPs displayed broad spectrum antimicrobial activity against both Gram-positive *S. aureus* and Gram-negative *E. coli*, whereas the DA SMAMPs, which contained a polar amide bond in between the hydrophobic moieties, only exhibited activity toward *S. aureus*. Moreover, it is worth mentioning that this latter activity improves as the overall hydrophobicity increases (Figure 67). From this study, it turns out that for *S. aureus* the most important feature is hydrophobicity, while for *E. coli* the determining factor is amphiphilicity.

i.

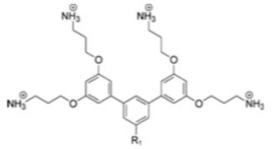

SMAMP	R_1	R_t[a] (min)	MIC (μg/ml) *S. aureus*	MIC (μg/ml) *E. coli*	HC_{50} (μg/ml)
1		28.8	12.5	3.13	537
2		30.2	0.78	3.13	279
3		30.6	1.56	6.25	634
4		34.6	1.56	3.13	41
5		35.4	1.56	6.25	34
MSI-78[b]	-	-	8-16	16-32	120

ii.

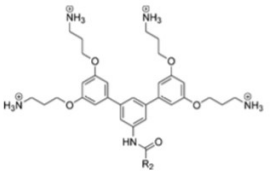

SMAMP	R_2	R_t[a] (min)	MIC (μg/ml) *S. aureus*	MIC (μg/ml) *E. coli*	HC_{50} (μg/ml)
6		26.1	50	>50	>1000
7		26.7	12.5	>50	519
8		30.8	6.25	>50	422
9		33.2	1.56	25	113

[a] Measured by HPLC using a C8 column with a gradient of 1% acetonitrile/min starting with 100% water. *b)* Literature values[96]

Figure 67. Antimicrobial and hemolytic activities of the SMAMPs for: (i) FA topology and (ii) DA topology.

A recent study reports the design and development of small antibacterial peptoid monomers synthesized in only three steps.[97] In this minimalist design, the two positive charges are provided by a residue of L-lysine, while hydrophobicity is furnished by an aromatic core (anthracene, naphthalene or benzene) and an alkyl chain (Figure 68).

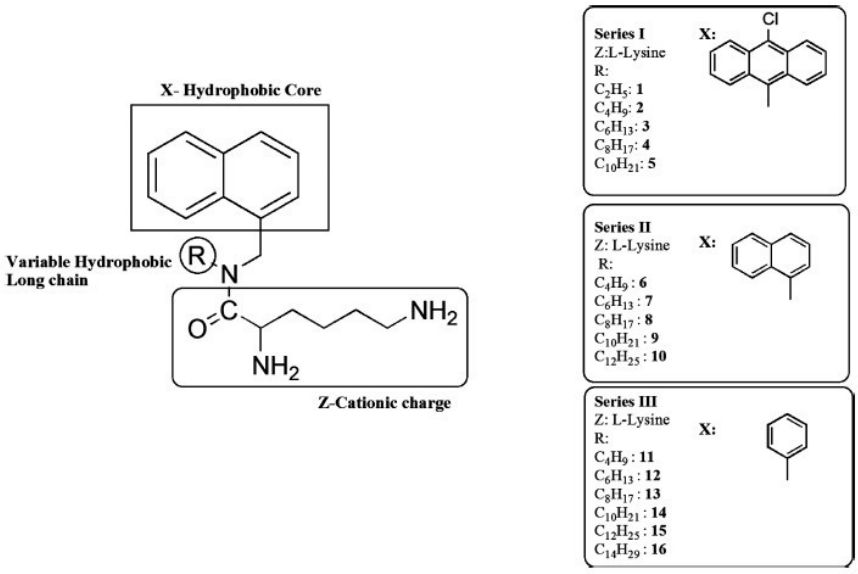

Figure 68. Structures of small molecular antibacterial peptoid mimics.

The hydrophobicity of the alkyl chains and bulky aromatic rings were varied in a systematic way, in order to understand the role of these parameters to the selective antibacterial activity. The antibacterial efficacy of these compounds was evaluated against Gram-positive (*S. aureus* and *E. faecium*) and Gram-negative bacteria (*E. coli*, *K. pneumoniae* and *P. aeruginosa*), including MRSA and VRE (Table 21).

Table 21. In Vitro Antibacterial and Haemolytic activity of the monomeric compounds.

	minimum inhibitory concentration (μg mL^{-1})								
	drug sensitive bacteria				drug resistant bacteria				
compd	*S. aureus*	*E. faecium*	*E. coli*	*P. aeruginosa*	MRSA	VRE	*K. pneumoniae*	HC_{50} (μg mL^{-1})	HPLC retention times (min)
1	11	13.6	25	4	21	7.2	31	118	11.8
2	5.3	4.5	4.8	1.9	6.3	5.3	17	91	12.4
3	2.4	3.3	3.5	1.6	2.8	5.2	16	82	13.6
4	2.2	2.5	2.9	3.8	2.3	3	4.3	64	14.6
5	7.1	4.9	26	11	4.6	5.6	7.6	71	15.6
6	>100	>100	>100	>100	>100	>100	>100	>1000	10.8
7	20	34	25	11	65	54	100	508	11.8
8	6.3	5.5	5	5.4	4.4	7	13	60	12.9
9	2.5	3.5	4	3	2.6	1.6	5.8	54	14.2
10	3	1.6	3.1	3.2	2.7	3.4	4	56	15.1
11	>100	>100	>100	>100	>100	ND[a]	>100	>1000	9.4
12	>100	>100	>100	>100	>100	ND	>100	>1000	10.6
13	46	60	51	60	>100	>100	>100	325	12.1
14	5.7	6.5	6.5	4	15.7	5.8	31	95	13.4
15	2.7	2.6	5	4	2.9	3.3	2.8	45	14.5
16	3.1	2	3.1	2.8	2.5	2.5	4	50	15.8
vancomycin	0.9	0.87	ND	ND	0.9	>100	ND	ND	ND
colistin	20	>100	0.4	0.4	54	>100	1.2	ND	ND
MSI-78	8–16[b]	64[b]*	16–32[b]	8–16[b]	16–32[b]	8[b]	8–16[b]	120[c]	ND

[a]ND stands for "not determined". [b]Literature values obtained from ref 36. * indicates value for *E. faecalis*, [c]Literature value obtained from ref 28. VRE (vancomycin-resistant *E. faecium*) and MRSA (methicillin-resistant *S. aureus*), *K. pneumoniae* is resistant to β-lactam antibiotics.

Compounds of series I (Figure 68) showed the best compromise between haemolytic activity and antibacterial properties, even against MRSA, VRE and *P. aeruginosa*. The latter is one of the major cause of hospital-acquired (nosocomial) infections and has a well-known ability to resist to almost all clinically approved antibiotics.[98]

Spectroscopic and microscopic studies through fluorescent dyes, reveals that depolarization and disruption of bacterial cell membranes are the primary mechanisms of their bactericidal action. Moreover, it is clear that in case of short alkyl chains (up to n-hexyl), the effect of the aromatic core is dominant over the one of the alkyl chain, the antibacterial activity decreasing, for the same length of the alkyl chain, moving from anthracene to naphthalene and benzene. For the octyl chain similar considerations apply, but the aromatic nucleus is no longer clearly dominant. With a decyl chain, very good MICs were always observed, even if the optimum activity is for the naphthalene derivative, while both anthracene and benzene derivatives are about two times less active. In this case, it is the alkyl chain that seems to dominate over the aromatic substituent.

Aminoglycoside antibiotics (AA) are a family of aminocyclitol drugs, widely used to treat infections caused by Gram-positive and Gram-negative bacteria. Their mechanism of action is based upon either the inhibition of protein synthesis, as they bind to the 16S rRNA, or the disruption of bacterial cell membrane. Aminoglycoside resistance mechanisms include:[99]

- the deactivation of aminoglycosides by N-acetylation, adenylylation or O-phosphorylation;
- the reduction of the intracellular concentration of aminoglycosides by changes in outer membrane permeability, decreased inner membrane transport, active efflux, and drug trapping;
- the alteration of the 30S ribosomal subunit target by mutation;
- methylation of the aminoglycoside binding site.

While AAs have a potent bactericidal activity, their widespread use has been compromised by toxicity and the development of resistant strains worldwide.[100]

Several studies were conducted to synthesize and test new classes of antibacterial amphiphilic aminoglycosides, like cationic 6''-thioether Tobramycin (TOB) analogues,[101] and the amphiphilic aminoglycoside-peptide triazole conjugates (APTCs).[102]

In a study of Schweizer et *al*.,[102c] some APTC derivatives (summarized in Figure 69) were synthesized exploiting a copper-mediated click-chemistry approach[103] between the azide-derivatized aminoglycosides (in red) and alkyne hydrophobic peptides (in green).

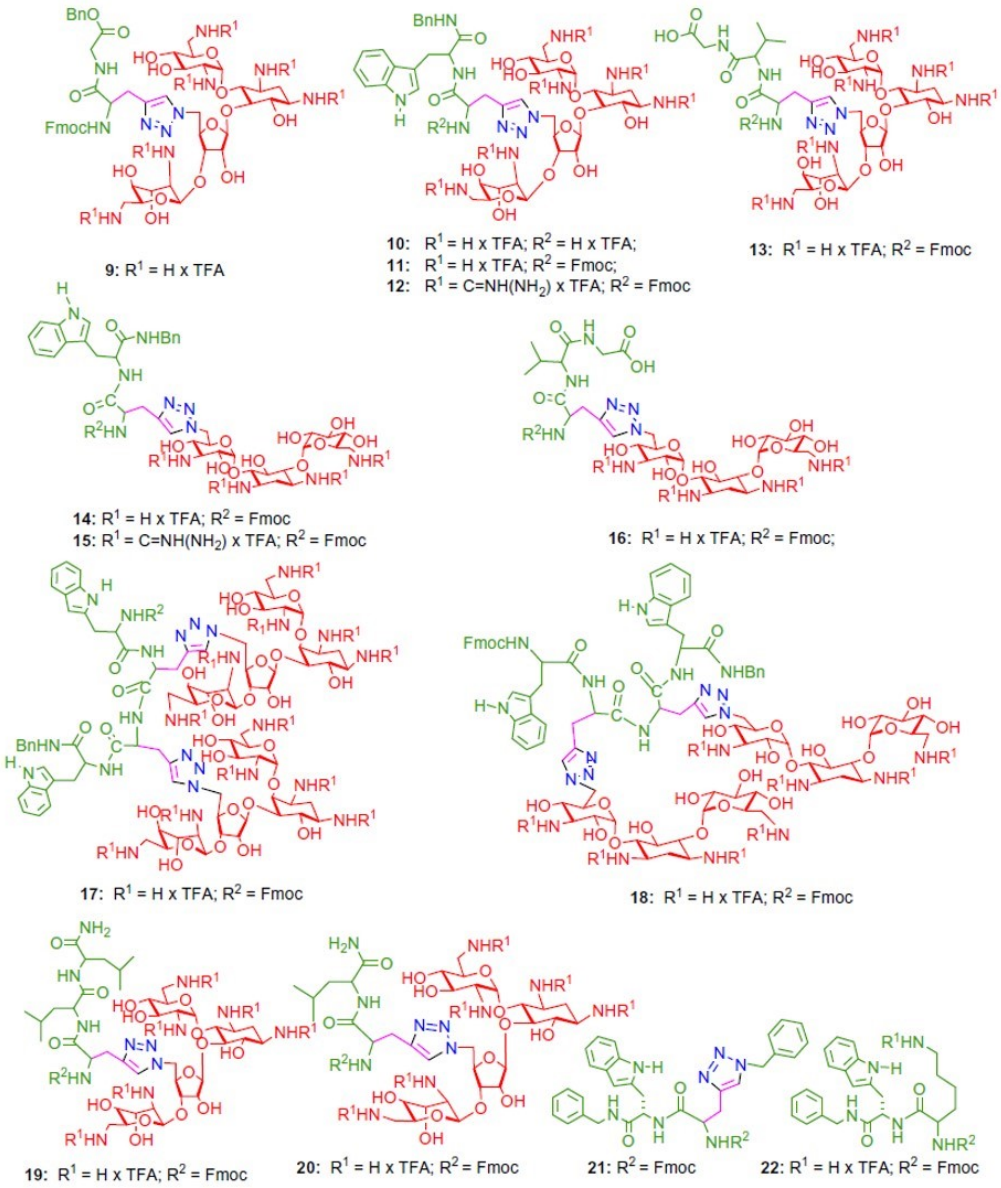

Figure 69. APTCs prepared by glycoconjugation of aminoglycoside azides (derivatives of neomycin B and kanamycin A) with suitable modified peptides (alkyne hydrophobic peptides). Peptides 21 and 22 represent negative controls.

APTCs were tested against a wide selection of Gram-positive and Gram-negative bacteria (Table 22), including three AA-resistant strains. The results demonstrate that APTCs show a higher antibacterial activity against methicillin-resistant *S. aureus* (MRSA, resistant to kanamycin A and neomycin B) and methicillin-resistant *S. epidermidis* (MRSE, resistant to kanamycin A and gentamicin). They also have a low hemolytic activity against mammalian erythrocytes at MIC concentrations, even if hemolysis occurs at higher concentrations.

However, most APTCs show reduced antibacterial activity against strains that are susceptible to kanamycin A and neomycin B. The structural similarities between the APTCs and AMPs suggest a membranolytic mechanism of action, which is supported by several

observations: the hemolytic concentration-dependent activity observed in all the APTCs and the need for a highly hydrophobic peptide segment to induce a potent antibacterial activity.

Table 22. MICs of APTCs 9-20, gentamicin, neomycin B, kanamycin A (positive controls) and 21,22 (negative controls) against Gram-positive and Gram-negative bacteria.

Organism	Compound																
	Genta-micin	Neo-mycin B	Kana-mycin A	**21**[m]	**22**	**9** *N*[k]	**10** *N*[k]	**11** *N*[k]	**12** *N*[k]	**13** *N*[k]	**14** *K*[l]	**15** *K*[l]	**16** *K*[l]	**17** *N*[k]	**18** *K*[l]	**19** *N*[k]	**20** *N*[l]
S. aureus[a]	1	1	4	128	512	16	32	8	4	16	16	4	16	8	32	32	32
MRSA[b]	2	256	>512	128	512	64	128	16	8	256	32	8	>256	16	32	32	32
S. epidermidis[c]	0.25	0.25	2	128	256	4	8	4	1	8	8	2	4	2	8	16	8
MRSE[d]	32	0.25	128	64	512	8	8	8	2	8	16	8	64	4	16	16	16
S. pneumoniae[e]	4	8	8	128	>512	>512	>512	64	64	128	64	64	8	64	64	>128	>256
E. coli[f]	1	2	8	128	512	32	32	16	32	32	32	64	128	32	64	64	64
E. coli[g] (Gent-R)	128	4	16	128	512	32	32	32	64	32	32	64	32	64	64	128	64
E. coli[h] (Amik-R)	8	32	32	128	n.d.	64	n.d.	n.d.	64	256	32	64	>256	16	32	128	64
P. aeruginosa[i]	8	512	>512	128	>512	512	512	128	128	256	128	128	>256	128	128	128	>256
P. aeruginosa[j] (Gent-R)	128	512	>512	128	>512	512	256	64	128	256	16	128	>256	32	64	64	>256
(%) Hemolysis[n] at 100 μg/ml	n.d.	<0.5	<0.5	n.d	n.d	1.0	1.0	9.9	n.d	0.8	3.9	13.7	n.d	1.5	10.2	1.0	2.2

n.d. = not determined.
[a] ATCC 29213.
[b] Methicillin-resistant *S. aureus* ATCC 33592.
[c] *S. epidermidis* ATCC 14990.
[d] Methicillin-resistant *S. epidermidis* Canadian Intensive Care Unit (CAN-ICU) 61589.
[e] ATCC 49619.
[f] ATCC 25922.
[g] CAN-ICU 61714.
[h] CAN-ICU 63074.
[i] ATCC 27853.
[j] CAN-ICU 62308.
[k] Neomycin B-based conjugate.
[l] Kanamycin A-based conjugate.
[m] Dissolved in DMSO and diluted with H_2O.
[n] Human erythrocytes.

CHAPTER 5:

α-Hydrazidoacid-based SMMAMP

5. α-HYDRAZIDO ACID-BASED SMMAMPS

5.1 Introduction

As reported above, there are numerous classes of compounds that are mimetics of natural antimicrobial peptides and are able to exert an antibiotic action. In all cases, the clear segregation of the lipophilic and hydrophilic moieties when the compounds interact with the bacterial membrane is critical for the antibacterial activity. In addition, as demonstrated in many cases (e.g. foldamers), the inherent stability of the amphiphilic conformation allows to obtain the best MICs.

From the studies on both conformationally constrained and unconstrained α-hydrazido acid oligomers (Chapter 1), it is evident that the oligomers of α-hydrazido acids have a pronounced proclivity to assume an 8-helix secondary structure, more specifically a sequence of hydrazido-turns. Moreover, the same tendency to the formation of 8-terms cycles also appears to be a common trait of α-hydrazido acids derivatized as amides at the C-terminal and as carbamates (or amides) at the N-terminal.

With the aim of creating inherently new amphiphilic structures, we have very recently undertaken the synthesis of properly derivatized monomeric α-hydrazido acids. In fact, even though it would be possible to synthesize amphiphilic oligomers, we preferred to point toward simpler compounds. The reasons are as follows:

- the overall yield in the case of oligomers is much lower than the ones for the corresponding monomers (many more synthetic steps; individual yields are generally lower);
- monomers are extremely cheaper than oligomers (much less reagents, reactants, solvent for reactions/purifications are needed to obtain the same amount of products);
- the synthesis of any single monomer is much more rapid;
- it is much easier and quicker to implement a diversity-oriented synthesis in a monomer, with the aim of obtaining an extended but complete library of compounds to be tested (e.g. 3 functionalities x 5 different groups for every functionality = 125 compounds!)

In light of the previous considerations, we pointed towards the optimization of a facile, short, high-yielding, cheap, and general synthesis of the amphiphilic structures reported in Figure 70. To this end, we exploited all the chemical knowledge acquired during the syntheses of monomers and foldamers described in Chapter 1, changing and/or optimizing the reaction conditions only when needed.

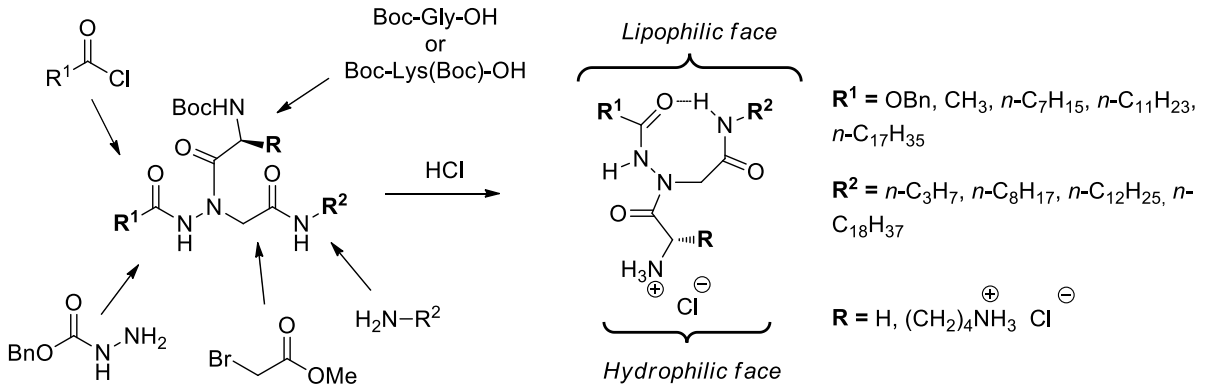

Figure 70. Starting compounds used for the synthesis, generic Boc-protected α-hydrazido acid monomers and amphiphilic α-hydrazido acid SMAMPs synthesized, with the putative 8-term intramolecular H-bond.

5.2. Results and discussion

5.2.1 Synthesis of compounds

The synthesis of the key intermediate **1** was performed in a multigram scale starting from benzyl carbazate and methyl bromoacetate, exploiting the already reported methodology (Chapter 1). Thus, the peptide coupling of compound **1** with the suitable NH-Boc protected amino acids (glycine or lysine) was optimized testing a lot of different experimental conditions (Table 23).

Table 23. Optimization of reaction conditions for the synthesis of the key C-terminal ester monomers.

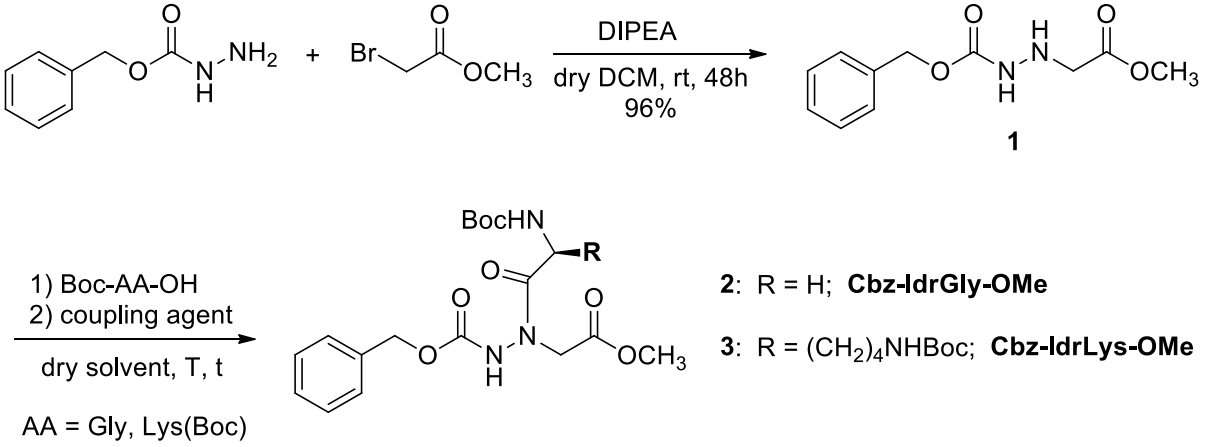

PRODUCT	COUPLING AGENT (eq)	SOLVENT (amount in mL per mmol 1)	TEMPERATURE (T) AND TIME (t)	YIELD (%)
2	DCC (1.3)	DCM (1 mL/mmol)	rt, 1h	42
	DCC (1.3)	DCM (2 mL/mmol)	rt, 1h	61
	DCC (1.7)	DCM (2 mL/mmol)	rt, 1h	55
	EDCI (1.5)	DCM (1 mL/mmol)	rt, 1h	63
	EDCI (1.5)	DCM (0.5 mL/mmol)	0 °C to rt, 1h[a]	71
	EDCI (1.5)	DCM (0.5 mL/mmol)	0 °C, 1h	84

	EDCI (1.5)	DCM (0.3 mL/mmol)	0 °C, 1h	83
	EDCI (1.5)	**DCM (0.5 mL/mmol)**	**-20 °C, 1h**	**86**
3	PyBOP (1.5) + DIPEA (2.5)	DCM (1 mL/mmol)	-20 °C, 2h then rt, 16h	no reaction
	PyBOP (1.3) + DIPEA (1.5)	DMF (0.5 mL/mmol)	rt, 16h	traces
	PyBOP (1.3) + DIPEA (1.5)	DMF (0.25 mL/mmol)	rt, 16h	16
	EDCI (1.2) + HOBT (1)	DCM (0.3 mL/mmol)	-20 °C, 2h then rt, 16h	17
	EDCI (1.5)	DCM (1 mL/mmol)	rt, 1h	22
	EDCI (1.2)	DCM (0.3 mL/mmol)	rt, 1h	38
	EDCI (1.1)	**DCM (0.5 mL/mmol)**	**0 °C, 2h**	**45**
	EDCI (1.2)	DMF (0.25 mL/mmol)	0 °C, 1h	44
	EDCI (1.2)	DMF (0.5 mL/mmol)	-30 °C, 1h then 0 °C, 1h	42
	DCC (1.2)	DMF (0.5 mL/mmol)	0 °C, 1h	41[b]
	DCC (1.2)	DMF (0.5 mL/mmol)	-20 °C, 1h	45[b]

[a] Cooling bath immediately removed after the addition of coupling agent. [b] Product contaminated by about 10% dicyclohexylurea.

As expected from the known reduced nucleophilicity of carbazates (see previous chapter) and from the fact that **1** is an N-alkylated carbazate, thus being less reactive due to the steric encumbrance, the coupling reactions turned out to be challenging, especially when the less reactive lysine was used. In both cases (Gly and Lys), a reaction temperature below the room temperature turned out to improve the yields, even if an excessive decrease led to an exaggerate viscosity of reaction mixtures, with a concomitant drop of the amounts of products obtained (Table 23).

Due to the occurrence of side-reactions, which very likely elicited the intramolecular decomposition of the activated amino acids, prolonged reaction times did not have a beneficial effect on the reaction yields. On the contrary, the use of the highest possible concentrations led to substantial increases in yields. Moreover, the formation of less reactive benzotriazol-1-yl intermediates, using either PyBOP or EDCI + HOBt, was proven to be ineffective. In all cases, the use of carbodiimmide coupling agents, keeping all the other experimental conditions constants, led to the best yields. Unfortunately, the DCU (dicyclohexylurea) produced in the reactions always contaminated the reaction products, so that EDCI (1-ethyl-3-(3-dimethylaminopropyl)carbodiimmide) became the reagent of choice.

With the suitable monomers in our hands, the derivatization reactions necessary to obtain the desired N-terminal and the C-terminal derivatives were easily accomplished as reported in Table 24 and Table 25. The first series, having yet the N-benzyloxycarbonyl functionality (series **Aa-e**), was directly obtained by simple ammonolysis with amines R^2NH_2. The reflux of compounds **2** and **3** with the suitable amines in dry MeOH gave the respective amides (**2,3 Aa-e**) in good to excellent yields (Table 24).

Table 24. Synthesis of N-Cbz protected C-terminal amides 2Aa-d and 3Aa-d.

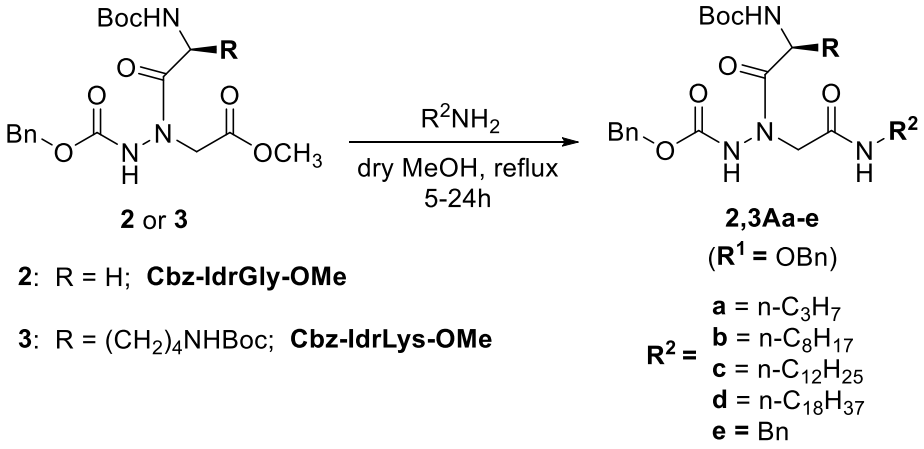

2 or **3**

2,3Aa-e
(**R1 =** OBn)

2: R = H; **Cbz-IdrGly-OMe**

3: R = $(CH_2)_4NHBoc$; **Cbz-IdrLys-OMe**

R2 =
a = n-C_3H_7
b = n-C_8H_{17}
c = n-$C_{12}H_{25}$
d = n-$C_{18}H_{37}$
e = Bn

SERIES	COMPOUND	EXTENDED NAME	YIELD (%)
2	**2Aa**	Cbz-IdrGly-NHC_3H_7	94
	2Ab	Cbz-IdrGly-NHC_8H_{17}	88
	2Ac	Cbz-IdrGly-$NHC_{12}H_{25}$	88
	2Ad	Cbz-IdrGly-$NHC_{18}H_{37}$	90
	2Ae	Cbz-IdrGly-NHBn	99
3	**3Ab**	Cbz-IdrLys(Boc)-NHC_8H_{17}	82
	3Ac	Cbz-IdrLys(Boc)-$NHC_{12}H_{25}$	85
	3Ad	Cbz-IdrLys(Boc)-$NHC_{18}H_{37}$	88

The change in the N-terminal derivatization was carried out by removal of the Cbz-protecting group by hydrogenolysis with formic acid and Pd/C, followed by acylation of the free hydrazide intermediate by reaction with the proper acyl chloride and pyridine in dry DCM, exploiting the optimized experimental conditions reported in Chapter 1 (Table 25).

Table 25. Synthesis of N-acyl derivatives 2B-Ia-e and 3B-Ia-e.

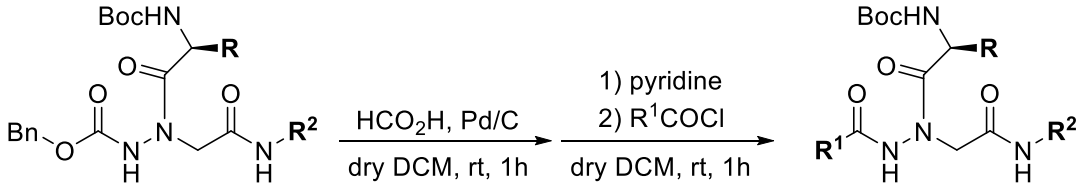

2,3Aa-e

2,3B-Ia-e

R1 =
B = CH_3
C = n-C_7H_{15}
D = n-$C_{11}H_{23}$
E = n-$C_{17}H_{35}$
F = Ph
G = t-Bu
H = Naphthyl
I = 9-Fluorenylmethyloxy

R2 =
a = n-C_3H_7
b = n-C_8H_{17}
c = n-$C_{12}H_{25}$
d = n-$C_{18}H_{37}$
e = Bn

SERIES	COMPOUND	COMPOUND EXTENDED NAME	YIELD (%)
2	**2Bb**	CH_3CO-IdrGly-NHC_8H_{17}	77
	2Bc	CH_3CO-IdrGly-$NHC_{12}H_{25}$	79
	2Bd	CH_3CO-IdrGly-$NHC_{18}H_{37}$	81

	2Ca	C_7H_{15}CO-IdrGly-NHC$_3$H$_7$	90
	2Cb	C_7H_{15}CO-IdrGly-NHC$_8$H$_{17}$	84
	2Cc	C_7H_{15}CO-IdrGly-NHC$_{12}$H$_{25}$	83
	2Cd	C_7H_{15}CO-IdrGly-NHC$_{18}$H$_{37}$	83
	2Da	$C_{11}H_{23}$CO-IdrGly-NHC$_3$H$_7$	94
	2Db	$C_{11}H_{23}$CO-IdrGly-NHC$_8$H$_{17}$	88
	2Dc	$C_{11}H_{23}$CO-IdrGly-NHC$_{12}$H$_{25}$	86
	2Eb	$C_{17}H_{35}$CO-IdrGly-NHC$_8$H$_{17}$	83
	2Ed	$C_{17}H_{35}$CO-IdrGly-NHC$_{18}$H$_{37}$	80
	2Fb	PhCO-IdrGly-NHC$_8$H$_{17}$	92
	2Fc	PhCO-IdrGly-NHC$_{12}$H$_{25}$	81
	2Gc	*t*-BuCO-IdrGly-NHC$_{12}$H$_{25}$	90
	2Hc	1-NaphthylCO-IdrGly-NHC$_{12}$H$_{25}$	79
	2Ic	Fmoc-IdrGly-NHC$_{12}$H$_{25}$	77
3	**3Ed**	$C_{17}H_{35}$CO-IdrLys(Boc)-NHC$_{18}$H$_{37}$	77

In order to evaluate the biological activity of our compounds, the removal of Boc-protecting groups, with the concomitant generation of the corresponding hydrochlorides, was carried out using either a methanolic solution of dry HCl or a mixture DCM:TFA = 3:1. The use of DCM:TFA instead of dry HCl/MeOH lies in the fact that, in some cases, the latter procedure caused the partial removal of the N-terminal substituent. Despite the fact that all the reaction were quite clean, we preferred to carry out the MIC tests with pure compounds. Thus, after extraction with a basic aqueous solution, the free amines were purified by flash chromatography using distilled DCM and methanol, and then re-protonated with few drops of HCl 3M in sterile water, obtaining the corresponding pure hydrochlorides in good to excellent yields (Table 26).

Table 26. Synthesis of hydrochlorides 4A-Ga-e and 5A-Ga-e.

R^1 = **A =** OBn; **B =** CH_3; **C =** n-C_7H_{15}; **D =** n-$C_{11}H_{23}$; **E =** n-$C_{17}H_{35}$; **F =** Ph; **G =** t-Bu; **H =** Naphthyl; **I =** 9-Fluorenylmethyloxy

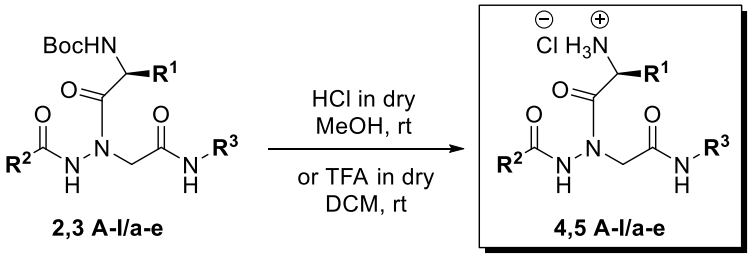

R^2 = **a** = n-C_3H_7; **b** = n-C_8H_{17}; **c** = n-$C_{12}H_{25}$; **d** = n-C_{18}-H_{37}; **e** = Bn

4: R = H; **R^{1}CO-IdrGly-NHR^2· HCl**

5: R = $(CH_2)_4\overset{\oplus}{N}H_3\overset{\ominus}{Cl}$; **R^{1}CO-IdrLys-NHR^2 · 2 HCl**

SERIES	COMPOUND	COMPOUND EXTENDED NAME	PROCEDURE	YIELD %
4	**4Aa**	Cbz-IdrGly-NHC$_3$H$_7$ · HCl	HCl	98
	4Ab	Cbz-IdrGly-NHC$_8$H$_{17}$ · HCl	HCl	90
	4Ac	Cbz-IdrGly-NHC$_{12}$H$_{25}$ · HCl	HCl	88
	4Ad	Cbz-IdrGly-NHC$_{18}$H$_{37}$ · HCl	TFA	82

	4Bb	CH_3CO-IdrGly-NHC_8H_{17} · HCl	TFA	68
	4Bc	CH_3CO-IdrGly-$NHC_{12}H_{25}$ · HCl	TFA	70
	4Bd	CH_3CO-IdrGly-$NHC_{18}H_{37}$ · HCl	TFA	89
	4Ca	$C_7H_{15}CO$-IdrGly-NHC_3H_7 · HCl	TFA	95
	4Cb	$C_7H_{15}CO$-IdrGly-NHC_8H_{17} · HCl	HCl	87
	4Cc	$C_7H_{15}CO$-IdrGly-$NHC_{12}H_{25}$ · HCl	HCl	84
	4Cd	$C_7H_{15}CO$-IdrGly-$NHC_{18}H_{37}$ · HCl	HCl	81
	4Da	$C_{12}H_{25}CO$-IdrGly-NHC_3H_7 · HCl	TFA	84
	4Db	$C_{11}H_{23}CO$-IdrGly-NHC_8H_{17} · HCl	HCl	89
	4Dc	$C_{11}H_{23}CO$-IdrGly-$NHC_{12}H_{25}$ · HCl	HCl	82
	4Eb	$C_{17}H_{35}CO$-IdrGly-NHC_8H_{17} · HCl	HCl	80
	4Ed	$C_{17}H_{35}CO$-IdrGly-$NHC_{18}H_{37}$ · HCl	TFA	82
	4Fc	$PhCO$-IdrGly-$NHC_{12}H_{25}$ · HCl	TFA	79
	4Gc	*t*-$BuCO$-IdrGly-$NHC_{12}H_{25}$ · HCl	TFA	85
5	**5Ab**	Cbz-IdrLys-NHC_8H_{17} · 2 HCl	TFA	76
	5Ac	Cbz-IdrLys-$NHC_{12}H_{25}$ · 2 HCl	TFA	77
	5Ad	Cbz-IdrLys-$NHC_{18}H_{37}$ · 2 HCl	TFA	70
	5Ed	$C_{17}H_{35}CO$-IdrLys-$NHC_{18}H_{37}$ · 2 HCl	TFA	67

5.2.2 Antimicrobial activity

The antimicrobial activity of the hydrochlorides reported in Table 26 was evaluated by determining the minimum inhibitory concentration (MIC) of the substance required to inhibit the growth of a given microorganism. In order to evaluate the MICs, the microbroth dilution test was carried out according to the CLSI manual.[104]

The antimicrobial activity was evaluated against the following strains:

- *E. faecalis* ATCC 29212 (Gram-positive);
- *E. faecium* 135562(35C) (Gram-positive);
- *S. aureus* ATCC 29123 (Gram-positive);
- *E. coli* ATCC 25922 (Gram-negative);
- *P. aeruginosa* ATCC 27853 (Gram-negative)

During the first trials, stock solutions in sterile DMSO (ranging from 2500 to 10000 μg/mL) were used, due the limited solubility of some compounds in water. Anyway, some compounds showed a very pronounced tendency to the formation of precipitates during the dilution procedure. On the other hand, using the most diluted stock solutions led to unacceptable percentages of DMSO (more than 3%) after the microbroth dilution, thus giving false MIC values due to the effect of dimethylsulfoxide itself.[105] Thus, the highest possible concentrations of hydrochlorides **4** and **5** directly dissolved in sterile water were subsequently used, discarding

for the moment the compounds with a very low solubility, namely less than 256 μg/mL, due to the difficulties in ascertaining the absence of a precipitate for such diluted solutions. In the case of compound **4Cd**, the solutions in the first wells were colloidal and very turbid, so leading to an additional uncertainty, but no actual precipitate was observed. All the previous results obtained exploiting stock solutions in DMSO were also discarded, even when the percentage of DMSO in the wells was below 3%, in order to avoid the use of MICs obtained with two different methodologies.

It should be noted at this point that, due to the problems reported above in the assessment of a correct and reliable procedure, the preliminary data reported in Table 27 are not the average values of at least three independent experiments, as it should be done correctly, but they are the results of the only trial available so far for each compound tested. Thus, they should be considered with caution and they could change when a larger and more complete dataset will be available.

Table 27. Antimicrobial activity (MIC) values for the hydrochlorides tested.

COMPOUND				**MIC (μg/mL)**				
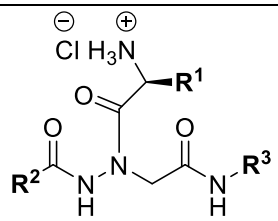				**GRAM-POSITIVE**			**GRAM-NEGATIVE**	
COMPOUND	**R^1**	**R^2**	**R^3**	***E. faecalis ATCC 29212***	***E. faecium 35C***	***S. aureus ATCC 29213***	***E. coli ATCC 25922***	***P. aeruginosa ATCC 27853***
4Aa	H	OBn	C_3H_7	>512	>512	>512	>512	>512
4Ab	H	OBn	C_8H_{17}	128	64	64	64	128
4Ac	H	OBn	$C_{12}H_{25}$	8	32	32	32	128
4Ad[a]	H	OBn	$C_{18}H_{37}$	64	16	128	---	---
4Bd	H	CH_3	$C_{18}H_{37}$	256	16	128	256	---
4Cb	H	C_7H_{15}	C_8H_{17}	16	16	32	64	128
4Cc	H	C_7H_{15}	$C_{12}H_{25}$	4	2	4	128	64
4Cd	H	C_7H_{15}	$C_{18}H_{37}$	1024	1024	1024	1024	---
4Db	H	$C_{11}H_{23}$	C_8H_{17}	4	8	8	---	---
4Dc	H	$C_{11}H_{23}$	$C_{12}H_{25}$	32	32	32	128	64
4Eb	H	$C_{17}H_{35}$	C_8H_{17}	64	64	128	256	128

4Ed[a]	H	$C_{17}H_{35}$	$C_{18}H_{37}$	256	64	64	128	128
4Fc	H	Ph	$C_{12}H_{25}$	16	4	4	4	32
4Gc	H	*t*-Bu	$C_{12}H_{25}$	16	8	4	8	16
5Ab	$(CH_2)_4NH_3^+Cl^-$	OBn	C_8H_{17}	256	128	32	256	256
5Ac	$(CH_2)_4NH_3^+Cl^-$	OBn	$C_{12}H_{25}$	16	16	16	64	256

[a] MIC values for compound **4Ad** and **4Ed** are not reliable because related to %DMSO upper to 3%.

Even if a comparison based on a sound quantitative basis is obviously impossible at the moment, nevertheless some qualitative indications can be drawn, and this is more true for the "monocharged" series **4**, for which much more data are available.

Preliminary trials furnished very good antibacterial activities, of the same order of magnitude of the best values reported in literature for compounds having a membranolytic action (see previous Paragraphs). A globally too large (**4Cd**) or too small (**4Aa**) lipophilic portion always led to a decrease, or even to a complete loss, of activity. Moreover, the shortest and longest chains never led to best antibacterial activities, regardless of their positioning (N- or C-terminal). Both compounds with N- and C-terminal chains of comparable lengths, that is octanoyl/octyl (**4Cb**) and lauroyl/lauryl (**4Dc**) derivatives, are less potent than both compounds with "mixed" groups (**4Cc** and **4Db**). Compounds **4Cc** and **4Db** are also among the most active against Gram-positive bacteria.

Anyway, the effect of an inversion of placement of C8 and C18 chains in **4Cd** and **4Eb** gave unexpectedly different activities, while this striking contrast was not observed for compounds having two medium-length aliphatic chains (C8 and C12), like **4Cc** e **4Db**, which presents very similar MICs (Table 27 and Figure 71). Anyway, this observation could also be related to the behaviour of **4Cd** described above. Thus, it appears to be likely that the right placement of the lipophilic chains might influence the activity of the compounds only when a certain degree of global hydrophobicity is reached. However, this hypothesis has not been rationalized or confirmed yet, and some discrepancies could also be ascribed to solubility losses not visible to naked eye.

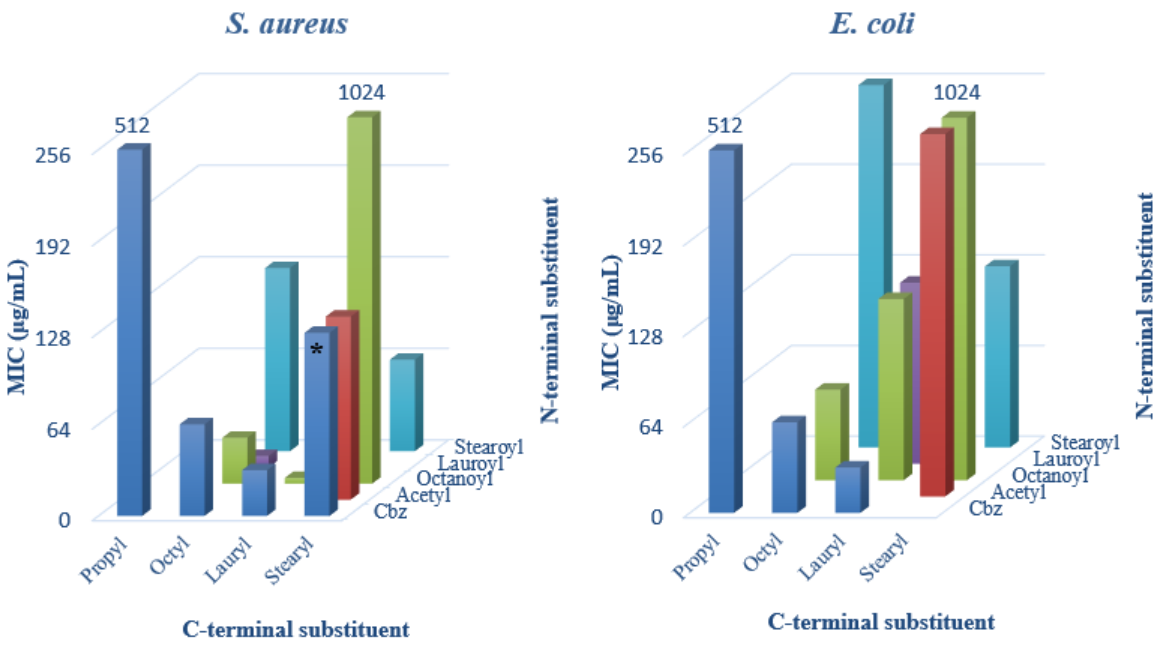

Figure 71. Variation of the antimicrobial activity against *S. aureus* (Gram-positive) and *E. coli* (Gram-negative) in relationship to the C- and N-terminal substituents for some compounds of series 4. Compound 4Ad (*) shows an unreliable MIC value due its high content (> 3%) of DMSO during the evaluation of MIC.

In general, as it is evident from Table 27 and Figure 71, compounds with the lauryl substituent at the C-terminal show the best antimicrobial activity. Thus, we decided to synthesize a series of compounds characterized by having different substituents at the N-ter, like a branched alkyl chain (*t*-Bu, **4Gc**) and aromatic functionalities (Ph, **4Fc**; 1-naphthyl, **4Hc**, fluorenylmethyloxy, **4Ic**). Unfortunately, due to solubility issues, it was possible test only compounds **4Gc** and **4Fc**. This last two compounds, as reported in Figure 72, show excellent antimicrobial values, especially against *P. aeruginosa*, one of the most problematic nosocomial Gram-negative pathogen.

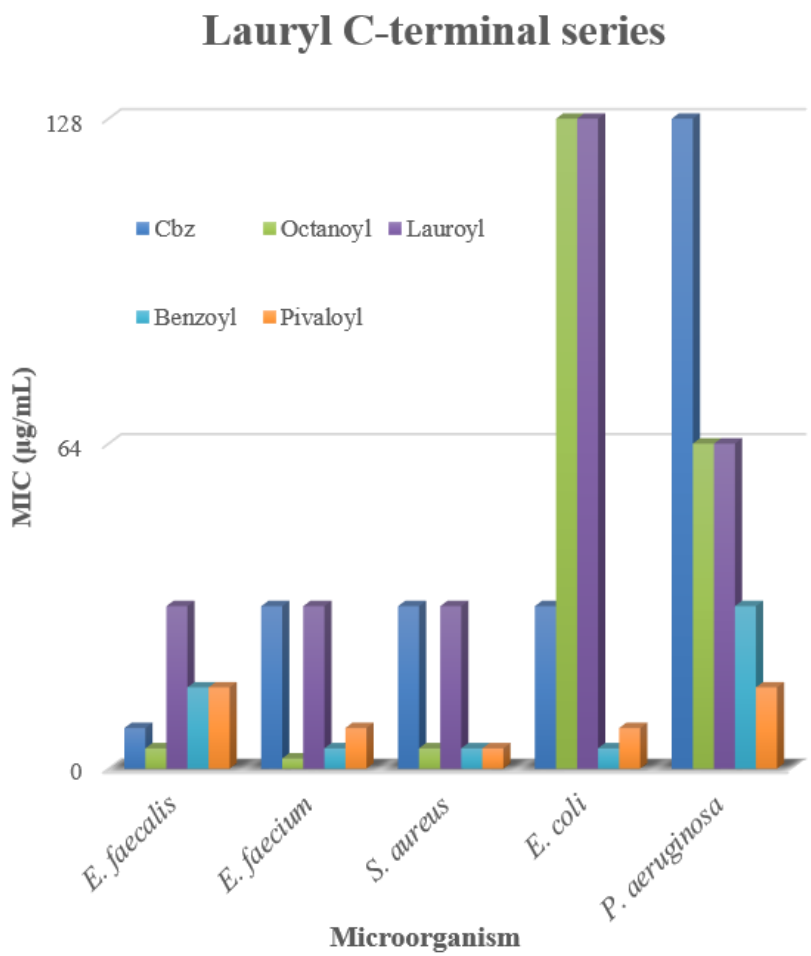

Figure 72. Variation of the antimicrobial activity in relationship to the N-ter substituents for the compounds of series 4, having a C-ter lauryl chain.

As expected, almost all compounds turned out to be more active against Gram-positive bacteria, whose cell membrane is more negatively charged, than towards the Gram-negative ones, with the exception of compounds **4Gc** and **4Fc**, as reported in Figure 73. In fact, compounds **4Fc**, which has an N-terminal benzoyl group without easily rotatable bonds (due to conjugation), and **4Gc**, which has a symmetrical *t*-butyl group, showed unexpectedly high activities towards Gram-positive and, most notably, Gram-negative bacteria, despite of the relatively small sizes of their N-terminal substituents.

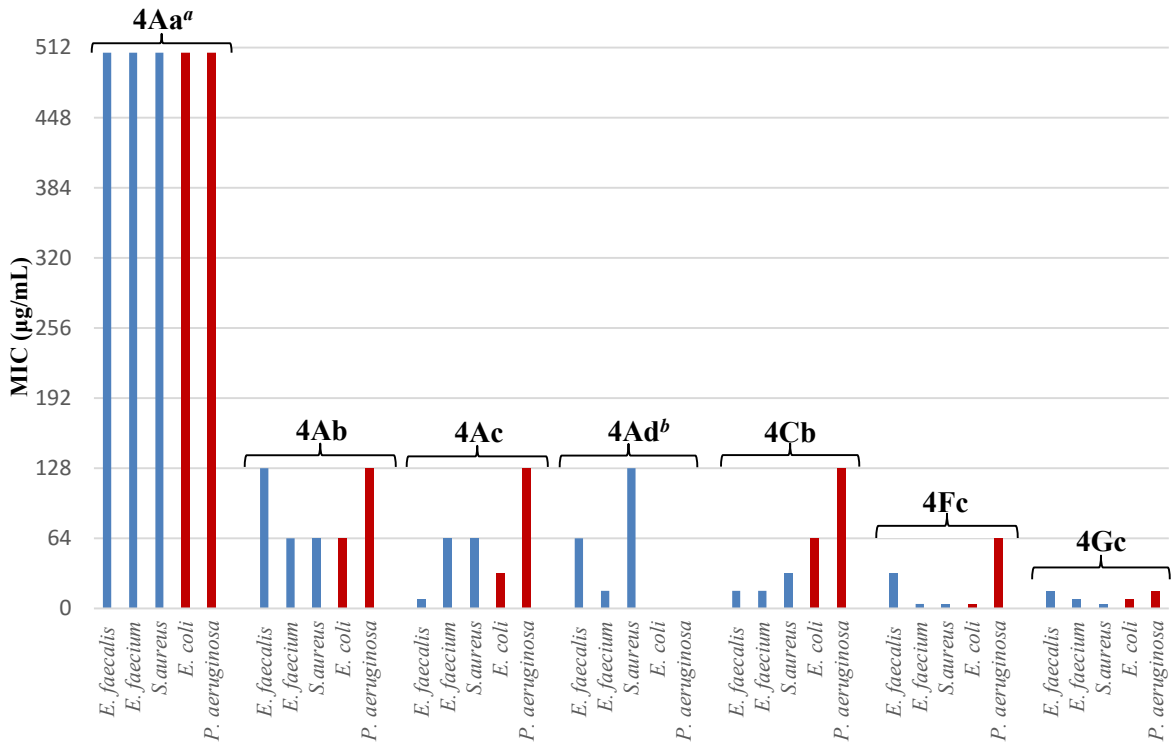

Figure 73. Biological activity of the Cbz N-ter series and some of the most active compounds with a C12 chain at the C-ter. In blue: Gram-positive bacteria; in red: Gram-negative bacteria. [a] Compound 4Aa has MIC values >512 µg/mL, but for clarity they were reported equal to 512. [b] compound 4Ad was tested with a DMSO percentage >3%.

The only exceptions among derivatives with only linear alkyl substituents were compounds **4Cb**, **4Dc**, and **4Eb**, which all have a quite large overall hydrophobic moiety. Indeed, they showed a reduced difference in activities against Gram-positive and Gram-negative bacteria, although the potency towards the positive ones remained slightly greater.

Considering the series **4** (Cbz group at the N-terminal) and alkyl chains of increasing lengths at the C-terminal (compounds **4Aa**, **4Ab**, **4Ac** and **4Ad**), the lauryl chain (**4Ac**) seemed to offer the best overall bacteriostatic activity, thus having the best matching between the charged and lipophilic moieties, whereas compound **4Aa**, whose C-terminal chain (n-propyl) is the shortest one, resulted to be completely inactive.

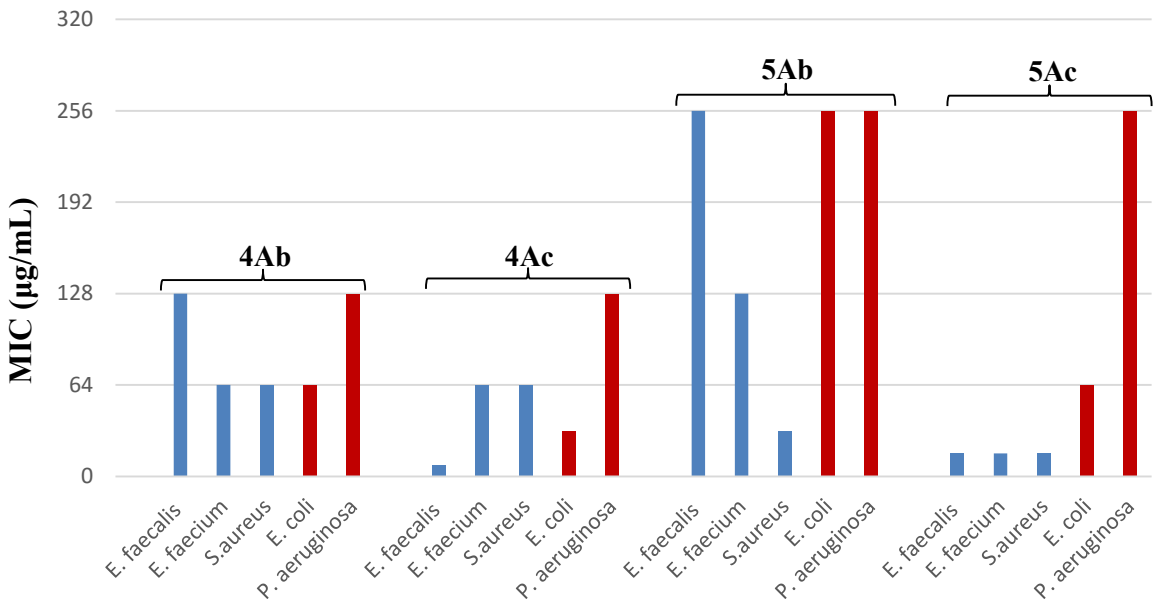

Figure 74. Comparison between the biological activity of mono and bi-charged derivatives with the same side chains R^2 e R^3. In blue: Gram-positive bacteria; in red: Gram-negative bacteria.

The two bicharged lysine derivatives gave contradictory results. In fact, while the Cbz-octyl derivative **5Ab** showed a somewhat lower activity in comparison to its monocharged counterpart **4Ab**, the Cbz-lauryl derivative **5Ac** exhibited an activity comparable to, and sometimes better than, that of the corresponding monocationic compound **4Ac**.

Although they are derived from preliminary and incomplete trials, these first experimental results confirm what has been reported in pre-existing studies, in which a good balance between the polar and the hydrophobic portion was demonstrated to be mandatory to get a good antimicrobial activity.

In addition to MICs evaluation, the relationship between the overall lipophilicity and the antimicrobial activity was also evaluated. Generally, in literature the retention time (t_R) in reverse-phase HPLC (RP-HPLC) is used as a reliable indicator of the global lipophilicity, as previously reported (Paragraph 4.3 Synthetic Mimics of AntiMicrobial Peptides (SMAMPs)). Table 28 reports the t_R relative to the all the hydrochlorides synthesized.

Table 28. Retention times t_R (min) in RP-HPLC of the hydrochlorides synthesized.

COMPOUND	COMPOUND EXTENDED NAME	RETENTION TIME t_R (min)
4Aa	Cbz-IdrGly-NHC_3H_7 · HCl	8,15
4Ab	Cbz-IdrGly-NHC_8H_{17} · HCl	18,95
4Ac	Cbz-IdrGly-$NHC_{12}H_{25}$ · HCl	25,91
4Ad	Cbz-IdrGly-$NHC_{18}H_{37}$ · HCl	35,64
4Ae	Cbz-IdrGly-NHBn · HCl	10,65

4Bd	CH_3CO-IdrGly-$NHC_{18}H_{37}$ · HCl	32,69
4Ca	$C_7H_{15}CO$-IdrGly-NHC_3H_7 · HCl	9,94
4Cb	$C_7H_{15}CO$-IdrGly-NHC_8H_{17} · HCl	22,48
4Cc	$C_7H_{15}CO$-IdrGly-$NHC_{12}H_{25}$ · HCl	28,71
4Cd	$C_7H_{15}CO$-IdrGly-$NHC_{18}H_{37}$ · HCl	37,75
4Da	$C_{11}H_{23}CO$-IdrGly-NHC_3H_7 · HCl	21,33
4Db	$C_{11}H_{23}CO$-IdrGly-NHC_8H_{17} · HCl	28,16
4Dc	$C_{11}H_{23}CO$-IdrGly-$NHC_{12}H_{25}$ · HCl	33,84
4Eb	$C_{17}H_{35}CO$-IdrGly-NHC_8H_{17} · HCl	36,94
4Ed	$C_{17}H_{35}CO$-IdrGly-$NHC_{18}H_{37}$ · HCl	46,48
4Fc	PhCO-IdrGly-$NHC_{12}H_{25}$ · HCl	24,40
4Gc	*t*-BuCO-IdrGly-$NHC_{12}H_{25}$ · HCl	24,47
4Hc[a]	1-NaphthylCO-IdrGly-$NHC_{12}H_{25}$· HCl	26,30
4Ic[a]	Fmoc-IdrGly-$NHC_{12}H_{25}$ · HCl	29,81
5Ab	Cbz-IdrLys-NHC_8H_{17} · 2 HCl	15,95
5Ac	Cbz-IdrLys-$NHC_{12}H_{25}$ · 2 HCl	22,78
5Ad	Cbz-IdrLys-$NHC_{18}H_{37}$ · 2 HCl	32,12
5Ed	$C_{17}H_{35}CO$-IdrLys-$NHC_{18}H_{37}$ · 2 HCl	43,10

[a] Compounds **4Hc** and **4Ic** were directly deprotected following the TFA/DCA methodology and analysed as crude compounds.

The data obtained show how the activity of these compounds is strongly influenced by the degree of the overall hydrophobicity, although of course it is impossible to obtain a trend that correlates perfectly all the points (Figure 75). Anyway, the range that encompasses the "best overall lipophilicity" (t_R = 15-30 minutes), is readily evident. In fact, molecules with an insufficient or excessive overall lipophilicity show a very low or no activity.

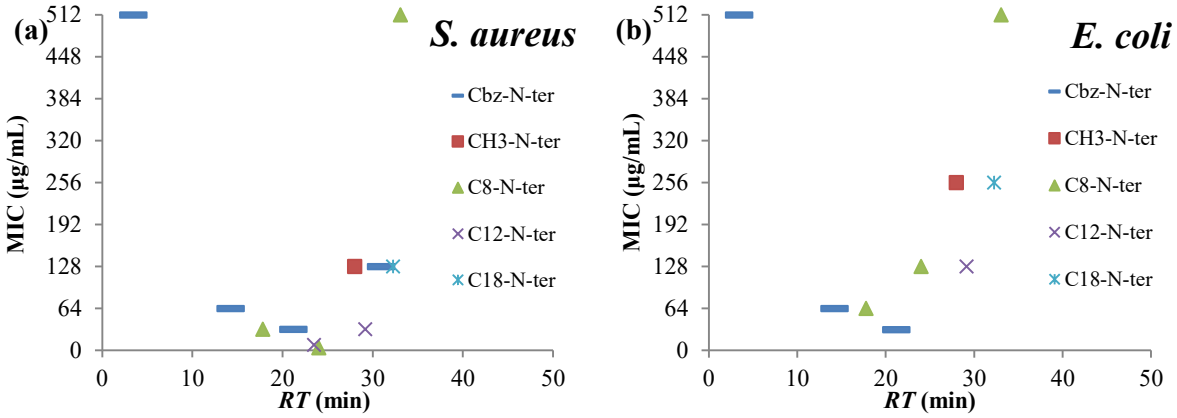

Figure 75. Correlation between the overall lipophilicity and the antimicrobial activity of the hydrochlorides synthesized. (a) Activity against *S. aureus* (Gram-positive), (b) activity against *E. coli* (Gram-negative). Compound 4Ad was not considered, due to the high content of DMSO (> 3%) during the evaluation of MIC.

The correlation between global lipophilicity and MIC easily explains why compounds with the same type of substituents (all with linear alkyl groups) at both N- and C-ter, as

octanoyl/octyl (**4Cb**) and lauroyl/lauryl (**4Dc**), are less active than compounds characterized by "mixed" groups, such as **4Cc** and **4Db** (Table 27).

A possible explanation relies on the fact that the two derivatives **4Cc** and **4Db** have very similar lipophilic moieties and the proper overall size, as witnessed by the extreme similarity of both their MICs and retention times. Instead, the octanoyl/octyl (**4Cb**) derivative may have an overall lipophilicity slightly lower than the optimal value for linear aliphatic chains, while the contrary applies to the lauroyl/lauryl compound, where the global lipophilicity is slightly too high (**4Dc**). However, there are not yet enough experimental evidences to safely confirm this hypothesis.

In general, all the previous preliminary observations demonstrate that, even using a very simple basis structure, there is an evident possibility to obtain compounds provided with very good antibacterial activities. Moreover, there is plenty of room for improvement, simply changing the three substituents that are present on the α-hydrazido acid skeleton.

5.3 Conclusions

Starting from the simple and easily derivatizable α-hydrazido acidic basis structure, many different hydrochlorides displaying an adjustable antibacterial activity were synthesized exploiting a short, cheap, general, well-tolerating and high-yielding synthesis.

The first *in vitro* trials against different Gram-positive and Gram-negative bacteria highlighted the possibility to obtain very good antimicrobial activities, even though, as expected, the Gram-positive ones seemed to be inherently more susceptible to the membranolytic action of our compounds. In addition, a qualitative structure-activity relationship between the global lipophilicity and the antibacterial activity was assessed. Furthermore, the possibility to tune finely the antibacterial activity by using different substituents turned out to be evident.

With the aim to verify the subsistence of a potential therapeutic window, the hemolyticity and toxicity towards mammalian cells will also be evaluated. These results will be reported in due course, together with the time-killing curves and the trials devoted to the evaluation of the development of resistance. Moreover, the assessment of the possible synergistic effect with first-line antibiotics will be carried out, against both sensitive and resistant strains.

Furthermore, when the complete scenario of bioactivities will be available for all the compounds reported in the text, an *ad hoc* optimization of the best performing antimicrobials

will be conducted, using both *in vitro* and *in vivo* trials, in view of a future practical implementation.

5.4 Experimental

5.4.1 General methods and materials for the synthesis of products

Melting points were obtained on an Electrothermal IA 9000 apparatus and are uncorrected. ^{1}H and ^{13}C-NMR spectra were determined at 25 °C on a Varian MR400 spectrometer, at 400 and 100 MHz for ^{1}H and ^{13}C, respectively, in $CDCl_3$ unless otherwise reported. Chemical shifts are reported in ppm relative to residual solvent signals (δ = 7.26 and 77.16 ppm for ^{1}H and ^{13}C NMR, respectively), and coupling constants (J) are given in Hz. LC electrospray ionization mass spectra were obtained with a Finnigan Navigator LC/MS single-quadrupole mass spectrometer, cone voltage 25 V and capillary voltage 3.5 kV, injecting samples dissolved in methanol. HPLC analysis was performed injecting the samples, previously dissolved in isopropyl alcohol (iPrOH), using a Hewlett-Packard 1100 chromatograph equipped with a Lichrosorb RP 18 5 μm, L x I.D. 200 x 4.6 mm column and a UV/VIS detector, eluting with water and iPrOH both containing 0.1% TFA. The elution was performed through a linear gradient of 30-90% iPrOH in H_2O in 40 min, with a 0.5 mL/min flow rate and 210 nm wavelength.

Column chromatography was performed using Kieselgel 60 Merck (230-400 mesh ASTM) as the stationary phase and distilled solvents as the eluents. To eliminate traces of eluents from the pure chromatographed products, these were submitted for three times to the dissolution in a few millilitres of distilled anhydrous dichloromethane, followed by in vacuo evaporation. DCM, MeOH and DMF were freshly distilled from calcium hydride, sodium and P_4O_{10}, respectively, under an argon atmosphere. Ethyl acetate and cyclohexane used as eluents were distilled by evaporation under vacuum. The TLC analysis was performed with sheets of silica gel Fluka TLC-PET, using exposure to UV light and immersion in aqueous $KMnO_4$, followed by heating and by possible immersion in H_2SO_4 9 M.

All reagents and solvents used were purchased from commercial suppliers and used as received, except in cases of anhydrous solvents, stearoyl chloride and Boc-Lys(Boc)-OH. The stearoyl chloride was obtained starting from stearic acid and thionyl chloride (1 mL/mmol) and, after 3 h reflux, all the volatiles were evaporated under vacuum and the crude product was azeotropically dried by dissolution in dry DCM followed by rotary evaporation (2 times), and

then used in the next synthetic step without further purifications. Boc-Lys(Boc)-OH was obtained following the synthetic procedure reported by Ghosh et al.[97]

The methanolic solution of anhydrous HCl for the formation of hydrochlorides was obtained by addition of acetyl chloride (15 mmol) in anhydrous MeOH (5 mL) at 0 °C under vigorous stirring, then the reaction was left to rise at room temperature.

The abbreviated nomenclature adopted is as follows: dichloromethane (DCM); methanol (MeOH); isopropyl alcohol (iPrOH); trifluoroacetic acid (TFA) dimethylformamide (DMF); acetyl chloride (AcCl); cyclohexane (*c*-EX); ethyl acetate (AcOEt); diethyl ether (Et_2O); N,N-diisopropylethylamine (DIPEA), 1-ethyl-3-(3-dimethylaminopropyl) carbodiimmide (EDCI).

5.4.2 Procedures for the evaluation of MICs

The antibacterial activities of the mono- and bi-cationic (series **4** and **5**, as reported in Table 26) α-hydrazido acid SMMAMPs were reported as minimum inhibitory concentration (MIC), the lowest concentration of the antimicrobial agent that inhibits the growth of a microorganism after overnight incubation. MICs were determined by the microbroth dilution method, following the recommended guide lines reported in CLSI manual.[104] All the final compounds tested were water soluble.

5.4.3 Synthetic procedures and characterizations

Synthesis of benzyl 2-(2-methoxy-2-oxoethyl)hydrazine-1-carboxylate, Cbz-Idr-OMe 1

To a solution of benzyl carbazate (105 mmol, 17.45 g) and methyl bromoacetate (100 mmol, 9.76 mL) in anhydrous DCM (50 mL) at room temperature under inert atmosphere, DIPEA (105 mmol, 18.34 ml) was added and the reaction was stirred for 48 hours. After evaporation under vacuum, the residue was extracted using a mixture of cyclohexane/ethyl acetate 1:1 (400 mL) as the organic phase and water (100 mL). The organic phase was washed with HCl 1 M (2 × 10 mL) and water (10 mL), then the aqueous phases were sequentially extracted with additional 400 mL of *c*-Ex/AcOEt 1:1. The second organic phase was washed with HCl 1 M (2 × 10 mL) and water (10 mL), then the reunited organic phases were dried over anhydrous sodium sulphate. After evaporation under vacuum, the crude product was purified by flash chromatography on silica gel (*c*-Ex/AcOEt), obtaining the pure product **1** as a colourless oil in a 96% yield (96 mmol, 22.87 g).

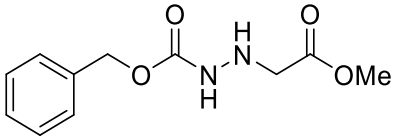

R_f = 0.32 (*c*-Ex:AcOEt = 1:1). ^{1}H NMR (400 MHz, $CDCl_3$): δ 3.69 (s, 2H), 3.72 (s, 3H), 5.13 (s, 2H), 6.93 (bs, 1NH), 7.31 (bs, 1NH), 7.34 (s, 5ArH). ^{13}C NMR (100 MHz, $CDCl_3$): δ 52.2, 52.6, 67.4, 128.4, 128.5, 128.7, 135.9, 156.9, 171.5. MS (ESI): *m/z* = 261.1 $[M+Na]^+$.

Synthesis of benzyl 2-((*tert*-Butoxycarbonyl)glycyl)-2-(2-methoxy-2-oxoethyl)hydrazine-1-carboxylate, Cbz-IdrGly-OMe 2

To a solution of compound **1** (45 mmol, 10.72 g) in dry DCM (22.5 mL) under inert atmosphere, Boc-Gly-OH (58.5 mmol, 10.04 g) was added and the reaction mixture was thermostated at -20 °C. EDCI (67.5 mmol, 12.94 g) was added and the mixture was stirred vigorously at -20 °C for 1 hour, then the reaction mixture was diluted with AcOEt (400 mL) and water (50 mL). After separation, the organic phase was sequentially washed with HCl 1 M (3 × 10 mL) and a saturated solution of Na_2CO_3 (3 × 10 mL). The aqueous phases were sequentially extracted with AcOEt (250 mL) and the organic phase was washed with HCl 1 M (3 × 5 mL) and water (50 mL). The combined organic phases were dried over anhydrous Na_2SO_4, the solvent was evaporated under reduced pressure and the residue was purified by silica gel chromatography (*c*-Ex/AcOEt) to give the pure compound **2** as a colourless wax in 86% yield (38.7 mmol, 15.30 g).

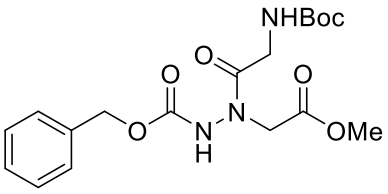

R_f = 0.50 (*c*-Ex:AcOEt = 1:1). ^{1}H NMR (400 MHz, $CDCl_3$): δ 1.42 (s, 9H), 3.70 (s, 3H), 4.07 (bs, 3H), 5.10 (bs, 1H), 5.15 (s, 2H), 5.27 (bs, 1NH), 7.31-7.38 (m, 5ArH), 7.77 (bs, 1NH). MS (ESI): *m/z* = 418.0 $[M+Na]^+$.

Synthesis of benzyl 2-(N^2,N^6-bis(*tert*-butoxycarbonyl)-*L*-lysyl)-2-(2-methoxy-2-oxoethyl)hydrazine-1-carboxylate, Cbz-IdrLys-OMe 3

To a solution of compound **1** (45 mmol, 25.50 g) in dry DCM (22.5 mL) at room temperature under inert atmosphere, Boc-Lys(Boc)-OH (67.5 mmol, 23.38 g) was added and the reaction mixture was thermostated at 0 °C. EDCI was added (49.5 mmol, 9.49 g) and the mixture was stirred vigorously at 0 °C for 2 hours, then the reaction mixture was diluted with AcOEt (400 mL) and water (50 mL). After separation, the organic phase was sequentially washed with HCl 1 M (3 × 10 mL) and a saturated solution of Na_2CO_3 (3 × 10 mL). The neutral aqueous phases were sequentially extracted with AcOEt (250 mL) and the organic phase was washed with HCl

1 M (3 × 5 mL) and water (50 mL). The combined organic phases were dried over anhydrous Na_2SO_4, the solvent was evaporated under reduced pressure and the residue was purified by silica gel chromatography (*c*-Ex/AcOEt) to give the pure compound **3** as a colourless waxy solid in 45% yield (20.25 mmol, 11.47 g).

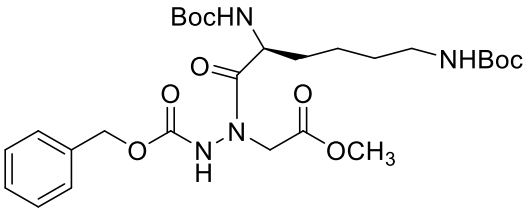

R_f = 0.43 (*c*-Ex:AcOEt = 1:1). MS (ESI): *m/z* = 589.3 $[M+Na]^+$.

General procedure for the synthesis of the C-terminal derivatives and their characterization.

Note: representative procedure referred to 1 mmol of starting compound; the actual amounts of starting compounds used in the reactions are reported below.

To a solution of compound **2** or **3** in dry MeOH (0.5 mL) under inert atmosphere, the suitable amine was added (3 eq. for propylamine and 1.5 eq. for octylamine, dodecylamine and octadecylamine). The reaction was stirred for 7 hours at room temperature for the synthesis of compound **2Aa**, and refluxed for 7, 15 and 30 hours, for the syntheses of compounds **2,3Ab**, **2,3Ac** and **2,3Ad**, respectively. Thus, the volatile species were removed under vacuum and the residue was submitted for three times to the dissolution in few millilitres of anhydrous dichloromethane, followed by *in vacuo* evaporation. The residue was purified by silica gel chromatography (*c*-Ex/AcOEt) to give the corresponding pure compound. The identity of all the products was ascertained only by mass spectra.

Benzyl 2-((*tert*-butoxycarbonyl)glycyl)-2-(2-oxo-2-(propylamino)ethyl)hydrazine-1-carboxylate, Cbz-IdrGly-NHC$_3$H$_7$ 2Aa

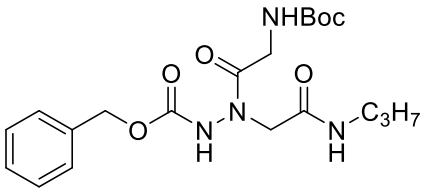

Starting from **2** (2 mmol, 791 mg) and following the general procedure, compound **2Aa** was obtained in 94% yield (1.88 mmol, 794 mg) as a white amorphous solid.

R_f = 0.55 (*c*-Ex:AcOEt = 2:8). m.p. = 49-50 °C. MS (ESI): *m/z* = 445.3 $[M+Na]^+$.

Benzyl 2-((*tert*-butoxycarbonyl)glycyl)-2-(2-(octylamino)-2-oxoethyl)hydrazine-1-carboxylate, Cbz-IdrGly-NHC$_8$H$_{17}$ 2Ab

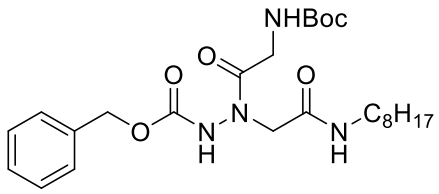

Starting from **2** (5 mmol, 1.98 g) and following the general procedure, compound **2Ab** was obtained in 88% yield (4.4 mmol, 2.17 g) as a white waxy solid.

R_f = 0.60 (*c*-Ex:AcOEt = 2:8). m.p. = 74-76 °C. MS (ESI): *m/z* = 515.3 $[M+Na]^+$.

Benzyl 2-(N^2,N^6-bis(*tert*-butoxycarbonyl)-*L*-lysyl)-2-(2-(octylamino)-2-oxoethyl)hydrazine-1-carboxylate, Cbz-IdrLys-NHC$_8$H$_{17}$ 3Ab

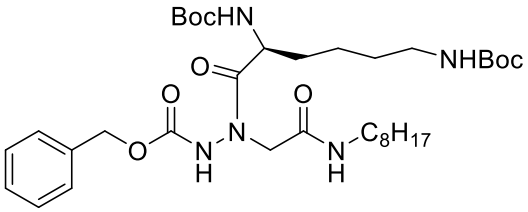

Starting from **3** (4.60 mmol, 2.61 g) and following the general procedure, compound **3Ab** was obtained in 82% yield (3.77 mmol, 2.50 g) as a white waxy solid.

R_f = 0.77 (*c*-Ex:AcOEt = 4:6). MS (ESI): *m/z* = 686.4 $[M+Na]^+$.

Benzyl 2-((*tert*-butoxycarbonyl)glycyl)-2-(2-(dodecylamino)-2-oxoethyl)hydrazine-1-carboxylate, Cbz-IdrGly-NHC$_{12}$H$_{25}$ 2Ac

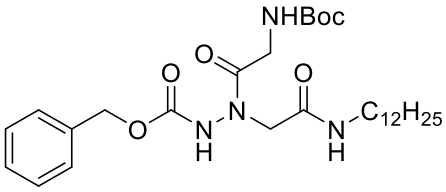

Starting from **2** (5 mmol, 1.98 g) and following the general procedure, compound **2Ac** was obtained in 88% yield (4.4 mmol, 2.41 g) as a white amorphous solid.

R_f = 0.43 (*c*-Ex:AcOEt = 1:1). m.p. = 76-78 °C. MS (ESI): *m/z* = 571.4 $[M+Na]^+$.

Benzyl 2-(N^2,N^6-bis(*tert*-butoxycarbonyl)-*L*-lysyl)-2-(2-(dodecylamino)-2-oxoethyl)hydrazine-1-carboxylate, Cbz-IdrLys-NHC$_{12}$H$_{25}$ 3Ac

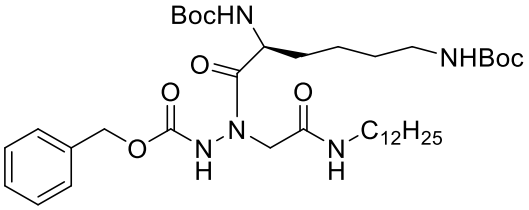

Starting from **3** (4.6 mmol, 2.61 g) and following the general procedure, compound **3Ac** was obtained in 85% yield (3.91 mmol, 2.82 g) as a colourless waxy solid.

R_f = 0.54 (*c*-Ex:AcOEt = 3:7). MS (ESI): *m/z* = 742.5 $[M+Na]^+$.

Benzyl 2-((*tert*-butoxycarbonyl)glycyl)-2-(2-(octadecylamino)-2-oxoethyl)hydrazine-1-carboxylate, Cbz-IdrGly-NHC$_{18}$H$_{37}$ 2Ad

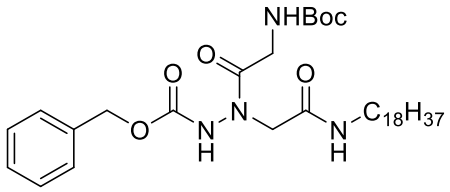

Starting from **2** (5 mmol, 1.98 g) and following the general procedure, the compound **2Ad** was obtained in 90% yield (4.5 mmol, 2.85 g,) as a white waxy solid.

R_f = 0.63 (*c*-Ex:AcOEt = 2:8). m.p. = 84-86 °C. MS (ESI): *m/z* = 655.5 $[M+Na]^+$.

Benzyl 2-(N^2,N^6-bis(*tert*-butoxycarbonyl)-*L*-lysyl)-2-(2-(octadecylamino)-2-oxoethyl)hydrazine-1-carboxylate, Cbz-IdrLys-NHC$_{18}$H$_{37}$ 3Ad

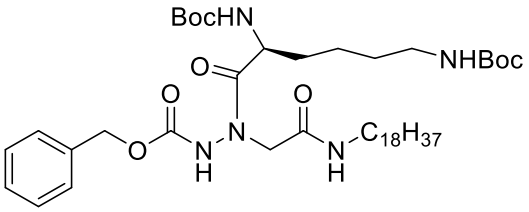

Starting from **3** (4.6 mmol, 2.61 g) and following the general procedure, compound **3Ad** was obtained in 88% yield (4.05 mmol, 3.26 g) as a white waxy solid.

R_f = 0.45 (*c*-Ex:AcOEt = 4:6). MS (ESI): *m/z* = 826.6 $[M+Na]^+$.

Benzyl 2-(2-(benzylamino)-2-oxoethyl)-2-((*tert*-butoxycarbonyl)glycyl)hydrazine-1-carboxylate, Cbz-IdrLys-NHBn 2Ae

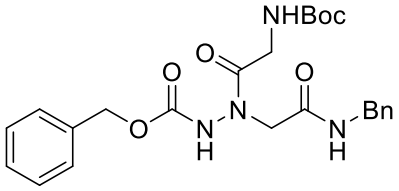

Starting from **2** (2 mmol, 791 mg) and following the general procedure, compound **2Ae** was obtained in 99% yield (1.98 mmol, 931 mg) as a white waxy solid.
R_f = 0.34 (*c*-Ex:AcOEt = 4:6). MS (ESI): *m/z* = 493.3 $[M+Na]^+$.

General procedure for the synthesis of the N-terminal derivatives and their characterization.

Note: representative procedure referred to 1 mmol of starting compound; the actual amounts of starting compounds used in the reactions are reported below.

To a solution of compound **2Aa-e** or **3Aa-e** dissolved in dry DCM (2 mL) under inert atmosphere at room temperature, Pd/C (100 mg) and formic acid (76 μL) were sequentially added and the mixture was stirred for 1 hour. Thus, the volatile species were removed under vacuum at room temperature, then DCM (20 mL) was added and the reaction mixture was filtered through Celite, washing with DCM (3 × 10 mL). The organic phase was washed with a saturated solution of Na_2CO_3 (5 mL), then the aqueous phase was newly extracted with DCM (25 mL) and, after separation, the organic phase was washed with a saturated solution of Na_2CO_3 (5 mL). The combined organic phases were dried over anhydrous Na_2SO_4, the solvent was evaporated under vacuum at room temperature and the free hydrazide intermediate was directly submitted to the following acylation reaction or stored at -18 °C.

To a solution of the suitable free hydrazide intermediate in dry DCM (5 mL) under inert atmosphere, pyridine (121 μL) was added, followed by dropwise addition of the suitable acyl chloride (1.1 eq). The solution was stirred for 1 hour, then all the volatile species were removed *in vacuo* at room temperature and the residue was diluted with AcOEt (30 mL) and water (5 mL). After separation, the organic phase was washed with HCl 1 M (2 × 3 mL), saturated aqueous sodium carbonate (5 mL) and water (5 mL). The aqueous phases were sequentially extracted with additional 30 mL of ethyl acetate, then the second organic phase was washed with HCl 1 M (2 × 3 mL), saturated aqueous sodium carbonate (5 mL) and water (5 mL). The combined organic phases were dried over anhydrous sodium sulphate and evaporated under

vacuum, then the crude product was purified by column chromatography on silica gel (*c*-Ex/AcOEt), to give the pure compound.

***tert*-Butyl (2-(2-acetyl-1-(2-(octylamino)-2-oxoethyl)hydrazinyl)-2-oxoethyl)carbamate, CH_3CO-IdrGly-NHC_8H_{17} 2Bb**

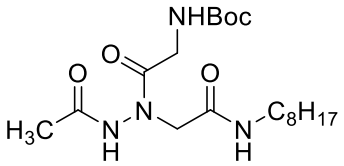

Starting from **2Ab** (1.1 mmol, 542 mg) and following the general procedure, compound **2Bb** was obtained in 77% yield (0.85 mmol, 340 mg) as a white waxy solid.
R_f = 0.22 (AcOEt). MS (ESI): *m/z* = 423.4 $[M+Na]^+$.

***tert*-Butyl (2-(2-acetyl-1-(2-(dodecylamino)-2-oxoethyl)hydrazinyl)-2-oxoethyl)carbamate, CH_3CO-IdrGly-$NHC_{12}H_{25}$ 2Bc**

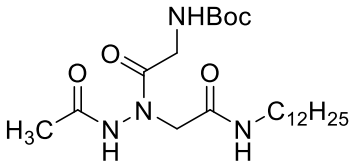

Starting from **2Ac** (1.15 mmol, 631 mg) and following the general procedure, compound **2Bc** was obtained in 79% yield (0.91 mmol, 415 mg) as a white waxy solid.
R_f = 0.14 (AcOEt). MS (ESI): *m/z* = 479.4 $[M+Na]^+$.

***tert*-Butyl (2-(2-acetyl-1-(2-(octadecylamino)-2-oxoethyl)hydrazinyl)-2-oxoethyl)carbamate, CH_3CO-IdrGly-$NHC_{18}H_{37}$ 2Bd**

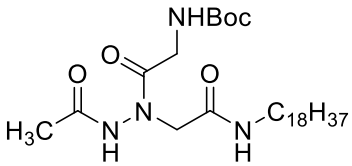

Starting from **2Ad** (1 mmol, 633 mg) and following the general procedure, compound **2Bd** was obtained in 81% yield (0.81 mmol, 438 mg) as a white waxy solid.
R_f = 0.32 (AcOEt). m.p. = 77-79 °C. MS (ESI): *m/z* = 563.5 $[M+Na]^+$.

***tert*-Butyl (2-(2-octanoyl-1-(2-oxo-2-(propylamino)ethyl)hydrazinyl)-2-oxoethyl)carbamate 2Ca**

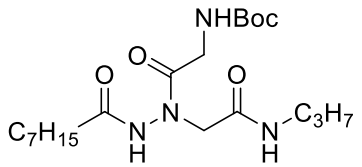

Starting from **2Aa** (1 mmol, 422 mg) and following the general procedure, compound **2Ca** was obtained in 90% yield (0.9 mmol, 373 mg) as a white waxy solid.

R_f = 0.4 (*c*-Ex:AcOEt = 2:8). MS (ESI): *m/z* = 436.3 $[M+Na]^+$.

***tert*-Butyl (2-(2-octanoyl-1-(2-(octylamino)-2-oxoethyl)hydrazinyl)-2-oxoethyl)carbamate, $C_7H_{15}CO$-IdrGly-NHC_8H_{17} 2Cb**

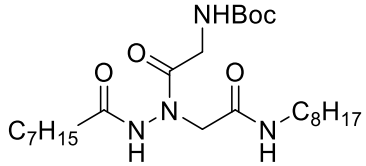

Starting from **2Ab** (0.9 mmol, 443mg) and following the general procedure, compound **2Cb** was obtained in 84% yield (756 μmol, 366 mg) as a white waxy solid.

R_f = 0.47 (AcOEt). m.p. = 77-79 °C. MS (ESI): *m/z* = 507.4 $[M+Na]^+$.

***tert*-Butyl (2-(1-(2-(dodecylamino)-2-oxoethyl)-2-octanoylhydrazinyl)-2-oxoethyl)carbamate, $C_7H_{15}CO$-IdrGly-$NHC_{12}H_{25}$ 2Cc**

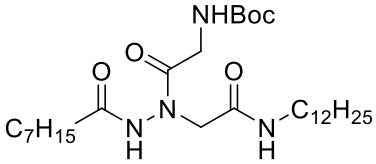

Starting from **2Ac** (390 μmol, 214 mg) and following the general procedure, compound **2Cc** was obtained in 83% yield (324 μmol, 175 mg) as a white amorphous solid.

R_f = 0.35 (AcOEt). m.p. = 81-83 °C. MS (ESI): *m/z* = 563.5 $[M+Na]^+$.

***tert*-Butyl (2-(1-(2-(octadecylamino)-2-oxoethyl)-2-octanoylhydrazinyl)-2-oxoethyl)carbamate, $C_7H_{15}CO$-IdrGly-$NHC_{18}H_{37}$ 2Cd**

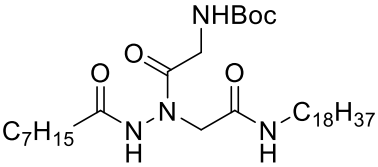

Starting from **2Ad** (525 μmol, 332 mg) and following the general procedure, compound **2Cd** was obtained in 83% yield (436 μmol, 272 mg) as a white amorphous solid.
R_f = 0.75 (AcOEt). m.p. = 83-85 °C. MS (ESI): *m/z* = 647.5 $[M+Na]^+$.

***tert*-Butyl (2-(2-dodecanoyl-1-(2-oxo-2-(propylamino)ethyl)hydrazinyl)-2-oxoethyl)carbamate 2Da**

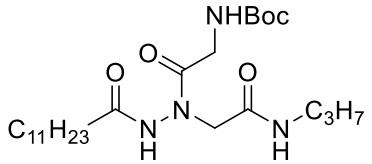

Starting from **2Aa** (1 mmol, 422 mg) and following the general procedure, compound **2Da** was obtained in 94% yield (0.94 mmol, 422 mg) as a white amorphous solid.
R_f = 0.33 (*c*-Ex:AcOEt = 2:8). MS (ESI): *m/z* = 493.4 $[M+Na]^+$.

***tert*-Butyl (2-(2-dodecanoyl-1-(2-(octylamino)-2-oxoethyl)hydrazinyl)-2-oxoethyl)carbamate, $C_{11}H_{23}CO$-IdrGly-NHC_8H_{17} 2Db**

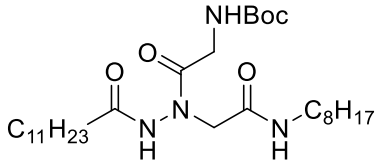

Starting from **2Ab** (628 μmol, 309 mg) and following the general procedure, compound **2Db** was obtained in 88% yield (553 μmol, 299 mg) as a white amorphous solid.
R_f = 0.38 (*c*-Ex:AcOEt = 2:8). m.p. = 67-69 °C. MS (ESI): *m/z* = 563.3 $[M+Na]^+$.

***tert*-Butyl (2-(2-dodecanoyl-1-(2-(dodecylamino)-2-oxoethyl)hydrazinyl)-2-oxoethyl)carbamate, $C_{11}H_{23}CO$-IdrGly-NH-$C_{12}H_{25}$ 2Dc**

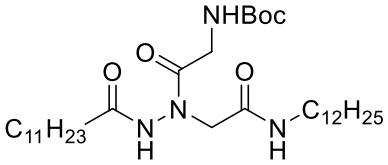

Starting from **2Ac** (600 μmol, 329 mg) and following the general procedure, compound **2Dc** was obtained in 86% yield (516 μmol, 308 mg) as a white amorphous solid.
R_f = 0.44 (AcOEt). m.p. = 63-65 °C. MS (ESI): *m/z* = 619.6 $[M+Na]^+$.

***tert*-Butyl (2-(1-(2-(octylamino)-2-oxoethyl)-2-stearoylhydrazinyl)-2-oxoethyl)carbamate, $C_{17}H_{35}CO$-IdrGly-NHC_8H_{17} 2Eb**

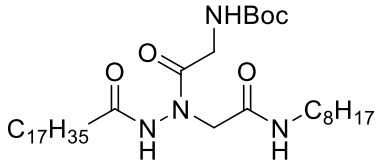

Starting from **2Ab** (375 μmol, 185 mg) and following the general procedure, compound **2Eb** was obtained in 83% yield (311 μmol, 194 mg) as a white amorphous solid.
R_f = 0.61 (DCM:MeOH = 9:1). m.p. = 125-127 °C. MS (ESI): *m/z* = 647.6 $[M+Na]^+$.

***tert*-Butyl (2-(1-(2-(octadecylamino)-2-oxoethyl)-2-stearoylhydrazinyl)-2-oxoethyl)carbamate, $C_{17}H_{35}CO$-IdrGly-$NHC_{18}H_{37}$ 2Ed**

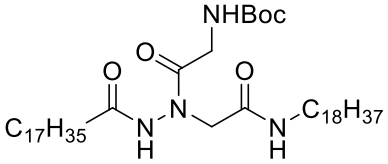

Starting from **2Ad** (347 μmol, 220 mg) and following the general procedure, compound **2Ad** was obtained in 80% yield (277 μmol, 212 mg) as a white waxy solid.
R_f = 0.82 (AcOEt). m.p. = 89-90 °C. MS (ESI): *m/z* = 787.8 $[M+Na]^+$.

Di-*tert*-Butyl (6-(1-(2-(octadecylamino)-2-oxoethyl)-2-stearoylhydrazinyl)-6-oxohexane-1,5-diyl)(*S*)-dicarbamate, $C_{17}H_{35}CO$-IdrLys-$NHC_{18}H_{37}$ 3Ed

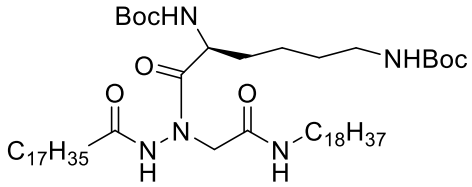

Starting from **3Ad** (323 μmol, 260 mg) and following the general procedure, compound **3Ed** was obtained in 77% yield (249 μmol, 233 mg) as a white waxy solid.
R_f = 0.36 (*c*-Ex:AcOEt = 4:6). MS (ESI): *m/z* = 958.9 $[M+Na]^+$.

***tert*-Butyl (2-(2-benzoyl-1-(2-(octylamino)-2-oxoethyl)hydrazinyl)-2-oxoethyl)carbamate 2Fb**

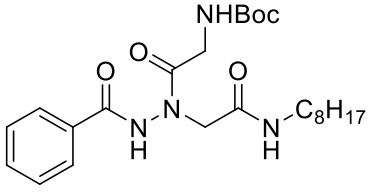

Starting from **2Ab** (0.9 mmol, 443mg) and following the general procedure, compound **2Fb** was obtained in 92% yield (0.83 μmol, 384 mg) as a white amorphous solid.
R_f = 0.16 (AcOEt). MS (ESI): *m/z* = 485.3 $[M+Na]^+$.

***tert*-Butyl (2-(2-benzoyl-1-(2-(dodecylamino)-2-oxoethyl)hydrazinyl)-2-oxoethyl)carbamate, PhCO-IdrGly-NHC$_{12}$H$_{25}$ 2Fc**

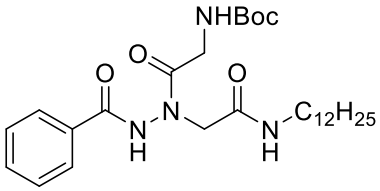

Starting from **2Ac** (424 μmol, 233 mg) and following the general procedure, compound **2Fc** was obtained in 81% yield (343 μmol, 178 mg) as a white amorphous solid.
R_f = 0.56 (AcOEt). m.p. = 123-125 °C. MS (ESI): *m/z* = 541.4 $[M+Na]^+$.

***tert*-Butyl (2-(1-(2-(dodecylamino)-2-oxoethyl)-2-pivaloylhydrazinyl)-2-oxoethyl)carbamate, *t*BuCO-IdrGly-NHC$_{12}$H$_{25}$ 2Gc**

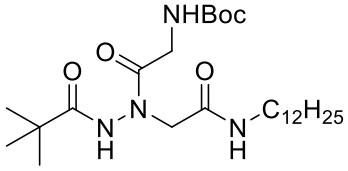

Starting from **2Ac** (673 μmol, 369 mg) and following the general procedure, compound **2Gc** was obtained in 90% yield (607 μmol, 303 mg) as a colourless waxy solid.
R_f = 0.49 (AcOEt). MS (ESI): *m/z* = 521.4 $[M+Na]^+$.

***tert*-Butyl (2-(2-(2-naphthoyl)-1-(2-(dodecylamino)-2-oxoethyl)hydrazinyl)-2-oxoethyl)carbamate, NaphthylCO-IdrGly-NHC$_{12}$H$_{25}$ 2Hc**

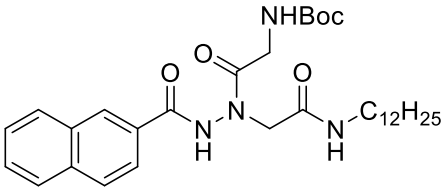

Starting from **2Ac** (315 μmol, 173 mg) and following the general procedure, compound **2Hc** was obtained in 79% yield (250 μmol, 142 mg) as a colourless waxy solid.
R_f = 0.40 (DCM:MeOH = 95:5). MS (ESI): *m/z* = 591.5 $[M+Na]^+$.

(9H-Fluoren-9-yl)methyl 2-((*tert*-butoxycarbonyl)glycyl)-2-(2-(dodecylamino)-2-oxoethyl)hydrazine-1-carboxylate, Fmoc-IdrGly-NHC$_{12}$H$_{25}$ 2 Ic

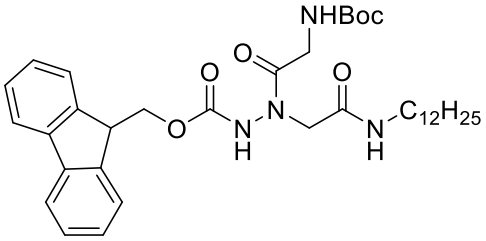

Starting from **2 Ac** (358 μmol, 196 mg) and following the general procedure, compound **2Ic** was obtained in 77% yield (276 μmol, 176 mg) as a colourless waxy solid.
R_f = 0.68 (AcOEt). MS (ESI): *m/z* = 662.5 $[M+Na]^+$.

General procedure for the synthesis of hydrochlorides and their characterization.
Note: representative procedures are referred to 1 mmol of starting compound; the actual amounts of starting compounds used in the reactions are reported below.
Procedure i. The suitable compound was dissolved in dry methanolic 3 M HCl solution and the reaction was stirred at room temperature for 90 minutes. All the volatile species were removed at reduced pressure without using the thermostating bath, then the residue was dissolved in dry DCM and evaporated under vacuum (procedure repeated three times). The residue was diluted with DCM (10 mL) and a saturated solution of Na_2CO_3 (3 mL), then the phases were separated and the aqueous one was newly extracted with DCM (10 mL). After separation, the second organic phase was washed with a saturated solution of Na_2CO_3 (3 mL). The combined organic phases were dried over anhydrous Na_2SO_4, the solvent was evaporated under vacuum and the residue was purified by flash chromatography on silica gel, using the suitable mixtures of distilled DCM and MeOH as the eluents. The pure free amine was dissolved in dry DCM, few drops of a methanolic 3 M HCl solution were added and the mixture was evaporated at reduced pressure, without using the thermostating bath, then the residue was dissolved in dry DCM and evaporated under vacuum (procedure repeated three times), obtaining the desired pure hydrochlorides.
Procedure ii. The suitable compound was dissolved in dry DCM (3 mL), then was added TFA (1 mL) and the reaction was stirred at room temperature for 30 minutes. Thus, the work-up and purification processes were carried out as reported in *Procedure i*.

2-(2-((Benzyloxy)carbonyl)-1-(2-oxo-2-(propylamino)ethyl)hydrazinyl)-2-oxoethan-1-aminium chloride, Cbz-IdrGly-NHC$_3$H$_7$ · HCl 4Aa

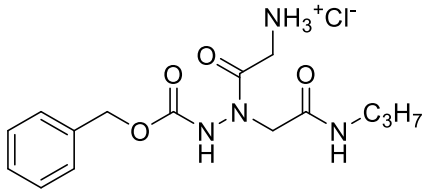

Starting from **2Aa** (263 µmol, 111 mg) and following *procedure i*, compound **4Aa** was obtained in 98% yield (259 µmol, 93 mg) as a colourless waxy solid.

R_f = 0.38 (free amine, DCM:MeOH = 9:1). m.p. = 100°C (decomposes). t_R = 8.15 min. MS (ESI): *m/z* = 345.3 $[M+Na]^+$.

2-(2-((Benzyloxy)carbonyl)-1-(2-(octylamino)-2-oxoethyl)hydrazinyl)-2-oxoethan-1-aminium chloride, Cbz-IdrGly-NH-C$_8$H$_{17}$ · HCl 4Ab

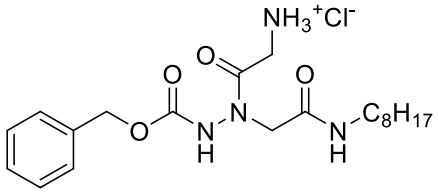

Starting from **2Ab** (356 µmol, 175 mg) and following *procedure i*, compound **4Ab** was obtained in 90% yield (322 µmol, 138 mg) as a colourless waxy solid.

R_f = 0.31 (free amine, DCM:MeOH = 95:5). m.p. = 105 °C (decomposes). t_R = 18.95 min. MS (ESI): *m/z* = 415.3 $[M+Na]^+$.

(*S*)-6-(2-((Benzyloxy)carbonyl)-1-(2-(octylamino)-2-oxoethyl)hydrazinyl)-6-oxohexane-1,5-diaminium chloride, Cbz-IdrLys-NH-C$_8$H$_{17}$ · 2HCl 5Ab

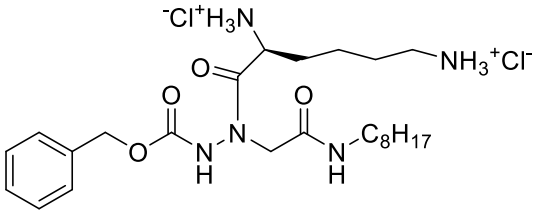

Starting from **3Ab** (246 µmol, 163 mg) and following *procedure ii*, compound **5Ab** was obtained in 76% yield (187 µmol, 100 mg) as a colourless waxy solid.

R_f = 0.54 (free amine, DCM:MeOH = 9:1). t_R = 15.95 min. MS (ESI): *m/z* = 487.4 $[M+Na]^+$.

2-(2-((Benzyloxy)carbonyl)-1-(2-(dodecylamino)-2-oxoethyl)hydrazinyl)-2-oxoethan-1-aminium chloride, Cbz-IdrGly-NHC$_{12}$H$_{25}$ · HCl 4 Ac

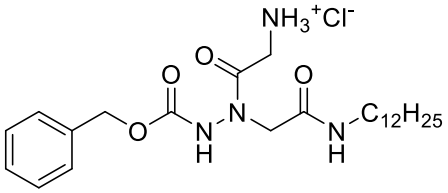

Starting from **2Ac** (155 µmol, 85 mg) and following *procedure i*, compound **4Ac** was obtained in 88% yield (136 µmol, 66 mg) as a white waxy solid.

R_f = 0.07 (free amine, DCM:MeOH = 9:1). t_R = 25.91 min. MS (ESI): *m/z* = 471.4 $[M+Na]^+$.

(*S*)-6-(2-((Benzyloxy)carbonyl)-1-(2-(dodecylamino)-2-oxoethyl)hydrazinyl)-6-oxohexane-1,5-diaminium chloride, Cbz-IdrLys-NH-C$_{12}$H$_{25}$ · 2HCl 5Ac

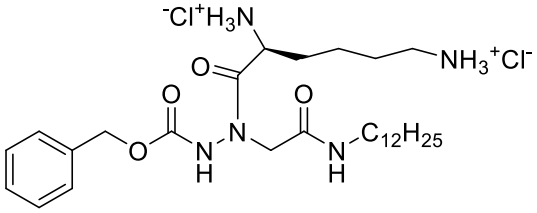

Starting from **3Ac** (158 µmol, 114 mg) and following the general procedure, compound **5Ac** was obtained in 77% yield (122 µmol, 72 mg) as a white waxy solid.

R_f = 0.57 (free amine, DCM:MeOH = 9:1). t_R = 22.78 min. MS (ESI): *m/z* = 542.5 $[M+Na]^+$.

2-(2-((Benzyloxy)carbonyl)-1-(2-(octadecylamino)-2-oxoethyl)hydrazinyl)-2-oxoethan-1-aminium chloride, Cbz-IdrGly(H)-NHC$_{18}$H$_{37}$ · HCl 4Ad

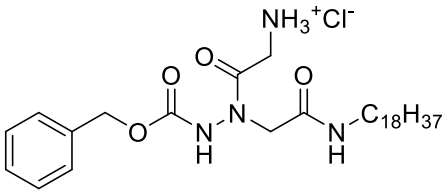

Starting from **2Ad** (152 µmol, 96 mg) and following *procedure ii*, compound **4Ad** was obtained in 82% yield (125 µmol, 71 mg) as a white waxy solid.

R_f = 0.16 (free amine DCM:MeOH = 95:5). t_R = 35.64 min. MS (ESI): *m/z* = 555.5 $[M+Na]^+$.

(*S*)-6-(2-((Benzyloxy)carbonyl)-1-(2-(octadecylamino)-2-oxoethyl)hydrazinyl)-6-oxohexane-1,5-diaminium chloride, Cbz-IdrLys-NHC$_{18}$H$_{37}$ · 2HCl 5Ad

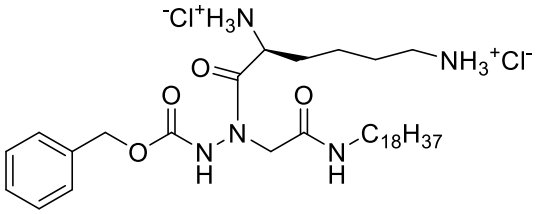

Starting from **3Ad** (276 μmol, 222 mg) and following *procedure ii*, compound **5Ad** was obtained in 70% yield (193 μmol, 131 mg) as a colourless waxy solid.

R_f = 0.65 (free amine, DCM:MeOH = 8:2). t_R = 32.12 min. MS (ESI): *m/z* = 626.6 $[M+Na]^+$.

2-(2-Acetyl-1-(2-(octylamino)-2-oxoethyl)hydrazinyl)-2-oxoethan-1-aminium chloride, CH$_3$CO-IdrGly-NHC$_8$H$_{17}$ · HCl 4Bb

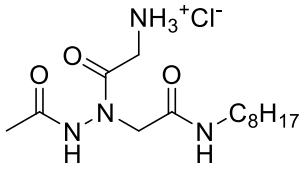

Starting from **2Ab** (356 μmol, 175 mg) and following *procedure ii*, compound **4Bb** was obtained in 68% yield (243 μmol, 82 mg) as a colourless waxy solid.

R_f = 0.13 (free amine, DCM:MeOH = 9:1). t_R = 13.99 min. MS (ESI): *m/z* = 323.3 $[M+Na]^+$.

2-(2-Acetyl-1-(2-(dodecylamino)-2-oxoethyl)hydrazinyl)-2-oxoethan-1-aminium chloride, CH$_3$CO-IdrGly-NHC$_{12}$H$_{25}$ · HCl 4Bc

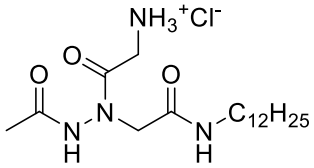

Starting from **2Ac** (175 μmol, 96 mg) and following *procedure ii*, compound **4Bc** was obtained in 70% yield (123 μmol, 48 mg) as a colourless waxy solid.

R_f = 0.42 (free amine, DCM:MeOH = 7:3). t_R = 22.17 min. MS (ESI): *m/z* = 379.3 $[M+Na]^+$.

2-(2-Acetyl-1-(2-(octadecylamino)-2-oxoethyl)hydrazinyl)-2-oxoethan-1-aminium chloride, CH$_3$CO-IdrGly-NHC$_{18}$H$_{37}$ · HCl 4Bd

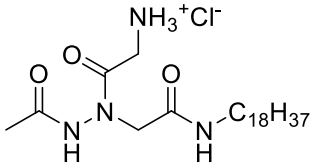

Starting from **2Bd** (262 μmol, 142 mg) and following *procedure ii*, compound **4Bd** was obtained in 89% yield (233 μmol, 111 mg) as a white waxy solid.

R_f = 0.29 (free amine, DCM:MeOH = 85:15). t_R = 32.69 min. MS (ESI): *m/z* = 463.5 $[M+Na]^+$.

2-(2-Octanoyl-1-(2-oxo-2-(propylamino)ethyl)hydrazinyl)-2-oxoethan-1-aminium chloride, CH_3CO-IdrGly-NHC_3H_7 · HCl 4Ca

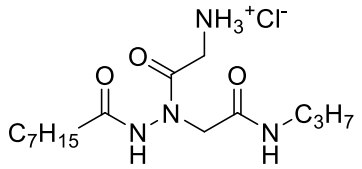

Starting from **2Ca** (260 μmol, 108 mg) and following *procedure ii*, compound **4Ca** was obtained in 95% yield (247 μmol, 87 mg) as a white waxy solid.

R_f = 0.47 (free amine, DCM:MeOH = 8:2). t_R = 9.94 min. MS (ESI): *m/z* = 337.2 $[M+Na]^+$.

2-(2-Octanoyl-1-(2-(octylamino)-2-oxoethyl)hydrazinyl)-2-oxoethan-1-aminium chloride, $C_7H_{15}CO$-IdrGly-NHC_8H_{17} · HCl 4Cb

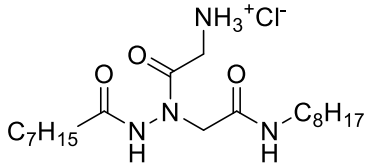

Starting from **2Cb** (192 μmol, 93 mg) and following *procedure i*, compound **4Cb** was obtained in 87% yield (167 μmol, 70 mg) as a white waxy solid.

R_f = 0.28 (free amine, DCM:MeOH = 1:1). m.p. (hydrochloride) = 120-123 °C (decomposes). t_R = 22.48 min. MS (ESI): *m/z* = 407.4 $[M+Na]^+$.

2-(1-(2-(Dodecylamino)-2-oxoethyl)-2-octanoylhydrazinyl)-2-oxoethan-1-aminium chloride, $C_7H_{15}CO$-IdrGly-$NHC_{12}H_{25}$ · HCl, 4Cc

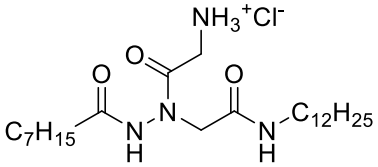

Starting from **2Cc** (135 μmol, 73 mg) and following *procedure i*, compound **4Cc** was obtained in 84% yield (113 μmol, 54 mg) as a colourless waxy solid.

R_f = 0.06 (free amine, DCM:MeOH = 9:1). t_R = 28.71 min. MS (ESI): *m/z* = 463.5 $[M+Na]^+$.

2-(1-(2-(Octadecylamino)-2-oxoethyl)-2-octanoylhydrazinyl)-2-oxoethan-1-aminium chloride, $C_7H_{15}CO$-IdrGly-$NHC_{18}H_{37}$ · HCl 4Cd

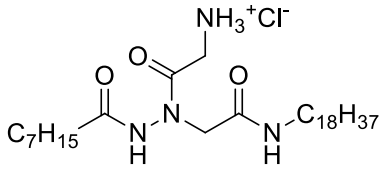

Starting from **2Cd** (174 μmol, 109 mg) and following *procedure i*, compound **4Cd** was obtained in 81% yield (141 μmol, 79 mg) as a white waxy solid.

R_f = 0.09 (free amine, DCM:MeOH = 95:5). m.p. = 135-137 °C (decomposes). MS (ESI): *m/z* = 547.6 $[M+Na]^+$.

2-(2-dodecanoyl-1-(2-oxo-2-(propylamino)ethyl)hydrazinyl)-2-oxoethan-1-aminium chloride, $C_{11}H_{23}CO$-IdrGly-NHC_3H_7 · HCl 4Da

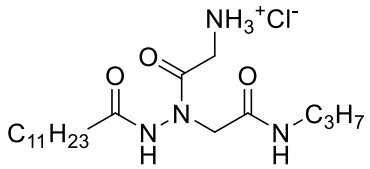

Starting from **2Da** (180 μmol, 85 mg) and following *procedure ii*, compound **4CDa** was obtained in 84% yield (152 μmol, 62 mg) as a white waxy solid.

R_f = 0.4 (free amine, AcOEt:MeOH = 8:2). t_R = 21.33 min. MS (ESI): *m/z* = 393.3 $[M+Na]^+$.

2-(2-Dodecanoyl-1-(2-(octylamino)-2-oxoethyl)hydrazinyl)-2-oxoethan-1-aminium chloride, $C_{11}H_{23}CO$-IdrGly-NHC_8H_{17} · HCl 4Db

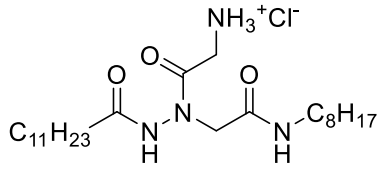

Starting from **2Db** (169 μmol, 91 mg) and following *procedure i*, compound **4Db** was obtained in 89% yield (151 μmol, 72 mg) as a white waxy solid.

R_f = 0.08 (free amine, DCM:MeOH = 9:1). t_R = 28.16 min. MS (ESI): *m/z* = 463.5 $[M+Na]^+$.

2-(2-Dodecanoyl-1-(2-(dodecylamino)-2-oxoethyl)hydrazinyl)-2-oxoethan-1-aminium chloride, $C_{11}H_{23}CO$-IdrGly-$NHC_{12}H_{25}$ · HCl 4Dc

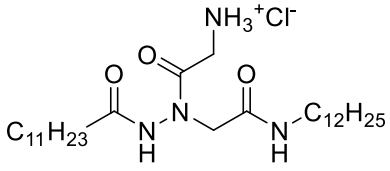

Starting from **2Dc** (253 μmol, 151 mg) and following *procedure i* compound **4Dc** was obtained in 82% yield (207 μmol, 110 mg) as a colourless waxy solid.

R_f = 0.11 (free amine, DCM:MeOH = 9:1). t_R = 33.84 min. MS (ESI): *m/z* = 519.5 $[M+Na]^+$.

2-(1-(2-(Octylamino)-2-oxoethyl)-2-stearoylhydrazinyl)-2-oxoethan-1-aminium chloride, $C_{17}H_{35}CO$-IdrGly-NHC_8H_{17} · HCl 4Eb

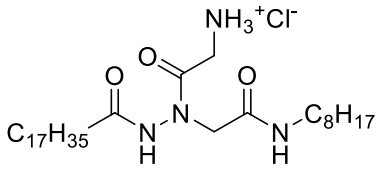

Starting from **2Eb** (174 μmol, 109 mg) and following *procedure i*, compound **4Eb** was obtained in 80% yield (139 μmol, 78 mg) as a white waxy solid.

R_f = 0.35 (free amine, DCM:MeOH = 9:1). t_R = 36.94 min. m.p. = 120-123 °C (decomposes). MS (ESI): *m/z* = 547.6 $[M+Na]^+$.

2-(1-(2-(Octadecylamino)-2-oxoethyl)-2-stearoylhydrazinyl)-2-oxoethan-1-aminium, $C_{17}H_{35}CO$-IdrGly-$NHC_{18}H_{37}$ · HCl 4Ed

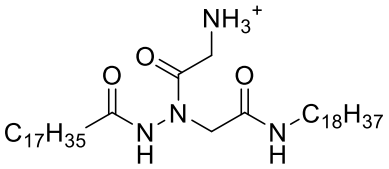

Starting from **2Ed** (141 μmol, 108 mg) and following *procedure ii*, the compound **4Ed** was obtained in 82% yield (116 μmol, 77 mg) as a white waxy solid.

R_f = 0.40 (free amine, DCM:MeOH = 9:1). m.p. (hydrochloride) = 150-152 °C (decomposes). t_R = 46.48 min.MS (ESI): *m/z* = 687.7 $[M+Na]^+$.

(*S*)-6-(1-(2-(Octadecylamino)-2-oxoethyl)-2-stearoylhydrazinyl)-6-oxohexane-1,5-diaminium chloride, $C_{17}H_{35}CO$-IdrLys-$NHC_{18}H_{37}$ · 2HCl 5Ed

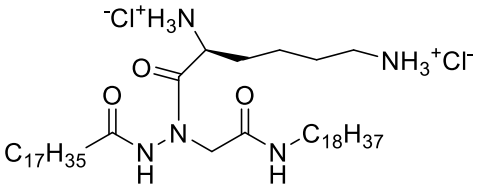

Starting from **3Ed** (128 μmol, 120 mg) and following *procedure ii*, compound **5Ed** was obtained in 67% yield (86 μmol, 69 mg) as a white waxy solid.

R_f = 0.32 (free amine, DCM:MeOH = 85:15). t_R = 43.10 min. MS (ESI): *m/z* = 758.8 $[M+Na]^+$.

2-(2-Benzoyl-1-(2-(dodecylamino)-2-oxoethyl)hydrazinyl)-2-oxoethan-1-aminium chloride, PhCO-IdrGly-NHC$_{12}$H$_{25}$ · HCl 4Fc

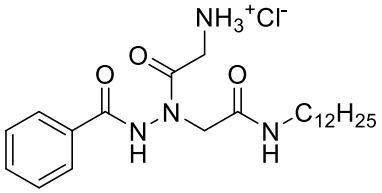

Starting from **2Fc** (183 μmol, 95 mg) and following *procedure ii*, compound **4Fc** was obtained in 79% yield (145 μmol, 66 mg) as a colourless waxy solid.

R_f = 0.12 (free amine, DCM:MeOH = 9:1). t_R = 24.40 min. MS (ESI): *m/z* = 441.4 $[M+Na]^+$.

2-(1-(2-(Dodecylamino)-2-oxoethyl)-2-pivaloylhydrazinyl)-2-oxoethan-1-aminium chloride, *t*-BuCO-IdrGly-NHC$_{12}$H$_{25}$ · HCl 4Gc

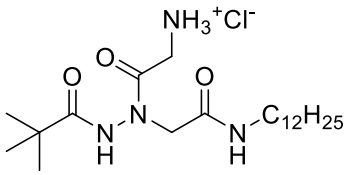

Starting from **2Gc** (222 μmol, 111 mg) and following the general procedure, compound **4Gc** was obtained in 85% yield (189 μmol, 82 mg) as a colourless waxy solid.

R_f = 0.07 (free amine, DCM:MeOH = 9:1). t_R = 24.47 min. MS (ESI): *m/z* = 421.4 $[M+Na]^+$.

REFERENCES

[1] For leading references, see: (*a*) D. Seebach, J. L. Matthews, *J. Chem. Soc., Chem. Commun.* **1997**, 2015; (*b*) S. H. Gellman, *Acc. Chem. Res*. **1998**, *31*, 173; (*c*) K. D. Stigers, M. J. Soth, J. S. Nowick, *Curr. Opin. Chem. Biol.* **1999**, *3*, 714; (*d*) R. P. Cheng, S. H. Gellman, W. F. DeGrado, *Chem. Rev.* **2001**, *101*, 3219; (*e*) D. J. Hill, M. J. Mio, R. B. Prince, T. S. Hughes, J. S. Moore, *Chem. Rev.* **2001**, *101*, 3893; (*f*) A. R. Sanford, B. Gong., *Curr. Org. Chem.* **2003**, *7*, 1649; (*g*) I. Huc, *Eur. J. Org. Chem.* **2004**, 17; (*h*) R. P. Cheng, *Curr. Opin. Struct. Biol.* **2004**, *14*, 512; (*i*) M. A. Balbo Block, C. Kaiser, A. Khan, S. Hecht, *Top. Curr. Chem.* **2005**, *245*, 89; (*j*) D. Seebach, D. F. Hook, A. Glättli, *Biopolymers (Pept. Sci.)* **2006**, *84*, 23; (*k*) F. Fülöp, T. A. Martinek, G. K. Tóth, *Chem. Soc. Rev*. **2006**, *35*, 323; (*l*) S. Hecht, I. Huc, *Foldamers: Structure, Properties, and Applications*, Wiley-VCH, Weinheim, **2007**; (*m*) C. M. Goodman, S. Choi, S. Shandler, W. F. DeGrado, *Nat. Chem. Biol.* **2007**, *3*, 252; (*n*) A. D. Bautista, C. J. Craig, E. A. Harker, A. Schepartz, *Curr. Opin. Chem. Biol.* **2007**, 11, 685; (*o*) W. S. Horne, S. H. Gellman, *Acc. Chem. Res.* **2008**, *41*, 1399; (*p*) I. Saraogi, A. D. Hamilton, *Chem. Soc. Rev.* **2009**, *38*, 1726; (*q*) H. Juwarker, K.-S. Jeong, *Chem. Soc. Rev.* **2010**, *39*, 3664; (*r*) G. Guichard, I. Huc, *Chem. Commun.* **2011**, *47*, 5933; (*s*) W. S. Horne, *Expert Opin. Drug Discov.* **2011**, *6*, 1247; (*t*) T. A. Martinek, F. Fülöp, *Chem. Soc. Rev.* **2012**, *41*, 687; (*u*) P. Prabhakaran, G. Priya, G. J. Sanjayan, *Angew. Chem. Int. Ed.* **2012**, *51*, 4006; (*v*) D.-W. Zhang, X. Zhao, J.-L. Hou, Z.-T. Li, *Chem. Rev.* **2012**, *112*, 5271; (*w*) R. V. Nair, K. N. Vijayadas, A. Roy, G. J. Sanjayan, *Eur. J. Org. Chem.* **2014**, 7763; (*x*) I. M. Mándity, F. Fülöp, *Expert Opin. Drug Discov.* **2015**, *10*, 1163.

[2] A. Banerjee, P. Balaram, *Curr. Science,* **1997**, *73*, 1067.

[3] D. H. Appella, L. A. Christianson, I. L. Karle, D. R. Powell, S. H. Gellman, *J. Am. Chem. Soc.*, **1996**, *118*, 13071.

[4] H. Bestian, *Angew. Chem. Int. Ed. Engl.*, **1968**, *7*, 278.

[5] (*a*) J. Kovács, R. Ballina, R. L. Rodin, D. Balasubramanian, J. Applequist, *J Am. Chem. Soc.* **1965**, *87*, 119; (*b*) J. Bella, C. Alemán, J. M. Fernandez-Santin, C. Alegre, J. A. Subirana, *Macromolecules* **1992**, *25*, 5225; (*c*) D. Seebach, E. P. Ciceri, M. Overhand, B. Juan, D. Rigo, L. Oberer, U. Hommel, R. Amstutz, H. Widmer, *Helv. Chim. Acta* **1996**, *79*, 2043; (*d*) Y. Hamuro, J. P. Schneider, W. F. DeGrado, *J. Peptide Res.* **1999**, *54*, 206; (*e*) R. Günther, H.-J. Hofmann, K. Kuczera, *J. Phys. Chem. B* **2001**, *105*, 5559.

[6] (*a*) T. Beke, C. Somlai, A. Perczel, *J. Comput. Chem*. **2006**, *27*, 20; (*b*) T. Beke, I. G. Csizmadia, A. Perczel, *J. Am. Chem. Soc.* **2006**, *128*, 14548; (*c*) G. Pohl, T. Beke, I. G. Csizmadia, A. Perczel, *J. Phys. Chem. B* **2010**, *114*, 9338; (*d*) I.-S. Park, Y.-R. Yoon, M. Jung, K. Kim, S.-B. Park, S. Shin, Y.-B. Lim, M. Lee, *Chem. Asian J.* **2011**, *6*, 452.

[7] (*a*) D. Seebach, S. Abele, K. Gademann, G. Guichard, T. Hintermann, B. Jaun, J. L. Matthews, J. V. Schreiber, L. Oberer, U. Hommel, H. Widmer, *Helv. Chim. Acta* **1998**, *81*, 932; (*b*) D.

Seebach, K. Gademann, J. V. Schreiber, J. L. Matthews, T. Hintermann, B. Jaun, L. Oberer, U. Hommel, H. Widmer, *Helv. Chim. Acta* **1997**, *80*, 2033.

[8] (*a*) D. H. Appella, L. A. Christianson, I. L. Karle, D. R. Powell, S. H. Gellman, *J. Am. Chem. Soc.* **1996**, *118*, 13071; (*b*) D. H. Appella, L. A. Christianson, D. A. Klein, D. R. Powell, S. H. Gellman, *Nature* **1997**, *387*, 381; (*c*) J. Applequist, K. A. Bode, D. H. Appella, L. A. Christianson, S. A. Gellman, *J. Am. Chem. Soc.* **1998**, *120*, 4891; (*d*) D. H. Appella, L. A. Christianson, D. A. Klein, M. R. Richards, D. R. Powell, S. H. Gellman, *J. Am. Chem. Soc.* **1999**, *121*, 7574; (*e*) E. A. Porter, X. Wang, H.-S. Lee, B. Weisblum, S. H. Gellman, *Nature* **2000**, *404*, 565; (*f*) J. J. Barchi, X. L. Huang, D. H. Appella, L. A. Christianson, A. R. Durell, S. H. Gellman, *J. Am. Chem. Soc.* **2000**, *122*, 2711; (*g*) X. Wang, J. F. Espinosa, S. H. Gellman, *J. Am. Chem. Soc.* **2000**, *122*, 4821; (*h*) H.-S. Lee, F. A. Syud, X. Wang, S. H. Gellman, *J. Am. Chem. Soc.* **2001**, *123*, 7721; (*i*) E. A. Porter, B. Weisblum, S. H. Gellman, *J. Am. Chem. Soc.* **2002**, *124*, 7324.

[9] X. Li, Y.-D. Wu, D. Yang, *Acc. Chem. Res.* **2008**, *41*, 1428 and references cited therein.

[10] (*a*) G. Lelais, D. Seebach, *Helv. Chim. Acta* **2003**, *86*, 4152 and references cited therein; (*b*) A. Salaün, M. Potel, T. Roisnel, P. Gall, P. Le Grel, *J. Org. Chem.* **2005**, *70*, 6499; (*c*) A. Salaün, A. Favre, B. Le Grel, M. Potel, P. Le Grel, *J. Org. Chem.* **2006**, *71*, 150; (*d*) P. Le Grel, A. Salaün, M. Potel, L B. e Grel, V. Lassagne, *J. Org. Chem.* **2006**, *71*, 5638; (*e*) C. Simo, A. Salaün, C. Arnarez, L. Delemotte, A. Haegy, A. Kachmar, A. D. Laurent, T J. homas, B. Jamart-Grégoire, P. Le Grel, A. *J.* Hocquet, *Mol. Struc. THEOCHEM* **2008**, *869*, 41; (*f*) P. Le Grel, A. Salaün, C. Mocquet, B. Le Grel, T. Roisnel, M. Potel, *J. Org. Chem.* **2008**, *73*, 1306; (*g*) A. Salaün, C. Mocquet, R. Perochon, A. Lecorgne, B. Le Grel, M. Potel, P. Le Grel, *J. Org. Chem.* **2008**, *73*, 8579; (*h*) P. Le Grel, A. Asprogenidi, P. Huez, B. Le Grel, A. Salaün, T. Roisnel, M. Potel, E. Rasti, A. Hocquet, *Chirality* **2013**, *25*, 341.

[11] (*a*) I. Menegazzo, A. Fries, S. Mammi, R. Galeazzi, G. Martelli, M. Orena, S. Rinaldi, *Chem. Commun.* **2006**, 4915; (*b*) R. Galeazzi, G. Martelli, A. Mazzanti, M. Orena, S. Rinaldi, *Chem., Eur. J.* **2011**, *17*, 12564.

[12] (*a*) S. Abele, P. Seiler, D. Seebach, *Helv. Chim. Acta* **1999**, *82*, 1559 (derived from 1-(aminomethyl)cyclopropanecarboxylic acid); (*b*) J. D. Winkler, E. L. Piatnitski, J. Mehlmann, J. Kasparec, P. H. Axelsen, *Angew. Chem. Int. Ed.* **2001**, *40*, 743 (derived from a *trans*-β-amino acid tethered on an antracene Diels-Alder adduct); (*c*) R. J. Doerksen, B. Chen, J. Yuan, J. D. Winkler, M. L. Klein, *Chem. Commun.* **2003**, 2534 (derived from a *trans*-oxanorbornene-β-amino acid); (*d*) R. Threlfall, A. Davies, N. M. Howarth, J. Fisher, R. Cosstick, *Chem. Commun.* **2008**, 585 (derived from a *trans*-nucleoside-β-amino acid); (*e*) E. Gorrea, G. Pohl, P. Nolis, S. Celis, K. K. Burusco, V. Branchadell, A. Perczel, R. M. Ortuño, *J. Org. Chem.* **2012**, *77*, 9795 (derived from *trans*-2-aminocyclobutane-1-carboxylic acid).

[13] Another putative 8-helix was found for α-hydroxy-β-amino acids: K. Gademann, A. Häne, M. Rueping, B. Jaun, D. Seebach, *Angew. Chem. Int. Ed.* **2003**, *42*, 1534. Anyway, this case is ambiguous, because a subsequent thorough molecular dynamics analysis pointed toward the

preference for the 12-helix over the 8-helix: A. Glättli, W. F. van Gunsteren, *Angew. Chem. Int. Ed.* **2004**, *43*, 6312.

[14] (*a*) A. Altmayer-Henzien, V. Declerck, D. Merlet, J. P. Baltaze, J. Farjon, R. Guillot, D. J. Aitken, *J. Org. Chem.* **2013**, *78*, 6031; (*b*) A. Altmayer-Henzien, V. Declerck, J. Farjon, D. Merlet, R. Guillot, D. J. Aitken, *Angew. Chem. Int. Ed.* **2015**, *54*, 10807.

[15] (*a*) F. Sgolastra - Design and synthesis of biomimetic compounds with pharmacological activity, Università Politecnica delle Marche, Doctoral Thesis, 2009/2010, http://openarchive.univpm.it/jspui/handle/123456789/304; (*b*) N. B. Hassen, M. Sc. thesis in Applied Biology, A.Y. 2009-2010, Università Politecnica delle Marche.

[16] R. Häner, B. Olano, D. Seebach, *Helv. Chim. Acta* **1987**, *70*, 1676.

[17] S. K. Mishra, N. Suryaprakash, *Phys. Chem. Chem. Phys.* **2015**, *17*, 15226.

[18] T. D. W. Claridge, J. M. Goodman, A. Moreno, D. Angus, S. F. Barker, C. Taillefumier, M. P. Watterson, G. W. J. Fleet, *Tetrahedron Lett.* **2001**, *42*, 4251.

[19] X. Zhao, X.-Z. Wang, X.-K. Jiang, Y.-Q. Chen, Z.-T. Li, G.-J. Chen, *J. Am. Chem. Soc.* **2003**, *125*, 15128.

[20] (*a*) I. M. Klotz, J. S. Franzen, *J. Am. Chem. Soc.* **1962**, *84*, 3461; (*b*) S. E. Krikorian, *J. Phys. Chem.* **1982**, *86*, 1875.

[21] S. H. Gellman, G. Dado, G. B. Liang, B. Adams, *J. Am. Chem. Soc.* **1991**, *113*, 1164.

[22] H. Kessler, *Ang. Chem. Int. Ed.* **1982**, *21*, 512.

[23] See, for example: (*a*) N. J. Baxter, M. P. Williamson, *J. Biomol. NMR* **1997**, *9*, 359; (*b*) N. H. Andersen, J. W. Neidigh, S. M. Harris, G. M. Lee, Z. Liu, H. Tong, *J. Am. Chem. Soc.* **1997**, *119*, 8547; (*c*) T. Cierpicki, J. Otlewski, *J. Biomol. NMR* **2001**, *21*, 249, and references cited therein.

[24] See, for example: (*a*) L. Belvisi, A. Bernardi, L. Manzoni, D. Potenza, C. Scolastico, *Eur. J. Org. Chem.* **2000**, 2563; (*b*) D. Yang, B. Li, F.-F. Ng, Y,-L. Yan, J. Qu, Y.-D. Wu, *J. Org. Chem.* **2001**, *66*, 7303; (*c*) M. M. Fernandez, A. Diez, M. Rubiralta, E. Montenegro, N. Casamitjana, M. J. Kogan, E. Giralt, *J. Org. Chem*. **2002**, *67*, 7587; (*d*) A. Trabocchi, E. G. Occhiato, D. Potenza, A. Guarna, *J. Org. Chem*. **2002**, *67*, 7483; (*e*) B.-h. Baek, M.-r. Lee, K.-Y. Kim, U.-i. Cho, D. W. Boo, I. Shin, *Org. Lett.* **2003**, *5*, 971.

[25] See, for example: C. Tomasini, G. Luppi, M. Monari, *J. Am. Chem. Soc.* **2006**, *128*, 2410 and references cited therein.

[26] A. Glättli, X. Daura, D. Seebach, W. F. van Gunsteren, *J. Am. Chem. Soc.* **2002**, *124*, 12972.

[27] D. Yang, J. Qu, B. Li, F.-F. Ng, X.-C. Wang, K.-K. Cheung, D.-P. Wang, Y.-D. Wu, *J. Am. Chem. Soc.* **1999**, *121*, 589.

[28] See, for example: D. Seebach, J. V. Schreiber, S. Abele, X. Daura, W. F. van Gusteren, *Helv. Chim. Acta* **2000**, *83*, 34.

[29] D. H. Appella, J. J. Barchi, S. R. Durell, S. H. Gellman, *J. Am. Chem. Soc.* **1999**, *121*, 2309.

[30] D. A. Case, T. A. Darden, T. E. III Cheatham, C. L. Simmerling, J. Wang, R. E. Duke, R. Luo, R. C. Walker, W. Zhang, K. M. Merz, B. Roberts, B. Wang, S. Hayik, A. Roitberg, G. Seabra, I. Kolossváry, K. F. Wong, F. Paesani, J. Vanicek, J. Liu, X. Wu, S. R. Brozell, T. Steinbrecher, H. Gohlke, Q. Cai, X. Ye, J. Wang, M.-J. Hsieh, G. Cui, D.R. Roe, D. H.

Mathews, M. G. Seetin, C. Sagui, V. Babin, T. Luchko, S. Gusarov, A. Kovalenko, P.A. Kollman, AMBER 11, University of California, San Francisco, **2010**.
[31] J. Wang, R. M. Wolf, J. W. Caldwell, P. A. Kollman, D. A. Case, *J. Comput. Chem.* **2004**, *25*, 1157.
[32] J. Wang, W. Wang, P. A. Kollman, D. A. Case, *J. Mol. Graph. Model*. **2006**, *25*, 247.
[33] (*a*) I. Daidone, A. Amadei, *WIREs Comput. Mol. Sci*. **2012**, *2*, 762; (*b*) S. Fermani, X. Trivelli, F. Sparla, A. Thumiger, M. Calvaresi, L. Marri, G. Falini, F. Zerbetto, P. Trost, *J. Biol. Chem*. **2012**, *287*, 21372.
[34] K. A. Bode, J. Applequist, *Macromolecules* **1997**, *30*, 2144.
[35] B. Moon, S. Han, D. Kim, *Org. Lett.* **2005**, *7*, 3359.
[36] R. Häner, B. Olano, D. Seebach, *Helv. Chim. Acta* **1987**, *70*, 1676.
[37] P. Le Grel, A. Salaün, C. Mocquet, B. Le Grel, T. Roisnel, M. Potel, *J. Org. Chem.* **2008**, *73*, 1306.
[38] J.-S. Chen, R. B. Shirts, *J. Phys. Chem.* **1985**, *89*, 1643.
[39] H. S. Gutowsky, A. Saika, *J. Chem. Phys.* **1953**, *21,* 1688.
[40] A. D. Becke, *J. Chem. Phys*. **1993**, *98*, 5648.
[41] (*a*) M. Cossi, V. Barone, B. Mennucci, J. Tomasi, *Chem. Phys. Lett.*, **1998**, *286*, 253; (*b*) B. Mennucci, J. Tomasi, *J. Chem. Phys.*, **1997**, *106*, 5151-5158; (*c*) U. C. Singh, P. A. Kollman, *J. Comput. Chem*., **1983**, *4*, 129.
[42] All the calculations were performed using the software Gaussian 09: Gaussian 09, Revision A.1, M. J. Frisch, G. W. Trucks, H. B. Schlegel, G. E. Scuseria, M. A. Robb, J. R. Cheeseman, G. Scalmani, V. Barone, B. Mennucci, G. A. Petersson, H. Nakatsuji, M. Caricato, X. Li, H. P. Hratchian, A. F. Izmaylov, J. Bloino, G. Zheng, J. L. Sonnenberg, M. Hada, M. Ehara, K. Toyota, R. Fukuda, J. Hasegawa, M. Ishida, T. Nakajima, Y. Honda, O. Kitao, H. Nakai, T. Vreven, J. A. Montgomery, Jr., J. E. Peralta, F. Ogliaro, M. Bearpark, J. J. Heyd, E. Brothers, K. N. Kudin, V. N. Staroverov, R. Kobayashi, J. Normand, K. Raghavachari, A. Rendell, J. C. Burant, S. S. Iyengar, J. Tomasi, M. Cossi, N. Rega, N. J. Millam, M. Klene, J. E. Knox, J. B. Cross, V. Bakken, C. Adamo, J. Jaramillo, R. Gomperts, R. E. Stratmann, O. Yazyev, A. J. Austin, R. Cammi, C. Pomelli, J. W. Ochterski, R. L. Martin, K. Morokuma, V. G. Zakrzewski, G. A. Voth, P. Salvador, J. J. Dannenberg, S. Dapprich, A. D. Daniels, Ö. Farkas, J. B. Foresman, J. V. Ortiz, J. Cioslowski, D. J. Fox, Gaussian, Inc., Wallingford CT, **2009**.
[43] L. Bren, *FDA Consumer Magazine*, **2002**, *28.*
[44] M. R. Yeaman, N. Y. Yount, *Pharmacol. Rev.*, **2003**, *55*, 27.
[45] For a review, see: R.E.W. Hancock, *The Lancet* **2001***, 1,* 156.
[46] M. Zasloff, *Nature*, **2004**, *412*, 389.
[47] For a review, see: Brogden, K. A. *Nat. Rev. Microbiol.* **2005***, 3,* 238.
[48] For a review see: C. Sohlenkamp, O. Geiger, *FEMS Microbiol. Rev.*, **2016**, *40*, 133.
[49] H. Jenssen, P. Hamill and R. E. W. Hancock, *Clin. Microbiol. Rev.,* **2006**, *19(3)*, 491.
[50] R. E. W. Hancock, *The Lancet*, **1997**, *349*, 418.

[51] For a review see: (*a*) R. M. Epand, H. J. Vogel, *Biochimica et Biophysica Acta 1462*, **1999**, *11*; (*b*) R. E. W. Hancock, D. S. Chapel, *Antimicrob. Agents and Chemioter.*, **1999**, *43(6)*, 1317; (*c*) W. C. Wimley, *ACS Chem. Biol.*, **2010**, *5(10)*, 905.

[52] M. S. P. Sansom, *Eur. Biophys*, **1993**, *22*, 105.

[53] L. Yang, T. A. Harroun, T. M. Weiss, L. Ding, H. W. Huang, *Biophys. J.*, **2001**, *81*, 1475.

[54] (*a*) M. Cudic M, L. Jr. Otvos, Curr Drug Targets, **2002**, *3(2)*,101; (*b*) N. Y. Yount, M. R. Yeaman, Protein Pept. Lett., **2005**, *12(1)*, 49; (c) O. Toke, Biopolymers, **2005**, *80(6)*, 717.

[55] L. Jr. Otvos, *J. Peptide Sci.*, **2005**, *11*, 697.

[56] M. Zasloff; Antimicrobial Peptides of multicellular organisms. *Nature* **2002***, 415,* 389.

[57] For a review see: D. I. Andersson *et al.*, *Drug Resistance Updates*, **2016**, *26*, 43 and references cited therein.

[58] (*a*) E. A. Groisman, *Bioessays*, **1998**, *20*, 96; (*b*) R. P. Darveau, et al.*, Antimicrob. Agents Chemother.*, **1991**, *35*, 1153.

[59] V. J. Hruby, T. O. Matsunaga, In *Synthetic Peptides (2nd Edition),* G. A. Ed. Grant, Oxford University Press: New York, **2002**, 292.

[60] K. Luthman, U. Hacksell, In *Textbook of Drug Design and Discovery (3rd Edition),* P. Krogsgaard-Larsen, T. Liljefors, U. Eds. Madsen, Taylor & Francis: London, **2002**, 459.

[61] L. Gentilucci, *Curr. Top. Med. Chem*., **2004**, *4*, 19.

[62] Example of β-peptidic amphiphilic foldamer with 12-helix: E. A. Porter, X. Wang, H.-S. Lee, B. Weisblum, S. H. Gellman, *Nature*, **2000**, *404*, 565.

[63] Example of β-peptidic amphiphilic foldamer with 14-helix: (*a*) Y. Hamuro, J. P. Schneider, W. F. DeGrado, *J. Am. Chem. Soc*., **1999**, *121*, 12200; (*b*) D. Liu, W. F. DeGrado, *J. Am. Chem. Soc.* **2001**, *123*, 7553.

[64] (*a*) A. Som, S. Vemparala, I. Ivanov, G. N. Tew, *Biopolymers*, **2008**, *90*, 83; (*b*) S. Rotem, A. Mor, *Biochim. Biophys. Acta*, *Biomembr.* **2009**, *1788*, 1582.

[65] A. Violette, S. Fournel, K. Lamour, O. Chaloin, B. Frisch, J.-P. Briand, H. Monteil, G. Guichard, *Chem. Biol.,* **2006**, *13*, 531.

[66] A. E. Barron, J. A. Patch, *J. Am. Chem. Soc.*, **2003**, *125*, 12092.

[67] K. El-Refaie, S. D. Worley, R. Broughton, *BioMacromolecules*, **2007**, *8*, 1359.

[68] R. E. W. Hancock, H.-G. Sahl, *Nat. Biotechnol.,* **2006**, *24*, 1551.

[69] B. P. Mowery, S. E. Lee, D. A. Kissounko, R. F. Epand, R. M. Epand, B. Weisblum, S. S. Stahl, S. H. Gellman, *J. Am. Chem. Soc.*, **2007**, *129*, 15474.

[70] B. P. Mowery, A. H. Lindner, B. Weisblum, S. S. Syahl, S. H. Gellman, *J. Am. Chem. Soc.*, **2009**, *131*, 9735.

[71] Some practical application of polymeric SMAMPs: M. B. Patel, S. A. Patel, A. Ray, R. M. Patel, *J. Appl. Polym. Sci*. **2003**, *89*, 895.

[72] Some practical application of polymeric SMAMPs: E. S. Park, H.-J. Lee, H.-Y. Park, M.-N. Kim, K.-H. Chung, J.-S. Yoon, *J. Appl. Polym. Sci.* **2001**, *80*, 728.

[73] Some practical application of polymeric SMAMPs: E. Ranucci, P. Ferruti, *Polymer* **1991**, *32*, 2876.

[74] M. W. Lee, S. Chakraborty, N. W. Schmidt, R. Murgai, S. H. Gellman, G. C. Wong, *Biochim. Biophys Acta*, **2014,** *1839,* 2269.

[75] M. A. Gelman, B. Weisblum, D. M. Lynn, S. H. Gellman, *Org. Lett.*, **2004**, *6*, 557.

[76] L. Dias de Melo Carrasco, J. L. Mello Sampaio, A. M. Carmona-Ribeiro, *Int. J. Mol. Sci.,* **2015**, *16*, 6337.

[77] F. Nederberg, Y. Zhang, J. P. K. Tan, K. Xu, H. Wang, C. Yang, S. Gao, X. D. Guo, K. Fukushima, L. Li, J. L. Hedrick, Y.-Y. Yang, *Nat. Chem.*, **2011**, *3*, 409.

[78] J. Haldar, D. An, L. Alvarez de Cienfuegos, J. Chen, A. M. Klibanov, *PNAS*, **2006**, *103*, 17667.

[79] D. S. S. M. Uppu, P. Akkapeddi, G. B. Manjunath, V. Yarlagadda, J. Hoque, J. Haldar, *Chem. Commun.,* **2013**, *49*, 9389.

[80] T. Tashiro, *Macromol. Mater. Eng.*, **2001**, *286*, 63.

[81] J. C. Tiller, C.-J. Liao, K. Lewis, A. M. Klibanov, *Proc. Natl. Acad. Sci. U.S.A.* **2001**, *98*, 5981.

[82] F. Baudrion, A. Perichaud, S. Coen, *J. Appl. Polym. Sci*. **1998**, *70*, 2657.

[83] E. R. Kenawy, F. I. Abdel-Hay, A. E. R. R. El-Shanshoury, M. H. El-Newehy, *J. Controlled Release*, **1998**, *50*, 145.

[84] K. Kuroda, W. F. DeGrado, *J. Am. Chem. Soc.*, **2005**, *127*, 4128.

[85] V. Sambhy, B. R. Peterson, A. Sen, *Angew. Chem. Int. Ed.,* **2008,** *47,* 1250.

[86] (*a*) M. Buchmeiser, *Chem. Rev.* **2000**, *100*, 1565; (*b*) L. L. Kiessling, R. M. Owen, in *Handbook of Metathesis*, Wiley-VCH, Weinheim, **2003**, 180; (*c*) K. Lienkamp, A. E. Madkour, A. Musante, C. F. Nelson, K. Nüsslein, G. N. Tew, *J. Am. Chem. Soc*. **2008**, *130*, 9836.

[87] K. Lienkamp, K. N. Kumar, A. Som, K. Nüsslein, G. N. Tew, *Chemistry,* **2009**, *15*, 11710.

[88] For a review see: J. D. F. Hale, R. E. W. Hancock, *Expert Rev. Anti Infect. Ther*., **2007**, *5 (6)*, 951.

[89] For a review see: (*a*) W. Aoki, M. Ueda, *Pharmaceuticals,* **2013**, *6*, 1055; (*b*) A. A. Bahar, D. Ren, *Pharmaceuticals,* **2013**, *6*, 1543.

[90] For a review see: Z. Yu, W. Qin, J. Lin, S. Fang, J. Qiu, *BioMed Research International*, **2015**, *2015.*

[91] (*a*) R. F. Epand, P. B. Savage, R. M. Epand, *Biochim. Biophys. Acta*, **2007**, *1768*, 2500; (*b*) X. Z. Lai, Y. Feng, J. Pollard, J. N. Chin, M. J. Rybak, R. Bucki, R. F. Epand, R. M. Epand, P. B. Savage, *Acc. Chem. Res.*, **2008**, *41*, 1233.

[92] C. R. Raetz, G. D. Kantor, M. Nishijima, K. F. Newman, *J. Bacteriol*, **1979**, *139*, 544.

[93] J. A. Castillo, A. Pinazo, J. Carilla, M. R. Infante, M. A. Alsina, I. Haro, S. P. Clapee, *Langmuir*, **2004**, *20*, 3379.

[94] J. Hoque, P. Akkapeddi, V. Yarlagadda, D. S. Uppu, P. Kumar, J. Haldar, *Langmuir*, **2012**, *28*, 12225.

[95] H. D. Thaker, A. Cankaya, R. W. Scott, G. N. Tew, *ACS Med. Chem. Lett.*, **2013**, *4*, 481.

[96] H. D. Thaker, A. Som, F. Ayaz, D. Lui, W. Pan, R. W. Scott, J. Anguita, G. N. Tew, *J. Am. Chem. Soc.*, **2012**, *134*, 11088 and references cited therein.

[97] C. Ghosh, G. B. Manjunath, P. Akkapeddi, V. Yarlagadda, J.Hoque, D. S. S. M. Uppu, M. M. Konai, J. Haldar, *J. Med. Chem.*, **2014**, *57*, 1428.

[98] P. D. Lister, D. J. Wolter, N. D. Hanson, *Clin. Microbiol. Rev.*, **2009**, *22*, 582.

[99] S. Shakil, R. Khan, R. Zarrilli, U. Asad, *Khan Journal of Biomedical Science*, **2008** *15*, 5.

[100] S. B.Vakulenko, S. Mobashery, *Clin. Microbiol. Rev.*, **2003**, *16*, 430.

[101] I. M. Herzog, K. D. Green, Y. Berkov-Zrihen, M. Fedman, R. R. Vidavski, A. Eldar-Boock, R. Satchi-Fainaro, S. Garneau-Tsodikova, M. Fridman., *Angew. Chem. Int. Ed. Engl.*, **2012**, *51*, 5652.

[102] (*a*) S. Bera, G. G. Zhanel, F. Schweizer, *J. Med. Chem.*, **2010**, *53*, 3626; (*b*) I. Baussanne, A. Bussière, S. Halder, C. Ganem-Elbaz, M. Ouberai, M. Riou, J.-M. Paris, E. Ennifar, M.-P. Mingeot-Leclercg, J.-L. Décout, *J. Med. Chem.*, **2010**, *53,* 119; (*c*) S. Bera, G. G. Zhanel, F. Schweizer. *Bioorg. Med. Chem. Lett.*, **2010**, *20*, 3031; (*d*) S. Hannessian, K. Pachamuthu, J. Szychowski, A. Giguère, E. E. Swayze, M. T. Migawa, B. François, J. Kondo, E. Westhof., *Bioorg. Med. Chem.,* **2010,** *20,* 7097; (*e*) R. B. Yan, M. Yuan, Y. Wu, X. You, X. S. Ye, *Bioorg. Med. Chem*, **2011**, *19*, 30; (*f*) S. Bera, G. G. Zhanel, F. Schweizer, *Carbohydr. Res.*, **2011**, *346*, 560; (*g*) M. Ouberai, F. El Garch, A. Bussiere, M. Riou, D. Alsteens, L. Lins, I. Baussanne, Y. F. Dufrêne, R. Brasseur, J. L. Decout, M. P. Mingeot-Leclercg., *Biochim. Biophys. Acta*, **2011**, *1808*, 1716.

[103] V. V. Rostovtsev, L. G. Green, V. V. Fokin, K. B. Sharpless, *Angew. Chem., Int. Ed. Engl.* **2002**, *41*, 2596.

[104] CLSI, Methods for Dilution Antimicrobial Susceptibility Tests for Bacteria that Grow Aerobically, Approved Standard, 9th ed., CLSI document M07-A9. Clinical and Laboratory Standards Institute, 950 West Valley Road, Suite 2500, Wayne, Pennsylvania 19087, USA, **2012**.

[105] See for example: Wadhwani, T., Desai, K., Patel, D., Lawani, D., Bahaley, P., Joshi, P., Kothari V. *Internet J. Microbiol.* **2009**, *7(1)* and references cited therein.

Ringraziamenti

Questo lavoro di tesi è il risultato di tre anni entusiasmanti, nei quali ho avuto la possibilità di crescere non solo a livello scientifico, ma anche a livello personale. Sono troppe le emozioni da scrivere a riguardo, così per non dilungarmi, procederò con semplici pensieri.

Il primo ringraziamento va al mio tutor, mentore ed amico Dott. Samuele Rinaldi. Senza il suo talento messo totalmente a mia disposizione, questo lavoro non avrebbe mai preso il volo né vista la pubblicazione finale. Per i suoi consigli, il suo intuito, la passione smisurata per il lavoro, la precisione e l'impegno che mi ha trasmesso ogni giorno. Ti ringrazio per la battuta sempre pronta e che ti strappa sempre un sorriso, per l'esempio che mi hai dato, per avermi testimoniato che volere è potere, e che l'impegno ed il duro lavoro, sono alla base della riuscita di qualsiasi cosa. Ti sarò eterno debitore.

Un ringraziamento sentito va al Prof. Mario Orena, alla sua dedizione ed impegno professionale. E' sempre stato un punto di riferimento a livello accademico ed umano. La ringrazio Prof. per le "dritte" ma anche per le 'chiacchieratine' pomeridiane, un vero toccasana!

Ringrazio i collaboratori che, anno dopo anno, hanno contribuito a farmi concludere questo ciclo di Dottorato. La Dott.ssa Alessandra Tolomelli, il Dott. Matteo Calvaresi e la Dott.ssa Alessandra Petroli dell'Università "Alma Mater Studiorum" di Bologna per il supporto alle caratterizzazioni strutturali; la Prof.ssa Francesca Biavasco e la Dott.ssa Barbara Citterio delle "Università Politecnica delle Marche" di Ancona ed Università degli studi di Urbino "Carlo Bo" per i test di attività antimicrobica. Senza il vostro aiuto, questa tesi non esisterebbe. Vi ringrazio di cuore.

Un pensiero va a mia moglie Monica e alle mie famiglie; la fam. Amabili e la fam. Mazzaferro. Siete stati indispensabili. Senza la vostra presenza quotidiana la mia vita avrebbe poco senso. Grazie per il vostro totale supporto ed amore. Vi amo!

I miei amici di PDA e PSG sono stati fondamentali per alleviare la tensione emotiva durante tutta la mia attività lavorativa e nel tempo libero. Amici veri e leali. Senza i vostri sorrisi e la vostra presenza, sarei stata senz'altro una persona più sola ed infelice. Siete i migliori!

Un particolare ringraziamento va al team OCIII dell'Università di Bielefeld (Germania). In primis al Prof. Norbert Sewald, leader del team non solo a livello professionale. Grazie per avermi accolto come *guest-researcher* con la sua gentile disponibilità durante il semestre in Germania.

Ulla, Sandip, Guillermo ed Oliver. Siete stati fondamentali durante un periodo particolare della mia vita, una seconda famiglia. Spero di rivedervi presto!

Last but not least il "diparti-gruppo". Colleghi ma soprattutto amici. Annafelicia, Emiliano, Luca, Beatrice, Giovanni, Diego, Roberto, Sara, Giulia e tutti i laureandi che, giorno dopo giorno, mese dopo mese, anno dopo anno, hanno reso indimenticabile la mia esperienza lavorativa. Non scorderò le pause caffè, i pranzi fatti insieme…i *break* più belli della mia vita. Sarà difficile rimpiazzarvi in futuro. Vi ricorderò per sempre.

Infine, un saluto a tutti quelli che non ci sono più. So che ci siete stati, che ci siete e che ci sarete per sempre. Ci rivedremo un giorno…

GRAZIE A TUTTI!

Paolo